

# **Artificial Hormone Network for Adaptable Robots**

**Pitiwut Teerakittikul**

Degree of Ph.D.

University of York

Department of Electronics

January 2013

## **Abstract**

With current robotic technologies, it generally remains unreliable to use fully autonomous robots in high-risk robotic applications such as search and rescue, surveillance or exploration in disaster scenarios. One of the main issues comes from the fact that unstructured real-world environments are dynamic and full of interventions. Therefore, for autonomous robots to operate in such environments, the ability to adapt to both internal and external environmental changes is crucial. Being unable to deal with such changes not only could downgrade the performance of the robots but also potentially cause devastating consequences in risky environments. Looking towards nature, it can be observed that biological organisms can cope well with the dynamic unpredictability of real-world environments. One of the key properties which assist biological organisms is the ability to adapt to changing environments by the utilization of hormones in response to environmental cues. This biological feature provides an inspiration for this research which investigates a novel Artificial Hormone Network architecture in providing adaptability for autonomous robots to deal with both internal and external environmental changes in simulations of unstructured real-world environments. The Artificial Hormone Network architecture proposes a new method which allows constructions and interactions of several hormones in order to provide adaptability for autonomous robots in different application scenarios. Two Artificial Hormone Networks (AHN1 and AHN2) are proposed and investigated in this research. Results from experiments correspondingly report better performance in dealing with considered internal and external environmental changes on a robot implemented with the Artificial Hormone Networks than a robot implemented without them. Another important aspect of the Artificial Hormone Network architecture is the ability to be constructed automatically to provide particular adaptability using Cartesian Genetic Programming. Experiment results show that the construction of Artificial Hormone Networks can be evolved and that this evolved system not only performed to a level of adaptability that was acceptable but actually performed better than the “hand-coded” system.

# Table of Contents

<b>List of Tables .....</b>	<b>8</b>
<b>List of Figures .....</b>	<b>9</b>
<b>Acknowledgements.....</b>	<b>17</b>
<b>Chapter 1 Introduction.....</b>	<b>19</b>
1.1 The Chaos of Real-World Environments .....	20
1.2 Effects of Environmental changes.....	23
1.3 Exploiting Environmental Information .....	25
1.4 Hypothesis .....	27
1.5 Thesis Structure .....	28
<b>Chapter 2 Test Environments .....</b>	<b>30</b>
2.1 The Robocup Rescue Robot Competition .....	30
2.2 Gazebo: the 3D robot simulator .....	35
2.3 The Simulated Robot and Test Environments.....	37
2.4 The robot tasks and robot controller.....	43
2.4.1 The main robot tasks.....	43
2.4.2 The robot controller .....	43
2.5 The Performance Metrics .....	46
2.6 The Considered environmental changes.....	47
2.7 Summary .....	48
<b>Chapter 3 The Hormone System .....</b>	<b>50</b>
3.1 Utilization of Hormones for Adaptation in Biological Organisms .....	51

3.2 Endocrine System and Homeostasis.....	53
3.3 The Artificial Endocrine and Artificial Homeostatic Systems.....	54
3.3.1 Neuro-Endocrine System.....	55
3.3.2 Artificial Homeostatic Hormone System (AHHS).....	64
3.4 Discussion .....	69
3.5 Research Approach.....	70
3.6 Summary .....	71
<b>Chapter 4 Implementation of an Artificial Hormone System.....</b>	<b>73</b>
4.1 Artificial Hormone Mechanisms .....	73
4.1.1 Hormone Gland (HG).....	73
4.1.1.1 Hormone release function .....	74
4.1.1.2 Activation function.....	75
4.1.1.3 Signal pre-processor .....	75
4.1.1.4 Control feature.....	76
4.1.2 Hormone Receptor (HR).....	77
4.1.2.1 Receptor function .....	78
4.1.2.2 Receptor feature .....	78
4.2 Implementation with Terrain Excitation Hormone .....	79
4.2.1 Background.....	79
4.2.2 The Terrain Excitation Hormone.....	80
4.2.2.1 Hormone Gland 1 (HG1).....	81
4.2.2.2 Motion-Command Hormone Receptor (HR_MC) .....	82
4.3 Experiment Setup .....	83
4.4 Results .....	85
4.5 Discussion and Analysis.....	86
4.5.1 Hormone Concentration versus Terrain Roughness .....	86
4.5.2 Hormone Concentration versus Robot Speed.....	89
4.5.3 Robot Traces .....	91

4.5.4 Tip Over Positions .....	92
4.6 Summary .....	94
<b>Chapter 5 Implementation of an Artificial Hormone Network.....</b>	<b>96</b>
5.1 Artificial Hormone Network 1 (AHN1).....	96
5.1.1 Background.....	97
5.1.2 Implementation of AHN1 .....	98
5.1.3 Experiment Setup.....	104
5.1.4 Results.....	105
5.1.5 Discussion and Analysis .....	107
5.1.5.1 The Hormone Interactions.....	107
5.1.5.2 Tip Over Positions.....	112
5.2 Artificial Hormone Network 2 (AHN2).....	114
5.2.1 Background.....	114
5.2.2 Implementation of AHN2 .....	116
5.2.2.1 Hormone Glands in the AHN2.....	119
5.2.2.2 Hormone Receptors in the AHN2 .....	122
5.2.3 Experiment I: Flat Terrain Environment .....	126
5.2.3.1 Experiment Setup .....	126
5.2.3.2 Results .....	128
5.2.3.3 Discussion and Analysis.....	129
5.2.4 Experiment II: Rough Terrain Environment.....	137
5.2.4.1 Experiment Setup .....	137
5.2.4.2 Results .....	138
5.2.4.3 Discussion and Analysis.....	139
5.3 Summary .....	147
<b>Chapter 6 Cartesian Genetic Programming Artificial Hormone Network.....</b>	<b>150</b>
6.1 A Brief Introduction to Cartesian Genetic Programming.....	151

6.2 Implementation of Cartesian Genetic Programming Artificial Hormone Network (CGP-AHN).....	155
6.2.1 CGP-AHN Representation.....	156
6.2.1.1 Program Inputs (AHN Inputs).....	156
6.2.1.2 Computational nodes (Hormone Glands).....	158
6.2.1.3 Program Outputs (Hormone Receptors).....	163
6.2.2 Example of CGP-AHN Encoding.....	167
6.3 Experiments.....	169
6.3.1 Experiment I: Initial test on CGP-AHN .....	169
6.3.1.1 Experiment Setup .....	170
6.3.1.2 Results .....	178
6.3.1.3 Analyse and discussion .....	178
6.3.2 Experiment II: Comparing the performance of no AHN, AHN2 and the best CGP-AHN.....	182
6.3.2.1 Experiment Setup .....	182
6.3.2.2 Results .....	183
6.3.2.3 Discussion .....	184
6.3.3 Experiment III: Generalization Test .....	184
6.3.3.1 Experiment Setup .....	184
6.3.3.2 Results .....	186
6.3.3.3 Analysis and discussion .....	187
6.4 Summary .....	192
<b>Chapter 7 Generalisation Methodology .....</b>	<b>194</b>
7.1 Methodology for Extending the AHN1 and AHN2 .....	195
7.1.1 Extending the AHN1 for Other Types of Robots .....	195
7.1.2 Extending the AHN1 for Other Robotic Applications.....	196
7.1.3 Extending the AHN2 for Other Type of Robots.....	197

7.2 Methodology for Extending the AHN Architecture for Other Application Scenarios .....	200
7.3 Summary .....	203
<b>Chapter 8 Conclusions and Future Work.....</b>	<b>204</b>
8.1 Thesis Summary .....	204
8.1.1 Testing the Hypothesis .....	208
8.2 Contributions .....	210
8.3 Future Work.....	212
<b>Bibliography .....</b>	<b>215</b>

# List of Tables

Table 4.1: The setup of HG1 mechanisms .....	81
Table 4.2: The setup of HR_MC mechanisms .....	82
Table 4.3: The robot performances on the experiment of Terrain Excitation hormone .	85
Table 5.1: The values of $\alpha_g$ and $\beta_g$ of each hormone gland in AHN1 .....	104
Table 5.2: The values of $\alpha_g$ and $\beta_g$ of each hormone gland in the AHN2.....	127
Table 6.1: The 24 data inputs provided at the program inputs of the CGP-AHN.....	157
Table 6.2: The 16 primitive functions defined for the Signal Pre-processor and how the Signal parameter is used in each function.....	161
Table 6.3: The control features and their addresses.....	162
Table 6.4: The three primitive functions of the Activation function and how the Activation parameter is used in each function .....	163
Table 6.5: The two receptor features.....	165
Table 6.6: The 16 primitive functions of the Receptor function and how the Receptor parameter is used in each function .....	166
Table 6.7: The time spent to reach the target object on each test case. Each average time spent is calculated from the same fault case over five positions of the target object ...	188

# List of Figures

Figure 1.1: The Unimate robot.....	19
Figure 1.2: The Bigdog robot.....	24
Figure 1.3: Two Daphnia. One is developed in a predator induced environment (left). Another is developed in a predator-free environment (right) .....	26
Figure 2.1: Examples of test arenas used in the Robocup Rescue Robot competition ...	31
Figure 2.2: An example of simulated victims trapped in the Robocup Rescue Robot test arenas .....	32
Figure 2.3: Examples of maze, roll ramps and pitch ramps used in the yellow-area of the Robocup Rescue Robot competition.....	33
Figure 2.4: Examples of ramps and half-cubic step-fields used in the orange-area of the Robocup Rescue Robot competition.....	34
Figure 2.5: Examples of environments and full-cubic step-fields used in the red-area of the Robocup Rescue Robot competition.....	34
Figure 2.6: An example of Gazebo environments .....	35
Figure 2.7: (a) The actual Pioneer 2-AT robot (b) The Pioneer 2-AT robot simulated in Gazebo .....	37
Figure 2.8: A picture of all three half-cubic step-fields used in the Robocup Rescue Robot competition including flat, diagonal and hill layout step-fields.....	39
Figure 2.9: An example of the test environments created in Gazebo .....	39
Figure 2.10: (a) A top view of the half-cubic flat layout step-field simulated in Gazebo (b) Colour and number codes of wooden blocks constructed to create the half-cubic flat	

layout step-field. The numbers represent the height of each block in millimetre. (c) A picture of the half-cubic flat layout step-field comparing with the simulated Pioneer 2-AT robot.....	40
Figure 2.11: (a) A top view of the half-cubic diagonal layout step-field simulated in Gazebo (b) Colour and number codes of wooden blocks constructed to create the half-cubic diagonal layout step-field. The numbers represent the height of each block in millimetre (c) A picture of the half-cubic diagonal layout step-field comparing with the simulated Pioneer 2-AT robot.....	41
Figure 2.12: (a) A top view of the half-cubic hill layout step-field simulated in Gazebo (b) Colour and number codes of wooden blocks constructed to create the half-cubic hill layout step-field. The numbers represent the height of each block in millimetre. (c) A picture of the half-cubic hill layout step-field comparing with the simulated Pioneer 2-AT robot.....	42
Figure 2.13: The frontal area distance infrared sensor located in front of the robot.....	44
Figure 2.14: The behaviour-based architecture designed as the robot controller. Note that the encircle “s” at the output of each behaviour represent that the behaviours above can subsume the behaviours below (Subsumption architecture) .....	44
Figure 3.1: (a) Spadefoot tadpoles (b) Developmental acceleration of the tadpoles in response to the water levels: The triangular-marked line represents the development of the tadpoles in a constant-high-water level environment, while the circular-marked line shows the development of the tadpoles in a daily-decreased-water level environment. The dotted line illustrates the water level of the daily-decreased-water level environment .....	52
Figure 3.2: A simple artificial neuron.....	55
Figure 3.3: A simple neuro-endocrine interaction .....	57
Figure 3.4: A simple neuro-endocrine robot controller .....	58
Figure 3.5: A simple diagram of the adaptive neuro-endocrine system .....	60
Figure 3.6: The main components of the new AES from .....	61

Figure 3.7: A simple diagram of the interactions between the modified AES and NSGasNets .....	62
Figure 3.8: A system diagram showing the interaction between the main components in the artificial homeostatic system .....	63
Figure 3.9: An example of swarm robots aggregated together as a multi-modular robot organism .....	64
Figure 3.10: an example of a simple two-wheel robot implemented with an AHHS1 ..	65
Figure 3.11: The three main factors defining the production of hormones .....	67
Figure 3.12: A comparison between the implementations of rules in AHHS1 and AHHS2 .....	68
Figure 3.13: Some interesting gaits generated by AHHS2 on a 5-module modular robot .....	69
Figure 4.1: Fundamental mechanisms of Hormone Gland .....	74
Figure 4.2: Pseudo-code for the implementations of inhibitory and stimulatory control features .....	76
Figure 4.3: Implementations of negative and positive feedback control features.....	77
Figure 4.4: The structure of Hormone Receptor .....	77
Figure 4.5: The artificial hormone system responsible for the secretion of the Terrain Excitation Hormone and the interaction of the hormone system with the robot controller .....	81
Figure 4.6: Pseudo-code for HG1 .....	83
Figure 4.7: Pseudo-code for HR_MC .....	83
Figure 4.8: The test environment for the experiment of the Terrain Excitation hormone (a) a front view of the arena (b) a bird-eye view of the arena. The grey-rectangular-marking indicates the starting area of the robot.....	84

Figure 4.9: Changes of the hormone concentration ( $C_g$ ) and the hormone stimulation (ActLevel) against the variations of the robot pitch sensory information when $\alpha_g$ and $\beta_g$ are assigned as follow (a) $\alpha_g$ : 1.0 and $\beta_g$ : 0.9 (b) $\alpha_g$ : 0.5 and $\beta_g$ : 0.5 (c) $\alpha_g$ : 0.3 and $\beta_g$ :0.3. Note that data showing in each figure is acquired from a single robot run. ....	88
Figure 4.10: The comparisons between the wheel velocity commands originated from the main robot controller and the actual wheel velocity adjusting by the Terrain Excitation hormone in the test cases when $\alpha_g$ and $\beta_g$ are assigned as follow (a) $\alpha_g$ : 1.0 and $\beta_g$ : 0.9 (b) $\alpha_g$ : 0.5 and $\beta_g$ : 0.5 (c) $\alpha_g$ : 0.3 and $\beta_g$ :0.3 Note that data showing in each figure is acquired from a single robot run. ....	90
Figure 4.11: Examples of the traverse routes taken by the robot when (a) there is no hormone implemented on the robot (b) the Terrain Excitation hormone is applied on the robot .....	92
Figure 4.12: The reference numbers assigned on each step-field .....	93
Figure 4.13: The robot tip over positions when (a) there is no hormone implemented on the robot (b) the Terrain Excitation hormone is applied on the robot.....	93
Figure 5.1: The AHN1 and its connection with the main robot controller .....	99
Figure 5.2: The settings of (a) HG1 (b) HG2 (c) HG3 in the AHN1 .....	102
Figure 5.3: The robot and test arena used for the experiment of the AHN1 .....	104
Figure 5.4: The robot performance in the fault free scenario (a) reporting in Time out, Tip Over and Object Reach metrics (b) displaying in box plots of time spent the robot uses to reach the target object .....	105
Figure 5.5: The robot performance in the pitch fault scenario (a) reporting in Time out, Tip Over and Object Reach metrics (b) displaying in box plots of time spent the robot uses to reach the target object .....	106
Figure 5.6: (a) An example of the hormone interactions in AHN1 from a single robot run when the pitch fault is injected from the beginning of the run (b) The robot wheel velocity corresponding to the hormones shown in (a) .....	109

Figure 5.7: (a) An example of the hormone interactions in AHN1 from a single robot run when the pitch fault is injected after 9 seconds (b) The robot wheel velocity corresponding to the hormones shown in (a).....	110
Figure 5.8: (a) An example of the hormone interactions in AHN1 from a single robot run when the pitch fault is injected after 15 seconds (b) The robot wheel velocity corresponding to the hormones shown in (a).....	111
Figure 5.9: The tip over positions of the robot in the fault free scenario.....	112
Figure 5.10: The tip over positions of the robot in the pitch fault scenario.....	113
Figure 5.11: The Artificial Hormone Network 2 (AHN2).....	118
Figure 5.12: The settings of HG41 and HG42.....	119
Figure 5.13: The settings of HG51 and HG52.....	120
Figure 5.14: The settings of HG53 and HG54.....	121
Figure 5.15: The settings of HG61 and HG62.....	122
Figure 5.16: The AHN2 hormone receptors located on the main robot controller.....	123
Figure 5.17: The settings of HR_FL, HR_FR, HR_RL and HR_RR.....	123
Figure 5.18: The settings up of (a) HR_KINEMATICS_RIGHT (b) HR_KINEMATICS_LEFT.....	125
Figure 5.19: The robot and the test arena employed in Experiment I.....	127
Figure 5.20: The experiment results of the robot operating in the flat terrain environment (a) reporting the robot performance in Time Out, Tip Over and Object Reach metrics (b) showing Time Spent the robot used to reach the target object.....	128
Figure 5.21: The robot traces when the AHN is and is not implemented on the robot in the cases of (a) no wheel fault (b) rear-right wheel fault (c) front-left wheel fault. (d) An example of robot trace in the case of Time Out.....	131

Figure 5.22: (a) the changes of HG41 and HG42 hormone concentrations based on the conflicts between the robot's target and the robot's actual turn velocity (b) the changes of the right side kinematic factor influenced by HG51 and HG52 hormones (c) the variation of the robot's actual right wheel velocities induced by the AHN2 hormones. Note that data in each figure is obtained from a single robot run. ....	134
Figure 5.23: (a) the variations of the HG61 hormone based on hormone concentrations of the HG41 hormone (b) the variations of the HG62 hormone based on hormone concentrations of the HG42 hormone (c) The effects of HG61 and HG62 hormone concentrations on the front-left wheel velocity (d) The effects of HG61 and HG62 hormone concentrations on the front-right wheel velocity. Note that data in each figure is obtained from a single robot run. ....	136
Figure 5.24: The robot and test arena employed in Experiment II .....	137
Figure 5.25: The results of the robot performance in Experiment II (a) reporting in Time Out, Tip Over and Object Reach metrics (b) showing Time Spent the robot used to reach the target object .....	138
Figure 5.26: The maximum displacement (the green circles) and tip over (the blue crosses) positions in the case of no wheel fault (a) with no AHN (b) with the AHN implemented on the robot .....	141
Figure 5.27: The maximum displacement (the green circles) and tip over (the blue crosses) positions in the case of rear-right wheel fault (a) with no AHN (b) with the AHN implemented on the robot.....	142
Figure 5.28: The maximum displacement (the green circles) and tip over (the blue crosses) positions in the case of rear-left wheel fault (a) with no AHN (b) with the AHN implemented on the robot.....	143
Figure 5.29: The maximum displacement (the green circles) and tip over (the blue crosses) positions in the case of front-right wheel fault (a) with no AHN (b) with the AHN implemented on the robot.....	144

Figure 5.30: The maximum displacement (the green circles) and tip over (the blue crosses) positions in the case of front-left wheel fault (a) with no AHN (b) with the AHN implemented on the robot.....	145
Figure 6.1: General form of CGP .....	152
Figure 6.2: An example of CGP genotypes (a) and its representation as a digital combinational circuit (b) .....	154
Figure 6.3: The representation of CGP-AHN .....	155
Figure 6.4: (a) The mechanisms of Hormone Gland (b) The definition of each gene locus in the genotype of computational node.....	159
Figure 6.5: The eight Hormone Receptors represented by the program outputs .....	163
Figure 6.6: (a) The fundamental mechanisms of Hormone Receptor (b) The definition of each gene locus in the program output genotype.....	164
Figure 6.7: (a) An example of CGP-AHN genotype (b) The AHN decoded from the genotype shown in (a).....	167
Figure 6.8: The robot and test arena employed in Experiment I (note that only one target object is presented at a time in the experiment).....	170
Figure 6.9: The target object position in the rear-right wheel fault test case.....	171
Figure 6.10: The target object position in the rear-left wheel fault test case.....	171
Figure 6.11: The fitness function for evaluating CGP-AHN individuals .....	173
Figure 6.12: The measuring of displacement between the centre of the target object and the robot heading test vector .....	175
Figure 6.13: The fitness scores of 40 evolutionary runs in Experiment I.....	178
Figure 6.14: The best and average fitness scores over 500 generations from a single evolutionary run of (a) the Min AHN, (b) the Med AHN and (c) the Max AHN.....	180

Figure 6.15: The performance of the three systems in term of the fitness score obtained from 40 runs on each system.....	183
Figure 6.16: The robot and the test arena employed in Experiment III.....	185
Figure 6.17: The box plots present the fitness scores obtained from 40 runs on each system.....	187
Figure 6.18: The robot routes taken by each system in the case of (a) rear-right wheel fault (b) rear-left wheel fault (c) no wheel fault. Note that each trace colour represents routes taken to reach the target object at each particular position as follow: Black (Position1), Red (Position2), Orange (Position3), Purple (Position4) and Blue (Position5).....	190
Figure 7.1: The generalisation of AHN1 for other applications .....	196
Figure 7.2: The generalisation of AHN2 for other robots.....	199
Figure 7.3: The fundamental mechanisms of Hormone Gland.....	201
Figure 7.4: The fundamental mechanisms of Hormone Receptor .....	202

## **Acknowledgements**

I would like to start by thanking my supervisors, Andy Tyrrell and Gianluca Tempesti, for their support, encouragement, guidance and every other thing you have done for me over my time in York. Without you two, I would not have made it this far. Also, I would like to give a special thank to Martin Trefzer and James Walker for all you help and support on any technical issues.

In addition, I must thank all my friends in York, especially my football mates who help make York a second home for me. Without you guys, my life in York would have been so boring.

Finally, I would like to thank my parents and my other half, Nongnuch, for their unconditional love and support which always help push me through the hard time.

## **Author's declaration**

I declare that this thesis entitled “Artificial Hormone Network for Adaptable Robots” is the result of my own research except as cited in the references. Selected aspects of the research described in this thesis, as well as some earlier work has been documented and published in:

- Pitwut Teerakittikul, Gianluca Tempesti, and Andy M. Tyrrell, "Artificial hormone network for adaptive robot in a dynamic environment", *NASA/ESA Conference on Adaptive Hardware and Systems (AHS)*, pp. 129 – 136, 2012.

# Chapter 1

## Introduction

The first practical real-world robot was arguably employed in 1961 by General Motor, and was named “Unimate” [1]. This is an industrial robot used in an assembly line for welding automobile parts and its main task was to transport hot die casting to pools of cooling liquid [2] as shown in Figure 1.1. The robot obtained its renowned status mainly from its ability to be operated in such dangerous and dull task [3]. Since then, a significant amount of work has been done in developing industrial robots to perform in many other tasks. As a result, robots had been installed and implemented worldwide in various industries, leading by the automotive industry and with the electronics, rubber and plastics, food and beverage, as well as metal and machinery industries not-too-far behind [4, 5]. Industrial robots are widely used mainly because of their speed, accuracy, repeatability, controllability and cost-effectiveness which obviously bring enhanced productivity to many industries. However, their effectiveness can be manifested mostly in factory environments where working conditions are always kept static or very little interference is allowed, and also mostly indoor. This is one of the main reasons why most of the real-world practical robots so far are only used in industry settings [5].

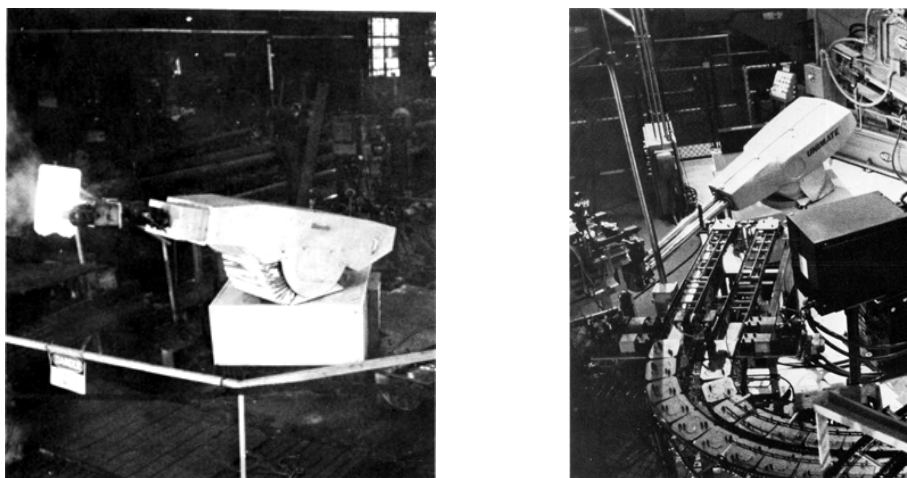


Figure 1.1: The Unimate robot [6, 7]

More recently robots have been brought out of structured environments (as in manufacturing environments) to other dynamic real-world environments such as households, battle-fields, nuclear plants and other planets, where objects in the environments can be changed dynamically and are generally very difficult to predict [5, 8]. However, because of the complex and unpredictable nature of unstructured real-world environments, only simple environments and not-so-critical tasks, such as the household vacuum cleaner, are allowed for robots to work autonomously. With the current robotic technology, fully autonomous operations in unstructured real-world environments remain restricted [5, 9]. This limitation, however, is imposed for good reasons. One of the main issues is the lag of the ability to adapt and survive the dynamic of real-world environments. Consequently, leaving the final decision to autonomous robots performing in any extremely sensitive tasks, for example rescue victims in collapsed building or taking gunfire in battlefields, is still considered too risky.

The research reported in this thesis considers this issue and attempts to provide biologically-inspired mechanisms which can help robots to adapt and work in dynamic real-world environments. Section 1.1 explains the need for adaptability on practical real-world robots while section 1.2 introduces the effects of dynamic real-world environments on the robots. Section 1.3 describes the ability of biological organisms in dealing with chaotic characteristics of the world, and the hypothesis of this research is given in section 1.4. Finally, section 1.5 explains the structure of this thesis.

## **1.1 The Chaos of Real-World Environments**

As stated previously, most of the current practical real-world robots are used in manufacturing plants, where environments are well preserved and variations are kept to a minimum, quite similar to when robots were first used more than 50 years ago. However, there are also robots which are currently being used in other unstructured real-world environments for examples, vacuum cleaning and lawn mowing robots used in household environments (e.g [10, 11]), medical robots employed for assisting surgery and therapy (e.g. [12, 13]), military robots exploited in exploring and reconnaissance applications (e.g. [14]) or space robots used in space exploration programs (e.g. [15]). Nevertheless, it is worth mentioning that most of these robots are not fully autonomous. Human operations in one way or another are always presented somewhere in the robot

control loop. Only some basic and “not-too-risky” tasks are currently affordable to be relied on for full autonomy [9].

Undoubtedly, there remains significant open technological issues which still require research in order to help create autonomous robots which are able to work effectively in unstructured real-world environments [5, 9, 16]. Some of these issues include:

- **Navigation in populated environments**

Research in robot navigation in static or laboratory conditions has been well developed [5, 17]. However, robust navigation in dynamic environments is still less well developed. In unstructured real-world environments, objects generally can be moved or changed position dynamically. Current static two-dimensional mapping and localization alone is not enough for robot navigation in dynamic environments. Therefore, the notion of research in *task-relevant semantic information* of surrounding objects and environments is considered potentially crucial for navigation in populated areas [5].

- **Robust dynamic task and path planning**

Similar to the previous example, robot task and path planning in structured environments is in constant development. However, planning in unstructured environments remains one of the main open problems in robotics [5]. In order to perform reliably in the real-world, the idea of *situation awareness* and *environmental affordances* are among the key features which can be useful in robust dynamic task and path planning. Performing a task such as approaching a victim in a collapsed building requires a robot to be aware of conditions and interactions with objects and environments in its planning processes [5]. For example, to reach the victim, the robot might have to consider which objects it is able to move out of its way without causing additional problems, which routes it can take without making further damage to the building or victims, and which methods it should use to help with first-aid for the victim. Therefore, the key idea here is, in unstructured environments, there are a vast number of constraints which can be differently imposed on robot tasks. When performing task and path planning in the environments, it is important for the robots to consider conditions and interactions with objects and environments existing on each task, in order to perform robustly and reliably [5, 9].

- **Sensing and perception**

This is one of the areas which is the key for improving the research discussed in the previous examples. More robust, higher-resolution and lower-cost sensors are vital for development of many algorithms which are able to help robots deal with constantly changing conditions of the real-world environments [5]. New kinds of sensors which can perform well in hazardous environments and can provide complex perception information (e.g. [18, 19]) is one of the important steps forward. In addition, sensor fusion is also regarded as one of the key areas in helping robot perception in dynamic environments by compensating the limitation of each sensor [9, 20].

- **Safe human robot interactions**

Safety is potentially one of the most significant criteria in determining whether autonomous robots can be used in close counters with human-beings in real-world environments. This issue requires work from the ground up both in terms of mechanical hardware and robot behaviours. Safety mechanisms which inherit *variable compliance* are desirable [5]. This property allows robots to adjust their behaviours based on reaction forces when the robots are in collision with different objects in the environments. In addition, safe robot behaviours which can anticipate serious or dangerous situations, and can avoid any severe physical contact with human-beings are also beneficial [5].

Even though a complete review of the open problems which require further research is beyond this thesis (because it is not entirely relevant and would require too much space), it can be understood, just from these examples, that the chaos in unstructured real-world environments plays a vital role in the requirements of further research. In order for robots to perform successfully in the environments, the capability to deal with dynamic and unpredictable changes of the environments is one of the most crucial issues. Therefore, adaptability is considered as one of the most important properties for pushing autonomous robots closer to the level at which they can be trusted and exploited in unstructured real-world environment applications.

## 1.2 Effects of Environmental changes

Generally, most current robots are designed to perform specific behaviours in certain environments [21], for example industrial welding robots which are designed for accuracy, precision and repeatability in welding car parts. However, for autonomous robots working in dynamic unstructured real-world environments, the ability to cope with uncertainty and to react quickly enough to changing environments is usually one of the most important requirements [5, 9].

Undoubtedly, the world is forever changing. When environmental changes do happen, they can occur in both internal and external systems of the robots. Thus, for robots to survive in such environments, the ability to adapt to both types of environmental variations is crucial. Some common external environmental changes are for examples: working in a crowded environment, robots need to be able to react quickly enough to other moving objects to avoid collision, or working in an extended mission, robots have to cope with performing in different lighting and weather conditions such as fog, rain or sunshine. In addition, one of the most common and obvious external environmental variations is the change of robot working terrain. The terrain is not always flat, instead it comes with significantly different height and roughness. It is also covered with many different types of substances which have various properties and also have different effects on robot motion. However, it is obvious that exploiting a dangerous and dynamic terrain is one of the key tasks expected to be employed by robots, such as in search and rescue in collapsed building and disaster environments [22, 23], exploring in nuclear plants [24] or reconnaissance in battlefields [25].

Considering robots working in different terrain environments, it is worth pointing to one of the most impressive robots reported called “Bigdog” [26] (Figure 1.2). It is a four-legged robot which is designed with the aim to develop a robotic system that can travel on almost any terrain on earth. The robot obtains the ability to travel on different terrain mainly because of its high-power and sophisticated mechanical, sensor and control systems. The robot actuator systems are primarily based on hydraulic systems which are powered by a two-stroke internal combustion engine. Almost 50 sensors are supplied on the robot to monitor robot functions and maintain its impressive locomotion [26]. The robot ability to deal with different terrain conditions is no doubt outstanding. However, as explained, it comes with bulky mechanical and complex hardware and software systems which certainly not every robotic system can afford. More importantly, it might

be unsuitable to some robotic systems for example swarm robotics [27] which is considered to be one of the promising future robotic systems [28, 29].

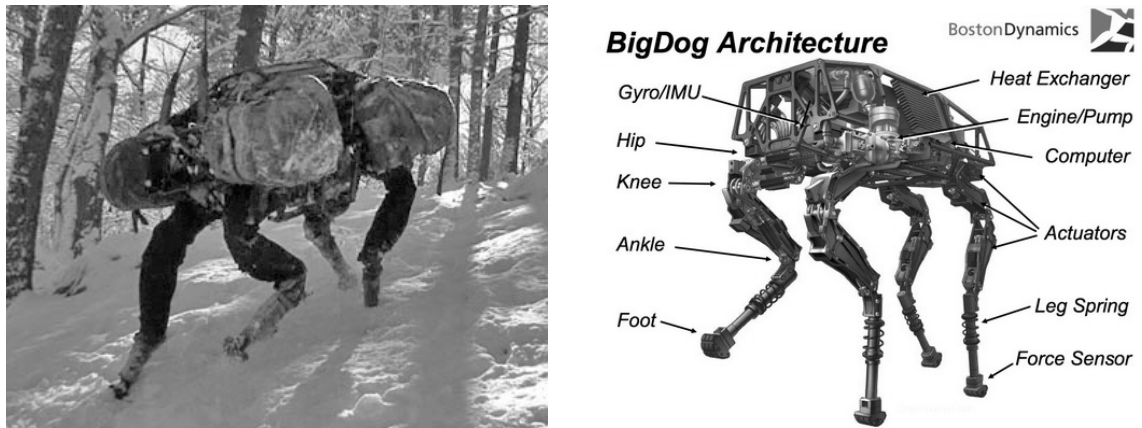


Figure 1.2: The Bigdog robot

Another important issue is that, as mentioned earlier, it is not only external environmental changes which effect robotic systems, but internal environmental changes also play a vital part in making practical real-world robots challenging. Often, robot components fail. For industrial or other robots working under human supervision, this might not cause significant problems. However, when components fail on autonomous robots working in unstructured real-world environments, it may cause catastrophic consequences or even ruin a whole robot mission as shown in the space explorer, Spirit [30].

Nevertheless, looking towards nature, biological organisms show a good deal of capabilities for dealing with the dynamic unpredictability of real-world environments. Certainly, there are a number of related mechanisms and systems functioning together that help biological organisms to thrive and survive in this world. One of the crucial properties which assist biological systems, however, is the ability to adapt to changing environments by exploiting environmental cues [31]. This issue is the main focus of the next section.

## 1.3 Exploiting Environmental Information

Coping with environmental variations is one of the key challenges for the survival of biological organisms [32]. In doing so, most biological organisms need to assess potential opportunities and keep away from danger, in order to increase their chances of survival. Thus, gathering as much environmental information as possible is crucial because this can reduce uncertainty of the real-world environments. However, because of the chaos in real-world environments, truly and completely observable information rarely exists [31]. Therefore, a method which biological organisms employ in order to react and adjust fast enough in order to survive or avoid any potentially dangerous conditions is by exploiting environmental cues [32].

An example of animal adaptation using environmental cues can be shown in a study of infant Rhesus monkeys [33]. It has been observed that the infant monkeys use the direction of human's gaze as an environmental cue for reacting to an approaching human intruder. The study shows that the infant monkeys react differently depending on whether the intruder stares at them or not. When the intruder stares at them, they react by making aggressive barking. On the other hand, if the intruder doesn't make an eye contact with them, they remain in their positions and stay quite. This adaptive behaviour using environmental cues is believed to be one of the key features for survival of biological organisms [33].

Moreover, apart from exploiting environmental cues for adaptation, many animals also use this feature to deal with some complex problems in their everyday lives, such as the navigation capability in vast open oceans shown by green sea-turtles [34]. Many animals are able to use environmental cues such as the sun, the stars, the geomagnetic field and local landmarks as compasses for navigating to specific destinations [35].

Another property which displays the use of environmental information for adaptation in biological organisms is phenotypic plasticity. This is a property which allows a developing organism to be able to gain its attributes in the way which suits the environments in which it develops [36, 37]. One of the examples showing phenotypic plasticity in biological organisms is the study of *Cyclomorphosis*<sup>1</sup> in *Daphnia*<sup>2</sup> [37, 38]. In this study, two individuals of *Daphnia* are separately exposed to different environments. One environment is blended with chemical substances representing the

---

<sup>1</sup> "Cyclic recurrent polymorphism in certain planktonic fauna in response to seasonal temperature or salinity changes"

<sup>2</sup> "one of the several small aquatic crustaceans commonly called water fleas"

existence of predatory fishes, while another is not. The result shows that the two individuals develop different phenotypic characteristics as shown in Figure 1.3. The one on the right, which shows a familiar body shape, is the individual which is developed in a predator-free environment. On the other hand, the individual which is developed in a predatory fish environment (on the left) showed the development of a different body shape. It is believed that the development of the sharp helmet and extended tail helps in protecting it from predators and enhances its chance of survival [37, 38].



Figure 1.3: Two Daphnia. One is developed in a predator induced environment (left). Another is developed in a predator-free environment (right) [39]

The ability of biological organisms for dealing with dynamic and uncertainty of real-world environments by exploiting environmental cues is intriguing. The research reported here is interested in this feature and is intended to create a mechanism which can provide this property to autonomous robots in order to help them perform in unstructured real-world environments. The hypothesis of the research is described in the next section.

## 1.4 Hypothesis

The challenges and issues explained above are the main focus of this research. The ability to cope with dynamic and the unpredictability of unstructured real-world environments is considered to be prominent for practical robot applications. The ability of biological organisms in exploiting environmental cues in order to adapt to the changing world is also inspiring. The hypothesis of this research can be stated as follow:

*“A flexible hormone-inspired architecture is able to exploit environmental cues in order to provide adaptability for autonomous robots to deal with variation effects of both internal and external environmental changes in simulations of unstructured real-world environments”*

In order to verify the accomplishment of this hypothesis, the following statements are used to measure its fulfilment.

1. By exploiting environmental cues, the proposed architecture must show that it can provide adaptability by responding to environmental information which does not directly identify the exact causes, instead the information should only imply potential situations.
2. To be classified as providing adaptability, the architecture must demonstrate that a robot implemented with the architecture can alter its behaviours or control systems in order to deal with environmental changes in the test scenarios. In addition, by dealing with environmental changes, the robot implemented with the architecture must perform better than the robot implemented without the architecture. The conditions which define that a robot does perform better are:
  - A robot must reach the target object more times (measured by the Object Reach metric)
  - If two robots obtain the same number of Object Reach metric, the robot that tips over less times is defined as the better (measured by the Tip Over metric)

Note that, by “more times” and “less times” indicated above, in experiments which results are measured in term of values of the metrics (chapter 5), the

differences of the values should be more than 10% where possible. However, in experiments which results are measured in terms of fitness scores (chapter 6), the results must show statistically differences.

Note also that the performance metrics and the test scenarios will be elucidated further in the next chapter.

3. To represent simulations of unstructured real-world environments, both test arenas and environmental variations applied must reflect at least one of the typical unstructured real-world robotic applications. Moreover, the environmental variations must include both internal and external environmental changes.
4. To be flexible, the proposed architecture must display these two features:
  - The ability to be automatically constructed to provide a specific adaptation using an intelligent design method.
  - The ability to be designed to provide different adaptability and to be applied to different robotic application scenarios using the fundamental mechanisms of the proposed architecture.

## 1.5 Thesis Structure

This thesis is organised as follow:

**Chapter 2** describes the test environments employed throughout this research. These include the robot, the test arenas and the test scenarios used in this research.

**Chapter 3** introduces the hormone system. Both the use of hormones in biological organisms and artificial organisms are illustrated. The research approaches are also elucidated.

**Chapter 4** provides an introduction to the fundamental mechanisms of the Artificial Hormone Network proposed in this research including an example of the hormone system for helping autonomous robots deal with the case of external environmental changes.

**Chapter 5** presents the implementations of two Artificial Hormone Networks on test scenarios concerning both internal and external environmental changes.

**Chapter 6** investigates the use of an evolutionary technique for the automatic construction of Artificial Hormone Networks.

**Chapter 7** discusses the methodologies for extending the Artificial Hormone Network on other robotic application scenarios.

**Chapter 8** provides a summary of the research reported and possible future work.

## **Chapter 2**

### **Test Environments**

As introduced in the previous chapter, autonomous robots working in unstructured real-world environments are the main focus of this research. However, because of the limitations in time and resources, implementing this research in real-world robots and environments is restricted. Therefore, simulations of real-world environments need to be considered instead. Consequently, careful considerations have to be made in every step to assure that simulated environments and test scenarios investigated in this research can be considered as a realistic reflection of unstructured real-world environments and situations as close as possible.

This chapter intends to provide details on the robot and environments implemented in this research in order to imitate unstructured real-world robotic environments. In addition, the environmental changes induced during experiments and the performance metrics used are also explained in this chapter. The chapter is structured as follows: Section 2.1 explains the Robocup Rescue Robot competition, which is used as a reference environment in this research. In section 2.2, the robot simulator used throughout this work, named Gazebo, is introduced. The robot and test environments implemented during the research are described in section 2.3. The tasks performed by the robot and its controller are described in section 2.4. The environmental changes performed and the performance metrics used are elaborated in section 2.5 and 2.6 respectively. Section 2.7 gives a summary of the chapter.

#### **2.1 The Robocup Rescue Robot Competition**

To undertake the research for this thesis any applied test environment must reflect a typical unstructured real-world robot environment. Undoubtedly, real-world robotic applications are huge and there are significant aspects of real-world robot environments which can be contemplated. However, one of the most active application areas is urban search and rescue. Because of the lesson learnt from the Kobe earthquake [40] in 1995,

the need for intelligent robots and robust machines for saving people in dynamic situations such as earthquake disaster have been realized [41]. In order to encourage the awareness on such issues and to bring about collaborations for development of practical urban search and rescue robots, the Robocup Rescue Robot competition [42] was introduced in 2001 and has been held annually ever since [43]. For the competition, in order to replicate the dynamic situations of earthquake disaster, the reference test arenas were developed; examples are shown in Figure 2.1. They are designed by the National Institute of Standards and Technology (NIST) and are based on many stages of real-world collapsed building [43, 44]. Given the well-developed nature of these test arenas, the research reported in this thesis also considers this as the representative environments.



Figure 2.1: Examples of test arenas used in the Robocup Rescue Robot competition [43]



Figure 2.2: An example of simulated victims trapped in the Robocup Rescue Robot test arenas [43]

In order to provide a more detailed insight of the environments, a general overview of the competition is given (based on the competition held in 2008 [45, 46]). Generally, robots entered in this competition are required to search for simulated victims (an example is shown in Figure 2.2) trapped in the test arenas within a specific time limit. Performance metrics are identified in order to evaluate the robots' capabilities. The main investigated capabilities and robot tasks include:

- **Searching for victims and identifying their conditions**

The simulated victims are human-models which are able to show some basic signs of life including heat, motion, sound and emitting carbon dioxide (which simulates breathing). Normally, the competing robots are required to search and approach the victims. In addition, the robots must show their abilities in identifying the victims' status.

- **Mapping of the search areas and locating the victims**

As the robots traverse through the test arenas, the robots must show the ability to create maps of the surrounding areas. Moreover, positions of detected victims must also be identified in the maps.

- **Negotiating different terrain environments and collapsed structures**

The robots display their mobility to negotiate the test arenas by exploring different-difficulty-levels in the test arenas. Generally, the level of terrain difficulty is defined by colour-codes. There are three colour-codes used, which are yellow, orange and red ordered by difficulty. The yellow area, which is the easiest-difficulty-level, is a wall-enclosed maze and 10 degree roll and pitch ramps as shown in Figure 2.3. The orange area, which is the intermediate-difficulty-level, contains 15 degree slopes as well as half-cubic flat, diagonal and hill layout step-fields as shown in Figure 2.4. Note that step-fields are obstacles designed to represent rubble. They are made of wooden blocks packed together. Each wooden block has a based size of 10cm x 10cm but a difference in height. For half-cubic step-fields, their heights vary from 2.5cm to 20cm. Finally, the red area, which is the highest-difficulty-level, includes mainly full-cubic flat, diagonal and hill step-fields as shown in Figure 2.5. The main difference between half-cubic and full-cubic step-fields is the height of wooden blocks. For the full-cubic step-fields, the height of wooden blocks is generally higher. They vary from 5cm to 40cm.

These are the three basic capabilities which the robots competing in the competition are required to exhibit. Undoubtedly, these capabilities are also demanded and are necessary for practical real-world robots working in urban search and rescue scenarios.

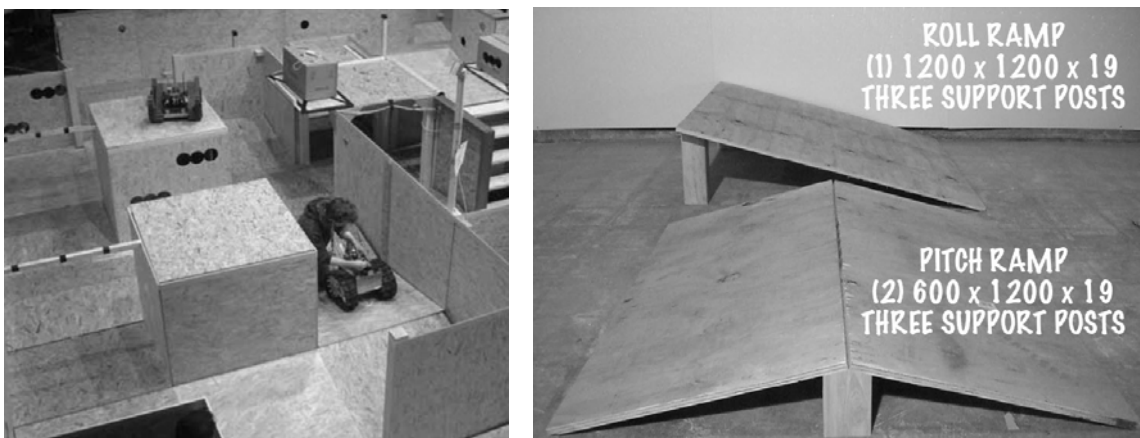


Figure 2.3: Examples of maze, roll ramps and pitch ramps used in the yellow-area of the Robocup Rescue Robot competition

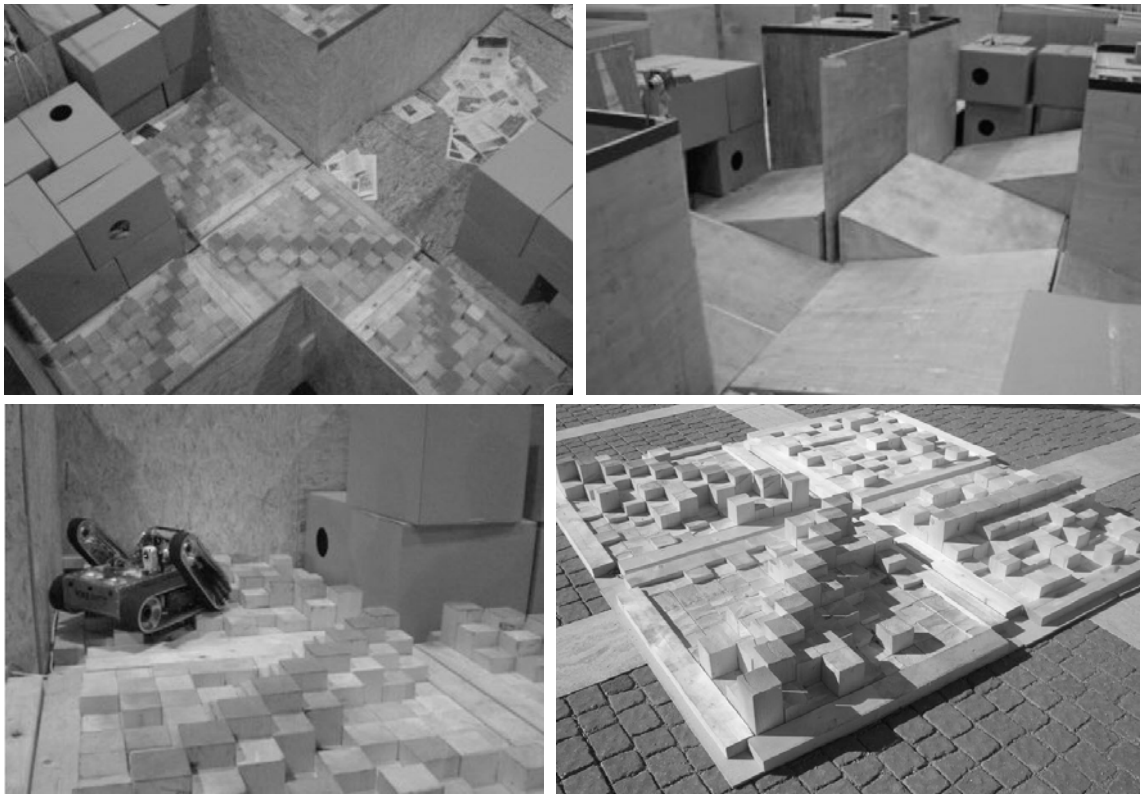


Figure 2.4: Examples of ramps and half-cubic step-fields used in the orange-area of the Robocup Rescue Robot competition

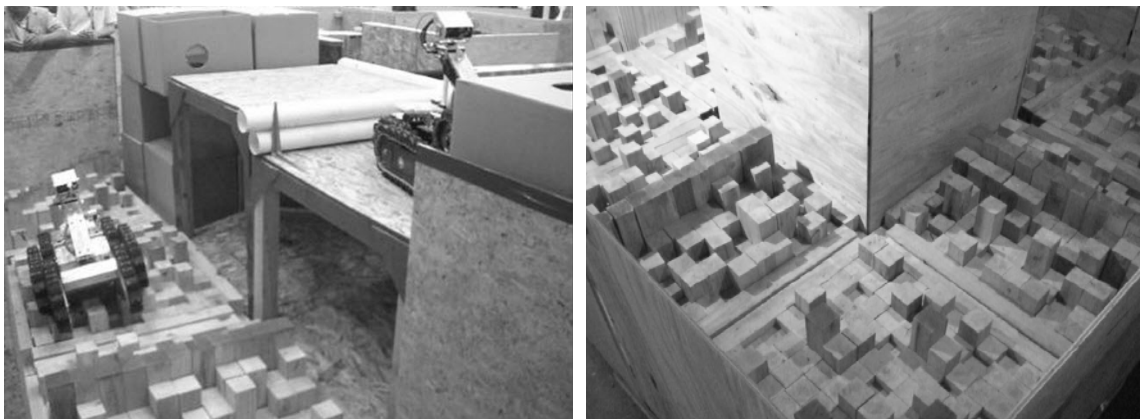


Figure 2.5: Examples of environments and full-cubic step-fields used in the red-area of the Robocup Rescue Robot competition

## 2.2 Gazebo: the 3D robot simulator

Focusing on real-world robotic applications, implementations on physical robots and environments are certainly logical. However, as stated previously, some limitations imposed on this research restrict these implementations. As a result, a robot simulation needed to be considered. The main constraint on the robot simulator was that it should be able to mimic real-world environments (as illustrated in section 2.1) as close as possible. Therefore, simulators, which are able to visualize three-dimensional objects and more importantly are able to simulate the dynamic interactions between objects and environments, are essential requirements. After research on the available robot simulators, the open-source 3D robot simulator named Gazebo [47, 48] is considered the most suitable platform for this research.



Figure 2.6: An example of Gazebo environments

Gazebo is a physically-realistic 3D robot simulator developed under the Player project [49, 50]. An example of robot environments created in Gazebo is illustrated in Figure 2.6. Generally, Gazebo is able to visualize 3D objects and environments, as well as to simulate the physical effects of interactions between the objects and environments using

the open-source 3D graphics engine called OGRE [51] and the open-source physics engine called the Open Dynamics Engine (ODE) [52]. This makes Gazebo suitable for simulating robots working in real-world environments because realistic sensor feedback and interactions between robots and environments can be included in the simulation. Usually, every simulated object has the kinematic and dynamic properties of rigid-body. This means every object in Gazebo has mass, size, velocity, density, friction and other related properties [48]. Therefore, most realistic situations can be simulated, for example, when a simulated robot hits another simulated object or robot; the outcome of the collision depends on the parameters relating to rigid-body kinematics and dynamics. The colliding robots or objects might bounce off each other, or one robot might climb on another. This is unlike other physically-unrealistic simulations in which the robots or objects would just stop when the collision happens.

Although Gazebo is able to display many aspects of real-world environments, it also has some limitations, for example:

- Terrain simulated within Gazebo can only be rigid. This means that the physically-realistic simulation of grass, soil, sand or any other flexible terrain remains infeasible [47].
- Every object created can only be a rigid-body object. Deformable objects are impossible [47].
- The simulation of fluid and thermal dynamics is not available [47].
- Although some static and dynamic parameters of simulated objects are able to be modified during simulation, some parameters, such as mass or size, have to be set before the simulation starts. They cannot be changed while the simulation is running.

Gazebo 0.9 was considered to be the most stable platform at the start of the simulation experiments of this research and thus, this version is used in every experiment reported in this thesis and every capability and limitation explained is also based on this version of the simulator.

## 2.3 The Simulated Robot and Test Environments

When utilizing the robot simulator, another consideration that is required is which robot(s) can be used and simulated in the simulator and also are relevant for the research. Arguably, any robots can be constructed and simulated in Gazebo. However, considering the rather not-well-documented manuals and tutorials of Gazebo, it was decided that using one of the well-developed and ready-made robots (which is also able to perform the desired tasks) in the simulator was considered desirable. As a consequence, the Pioneer2-AT [53], shown in Figure 2.7, qualified to be used in this research.

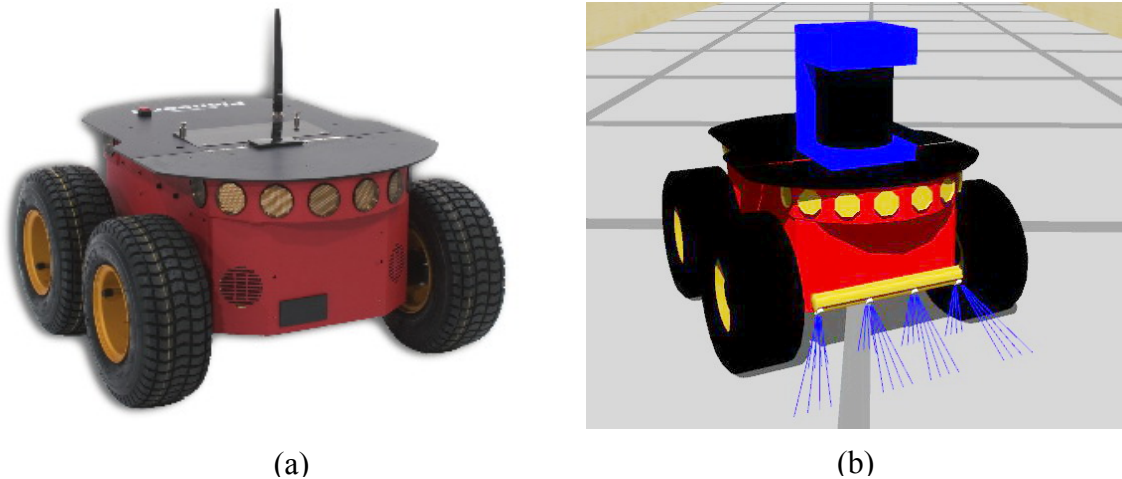


Figure 2.7: (a) The actual Pioneer 2-AT robot (b) The Pioneer 2-AT robot simulated in Gazebo

Regarding the test environments, as described in section 2.1, the reference test arenas of the Robocup Rescue Robot competitions were regarded as the test environments in this research. Nevertheless, as can be noticed, the competition test environments are designed to evaluate many aspects and features of search and rescue robots in collapsed building. Considering every aspect and feature presented in the Robocup Rescue Robot competition was considered unrealistic (nor required) for this research. Therefore, only some logical and implementable characteristics need to be selected. Consequently, the ability to traverse and negotiate unstructured terrain was chosen. One of the main reasons was because this feature is not only deemed as a key characteristic for the

robots competing in the competition but is also regarded as a fundamental capability for robots working in other unstructured real-world robotic applications.

As briefly explained in section 2.1, the terrain of test arenas in the Robocup Rescue Robot competition is built from different obstacles. Among them, the most challenging obstacles are the step-fields used in the orange and red areas. However, because of the size and performances of the Pioneer 2-AT robot used, only half-cubic step-fields (as shown in Figure 2.8) are considered in the test environments of this research.

An example of the test environments created in Gazebo is illustrated in Figure 2.9. The test arena is a wall-enclosed rectangular area. Generally, there are 12 half-cubic step-fields arranged and irregularly oriented in a format of 3 by 4. Six of them are flat layout, whereas the remaining six step-fields are composed of three diagonal and three hill layout step-fields. To provide an insight on the characteristic of the step-fields, more details of the three layout step-fields are displayed in Figure 2.10, Figure 2.11 and Figure 2.12 respectively.

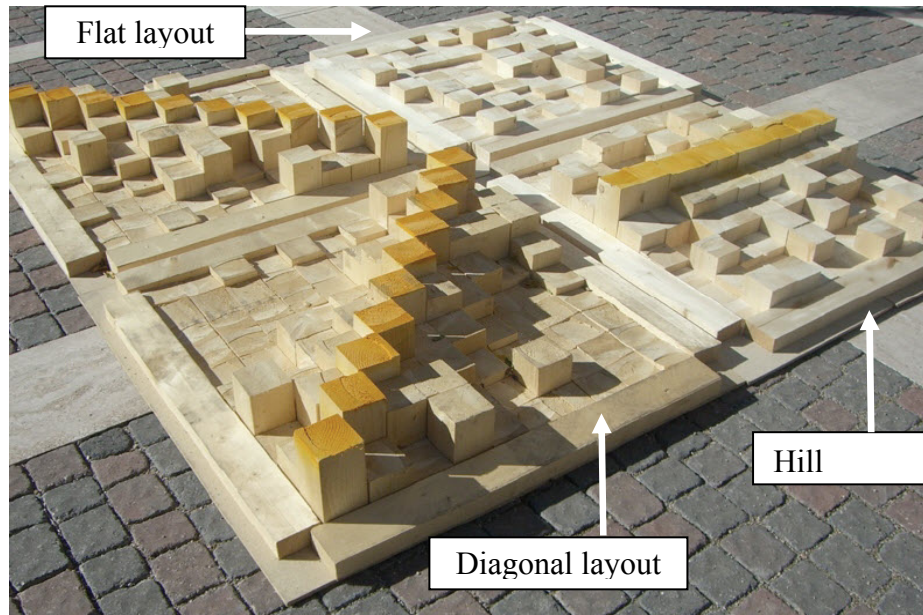


Figure 2.8: A picture of all three half-cubic step-fields used in the Robocup Rescue Robot competition including flat, diagonal and hill layout step-fields

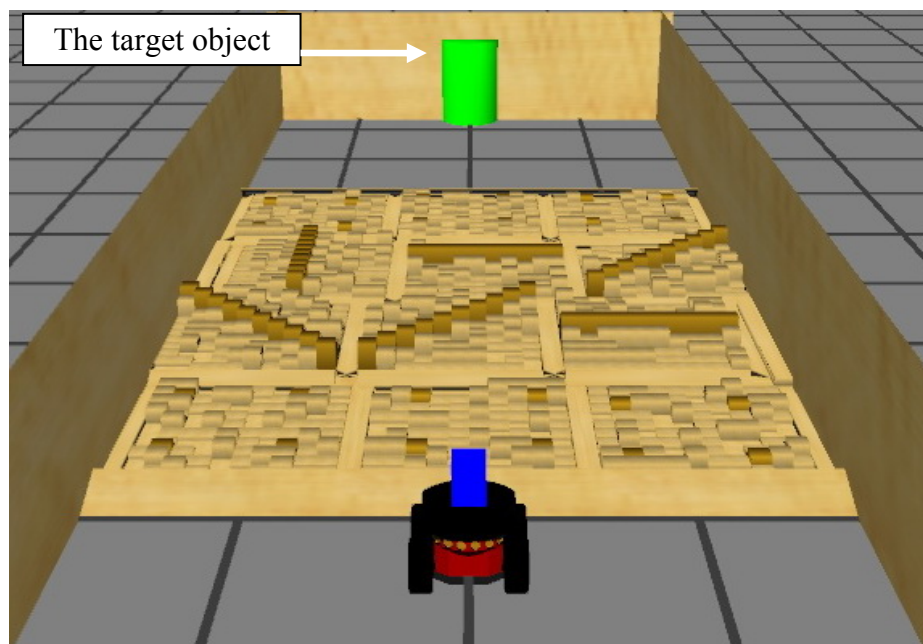
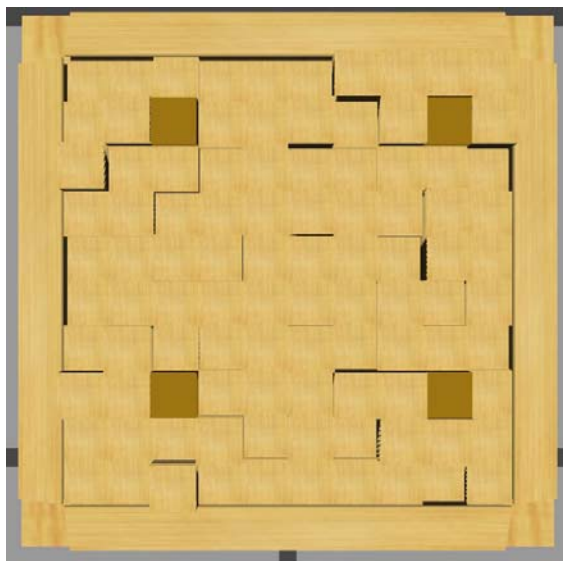


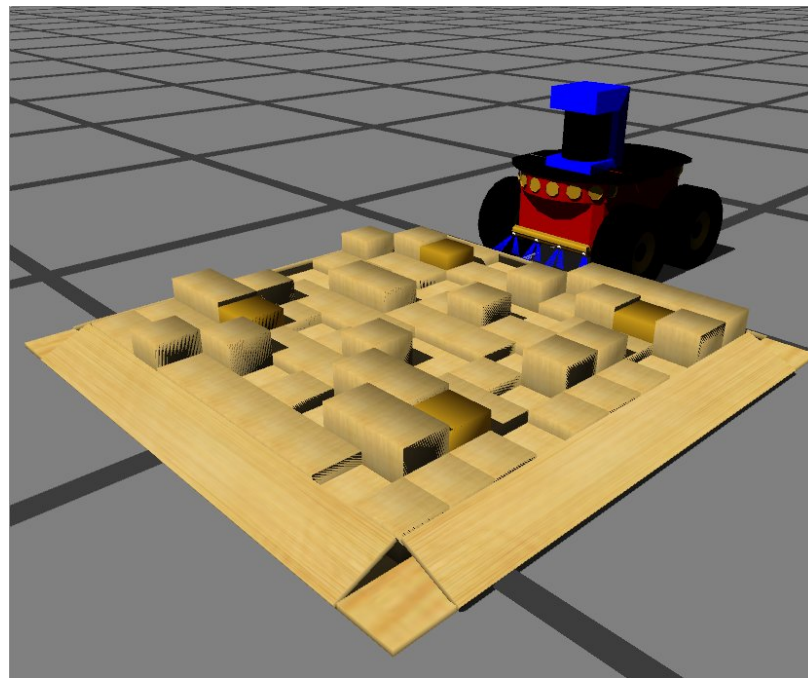
Figure 2.9: An example of the test environments created in Gazebo



(a)

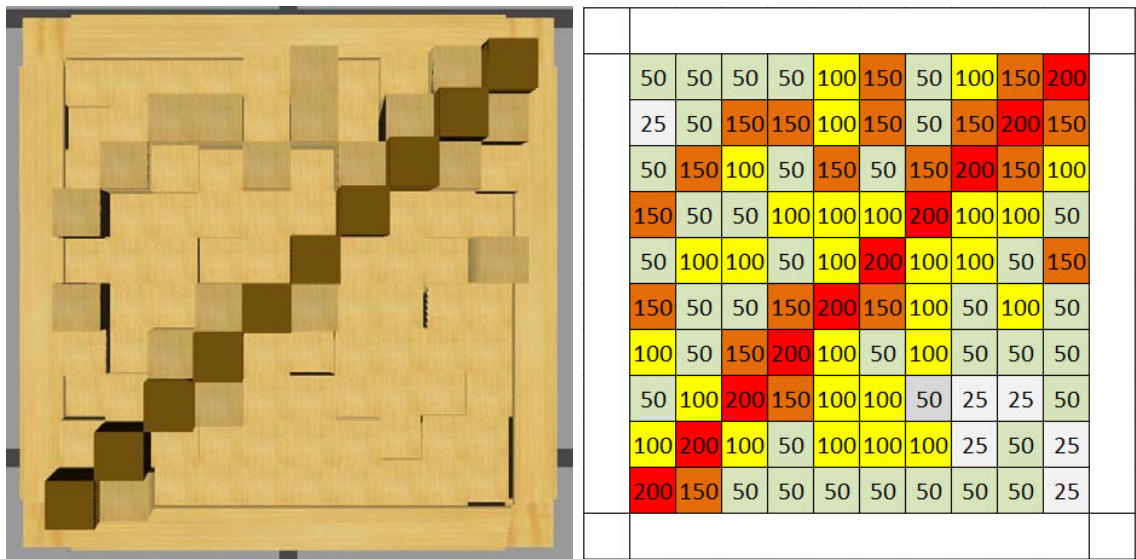
25	25	50	25	25	25	100	100	100	100
50	100	90	50	50	100	50	100	90	100
100	50	50	25	50	25	25	50	50	25
50	50	25	25	50	100	50	50	100	50
25	25	100	100	50	50	50	25	100	50
25	50	50	50	50	25	25	50	25	50
50	100	50	25	50	100	25	50	50	25
100	100	90	50	50	50	100	100	90	50
50	50	50	100	25	50	25	100	100	50
50	50	100	50	50	50	50	50	25	50

(b)



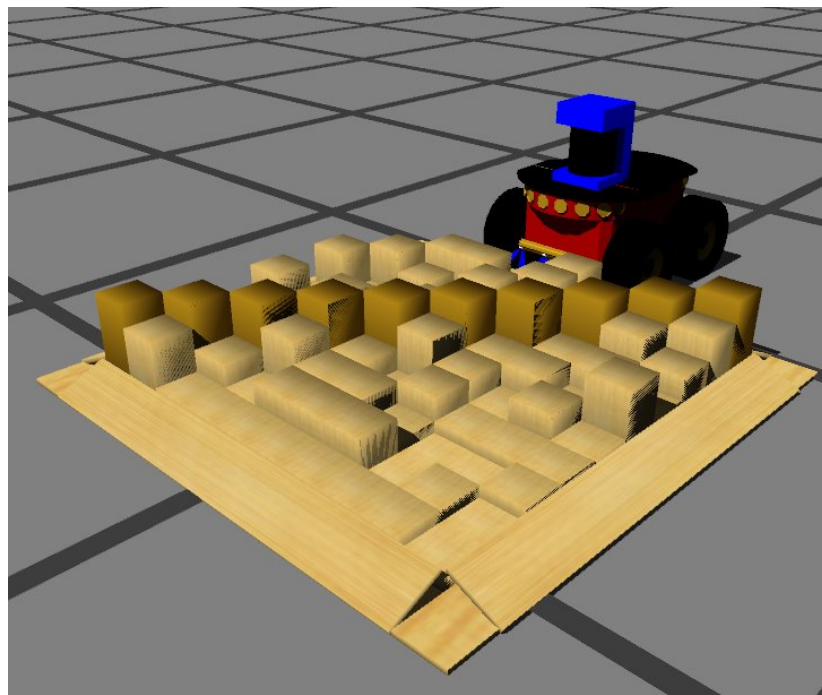
(c)

Figure 2.10: (a) A top view of the half-cubic flat layout step-field simulated in Gazebo (b) Colour and number codes of wooden blocks constructed to create the half-cubic flat layout step-field. The numbers represent the height of each block in millimetre. (c) A picture of the half-cubic flat layout step-field comparing with the simulated Pioneer 2-AT robot



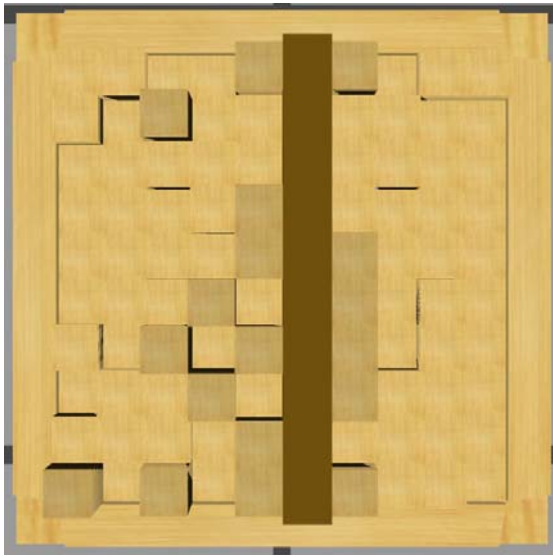
(a)

(b)



(c)

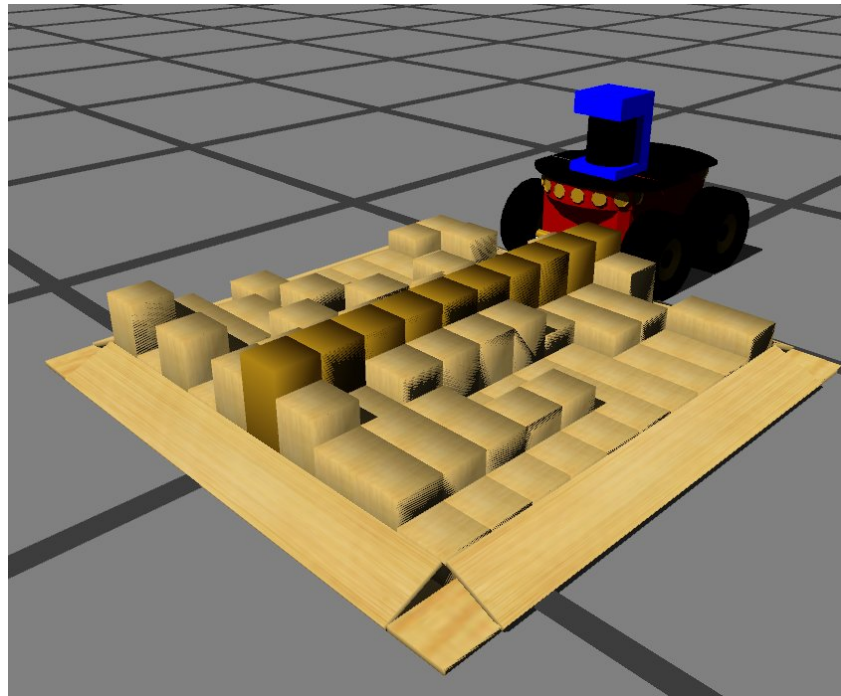
Figure 2.11: (a) A top view of the half-cubic diagonal layout step-field simulated in Gazebo (b) Colour and number codes of wooden blocks constructed to create the half-cubic diagonal layout step-field. The numbers represent the height of each block in millimetre (c) A picture of the half-cubic diagonal layout step-field comparing with the simulated Pioneer 2-AT robot



(a)

100	100	50	50	150	200	150	50	150	100	
100	50	150	50	100	200	100	100	50	50	
50	50	100	100	100	200	150	150	150	50	
50	50	50	100	150	200	100	50	50	50	
25	50	50	50	150	200	150	50	25	50	
50	25	100	25	100	200	150	50	100	50	
25	50	100	50	150	200	150	50	100	50	
50	25	100	25	100	200	150	100	100	50	
100	100	100	50	150	200	100	100	100	50	
150	50	150	50	150	200	150	100	100	50	

(b)



(c)

Figure 2.12: (a) A top view of the half-cubic hill layout step-field simulated in Gazebo (b) Colour and number codes of wooden blocks constructed to create the half-cubic hill layout step-field. The numbers represent the height of each block in millimetre. (c) A picture of the half-cubic hill layout step-field comparing with the simulated Pioneer 2-AT robot

## **2.4 The robot tasks and robot controller**

In the previous section, the simulated robot and test environments are elucidated. This section is dedicated to explaining the tasks that the robot is assigned to perform in the test environments and also its controller which is designed to perform the assigned tasks.

### **2.4.1 The main robot tasks**

As introduced, the main tasks for robots competing in the Robocup Rescue Robot competition are to search for victims and to negotiate unstructured terrain in the test arenas. Similarly, in this research, the main robot tasks are to search and approach a green cylinder object normally located at the end of the test arenas, as also shown in Figure 2.9. For the robot to perform the tasks in the test environments, it requires the ability to detect and approach the target object, and also the ability to deal with rough terrain filling the area between the target object and the robot's starting positions. The next sub-section is devoted to describing the sensors and controller implemented on the robot in order to help the robot to perform its tasks.

### **2.4.2 The robot controller**

As stated previously, the robot utilized in this research is the four-wheel-differential drive robot, Pioneer 2-AT. In order to perform its tasks, the robot is generally equipped with five different sensors including a scanning laser range sensor, a Global Positioning System (GPS), an Inertia Measurement Unit (IMU), a colour detection camera and a frontal area distance infrared sensor. The frontal area distance sensor is actually composed of eight infrared sensors which are mainly used to measure the distance between the robot and an area in front of the robot. This information gives the robot an idea of frontal terrain level. Four of these sensors are pointed straight down towards the floor in front of the robot and the other four sensors point forward at a 45 degree angle with respect to the first four sensors, as shown in Figure 2.13.

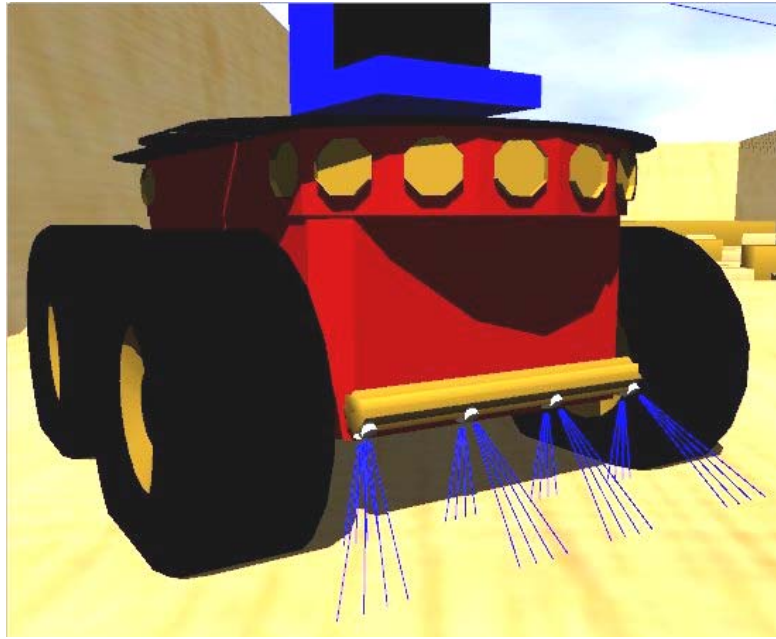


Figure 2.13: The frontal area distance infrared sensor located in front of the robot

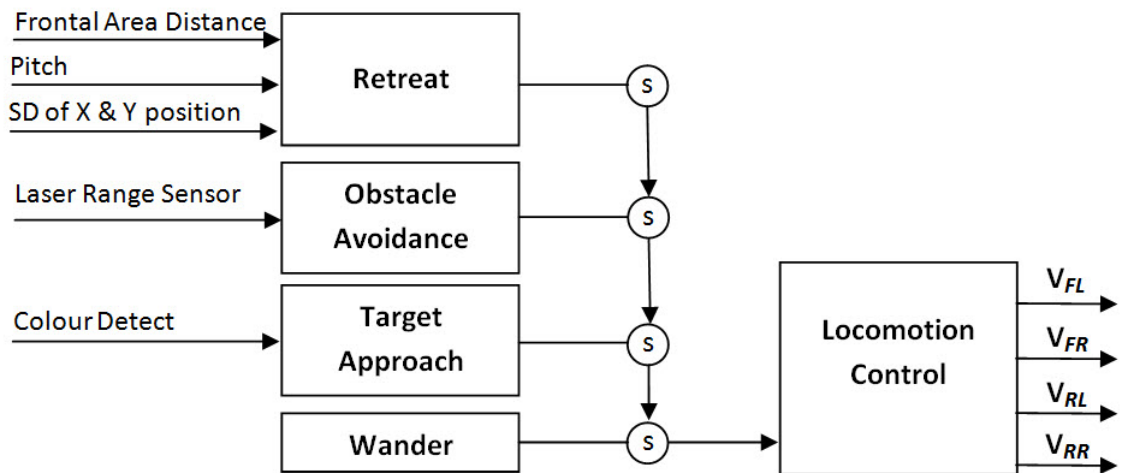


Figure 2.14: The behaviour-based architecture designed as the robot controller. Note that the encircle “s” at the output of each behaviour represent that the behaviours above can subsume the behaviours below (Subsumption architecture)

For the robot to perform the tasks, a behaviour-based controller using a subsumption architecture [54] was designed and implemented on the robot as shown in Figure 2.14. There are four main behaviours designed on the controller:

- **Wander**

This behaviour is at the lowest layer and basically causes the robot to move around in the arena. When this behaviour is activated, the robot first makes a turn for a random time step in a random direction. After that the robot then moves forward for another random time step.

- **Target Approach**

When the target object is detected by the colour detection camera, it activates Target Approach. This behaviour basically causes the robot to move toward the target object and to keep it in the centre of view.

- **Obstacle Avoidance**

This is a typical obstacle avoidance behaviour which helps the robot to move away from any obstacles which are closer to the robot than a set threshold. The distances between the robot and surrounding objects are measured using the scanning laser range sensor.

- **Retreat**

This is a crucial behaviour which helps the robot deal with rough terrain. Generally, this behaviour encourages the robot to retreat from critical terrain, by forcing the robot to move backward and then make a random turn.

There are three conditions that can activate this behaviour.

- 1) The robot is stuck. This condition is represented by a low standard deviation (SD) of the value of the robot's X and Y coordinates over a specified period of time.
- 2) The robot pitch orientation reaches a critical angle. This helps the robot from tipping over when negotiating a too steep terrain.
- 3) An area in front of the robot is too steep. This is represented by the distance reported from the frontal area distance infrared sensor.

Generally, the critical pitch angle and the threshold for the frontal area distance vary depending on the speed of the robot. The faster the robot moves, the lower the angle and the distance are.

It has to be noted that all behaviours generate the same output types, which are forward speed, forward direction, turn speed and turn direction of the robot. These outputs are

then fed through the Locomotion Control unit which is used to transform locomotion commands to velocity of robot's wheels (which are front-left velocity ( $V_{FL}$ ), front-right velocity ( $V_{FR}$ ), rear-left velocity ( $V_{RL}$ ) and rear-right velocity ( $V_{RR}$ )). The Locomotion Control unit basically contains a kinematic model of a four-wheel-differential drive system.

With this behaviour-based controller, normally the robot can search and approach the target object, as well as avoid the walls surrounding the test area. More importantly, the robot is also able to deal with the rough terrain by retreating from any critical area which can potentially cause the robot to tip over or get stuck. These robot capabilities are demonstrated and reported further in chapters 4 and 5.

## 2.5 The Performance Metrics

In order to investigate the robot performance, four main metrics are assigned for evaluating the robot performance when performing the assigned tasks. These metrics include:

- **Time Out**

This metric measures the number of times that the robot is unable to reach the target object but has not tipped over, when a set time limit has been exceeded.

- **Tip Over**

This metric shows the number of times that the robot has tipped over before reaching the target object.

- **Object Reach**

This metric displays the number of times that the robot reaches the target object before a set time limit has passed.

- **Time Spent**

This index reports time spent by the robot in cases when the robot is able to reach the target object.

These four indices are used, throughout experiments reported in chapters 4 and 5, to verify the robot capabilities in performing the assigned tasks. In addition, as mentioned

in the hypothesis section in chapter 1, *Tip Over* and *Object Reach* are used as the main metrics for investigating the robot performance. Generally, a better robot performance is identified by a higher value of *Object Reach* and a lower value of *Tip Over*.

## 2.6 The Considered environmental changes

As introduced in chapter one, for autonomous robots operating in unstructured real-world environments, dealing with both internal and external environmental changes is vital. In addition, the research reported in this thesis is also intended to provide a mechanism which can help autonomous robots cope with both types of environmental variations. Therefore, in order to evaluate the robot performance, both types of environmental variations need to be investigated. Nevertheless, it is obvious that there are a significant amount of environmental changes which can occur and can affect autonomous robots operating in unstructured real-world environments. Thus, in simulating such complex real-world environments, careful consideration was required in selecting both the internal and external environmental changes examined in this research.

There are some criteria set for determining the considered environmental changes. In general, the changes need to be common and are considered generally to happen in search and rescue robotic application and potentially in any other unstructured real-world robotic application. In addition, the considered changes must effect the performance of the simulated robot used (Pioneer 2-AT) in performing its dedicated tasks. Finally, the environmental changes must be able to be implemented in Gazebo. From these criteria, three principal environmental changes are selected including one external environmental change and two internal environmental changes. Even though more details of these environmental changes are discussed in chapters 4 and 5, the information below serves as an introduction to the considered environmental variations.

For the external environmental change, as mentioned previously, dealing with different terrain roughness is one of the most challenging issues for autonomous robots working in unstructured real-world environments. This challenge is considered not only in the Robocup Rescue Robot competition (which is the main referenced environment in this research) but also in many other unstructured real-world robot applications. Therefore,

different terrain roughness generated by the step-fields explained in section 2.3 was decided as the main external environmental change in this research.

Regarding the internal environmental changes, faults occurring in sensor and actuator units of the robot were chosen. In the case of sensor faults, a broken pitch sensory channel on the IMU sensor is selected. In general, this causes the sensor to report a constant value of zero and causes the robot to be unaware of its actual pitch angle. As the robot is set to traverse on unstructured terrain, this issue should affect the robot performance significantly. In the case of faults in the actuator unit, for wheeled-robots a fault occurring in one or more wheels appeared appropriate, especially on robots negotiating difficult terrain e.g. [30]. Therefore, the actuator fault considered in this research is the case when a robot wheel is broken. This issue causes one of the robot's wheels to be unresponsive to any commands from the robot controller. However, the wheel is still able to be turned freely when external forces are applied. Note that although both cases of internal environmental changes are in the form of robot components' faults, the proposed architecture in this research does not intend to perform as a fault recovery system. Instead, the proposed architecture focuses on maintaining homeostasis and providing adaptability for autonomous robots in the presences of both internal and external environmental changes. It is only because some cases of robot components' faults could be considered as internal environmental changes. This issue is discussed and illustrated further in chapter 5.

These are all three main environmental changes considered in this research. Nevertheless, as stated, more details of the effects from these environmental changes on the robot performance are further investigated and reported in chapter 4 and 5.

## **2.7 Summary**

This chapter provided detailed information about the simulated environments utilized and implemented in this research. Examining real-world robotic issues using a robot simulator requires careful consideration in every step in order to be certain that the simulated environments and situations are a close reflection of unstructured real-world environments and importantly correspond with the hypothesis.

In this chapter, Gazebo, the 3D physically-realistic robot simulator is introduced. Because of its main ability to simulate physical effects of interactions between rigid-

body objects and environments, the simulator is utilized in this research as a tool to create each test object and environment. In addition, some of the main issues of the test environments were also elaborated in this chapter including the robot's tasks, the test scenarios, the environmental changes and the metrics which are used to evaluate the robot performance.

Regarding the simulated test environments and test scenarios concerned in this research, the chapter described how these are inspired by one of the most well-established robot competitions, the Robocup Rescue Robot. As explained, the test environments of the competition are designed based on real-world collapsed buildings and the test scenarios also represented the actual requirements of urban search and rescue robot scenarios.

Dealing with both internal and external environmental changes is one of the main intentions of the research reported in this thesis. Both types of these environmental variations, which include different terrain roughness as well as pitch sensory information and robot wheel-motor faults, were also introduced in this chapter. Finally, the metrics identified for investigation of the robot and for evaluating the hypothesis were also introduced in this chapter. The robot performance investigated by these metrics is reported in chapters 4 and 5.

In the next chapter, a biologically-inspired mechanism proposed in this research is introduced. In addition, a review of its related work is also given.

## Chapter 3

### The Hormone System

As introduced in chapter one, real-world environments are dynamic and full of interventions. To survive in such environments, the ability to adapt to these changing environments, both internal and external, is crucial. In biological organisms, there are a number of mechanisms and systems functioning in a symbiotic manner in order to help living organisms cope with different situations and challenges from the unstructured world. For autonomous robots expected to work in such environments, even though the robots might not need every function and characteristic available in biological organisms (indeed they might not even be appropriate), adaptability remains one of the most essential features required to deal with the uncertainty in the real-world and to increase their chances of achieving assigned tasks [21, 55].

Exploitation of environmental information, such as changes in daylight length or temperature, as a cue for adaptation, is shown in biological organisms. This ability is considered to be one of the key features for coping with the dynamics of real-world environments [56]. In addition, one of the principle mechanisms used in biological organisms, which responds to environmental cues and provides adaptability for biological organisms, is the hormone system [56, 57]. This system is a main inspiration of the research reported in this thesis. As a consequence, the hormone system is considered in this research as a modelled mechanism to provide the ability to cope with both internal and external environmental changes for autonomous robots working in simulated unstructured real-world environments.

In section 3.1, some examples of adaptation shown in biological organisms using hormones are provided. Section 3.2 gives an introduction to two other systems strongly related to hormones, which are the endocrine and homeostatic systems, while the review of the artificial counterparts of these systems are illustrated in section 3.3, with the discussion of the two systems given in section 3.4. The research approach is identified in section 3.5 and the summary of this chapter is given in section 3.6.

### **3.1 Utilization of Hormones for Adaptation in Biological Organisms**

In general, there are a number of basic functions in biological organisms, such as respiration, circulation and digestion, which help keeping them alive and functioning in the world [58]. However, one of the main features which assists them to survive and cope with the dynamics and uncertainty of the world is adaptation. As the world is forever changing, biological organisms are usually exposed to a wide range of environmental conditions such as the changing of temperature, the changing of climate in different regions, the availability of food sources or even the changes in morphology of the organisms. Biological organisms might not be able to survive in the world without adaptation [59].

Not only do different groups of biological organisms have different methods of adaptation, but each type of biological organism also uses a number of different mechanisms to cope with environmental variations [60]. Nevertheless, one key source of adaptation used in many biological organisms is the utilization of hormones which respond to environmental cues [61, 62]. In general, hormones are exploited in a number of functions of an organism such as the regulation of growth, homeostasis or breeding. However, one of the underlying features of hormones is for regulating morphological, physiological and behavioural changes when facing environmental variations [60].

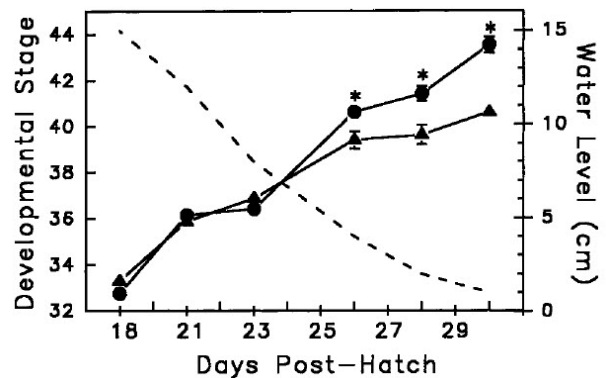
The utilization of hormones is shown in both plants and animals. Unlike animals, plants cannot simply walk away from unpleasant environments. Therefore, plant hormones generally play a very significant role in helping plants to survive in a vast variety of conditions that they might grow in. A good example is the use of the hormone *Auxin* which helps bend growing stems toward sources of light. Because light is so important for the growth and development of plants, this function helps ensure that plants can gain this valuable resource as efficiently as possible under their various growing conditions. This, in turn, helps increasing their chances of survival in varying environments [63].

There are also some good examples of the utilization of hormones for adaptation shown in animals, such as the decreasing of thyroid hormone level displayed in mammals adapting to warmer climates [64]. It is found that, for some agricultural animals, living in hot environments can cause heat stress, which is a condition in which the core body temperature is higher than a threshold for doing normal activities. Generally, these animals respond automatically by reducing food consumption and increasing water

intake. However, another important hormonal response is the reduction in the secretion of the thyroid hormone, which helps decrease internal heat production for these animals. This feature is found fundamental for mammals adapting to live in hot climates [65]. Another example of the adaptation to ensure the survival in changing environments using hormones is illustrated in some species of tadpoles. In the research reported in [66, 67], it is found that the growth and developmental rates in which spadefoot tadpoles transform into an adult state is dependent on the water availability, as shown in Figure 3.1. The studies indicate that the secretion of hormones related to the metamorphosis of the tadpoles can be varied based on the water levels in which the tadpoles are developing. Generally, the decrease of the water level can accelerate the secretion of the hormones, which in turn increases the rate in which the tadpoles develop to adults [68]. Hence with this hormone behaviour the survivability of the tadpoles before water runs out is increased.



(a)



(b)

Figure 3.1: (a) Spadefoot tadpoles (b) Developmental acceleration of the tadpoles in response to the water levels: The triangular-marked line represents the development of the tadpoles in a constant-high-water level environment, while the circular-marked line shows the development of the tadpoles in a daily-decreased-water level environment.

The dotted line illustrates the water level of the daily-decreased-water level environment [66]

There remain a number of other adaptations shown in biological organisms that exploit hormones in response to environmental cues. However, this section describes some examples in order to illustrate the roles and potential utilizations of the implementation of these mechanisms to provide adaptation for autonomous robots working in dynamic

real-world environments. In the next section, two other key hormone-related systems are introduced.

### **3.2 Endocrine System and Homeostasis**

Hormones are chemical substances in a regulatory class [69, 70]. Usually, there are a significant number of hormones generated by different special cells and each of these is produced for a different purpose [69]. However, in general, hormones act as signals released through a body. Upon reaching their target cells, hormones can then influence these cells. Hormones and their target cells can match each other using receptors. Usually, associated receptors of each hormone are located in or on their target cells in order for the target cells to detect the hormones and then allows specific responses on the target cells to be initiated [61].

The endocrine system is one of the principle systems which takes the main responsibility in the production and secretion of hormones. Generally, the endocrine system can be considered as a system of glands which secretes hormones to act on target cells that have receptors corresponding to the hormones. When hormones reach their target cells, the cells react by producing the appropriate responses [71].

Homeostasis is a phenomenon which is considered as one of the key features in the regulation process of internal states when faced with environmental changes in biological organisms. It is understood that this feature emerges from the interaction between the endocrine, the nervous and immune systems [72].

In order to recap on the relations between them (i.e. hormones, endocrine system and homeostasis) and to elucidate their roles in helping biological organisms to adapt and survive in constantly changing environments, generally there is a crucial phenomenon, known as homeostasis. This is a quality of organisms which controls their internal states, either by internal regulation processes or through interactions with environments, in order to cope with environmental variations [73]. It is understood that homeostasis is mainly influenced by complex interactions between the nervous, the endocrine and the immune systems. However, the endocrine system is considered as a major mechanism responsible for the internal state stabilizations of an organism [70, 74]. The endocrine system achieves the regulation of the internal states mainly by the production and secretion of hormones in response to environmental changes. The secretion of

hormones, when reaching their target cells, then causes the cells to perform appropriate responses, which in turn originates morphological, physiological or behavioural changes in the organisms [60, 69].

These biological phenomena have been used as a source of inspiration for much research in artificial systems. The review of this research is illustrated in the next section.

### **3.3 The Artificial Endocrine and Artificial Homeostatic Systems**

Because of the various usages of hormones and their relations with other systems in biological organisms, there are a number of examples which propose hormone-inspired or hormone-like mechanisms for different purposes in artificial systems. For example, in [75, 76], the authors suggest an adaptive communication for multi-modular self-reconfigurable robots. In this work, a hormone-inspired communication protocol is employed as a method for sending messages through each robot module in order to help set up appropriate actions on each module of the robot. Another example of a communication system inspired by the hormone system is shown in the work reported in [77, 78, 79]. This work takes its inspiration from endocrinology to create a communication system which helps provide fault-tolerance for multi-cellular electronic systems. In addition, research reported in [80, 81] proposes a task-distribution control system for a group of robots. The control system employs a hormone-inspired mechanism to help switching tasks between robots in a group based on their performances.

Nevertheless, the main interest of this review is on research which uses hormone-inspired systems to regulate internal states or to adjust system dynamics of artificial systems, especially autonomous robots, which is more related to the research reported in this thesis. Considered in this group of research, there are two mainstream architectures which have been investigating the “Neuro-Endocrine System” and “Artificial Homeostatic Hormone System”. For both architectures, although their general concepts are quite similar in that artificial hormones are employed mainly for adjusting systems’ behaviour, the implementations of each are rather different. In general, the neuro-endocrine system employs Artificial Neural Networks (ANN) as the main controller of robots and Artificial Endocrine System (AES) is used to adjust the behaviours of ANN

influenced by hormone concentrations. On the other hand, the artificial homeostatic hormone system generally utilizes hormone mechanisms individually as the main controller for robots. Emerged behaviours of robots are direct products of the homeostatic control of the robot's internal hormonal states. More details and various implementations of both systems are explained in the next two sub-sections.

### 3.3.1 Neuro-Endocrine System

Proposed in [70], the neuro-endocrine system is inspired from the homeostasis displayed in biological organisms. As introduced, it is understood that there are three main systems responsible for homeostasis, these being the nervous, endocrine and immune systems. However, this work mainly concentrates only on the interactions between the nervous and endocrine systems. As mentioned, this architecture generally employs an ANN as the main robot controller and an AES as a mechanism to alter a robot's behaviours, depending on environmental information. In order to help explain the interactions between both systems proposed in this work, Figure 3.2 **Error! Reference source not found.** illustrates a simple artificial neuron with its mathematical definition shown in equation 3.1 and 3.2. It is a neuron of a type generally found in networks called Multi-Layer Perceptrons (MLP)

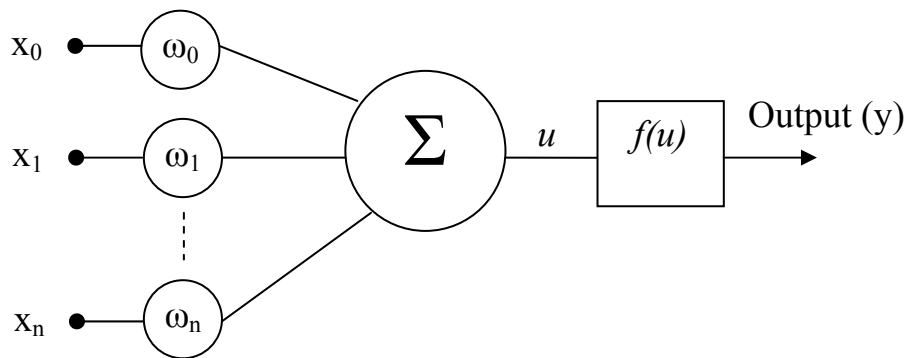


Figure 3.2: A simple artificial neuron (modified from [70])

$$u = \sum_{i=0}^{nx} \omega_i x_i \quad (3.1)$$

$$y = f(u) \quad (3.2)$$

Practically, each artificial neuron is usually connected together to form artificial neural networks. In addition, in order for ANNs to perform any particular tasks, the ANNs need to be set up or trained, and it is the input weights of ANNs which provide a fundamental channel for each ANN to be trained to perform a task and also to change its behaviour [82]. Therefore, in order to enable the interactions between an AES and an ANN, this work proposes the AES changes the input weights of an ANN. There are two main types of components in an AES which enable this aspect to take place: these are “Grand cells” and “Membrane receptors”. Grand cells are mechanisms designed with the main responsibility for secretion of hormones based on external stimuli. The hormone production quantity of each grand cell is defined by equation 3.3.

$$r_g = \alpha_g \sum_{i=0}^{ng} x_i \quad (3.3)$$

$$c_g(t+1) = (c_g(t) \cdot \beta) + r_g(t+1) \quad (3.4)$$

$r_g$  is a value of hormone production for gland  $g$  which is a product between the summation of every dedicated inputs on gland  $g$  and a stimulation rate ( $\alpha_g$ ). Note that  $ng$  is the number of inputs considered at gland cells  $g$ . However, every hormone concentration is usually subjected to decay. Therefore, as defined in equation 3.4, a hormone concentration at the next time step ( $c_g(t+1)$ ) is defined by the summation between a hormone concentration at a current time step  $c_g(t)$  which is subjected to a decay rate ( $\beta$ ) and a hormone production quantity at the next time step ( $r_g(t+1)$ ).

Membrane receptors are used as channels which allow an AES to influence an ANN. Thus ANNs usually are the places where membrane receptors are located. Similar to their biological counterparts, each membrane receptor is sensitive to a particular hormone(s). Therefore, only hormone concentrations secreted from associated gland cells can have some effects over a particular membrane receptor. This feature allows each part of ANNs to respond to different hormones.

A basic interaction between an AES and an artificial neuron is illustrated in Figure 3.3. As mentioned, this work suggests the use of an AES to influence the input weights of an ANN. Thus, the membrane receptor is located at the input weights of the artificial neuron.

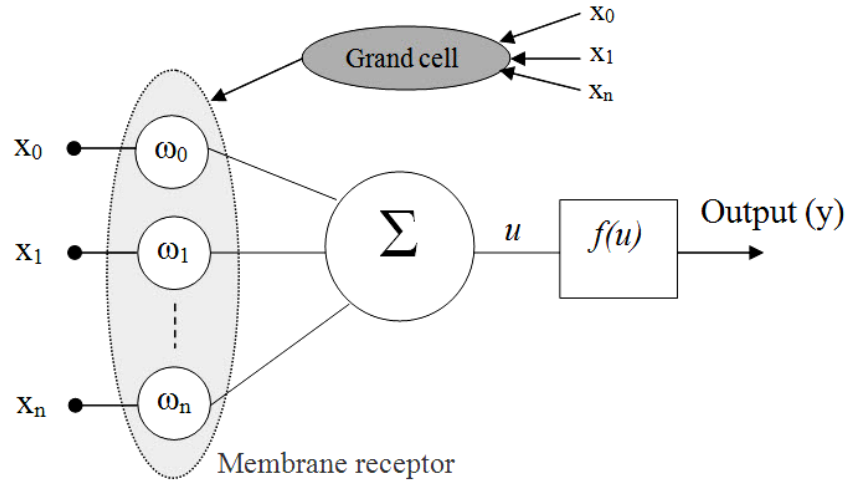


Figure 3.3: A simple neuro-endocrine interaction (modified from [70])

With the addition of a connection between an AES and an artificial neuron, equation 3.1 can be changed to equation 3.5 where  $C_g$  is the hormone concentration of gland cell  $g$ ,  $S_{ig}$  is the sensitivity of an input weight  $i$  to the hormone from gland cell  $g$ , and  $M_{ig}$  is the match between an input weight  $i$  to a gland cell  $g$ . The match is depended on the distance between them as defined in equation 3.6.

$$u = \sum_{i=0}^{nx} x_i \cdot \omega_i \cdot \sum_{g=0}^{ng} C_g \cdot S_{ig} \cdot M_{ig} \quad (3.5)$$

$$M_{ig} = \frac{1}{1+dis(i,g)} \quad (3.6)$$

It can be noticed from equation 3.5 that the extension of AES to the ANN allows the hormones to alter the input weights of the ANNs. This in turn enables the ANN to change its behaviour depending on the hormones levels which are subjected to environmental information. Then, the authors implement the neuro-endocrine system (shown in Figure 3.4) on a Pioneer 2DX robot, in order to investigate the system performance. In such a scheme, the sensory signals from 16 ultrasonic distance sensors are fed to both the fully-connected ANN and the AES. The ANN is created to perform simple obstacle avoidance and the two outputs of the ANN are connected directly to the robot motors. The robot is tested by exploring an approximately square arena with two

short cul-de-sac corridors. From the results, it can be analysed that, with the neuro-endocrine system, the robot is able to change its behaviours depending on the environments. The changing robot behaviours can be noticed from the ability of the robot to adjust its wall-approaching-distances based on the surrounding space. Generally, the robot approaches a wall more closely in an open space, while the approaching-distance is increased (the robot approaches a wall less closely) when the robot is in a tighter area. The robot also retreats from obstacles faster in a tight environment. The ability of the robot in changing the approaching-distance emerges directly from the secretion of hormone based on the stimulation of distance sensors connected to the hormone gland. The changes in the hormone concentration are then used to adjust the input weights in the ANN which results in the changing behaviours of the robot.

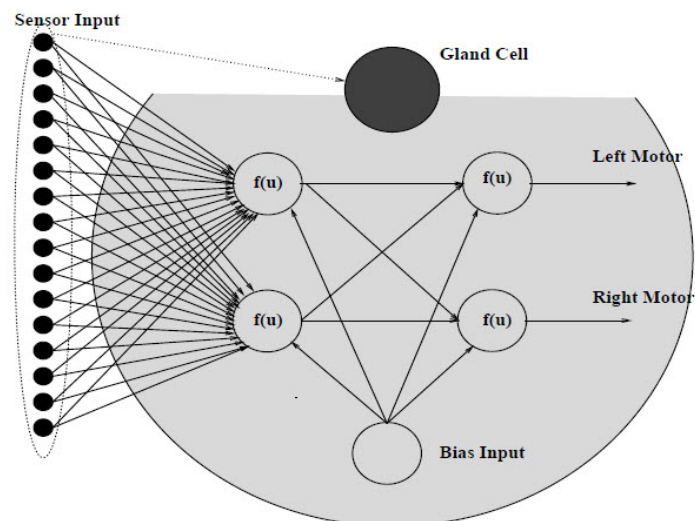


Figure 3.4: A simple neuro-endocrine robot controller [70]

The results shown in this work provide a good example of how an artificial hormone system can be used to adjust behaviours of robots based on the environment the robots are working in. There is also other work which envisages this feature, and applies the architecture further onto other robotic applications. For example, in research reported in [83], the neuro-endocrine system is implemented on a hexapod robot in order to help assist the robot to negotiate an unknown terrain. That work proposes a use of AES to adjust the robot's leg elevation levels based on the robot working terrain. In another

example, the neuro-endocrine system is also suggested to be used as a mechanism for helping autonomous robots working in long-term scenarios as reported in [84]. That work proposes utilization of the neuro-endocrine system to assist an ocean-monitoring sailing robot that operates autonomously for a long period of time. Even though this work had not actually been implemented due to technical problems, the proposed system gives an interesting insight into the use of hormone systems for helping autonomous robots facing environmental variations. That work suggests a use of several hormones for monitoring several essential states of the sailing robot such as the energy levels, actuator temperatures, environmental situations and mission priority level. Generally, the hormone concentration of each hormone can be changed depending on its associated states. Therefore, when the robot encounters different situations, the robot's behaviour can be altered based on the level of each hormone concentration in order to increase the chance of survival and prolong the robot working conditions for a longer period of time.

The utilization of the neuro-endocrine system is not only implemented on single-robot-scenarios but is also evaluated on swarm robots as in the example shown in [85]. In general, this work proposes the use of the neuro-endocrine system for helping robots in a swarm robotic system to work together in order to accomplish a collaborating task of picking up objects scattered in an environment and return them to a certain place. In addition, other work reported in [86], employs only the AES system and applies it onto motivation-based action selection architectures. In this work, motivation-based action selection architectures are designed as the main robot controllers. The AES is used to influence the inputs of motivation-based action selection architectures based on the changing environments. The results show changing of robot's behaviours depending on the situations presented in the test environments.

Apart from applying the neuro-endocrine system to other robotic applications as illustrated above, there is also research which aims to develop the mechanisms of the neuro-endocrine system further, for example, research reported in [87]. The main inspiration of this work is the fact that there is no neuro-endocrine system which is able to adapt to new environments (even though the system is shown to be able to help robots adapting to new environments, the mechanisms of the neuro-endocrine system itself are unable to adapt to new situations, if required). Therefore, this work studies the possibility to incorporate a learning technique with the neuro-endocrine system in order to create an adaptive neuro-endocrine system. The key idea of this work is the inclusion

of input weights at hormone gland inputs (quite similar to input weights generally applied in ANNs) in order to enable learning on AES to associate sensory signals while a robot is working online. A basic diagram of the new proposed system is exemplified in Figure 3.5.

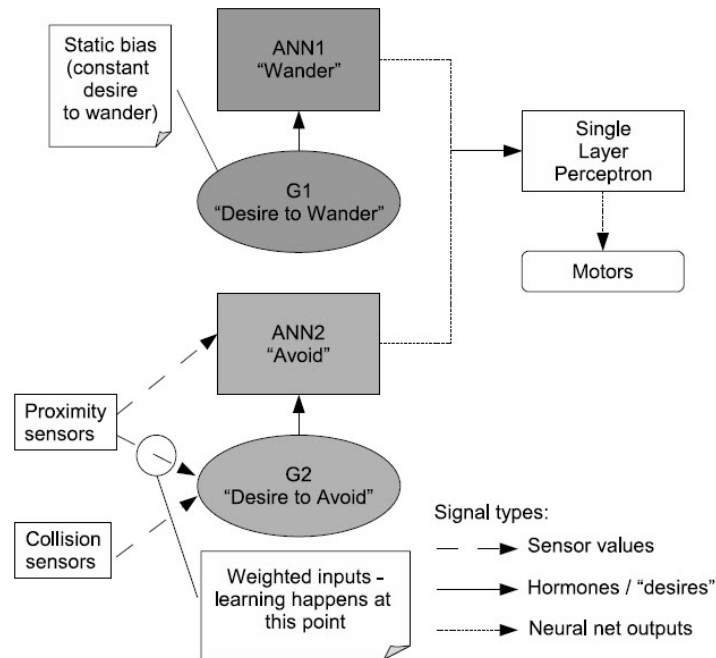


Figure 3.5: A simple diagram of the adaptive neuro-endocrine system [87]

The main objective of the scenario considered in this research is to enable an adaptive neuro-endocrine system to associate two input signals of a hormone gland. As can be seen in Figure 3.5, normally proximity sensors are used as inputs of an ANN to generate “Avoid” behaviour for a robot, while collision sensors are used to stimulate the secretion of hormone “Desire to Avoid”. However, because signals from both types of sensors are likely to be activated together when the robot operates, thus it is expected that the adaptive neuro-endocrine system should learn to associate both types of sensory signals together and later allow the stimulation of hormone “Desire to Avoid” to be influenced by signals from the proximity sensors too. In order to allow this adaptive feature to happen, this work suggests the use of a simple Hebbian learning approach applied on the input weights of signals from proximity sensors which are connected to the hormone gland G2 (as shown in Figure 3.5). The results of experiments on a robot exploring in a rectangular area filled with eight cylindrical obstacles show that the proposed system is able to associate between the signals from the proximity and

collision sensors as expected. The study in [87] illustrates a possible way of creating an adaptive endocrine system by exploiting a learning method. This is one of the interesting features to be acquired in artificial hormone systems, especially when they are expected to be used for autonomous robots encountering dynamic environments.

Another development of the AES is presented in [74]. In that work, the AES is redesigned with the aim to make it more “biologically plausible”. Generally, the overall ideas of the modified AES remain the same as the ones presented in the neuro-endocrine system; it is only the mechanisms of AES that are changed. Figure 3.6 illustrates the main components of the modified AES.

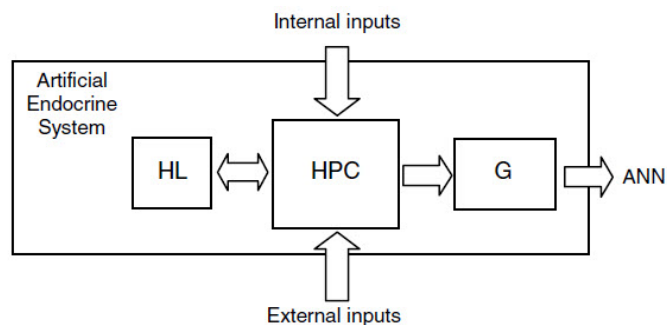


Figure 3.6: The main components of the new AES from [74]

In the modified AES from [74], there are three main components proposed, which are hormone level repository (HL), hormone production controller (HPC), and endocrine gland (G). The HL is proposed as a module which has a record of the hormone level. The HPC is the main mechanism used for controlling the production of hormone based on the record of hormone level as well as the internal and external states. Finally, G is a mechanism which is used to produce and secrete hormones when required. The main distinguished feature of the modified AES from the original AES is the presence of HPC, which controls the hormone production on the basis of both internal and external information. This feature is influential mainly because it helps provide a feedback mechanism for the AES. Generally, the secretion of hormones is proposed to have an effect on ANNs which, in turn, can alter the internal states of a robot. The changes of the internal states can then be detected by the HPC and so the secretion of hormones can be modified by this feedback. This is similar to the endocrine system presented in biological organisms which also functions under feedback mechanisms. The modified

AES is then investigated further in the research reported in [88, 89, 90]. For that research, instead of combining an AES with multi-layer perceptron neural networks (as generally applied in other examples of the neuro-endocrine system), this work investigates the interactions between the modified AES and two NSGasNets (a type of modified ANN [91, 92]). A diagram of the basic interactions between both systems is shown in Figure 3.7. The architecture is used to control robot movement. The two NSGasNets are evolved to help a robot perform specific tasks. The addition of the modified AES is to modify behaviours of the robot depending on the changes in the environments. This feature can occur because the robot velocity commands are directly generated from the modulation of the values between the outputs of the NSGasNets and the hormone level from the AES, which is the subject to be changed based on both internal and external states. In general, the modified AES can differently adjust the influence of each NSGasNet output on the robot motors in response to the changing environmental conditions. The results reported show good robot performances in switching its behaviours when facing different situations.

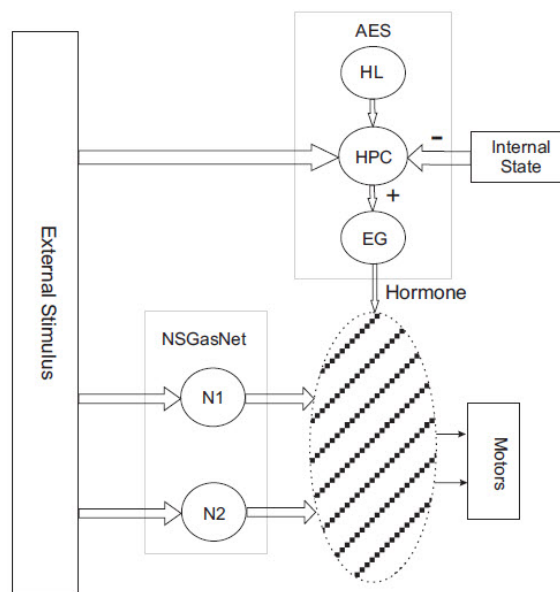


Figure 3.7: A simple diagram of the interactions between the modified AES and NSGasNets [88]

It is believed that the interactions between the neuron, endocrine and immune systems are the keys for homeostasis expressed in biological organisms. Therefore, achieving artificial homeostasis using the combination of the artificial neural system, the artificial

endocrine system and the artificial immune system is clearly intriguing. Although an artificial homeostatic system created from the interactions among the three systems has not practically been evaluated yet, work in [72] has proposed a conceptual framework for the integration of the three systems to accomplish artificially homeostatic systems. A general overview of the integration is shown in Figure 3.8.

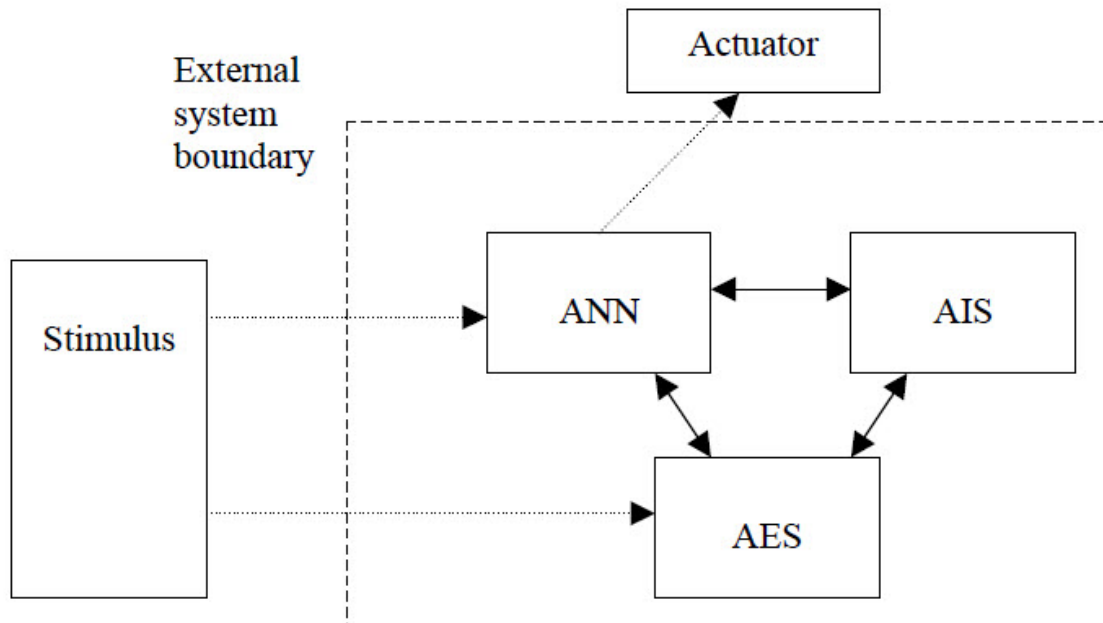


Figure 3.8: A system diagram showing the interaction between the main components in the artificial homeostatic system [72]

From Figure 3.8, it can be noticed that the interactions between the artificial neural network (ANN), artificial endocrine system (AES) and artificial immune system (AIS) is proposed to be inside an artificial organism. External information can only be detected via the ANN and AES. In addition, the artificial organism only interacts with the outside world via the functions of ANN. The proposed system is expected to perform as a self-organising developmental system. A broad idea is that each component of the three main systems is considered as a cell. These cells can be added over time to generate complex control systems for an artificial organism (development). The utilization of ANN and AES in this system, in general, is rather similar to the one usually proposed in the neuro-endocrine system reported previously. However, the addition of an AIS is mainly to help in performing developmental processes. Generally,

any added cells are monitored by the AIS which has the ability to kill the added cells. Nevertheless, because the killing process is performed at a particular rate, the added cells normally have time to show their usefulness. Normally, the concentration of a fitness hormone (from AES) is supposed to rise, if the added cells can provide benefit to the artificial organism which, in turn, can slow down the killing process of AIS and increase the survival chance of the added cells. On the other hand, if the added cells cannot show any benefits to the organism, the fitness hormone concentration would not be increased. This, in turn, speeds up the killing process of the AIS and the added cells then are likely to be eliminated. With this proposed mechanisms, complex controllers which can be developed over time in a self-organising fashion can emerge.

This subsection has reported a review of work done related to the neuro-endocrine architecture. The next subsection will consider work related to the artificial homeostatic hormone system.

### 3.3.2 Artificial Homeostatic Hormone System (AHHS)

The AHHS is mainly developed under SYMBRION and REPLICATOR projects [27]. One of the main focuses of these projects is to create a swarm of small autonomous robots which are able to automatically join together to create one or many symbiotic organisms; an example is shown in Figure 3.9. It is also expected that the control system of the robots will be created from a self-organising process using artificial evolution [93]. The AHHS is one of the controllers proposed to deliver this objective. There are two versions of AHHS which have been developed called “AHHS1” and “AHHS2”.



Figure 3.9: An example of swarm robots aggregated together as a multi-modular robot organism [94]

The first version AHHS1, is proposed and implemented both in a simulated robot [95] and in a real robot [93]. As stated, the AHHS is proposed to be used as a main robot controller which means, for this system, any stimulation on the sensory inputs of the system usually results in the secretion of associated hormones which, in turn, triggers the effects on the actuator outputs of the system directly. In order to allow this feature to happen, the notions of virtual internal space and system's compartments are introduced. To explain the concepts, Figure 3.10 gives an example of a simple two-wheeled robot implemented with an AHHS1.

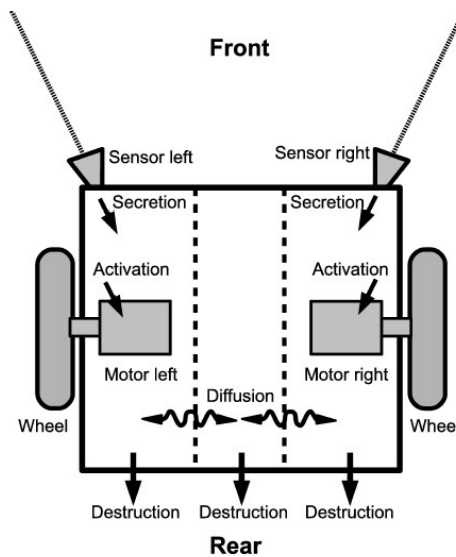


Figure 3.10: an example of a simple two-wheel robot implemented with an AHHS1 [93]

From the example presented, the internal space of the robot is virtually separated into three compartments (divided by the dotted lines). The left compartment contains one left sensor and one left motor, while the right compartment contains one right sensor and one right motor. The middle compartment contains no sensor or motor. For this system, the hormone secretion in any compartment can only be stimulated by the sensors associated with that particular compartment, but hormones can be diffused to adjacent compartments. For example a hormone in the left compartment can only be secreted by the stimulation of the left sensor but the hormone can also spread through to the middle compartment. In addition, the production of each hormone is the subject of its own production and decay rates and each hormone usually can affect any actuator in the system.

An example of the implementation of AHHS1 for the robot (shown in Figure 3.10) performing obstacle avoidance can be defined by equations 3.7 to 3.12. The robot has two distance sensor; one on the left ( $S_l(t)$ ) and another on the right ( $S_r(t)$ ).  $s^l$  is a scaling factor between the hormone unit and sensor value unit. Note that there is only one hormone implemented in the example which is denoted by  $H^l$ . However, the concentration of this hormone in any compartment is denoted by  $H_i^l$ . Thus,  $H_1^l$  represents hormone1 in the left compartment,  $H_2^l$  represents hormone1 in the middle compartment and  $H_3^l$  is hormone1 in the right compartment.

$$\frac{\Delta H_1^1}{\Delta t} = +H_{base}^1 - H_1^1(t)H_{decay}^1 + (S_l(t) > 40)s^1 S_l(t) + D_{1,2}^1(t) \quad (3.7)$$

$$\frac{\Delta H_2^1}{\Delta t} = +H_{base}^1 - H_2^1(t)H_{decay}^1 + D_{2,1}^1(t) + D_{2,3}^1(t) \quad (3.8)$$

$$\frac{\Delta H_3^1}{\Delta t} = +H_{base}^1 - H_3^1(t)H_{decay}^1 + (S_r(t) > 40)s^1 S_r(t) + D_{3,2}^1(t) \quad (3.9)$$

Equations 3.7 to 3.9 define the production of the hormone1 in the left, middle and right compartments respectively.  $H_{base}^l$  and  $H_{decay}^l$  define the base and decay rates of hormone1 respectively.  $D_{xy}^i(t)$  is used to define the diffusion of hormone  $H^i$  as described in equation 3.10. Note that  $d^i$  defines the constant diffusion coefficient of the hormone  $H^i$ .

$$D_{x,y}^i(t) = \frac{H_y^i(t) - H_x^i(t)}{2} d^i \quad (3.10)$$

It can be noticed that the production of hormones in any compartment is defined by three main factors, i) the hormone base and decay rates, ii) the sensor stimulation value and iii) the hormone diffusion value as shown in Figure 3.11. Because there is no sensor dedicated to the middle compartment, the sensor stimulation part is omitted from the equation 3.8.

$$\frac{\Delta H_1^1}{\Delta t} = \overbrace{+H_{base}^1 - H_1^1(t)H_{decay}^1}^{\text{Hormone base and decay rates}} + \overbrace{(S_l(t) > 40)s^1 S_l(t)}^{\text{Sensor stimulation value}} + \overbrace{D_{1,2}^1(t)}^{\text{Hormone diffusion value}}$$

Figure 3.11: The three main factors defining the production of hormones

How the hormone concentration in each compartment influences the robot motors is defined in equations 3.11 and 3.12. Note that  $a^l$  is a scaling factor between the hormone unit and motor value unit.  $A_l(t)$  represents the left motor and  $A_r(t)$  defines the right motor.

$$A_l(t) = a^1 H_1^1(t) \quad (3.11)$$

$$A_r(t) = a^1 H_3^1(t) \quad (3.12)$$

With these setups explained, generally when a distance sensor (either on the left or the right side of the robot) detects any obstacles the hormone will be secreted from its associated compartment. The increase in hormones will then speed up the motor on that side causing the robot to move away from an obstacle. In general, it can be seen that behaviours of the robot can be changed directly based on the stimulation from the environment which affect the internal hormone level of the robot. It can also be noted that other robot tasks or robot behaviours can be obtained by changing the constructions of hormones, compartments and their interactions.

The proposed AHHS1 is developed further in [96] by enabling an Evolutionary Algorithm (EA) to evolve the architecture for robots to perform specific tasks. In order to allow the proposed AHHS1 mechanisms to be evolved, this work introduces “hormone chromosome” and “rule chromosome” as the genome of the AHHS1. In general, the hormone chromosome contains the basic properties of the hormone such as the base and decay rates, and the diffusion coefficient. The rule chromosome generally contains the interactions between the components related to the virtual internal space such as how a sensor influences hormones, how hormones influence each other and how hormones influence actuators. The results on a simulated robot performing an exploring task in a tightly structured environment show some good results for a robot which is

able to avoid obstacles, and evolved controllers which can help the robot to explore the test environment.

The improved version of AHHS1, AHHS2, is then presented in [97] and [98]. The AHHS2 is designed with the main objective to make AHHS1 more evolvable by creating smoother fitness landscapes for the EA to evolve the controller. One of these changes is the introduction of rule type weights. For AHHS2, the rule types (encoded in the rule chromosome) which define the interactions between each component in the system are composed of four sub-rules: actuator sub-rule, sensor sub-rule, linear hormone-to-hormone sub-rule and nonlinear hormone-to-hormone sub-rule. More importantly, for the AHHS2, instead of having just one strict rule as in AHHS1, each rule of AHHS2 is proposed to be a combination of the four sub-rules and an idle sub-rule (as exemplified in Figure 3.12). The combination of sub-rules in each rule is defined by the proposed rule type weights. It has to be noted that the summation of the rule type weights is restricted to be equal to one. Therefore, in general, changing the weight of one sub-rule will affect the remaining weights in the same rule. This feature is expected to be key in helping to create smoother fitness landscapes because the introduction of the rule type weights should allow smoother transition of the system.

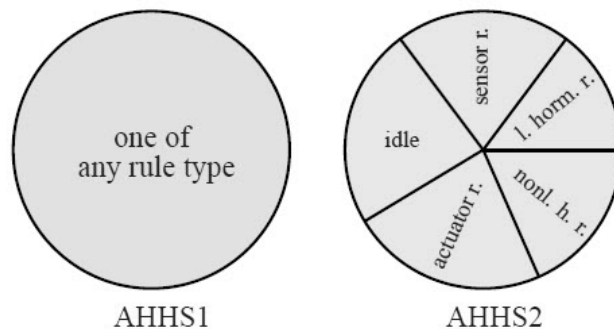


Figure 3.12: A comparison between the implementations of rules in AHHS1 and AHHS2 [98]

The AHHS2 is then implemented on some interesting applications such as gait learning in three and five modules of simulated modular robots connected in a chain [97, 98]. The AHHS2 is implemented on each robot module in a decentralized manner which means generally each module of the robots has no explicit knowledge of its position and topology. Therefore, each module needs to find out these aspects and coordinate with

other modules in order to generate gaits to move the whole robot. The results show that the robot can generate some different gaits such as walking, jumping, wrapping over the wall, and caterpillar-like gaits as shown in Figure 3.13.

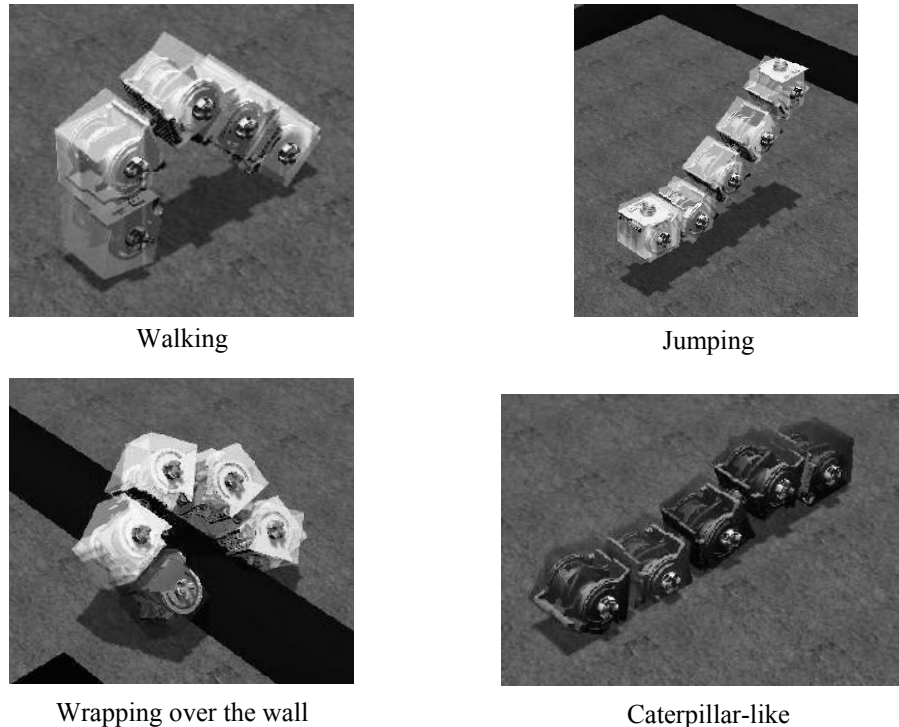


Figure 3.13: Some interesting gaits generated by AHHS2 on a 5-module modular robot

### 3.4 Discussion

In the last two sub-sections, the two mainstream architectures utilizing artificial hormones for maintaining internal states of autonomous robots and adjusting their behaviours have been reviewed. Both architectures show some interesting aspects of using hormones to help autonomous robots deal with different environments and situations but both also display some limitations.

For the AHHS, the system illustrates a good control architecture which is able to provide the emergence of different behaviours for autonomous robots working in different environments. In addition, the concepts of the architecture which enable the regulation of its internal states (which in turn change robot behaviours) when robots encounter different situations is a very interesting aspect. As is the case with biological organisms, the results shown from using this architecture also support the utilization of

hormones to provide adaptability for autonomous robots working in unstructured real-world environments. However, for the research reported in this thesis, we are more interested in creating an additional generic system which is able to be applied on top of other robotic control systems in order to provide adaptability, rather than implementing as a main control system.

As for the case of the neuro-endocrine system, the proposed artificial endocrine system provides an excellent fundamental system which can be developed to generate a generic system for autonomous robots to deal with the dynamics of real-world environments. However, as shown in biological organisms, the interactions between several different hormones in an organism also play a crucial role in the emergence of complex behaviours and the ability to adapt to changing environments. This issue has not been explicitly investigated in the neuro-endocrine system. However, this feature, which allows the interactions between hormones, is one of the main interests of the research reported in this thesis.

More importantly, both internal and external environmental changes are of major concern in autonomous robots working in unstructured real-world environments. Not only external environmental changes can affect the robot performances, but so can internal environmental changes (as shown in the case of Spirit [30]). However, from the review reported here, it can be noticed that there is no research investigating the use of hormones to help autonomous robots deal with internal environmental changes.

### **3.5 Research Approach**

The statements given below are intended to summarise the main focuses of the research reported in this thesis.

- 1) This research is intended to create a system which can provide adaptability for autonomous robots to deal with both internal and external environmental changes in unstructured real-world environments.
- 2) In order to provide adaptability, this research is interested in the concept of exploiting environmental cues as a method for adaptation as illustrated in biological organisms.
- 3) Utilization of hormones in response to environmental cues and in providing adaptability is the key inspiration of the proposed mechanisms in this research.

- 4) The mechanisms of the Artificial Endocrine System (AES) proposed in the neuro-endocrine system are considered as a fundamental system for the mechanisms proposed in this research. However, this research is interested in extending the original mechanisms further in order to allow interactions between hormones in the proposed system and to enable the creation of hormone networks.
- 5) The proposed system is expected to be a generic system. The main idea is that the system should be able to be manually or automatically constructed to create a system which can provide adaptability for different robotic application scenarios.

Note that the full detail explanation of the mechanisms of the proposed system is given in the next chapter.

### **3.6 Summary**

This chapter gives details of hormone systems in terms of both their uses in biological organisms and their implementations in artificial systems. Hormone systems are at the heart of the proposed system in this research, the artificial hormone network (AHN). The use of hormones which respond to environmental cues as a source of adaptation is presented in many biological organisms, and has been found to be one of the fundamental features which helps biological organisms deal with the dynamics of the world. This is definitely one of the key reasons for the interest in hormones in this research. The two systems which are mainly related to the hormone system are the endocrine and homeostatic systems. The endocrine system is a system of glands which can produce and secrete hormones into the bloodstream to act on their target cells. Each hormone, when reaching its target cell(s), can have some effects on the target cell(s) which, in turn, can cause adaptation in an organism. One of most important features of the endocrine system is the secretion of hormones in response to environmental changes in order to regulate internal states of an organism when encountering different environments, a phenomenon known as homeostasis. Because of these properties, both systems get attention from researches in the fields of artificial systems, and especially for robotic applications. Both artificial endocrine and artificial homeostatic systems have been studied and proposed. Among them, there are two key architectures which utilize hormone mechanisms for changing robot behaviours in different environments:

the neuro-endocrine system and the homeostatic hormone system. These two systems show some good examples of how hormones could be implemented to provide adaptability for autonomous robots. However, there are also some limitations in both systems.

In the next chapter, details of the mechanisms inside the proposed AHN are elucidated. In addition, the first implementation of an artificial hormone system and an initial experiment are also illustrated.

## Chapter 4

# Implementation of an Artificial Hormone System

This research aims to employ a hormone-inspired system to assist autonomous robots working in simulations of unstructured real-world environments in dealing with both internal and external environmental changes. An Artificial Hormone System is proposed as a mechanism capable of responding to environmental cues and providing appropriate adaptability for autonomous robots. The main objective of this chapter is to introduce and elucidate the fundamental structures and mechanisms of the artificial hormone system proposed in this research. In section 4.1, mechanisms of the proposed artificial hormone system are described. Section 4.2 exemplifies the implementation of a hormone created to help an autonomous robot deal with changes of terrain roughness. An experiment using this hormone implemented on an autonomous robot is illustrated in section 4.3 and the results are presented in section 4.4. Section 4.5 provides the analysis and discussion, while section 4.6 gives a summary of this chapter.

### 4.1 Artificial Hormone Mechanisms

There are two main types of mechanisms in the proposed artificial hormone system: a Hormone Gland (HG) and a Hormone Receptor (HR). A Hormone Gland is a mechanism which generates and secretes a hormone corresponding to the quantity and existence (i.e. time interval) of the particular environmental information presented at each gland, while a Hormone Receptor is used as a mechanism to determine the locations where hormones can express their validity and to specify what influences hormones can induce on the target systems.

#### 4.1.1 Hormone Gland (HG)

A structure of a HG is illustrated in Figure 4.1. In general, there are two types of inputs which can be connected to a HG. These are Control Inputs (*CI*) and Signal Inputs (*SI*).

The main difference between *CI* and *SI* is that, an input connected to a HG via *SI* is used directly for the calculation of the level of hormone stimulation in each gland. On the other hand, each *CI* input is only used to control the production of hormone (but not directly for the calculation of the hormone stimulation) based on a control feature set (which will be explained later). The *CI* essentially provides a way to enable the interactions among hormones and to create hormone networks. There are four fundamental mechanisms in the HG. These are Hormone release function, Activation function, Signal pre-processor and Control feature (as illustrated in Figure 4.1).

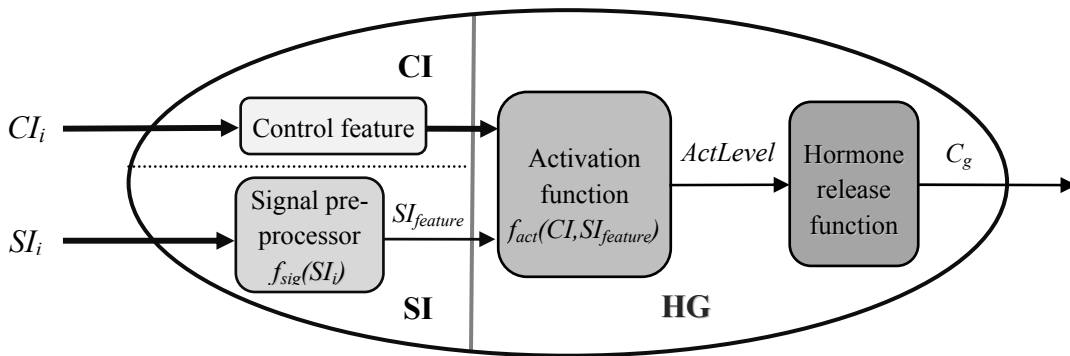


Figure 4.1: Fundamental mechanisms of Hormone Gland

#### 4.1.1.1 Hormone release function

The main responsibility of this mechanism is to identify the hormone concentration at each time step and let the HG secrete the appropriate concentration. Based on the work proposed in [70], the hormone concentration at each time step ( $C_g(t)$ ) is calculated from a summation of the two main terms given by equation 4.1.

$$C_g(t) = (\alpha_g \cdot ActLevel(t)) + (\beta_g \cdot C_g(t-1)) \quad (4.1)$$

The first term considers the stimulation level of hormone at a current time step ( $ActLevel(t)$ ) which is subject to a stimulation rate ( $\alpha_g$ ). The second term takes a hormone concentration at a previous time step ( $C_g(t-1)$ ) which is subjected to a linear decay rate ( $\beta_g$ ). Although other forms of decay rates can also be used, such as a non-linear decay rate (e.g. [74, 90, 98]), only a linear decay rate is investigated in this work.

Examining the uses of other forms of decay rates are left for future work. Note that  $C_g$ ,  $\alpha_g$  and  $\beta_g$  have values normalized between 0 and 1. From this mechanism, it can be noticed that each hormone is subjected to its own dedicated production and decay rates. The rate at which a hormone can be produced is controlled by  $\alpha_g$ , whereas when there is no hormone stimulation, the concentration of hormone will decline at a rate defined by  $\beta_g$ .

#### 4.1.1.2 Activation function

The level of the hormone stimulation at each time step ( $ActLevel(t)$ ) is determined by equation 4.2. The roles and properties of the Activation function ( $f_{act}(x,y)$ ) are rather similar to the activation function usually used in an ANN. Several different forms of functions can be set on the Activation function such as linear, step or sigmoid. The main duty of this mechanism is to determine the production of hormone based on the Control Input ( $CI$ ) and the associated aspects of environmental information ( $SI_{feature}$ ). These two mechanisms are explained further in the next two sub-sections.

$$ActLevel(t) = f_{act}(CI, SI_{feature}) \quad (4.2)$$

#### 4.1.1.3 Signal pre-processor

Equation 4.3 defines the Signal pre-processor mechanism. Its main purpose is to determine the aspects of environmental information ( $SI_{feature}$ ) which are considered to stimulate the production of a hormone. Similar to the  $f_{act}(x,y)$ , the Signal pre-processor function ( $f_{sig}(x)$ ) can take several different forms such as standard deviation, average or differentiation functions. The decision on which functions should be set on this mechanism is mainly based on how signal inputs can be interpreted related to the desired aspects of environmental information. For example, in a case that two signal inputs are connected to a HG and perhaps it is the difference between values of these two inputs which are expected to stimulate the production of hormone. In this case, the Signal pre-processor takes a form of differentiation function.

$$SI_{feature} = f_{sig}(SI_i) \quad (4.3)$$

#### 4.1.1.4 Control feature

As stated previously, any *CI* input can have an effect based on a feature set. Thus, the Control feature is used to set the features of *CI*. Each control input generally can be set to have one of the following features:

- **Inhibitory / Stimulatory control**

These control features provide a way to inhibit or to stimulate a hormone release depending on the existence or the lack of other sensory information or another hormone. When the value of sensory information or hormone concentration (which is connected to a HG via these control features) is higher than a threshold, the production of hormone can be inhibited or stimulated based on whether the feature is set to Inhibitory or Stimulatory, respectively. The implementations of these two features can be achieved by a simple if-then rule as shown in Figure 4.2.

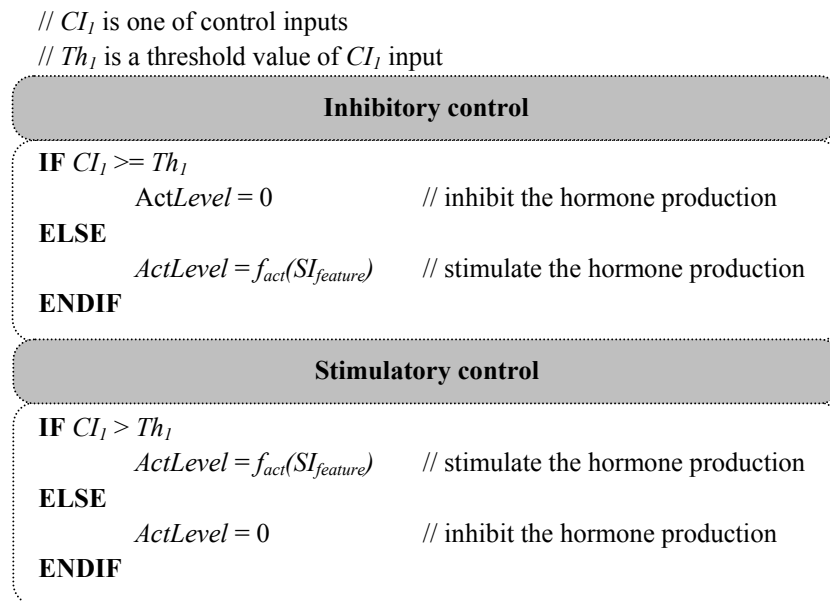


Figure 4.2: Pseudo-code for the implementations of inhibitory and stimulatory control features

- **Negative / Positive feedback control**

These control features are used as a procedure to decrease or increase hormone stimulation when other sensory information or hormone concentrations are built up. In general, if a *CI* input is set to have negative feedback control, signals from

the input will suppress the production of hormone on the gland and vice versa. These two control features can be implemented as shown in Figure 4.3.

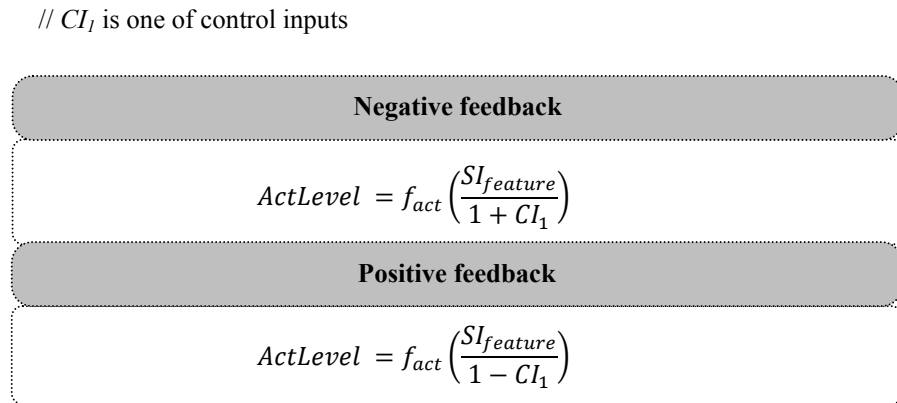


Figure 4.3: Implementations of negative and positive feedback control features

Note also that each  $CI$  input is normalized between 0 and 1.

#### 4.1.2 Hormone Receptor (HR)

Similar to the hormone system in biological organisms which have associated hormone receptors on their target cells, the HR acts as a mechanism which allows only associated hormones to influence their target systems. HR can be located both on the robot and the hormone system depending on which locations are subjected to be influenced by hormones. Therefore, any parameters, mechanisms or systems which are expected to be altered by hormones must have one or more HR associated with particular hormones in order to enable the interactions between the hormones and their target systems. Figure 4.4 shows the structure of an HR. Theoretically, only hormone signals can be presented at the inputs of an HR. Basically, the connections of hormones at the inputs of an HR define that the hormones is associated with that HR.

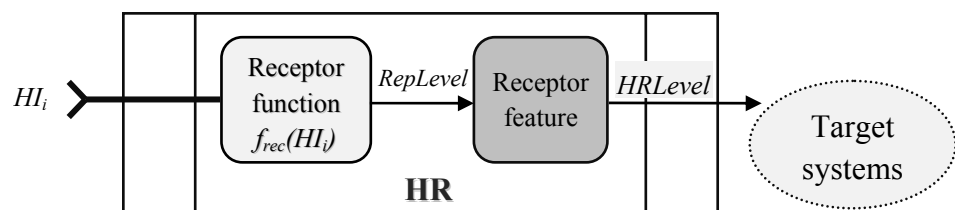


Figure 4.4: The structure of Hormone Receptor

There are two main mechanisms which are used to determine how associated hormones can influence their target systems. These are Receptor function and Receptor feature.

#### 4.1.2.1 Receptor function

Rather similar to the Signal pre-processor proposed in HG, the Receptor function can be set to perform a number of different functions. The main purpose of this mechanism is to identify how the values of associated hormones can determine the values of hormone receptor (*HRLevel*). Note that the value of *HRLevel* is mainly used to influence the target's systems.

#### 4.1.2.2 Receptor feature

This mechanism defines how the *HRLevel* values are built up (from the value generated by Receptor function (*RepLevel*)). The feature can be set to one of the following:

- **Direct effect**

This feature determines that the value of *RepLevel* at each time step directly determines the value of hormone receptor at that time step, as shown in equation 4.4.

$$HRLevel(t) = RepLevel(t) \quad (4.4)$$

- **Accumulative effect**

This feature determines that the value of hormone receptor at a current time step (*HRLevel(t)*) is influenced by the combination of the value of *RepLevel* at the current time step (*RepLevel(t)*) with the value of hormone receptor at a previous time step (*HRLevel(t-1)*), as defined in equation 4.5.

$$HRLevel(t) = RepLevel(t) + HRLevel(t-1) \quad (4.5)$$

In order to prevent the value going unbound, the value of hormone receptor can be restricted to any specified values (based on the problems applied) by the users. However, in this research, the value is restricted to 2 because this value

can cover the possible velocity range of the robot implemented. This will be explained later in the chapter 5.

These are the main structures and mechanisms of the artificial hormone system proposed in this research. Note that it would also be possible to implement a sensitivity function to the hormone inputs on HR, similar to the AES proposed in the neuro-endocrine system [70]. The sensitivity can be included simply by adding a sensitivity parameter on each input of HR. However, this feature is not investigated in this research. Therefore, the inclusion of the sensitivity parameters is omitted from the proposed HR.

In order to enhance the understanding of the proposed mechanisms of both the Hormone Gland and the Hormone Receptor, an implementation of an artificial hormone system to help an autonomous robot deal with an external environmental change is elucidated in the next section.

## **4.2 Implementation with Terrain Excitation Hormone**

The natural terrain is vast, dynamic and full of different surface configuration. Autonomous robots which are able to work in such environments are certainly considered essential and having numerous benefits [99]. In this research, the robot's ability to deal with unstructured terrain is considered. This section provides the background and describes an artificial hormone system configured for assisting an autonomous robot to deal with different terrain roughness, tested in simulation.

### **4.2.1 Background**

An autonomous robot which is able to modify its locomotion based on terrain profiles can undoubtedly provide an excellent foundation system for robots to be employed in a number of unstructured real-world robotic applications. However, attempting to gain exact knowledge of terrain configuration in order to adjust the robot movements may require sophisticated sensors and computational systems, as shown in [100, 101], which obviously not every robot designer/builder can afford.

Some of the main issues for a robot working on rough terrain environments are the unpredictability of surface traction and the probability of being tipped over because of the irregularity of the terrain. When a robot traverses over rough terrain, the profile of terrain can unpredictably force the robot to rotate and change the robot's orientations. This situation is likely to disturb the robot's stability and increases the chances of tipping over. One of the environmental cues which can imply the robot's stability and the effects of rough terrain on the robot is the variation of robot pitch angle. A robot can acquire this information simply using sensors such as IMUs and accelerometers. When a robot travels on rough terrain, the change of terrain roughness usually alters the robot pitch angle. Therefore, information about how the pitch angle of a robot changes over a specific period of time can potentially be used as an environmental cue which is linked with the terrain profile that a robot is working on.

In order to increase the robot's chances of survival (not tipping over when moving on rough terrain), the notion of adjusting robot movements based on changes of terrain roughness is considered for example the robot's speed can be decreased when the environmental cue indicates that the robot stability is reduced, and then speed up again when the robot is more stable. This should improve the robot's survivability. This insight is used on a robot by the inclusion of an artificial hormone system in an attempt to increase its stability in such rough terrains.

#### **4.2.2 The Terrain Excitation Hormone**

The hormone, proposed to assist a robot to deal with changes of terrain roughness, is called Terrain Excitation hormone. Figure 4.5 illustrates the artificial hormone system responsible for the production and secretion of the hormone, and the connection of the hormone system with the main robot controller. The implementations of the two main hormone mechanisms, which are the Hormone Gland (HG1) and Hormone Receptor (HR\_MC), are described.

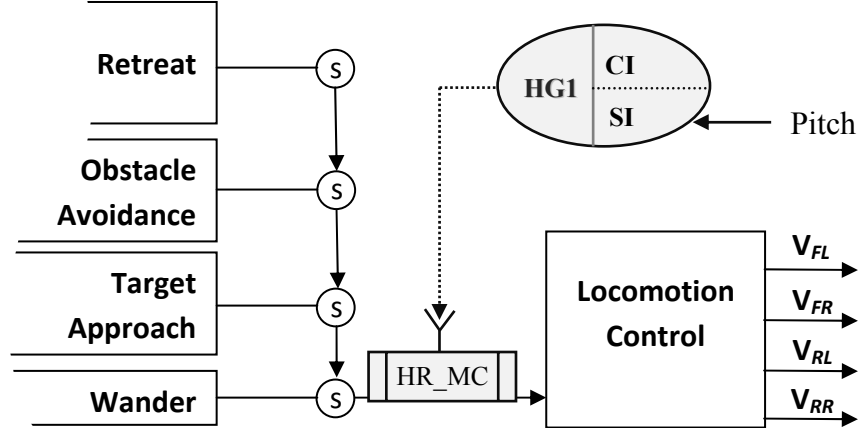


Figure 4.5: The artificial hormone system responsible for the secretion of the Terrain Excitation Hormone and the interaction of the hormone system with the robot controller

#### 4.2.2.1 Hormone Gland 1 (HG1)

Table 4.1 shows the setting up of inputs and mechanisms of HG1. This gland only takes one signal input from the robot pitch sensory information without having any control inputs. The environmental cue is extracted from the input by applying standard deviation on the pitch information over a specified period of time. The extracted environmental aspect is linearly scaled by a specific maximum-limit-SD-value ( $\text{maxLimitSD}$ ) and then directly stimulates the production of Terrain Excitation hormone.

Table 4.1: The setup of HG1 mechanisms

HG1		
<b>Signal inputs</b>	$SI_I$	Pitch angle of the robot (Pitch)
<b>Control inputs</b>	-	-
<b>Signal pre-processor</b>	Standard deviation (SD)	$SI_{feature} = SD(SI_I)$
<b>Control features</b>	-	-
<b>Activation function</b>	Scaling linear function	$ActLevel = SI_{feature} / \text{maxLimitSD}$ <b>IF</b> $ActLevel > 1$ $ActLevel = 1$

#### 4.2.2.2 Motion-Command Hormone Receptor (HR\_MC)

As shown in Figure 4.5, the HR\_MC is located at the output of the Behaviour-based robot controller (before connected to the Locomotion Control unit). Section 2.4.2 described that there are four types of output commands generated from the controller. These are forward speed, forward direction, turn speed and turn direction. Note that only forward speed and turn speed are connected with the HR\_MC, thus the Terrain Excitation hormone only influences the forward and turn speed of the robot. Table 4.2 presents the input and setup of the HR\_MC mechanisms. The HR\_MC is a receptor which associates to the hormone secreted from the HG1, therefore, HR\_MC only responds to the concentration of the Terrain Excitation hormone ( $C_gHG1$ ). The Receptor function is set to linearly scale down the hormone concentration by a factor of 0.9. The main purpose of this is to prevent the robot from stopping completely when the hormone concentration is at its highest level (which is one). The Receptor feature is set to Direct effect, thus the value of this hormone receptor at each time step is influenced directly by the value of  $RepLevel(t)$ . Finally, as this hormone is proposed to decrease the robot speed based on the concentration of the hormone, this feature is implemented as shown in Table 4.2. Generally, when the highest concentration of Terrain Excitation hormone is reached, the speed of the robot is forced to decrease by 90% of its original desired speed (from the Behaviour-based controller). However, when there is no Terrain Excitation hormone presented, the robot speed is set to be exactly as originally commanded, while the different hormone concentration levels can adjust the speed of the robot proportionally.

Table 4.2: The setup of HR\_MC mechanisms

HR_MC		
Hormone inputs	$HI_1$	$C_gHG1$
Receptor function	Scaling linear function	$RepLevel(t) = HI_1 \cdot 0.9$
Receptor feature	Direct effect	$HRLevel(t) = RepLevel(t)$
Target action	Robot forward speed	$forwardSpeed(t) \cdot (1 - HRLevel(t))$
	Robot turn speed	$turnSpeed(t) \cdot (1 - HRLevel(t))$

Pseudo-code for both the HG1 and HR\_MC are shown in Figure 4.6 and Figure 4.7 respectively. From the implementation of this hormone system, an autonomous robot

which is able to adapt its locomotion by adjusting its speed depending on the roughness of terrain can be postulated.

**Pseudo-code: HG1**

```

// SI1 is the input from robot pitch sensory information
// maxLimitSD is set to 8
// SD(X,Y) is a basic standard deviation function which calculates the SD
// value of input X over the number of sampling defined by Y

SIfeature = SD(SI1, 10) //Calculate standard deviation of robot pitch angle

Actlevel = SIfeature / maxLimitSD
IF Actlevel > 1
    Actlevel = 1
ENDIF

```

Figure 4.6: Pseudo-code for HG1

**Pseudo-code: HR\_MC**

```

// HI1 is the input from the Terrain Excitation hormone

RepLevel(t) = HI1 · 0.9 // Scaling linear function

HRlevel(t) = RepLevel(t) // Direct effect

forwardSpeed(t) = forwardSpeed(t) · (1 - HRlevel(t)) // Target action
turnSpeed(t) = turnSpeed(t) · (1 - HRlevel(t)) // Target action

```

Figure 4.7: Pseudo-code for HR\_MC

### 4.3 Experiment Setup

The main purpose of this experiment is to investigate the performances of the Terrain excitation hormone in helping an autonomous robot deal with the case of external environmental changes induced by rough terrain. As introduced in Chapter 2, all experiments in this research are implemented in Gazebo, the 3D robot simulator. The test environment and robot used in this experiment is shown in Figure 4.8. The size of the arena is measured 340 cm by 840 cm and is enclosed by walls. The robot is implemented with the controller explained in section 2.4.2 and the artificial hormone system described in the previous section. The main robot task is to approach the target object as also introduced in section 2.4.1.

As introduced in section 4.1.1.1, the secretion of each hormone is subject to its own production rate ( $\alpha_g$ ) and decay rate ( $\beta_g$ ). Generally, variations of these two parameters can alter the behaviour of the HG in the production and secretion of its hormones (which in turn affect the robot behaviour). In order to evaluate how the behaviour of the HG can be changed depending on the variations of these two parameters, this feature is considered as another objective of this experiment. Therefore, 17 test cases are set up in this experiment. They are established from the combinations of the different values of  $\alpha_g$  (1.0, 0.7, 0.5 and 0.3) and  $\beta_g$  (0.9, 0.7, 0.5 and 0.3), and a case when there is no hormone implemented on the robot. Each case is tested for 100 runs and the robot is allowed to perform the task for 15 minutes in each run. This time limit was acquired from a preliminary experiment which showed that in 90% of the total number of test runs the robot either reaches the object or tips over within 15 minutes. Note that at the beginning of each run, the starting position and orientation of the robot are randomly generated in order to avoid bias and to introduce randomness to the experiment. The starting positions of the robot, however, are restricted to be in the flat area at the beginning of the arena (as marked in Figure 4.8 (b)). Usually, the behaviour-based controller of the robot commands the robot to move at 30cm/s on average. The robot performances are measured using the performance metrics introduced in section 2.5 and the results are presented in the next section.

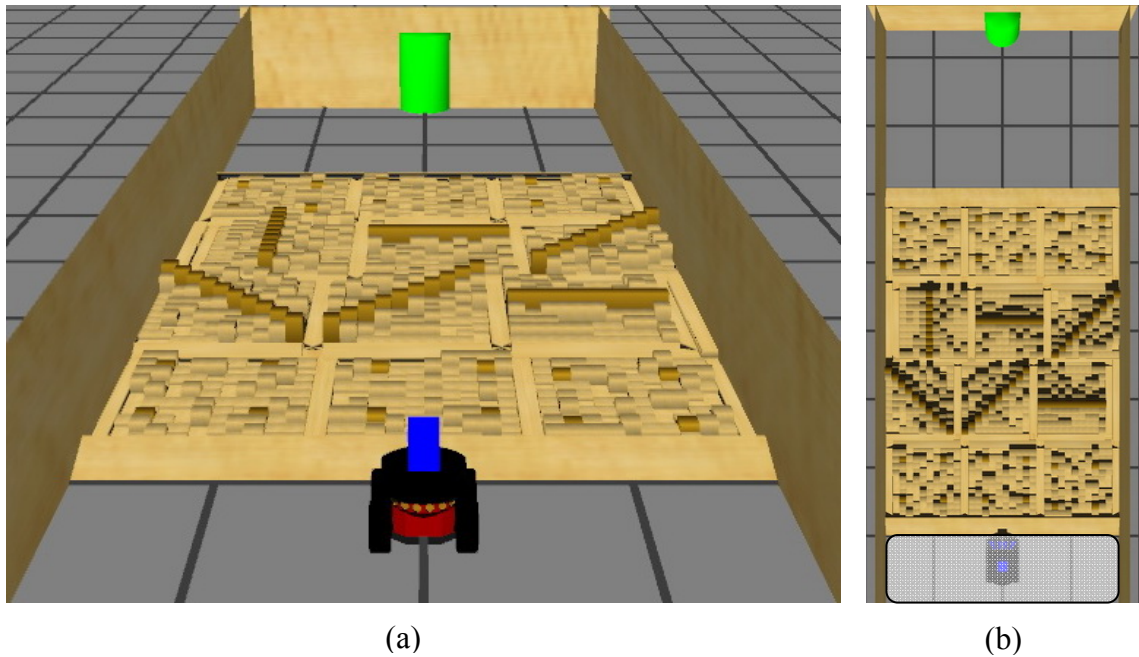


Figure 4.8: The test environment for the experiment of the Terrain Excitation hormone  
(a) a front view of the arena (b) a bird-eye view of the arena. The grey-rectangular-marking indicates the starting area of the robot

## 4.4 Results

The performance of the robot in achieving the assigned task is shown in Table 4.3.

Table 4.3: The robot performances on the experiment of Terrain Excitation hormone

	The number of			Time Spent to Reach	
	Time Out	Tip Over	Object Reach	Average (s)	SD
<b>No Hormone</b>	0	37	63	168	132.98
$\alpha_g: 1.0 \quad \beta_g: 0.9$	38	17	45	467	144.50
$\alpha_g: 1.0 \quad \beta_g: 0.7$	5	21	74	288	120.61
$\alpha_g: 1.0 \quad \beta_g: 0.5$	1	25	74	241	121.75
$\alpha_g: 1.0 \quad \beta_g: 0.3$	0	35	65	199	93.73
$\alpha_g: 0.7 \quad \beta_g: 0.9$	12	41	47	420	140.52
$\alpha_g: 0.7 \quad \beta_g: 0.7$	0	29	71	227	81.27
$\alpha_g: 0.7 \quad \beta_g: 0.5$	0	26	74	233	128.40
$\alpha_g: 0.7 \quad \beta_g: 0.3$	1	30	69	203	97.94
$\alpha_g: 0.5 \quad \beta_g: 0.9$	6	25	69	354	140.12
$\alpha_g: 0.5 \quad \beta_g: 0.7$	2	32	66	225	115.96
$\alpha_g: 0.5 \quad \beta_g: 0.5$	0	31	69	186	93.78
$\alpha_g: 0.5 \quad \beta_g: 0.3$	0	32	68	191	116.33
$\alpha_g: 0.3 \quad \beta_g: 0.9$	2	30	68	270	118.94
$\alpha_g: 0.3 \quad \beta_g: 0.7$	1	28	71	203	98.13
$\alpha_g: 0.3 \quad \beta_g: 0.5$	0	23	77	183	135.44
$\alpha_g: 0.3 \quad \beta_g: 0.3$	1	35	64	184	130.62

As stated in the hypothesis section, a better robot performance is defined by a higher Object Reach and a lower Tip Over. From the results shown in Table 4.3, some initial conclusions can be drawn:

- 1) It is clear from the results that the variations of  $\alpha_g$  and  $\beta_g$  can affect the robot's performance as can be noticed from the variations in each test case.

- 2) Although the robot's performance when the hormone system is implemented are not better than the robot without the hormone in all test cases, the robot with the hormone system still manages to reach the object more often in almost every test case (except the two cases of  $\alpha_g:1.0$  &  $\beta_g:0.9$ , and  $\alpha_g:0.7$  &  $\beta_g:0.9$ ). Note that without the implementation of the hormone on the robot, the Object Reach is already high at 63. This confirms that the Behaviour-based controller on the robot is capable of performing the tasks rather well, even without the hormone system.
- 3) The best robot performance is shown when  $\alpha_g$  and  $\beta_g$  are set to 0.3 and 0.5 respectively. In this case, the robot manages to increase the number of Object Reach by 14% (to 77%) comparing with the robot without the hormone.
- 4) The combination of high values of  $\alpha_g$  and  $\beta_g$  is likely to increase the Time Out as shown in the cases of  $\alpha_g:1.0$  and  $\beta_g:0.9$ , and  $\alpha_g:0.7$  and  $\beta_g:0.9$ . However, it is the  $\beta_g$  value which is likely to play a more significant role in rising of Time Out as there is no evidence of higher Time Out when  $\beta_g$  is low.
- 5) With this implementation of the hormone system, it can be noticed that the robot takes a longer time on average to reach the target object. In addition, the higher the values  $\alpha_g$  and  $\beta_g$  are a longer time required.

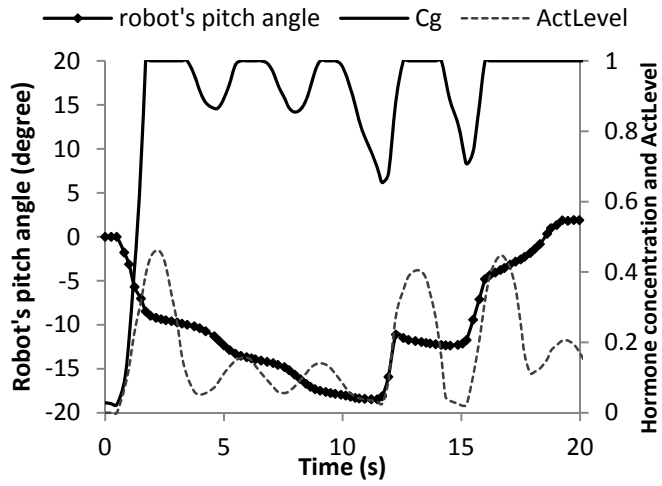
## 4.5 Discussion and Analysis

In order to further analyse the results obtained in the previous section and to understand the influences of the Terrain Excitation hormone in helping the robot deal with changes of terrain roughness, some issues are investigated further.

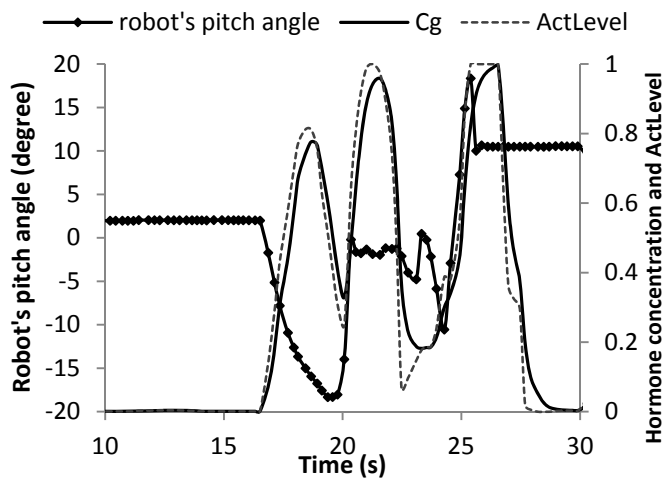
### 4.5.1 Hormone Concentration versus Terrain Roughness

Figure 4.9 exemplifies the behaviours of HG1 in the production and secretion of Terrain Excitation hormone in response to changes of terrain roughness. The figure shows the hormone behaviour in three test cases when the production rate ( $\alpha_g$ ) and decay rate ( $\beta_g$ ) of HG1 is set to 1.0 & 0.9, 0.5 & 0.5, and 0.3 & 0.3 respectively. Values of the robot's

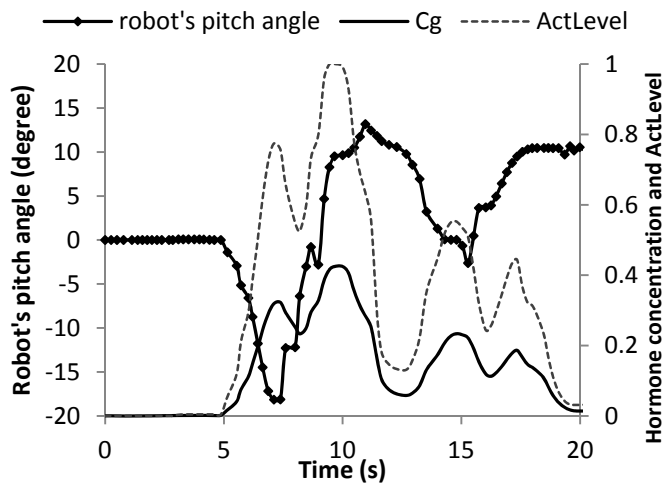
pitch sensory information are represented with the dotted full black lines. Negative values of this quantity mean that the robot is heading down with the degree angle reported by the values, while positive values mean the robot is heading up also with the degree angle reported by the values. The changes of the terrain roughness can be estimated by the changes of these robot pitch values. This quantity is also the key driver of the Terrain Excitation hormone. As explained in section 4.2.2.1, the HG1 responds to the variations of pitch sensory information (which is derived by the SD) and it is this information that stimulates the production of the hormone. This quantity is represented with the dotted lines in Figure 4.9. The hormone concentration (the solid lines) will then be changed corresponding to the hormone stimulation. However, the variations of  $\alpha_g$  and  $\beta_g$  influence the secretion of hormone concentration differently as can be noticed from the different behaviours shown between Figure 4.9 (a), (b) and (c). Generally,  $\alpha_g$  determines the sensitivity of the hormone production to its stimulation. Higher values of  $\alpha_g$  indicate that the hormone is more sensitive to its stimulation, thus only low hormone stimulations can rapidly raise the hormone concentration and the opposite is also true for the lower values. This is illustrated in the first few seconds shown in Figure 4.9 (a), in the figure it is shown that only such small hormone stimulations (less than 0.5) can immediately increase the hormone concentration to reach its maximum value. In contrast to Figure 4.9 (b) around 16s to 19s and Figure 4.9 (c) around 5s to 10s, even with the higher hormone stimulations, the concentrations of the hormone remain lower than the ones shown in Figure 4.9 (a). For the  $\beta_g$ , this attribute not only influences the accumulation of hormone concentration, but  $\beta_g$ , also crucially identifies the range of time period in which the built up hormone concentration is still presented when the hormone stimulation has already diminished or disappeared. One of the most obvious consequences of high  $\beta_g$  values is the longer time period in which the built up hormone concentration exist even without stimulations or with low stimulations of the hormone. As illustrated around 4s to 10s in Figure 4.9 (a), the concentration of the hormone remains high (more than 0.8), even when the hormone stimulation has decreased significantly. Comparing the last few seconds shown in Figure 4.9 (b), in which the hormone concentration has dropped off almost immediately after the hormone stimulations have inhibited. How these hormone dynamics influence the speed of the robot is illustrated in the next section.



(a)  $\alpha_g$ : 1.0 and  $\beta_g$ : 0.9



(b)  $\alpha_g$ : 0.5 and  $\beta_g$ : 0.5



(c)  $\alpha_g$ : 0.3 and  $\beta_g$ : 0.3

Figure 4.9: Changes of the hormone concentration ( $C_g$ ) and the hormone stimulation ( $ActLevel$ ) against the variations of the robot pitch sensory information when  $\alpha_g$  and  $\beta_g$  are assigned as follow (a)  $\alpha_g$ : 1.0 and  $\beta_g$ : 0.9 (b)  $\alpha_g$ : 0.5 and  $\beta_g$ : 0.5 (c)  $\alpha_g$ : 0.3 and  $\beta_g$ : 0.3.

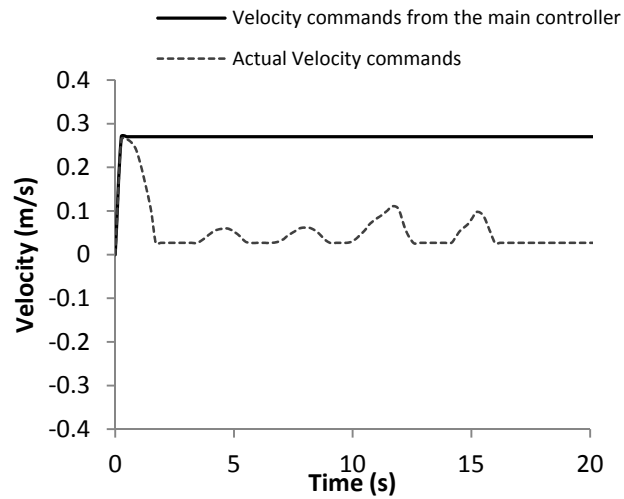
Note that data showing in each figure is acquired from a single robot run.

### 4.5.2 Hormone Concentration versus Robot Speed

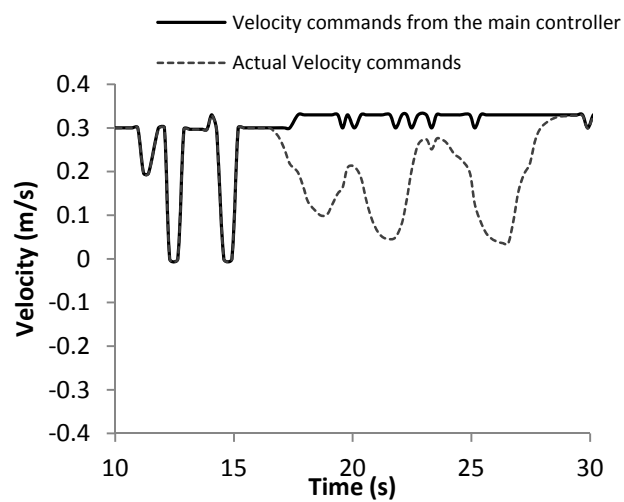
Figure 4.10 displays the comparisons between the velocity commands of a robot wheel originating from the main robot controller and the actual robot wheel velocity subjected to the hormone influences. Note that the results shown are acquired from the front-left wheel of the robot. In addition, the changes of the robot speed illustrated in Figure 4.10 (a), (b) and (c) correspond to the hormone concentration shown in Figure 4.9 (a), (b) and (c) respectively. A positive velocity means that the wheel is turning forward and a negative value means the wheel is rotating backward.

Considering Figure 4.9 and Figure 4.10, it is obvious that the Terrain Excitation hormone affects the robot by adjusting the robot speed depending on the level of hormone concentration at each particular time. In Figure 4.10 (a), when  $\alpha_g$  and  $\beta_g$  are high and the hormone concentration is increased, the actual speed of the robot is kept rather low almost all the time even though the original velocity commands are always high. In Figure 4.10 (b) and (c), it can be seen that the robot speed is closer to the original velocity commands than the speed shown in Figure 4.10 (a) which is mainly because the hormone concentrations in these two cases are lower.

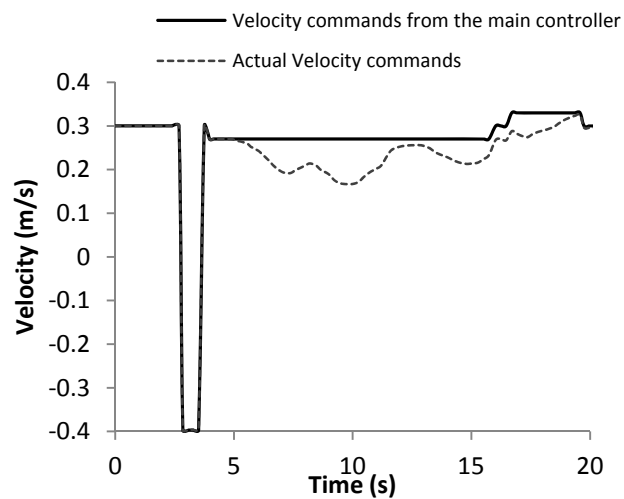
From these graphs, it can be stated that the influence of the hormone which decreases the robot speed based on the changes of terrain roughness is one of the main reasons for the longer time required for the robot to reach the target object as the robot is more likely to move slower when  $\alpha_g$  and  $\beta_g$  are higher.



(a)  $\alpha_g$ : 1.0 and  $\beta_g$ : 0.9



(b)  $\alpha_g$ : 0.5 and  $\beta_g$ : 0.5



(c)  $\alpha_g$ : 0.3 and  $\beta_g$ : 0.3

Figure 4.10: The comparisons between the wheel velocity commands originated from the main robot controller and the actual wheel velocity adjusting by the Terrain Excitation hormone in the test cases when  $\alpha_g$  and  $\beta_g$  are assigned as follow (a)  $\alpha_g$ : 1.0 and  $\beta_g$ : 0.9 (b)  $\alpha_g$ : 0.5 and  $\beta_g$ : 0.5 (c)  $\alpha_g$ : 0.3 and  $\beta_g$ : 0.3 Note that data showing in each figure is acquired from a single robot run.

### 4.5.3 Robot Traces

Figure 4.11 illustrates examples of a number of robot traverse routes when there is and there is no Terrain Excitation hormone implemented on the robot. Note that the robot traces shown when the hormone is implemented on the robot are obtained from the test case when the robot has its best performances. That is when  $\alpha_g$  is set to 0.3 and  $\beta_g$  is set to 0.5.

It can be noticed that, with the implementation of the Terrain Excitation hormone, the robot traverse routes are straighter. This happens because the effect of the speed reduction when facing rough terrain also helps the robot to negotiate steeper hill terrain. As explained previously in section 2.4.2 regarding the Retreat behaviour, the slower the robot moves, the higher the critical pitch angle is. Therefore, when the robot reduces its speed when encountering rough hills, the main controller allows the robot to negotiate steeper hills. These effects regularly assist the robot to move across a steep hill and prevent the robot from tipping over. Nevertheless, without the Terrain Excitation hormone, the robot is unable to adjust its speed based on changes of terrain roughness. Thus, when the robot is facing too steep a hill, the Retreat behaviour is activated and forces the robot to change its direction as can be observed from the frequent changes of the robot moving directions shown in the Figure 4.11 (a).

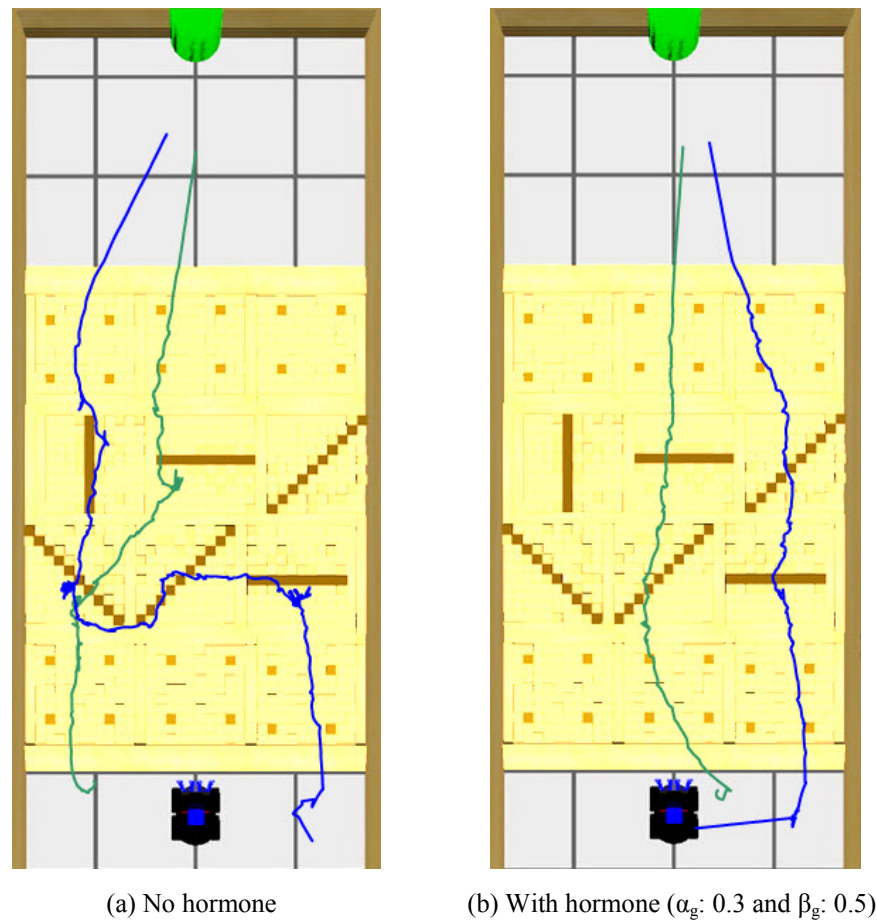


Figure 4.11: Examples of the traverse routes taken by the robot when (a) there is no hormone implemented on the robot (b) the Terrain Excitation hormone is applied on the robot

#### 4.5.4 Tip Over Positions

Figure 4.12 shows the reference numbers assigned for each step-field implemented on the test arena. The main proposed of the reference numbers is to help specify the areas when discussing the tip over positions. Figure 4.13 visualizes the tip over positions of the robot when there is and there is no hormone implemented on the robot. Similar to the previous sub-section, the tip over positions when the hormone is implemented are obtained from the test case when  $\alpha_g$  is 0.3 and  $\beta_g$  is 0.5.

From Figure 4.13 (a), it can be noticed that the tip over positions of the robot are spread throughout the areas of the hill and diagonal step-fields (2x and 3x). However, when the Terrain Excitation hormone is implemented on the robot (Figure 4.13 (b)), the areas in which the robot tips over are decreased. In this case, the robot tips over mostly around the upper part of step-fields 23 and 33. Investigating further on both areas is shown that

these two areas are the most difficult areas for the robot to deal with. This is fundamentally because the differences in height of some wooden blocks in these areas are too high for the robot. Tip over occurs mostly after the robot climbs over the hills of step-fields 23 and 33, and some areas in front of the robot are too steep and the robot is very likely to fall down the hills on to the lower areas in front.

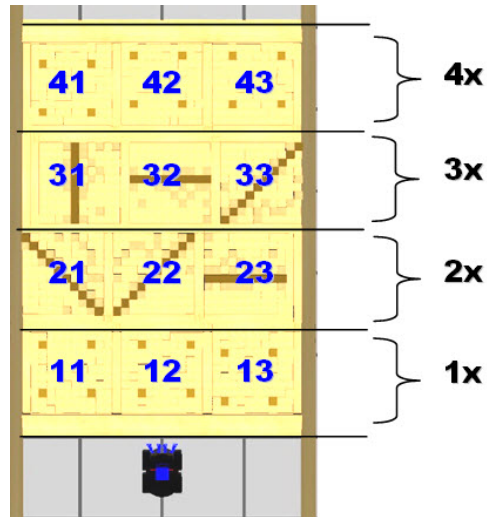


Figure 4.12: The reference numbers assigned on each step-field

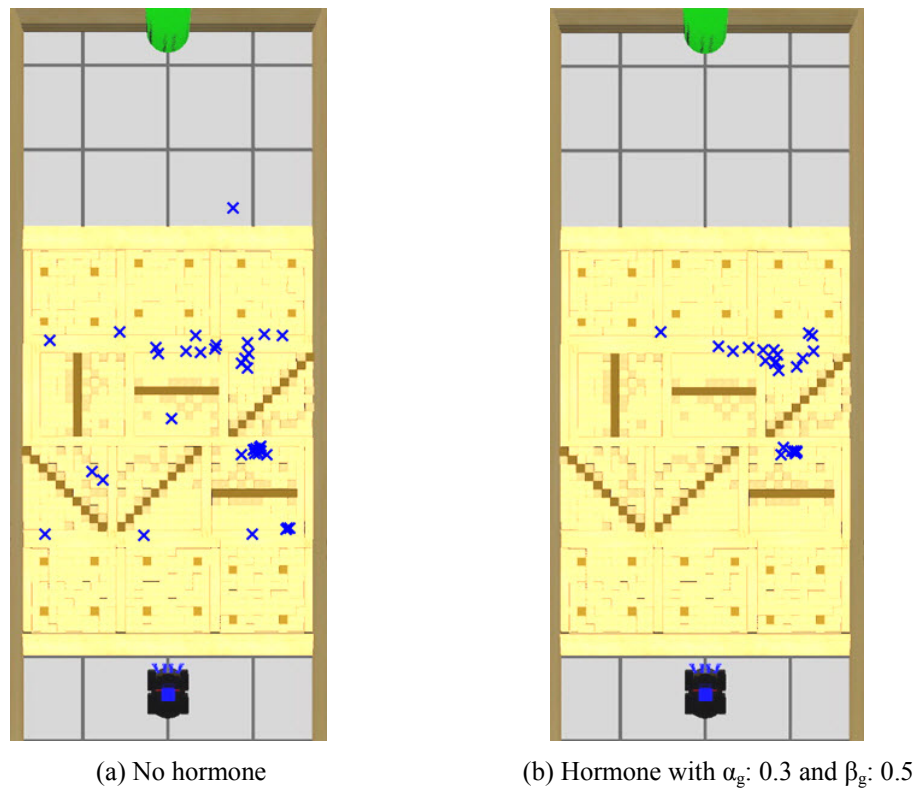


Figure 4.13: The robot tip over positions when (a) there is no hormone implemented on the robot (b) the Terrain Excitation hormone is applied on the robot

From the analysis, it can be stated that the Terrain Excitation hormone can assist the robot to increase the Object Reach and reduce the Tip Over by adjusting the robot speed based on the changes of terrain roughness. However, there remain some areas in the test arena which are too difficult for the robot and the Terrain Excitation hormone to cope with. The main reason is because the areas are too steep and simply decrease the speed of the robot is not enough to avoid tipping over in these areas.

## 4.6 Summary

In this chapter, the structures and mechanisms of the artificial hormone system proposed in this research are described. The first implementation of the hormone system is also exemplified. In the implementation, a Terrain Excitation hormone is proposed in order to help the robot deal with the external environment change considered in this research, the variations of terrain roughness. As identified in the hypothesis section, it is expected that the proposed system can exploit environmental cues to provide adaptability for autonomous robots. The Terrain Excitation hormone implemented in this chapter exploits the variations of the robot pitch angle as an environmental cue to help the robot cope with the changes of terrain roughness. It is noted that instead of attempting to acquire the exact roughness of the terrain to adjust the robot speed, this hormone influences the robot by altering its speed based on the cue from its own pitch sensory information. This information does not specifically identify the terrain profile. However, it can imply the roughness of the terrain and the stability of the robot. For example, if there is an indication of huge and frequent changes of the robot pitch sensory information, this may imply that the robot is moving on a very rough terrain and the stability of the robot is reduced.

From the experiment of the Terrain Excitation hormone, the results also indicate that, with the implementation of the hormone, the robot is likely to deal with the rough terrain better. Identifying with the performance metrics, it shows that, with the appropriate values of  $\alpha_g$  and  $\beta_g$  the robot performances can be improved by up to 14% comparing to when there is no hormone implemented on the robot, moving the robot performance above 75%.

Two other key attributes which have not been elucidated in this chapter but are among the main aspects concerned in this research are the robot's ability to deal with internal

changes and the notion of hormone interactions by the creation of hormone network.  
These two features will be considered in the next chapter.

## **Chapter 5**

# **Implementation of an Artificial Hormone Network**

In the previous chapter, fundamental structures and mechanisms of the artificial hormone system have been elucidated. The implementation of the artificial hormone system in helping an autonomous robot deal with a case of external environmental changes (the changes of terrain roughness) was also presented and discussed. However, this research proposes that the utilizations of the artificial hormone system can not only assist autonomous robots to cope with external environmental changes but also internal environmental changes. The main objective of this chapter is to further illustrate the implementations of the artificial hormone system with the introduction of Artificial Hormone Networks (AHNs) to help autonomous robots as they encounter both internal and external environmental changes. Additionally, this chapter also elucidates the interactions between several hormones by enabling the constructions of hormone networks and illustrating how this can bring benefits to autonomous robots.

There are two AHNs presented in this chapter. Both are proposed principally to handle the internal environmental changes introduced in section 2.6. These are the cases of sensor faults and actuator faults on an autonomous robot. The implementations, experiment results, as well as analysis and discussion of the robot dealing with both internal change scenarios using the AHNs are elucidated. Section 5.1 focuses on the utilization of an AHN to cope with the sensor fault scenario, while section 5.2 is dedicated for the actuator fault scenario. In addition, the summary of this chapter is given in section 5.3.

### **5.1 Artificial Hormone Network 1 (AHN1)**

This section describes the implementation of the Artificial Hormone Network 1 (AHN1), a hormone network designed to assist autonomous robots deal with a case of internal environmental variations induced by a malfunctioning sensor.

### 5.1.1 Background

From the implementation of the robot and the Terrain Excitation hormone explained in section 4.2, it is obvious that one of the key sensors in assisting the robot to deal with different terrain roughness is the pitch sensor. The pitch sensory information is used not only in the main robot controller as information activating the Retreat behaviour when the pitch angle of the robot is more than a critical threshold but the pitch sensory information is also utilized by the artificial hormone system as a cue to adjust the speed of the robot based on the changes of terrain roughness. Lacking the robot's pitch information or even incorrectly acquired data of the sensory information could severely affect the robot performance when the robot is operating in unstructured environments. Therefore, the pitch sensor is considered as an interesting component for applying faults and for investigating how the AHN could assist the robot in dealing with such internal environmental variation.

In biological organisms, there is a condition called "Kinetosis", better known as motion sickness. This is a condition which usually causes nausea and vomiting when there is a mismatch between visually perceived motion and the sense of motion acquired from the vestibular system (inner ears), common on automobile journeys [102, 103]. It is generally understood that the main reason for this condition is a defence against neurotoxin. One of the main reasons for the conflicts between the senses of motion acquired from the vision system and the balancing system is the hallucination occurring on one of them. In addition, because the hallucination can occur by poison ingestion, therefore, when the conflicts occur, the brain then attempts to get rid of the supposed poisons by the stimulation of vomiting [104, 105]. This process displays an interesting ability of biological organisms. This is a capability to obtain similar kind of information (i.e. sense of motion) from environmental cues acquired from different sources of sensory inputs (i.e. vision and vestibular systems) without requiring a dedicated spare system to provide redundancy. Moreover, the process is also able to exploit conflicts between information from both sources as environmental cues to cope with possible internal environmental changes that may affect an organism. It can be noticed that the main purpose of this process is simply to keep an organism functioning well and to increase its chances of survival in the presences of environmental changes. This biological process is the key inspiration of the AHN1 which is mainly proposed to help autonomous robots cope with internal environmental changes in the case of faults in their sensory systems.

From the implementation of the artificial hormone system explained in the previous chapter, apart from the data from the pitch sensor, there is another source of sensory information which can be used to imply the roughness of terrains. This is the sensory information from the frontal area distance infrared sensor. Note that the presence of this sensor on the robot is not directly to provide this information but, as introduced in section 2.4.2, the sensor is used mainly in the robot controller to provide approximate information of the terrain roughness in front of the robot and to activate the Retreat behaviour when an area in front of the robot is too steep. However, this sensory information is also able to provide useful environmental cues for the artificial hormone system to cope with environmental changes. In addition, for this particular robot system, the information obtained from the infrared sensor is normally directly correlated to the information acquired from the pitch sensor: changes in the infrared sensor data usually result in corresponding changes in the pitch sensory information of the robot. Therefore, when sensory conflicts between pitch and frontal area distance occur, these can imply that there might be faults or changes occurring on the sensors. For example, if changes are detected from the frontal area distance data, this can imply that the area in front of the robot is rough. However, if subsequently there are no changes detecting on the pitch sensory information, this can indicate that there might be faults occurring on the pitch sensor. The implementation of the AHN1 inspired from this insight is illustrated in the next sub-section.

### **5.1.2 Implementation of AHN1**

Figure 5.1 presents the structures of AHN1 and its connections to the main robot controller. There are three HGs and two HRs in this hormone network. Note that the HG1 and HR\_MC are the same components proposed in the artificial hormone system explained in the previous chapter. The two new additional HGs forming the hormone network are HG2 and HG3. HG2 is considered similar in functionality with the HG1 except that this particular gland responds to the sensory information from the frontal area distance infrared sensor, instead of the pitch sensory information. Therefore, the HG2 can also secrete the Terrain Excitation hormone (similar to the HG1). However, this gland utilizes the variations of the frontal area distance data as an environmental cue for the stimulation of the hormone.

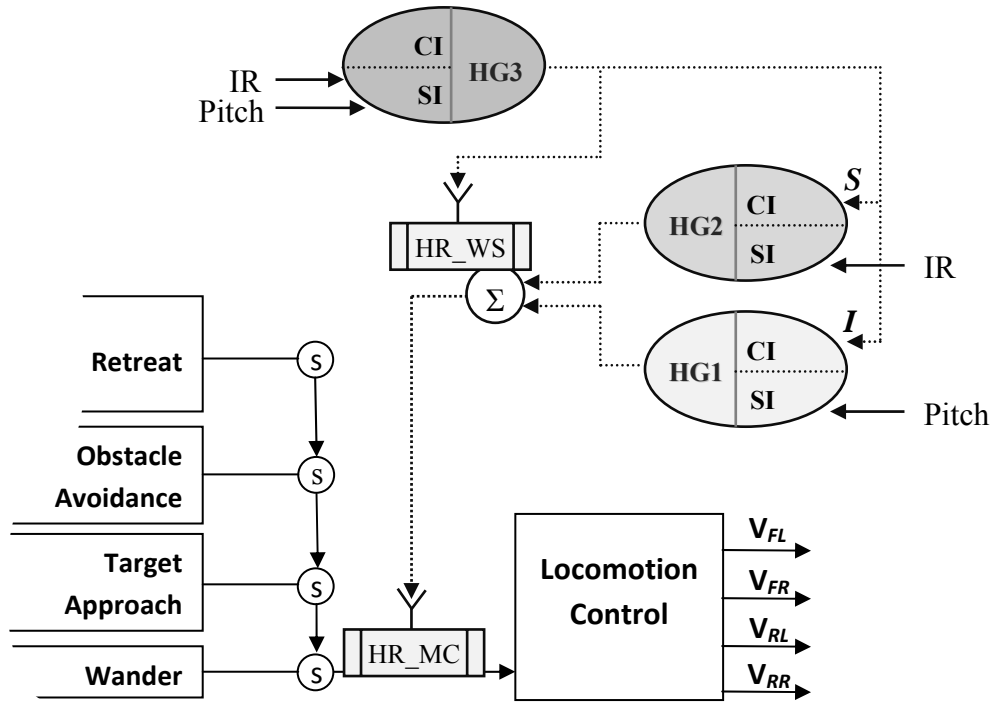


Figure 5.1: The AHN1 and its connection with the main robot controller

HG3 is responsible for the secretion of a hormone called Pitch-Conflict hormone. This HG secretes the hormone in response to the conflicts of the pitch sensory information from the frontal area distance data. As shown in Figure 5.1, HG3 takes pitch and frontal area distance information as its inputs. The environmental cues which are used as the key signals for the stimulation of the Pitch-Conflict hormone is the conflicts of the pitch sensory information from that of the frontal area distance data. The identifying conflicts are obtained from a preliminary experiment in the case when the pitch fault occurs. In this implementation, only the case of internal environmental changes induced by the pitch fault is considered because the robot mainly uses pitch sensory information to deal with terrain roughness, as previously illustrated in chapter 4. However, this is not restrictive. Environmental cues indicating faults in the infrared sensor or any other environmental changes can also be exploited. This issue will be further illustrated in chapter 7. In addition, it can be noticed that the Pitch-Conflict hormone is connected to both the *CI* inputs of HG1 and HG2. The hormone is connected to HG1 via the Inhibitory control feature but to HG2 via the Stimulatory control feature. This indicates that when the sensory conflict is not significant or does not permanently exist (resulting in a low concentration of Pitch-Conflict hormone), it motivates the HG1 to secrete the Terrain Excitation hormone but inhibits the secretion of the hormone from the HG2. On the contrary, when the Pitch-Conflict hormone concentration is increased to a certain

level (generally caused by the significant and frequent sensory conflicts), the production of HG1 hormone is inhibited and HG2 then starts to produce the Terrain Excitation hormone instead. This dynamic allows the AHN1 to alter its systems by changing the sensory information (environmental cue) used for the secretion of the Terrain Excitation hormone depending on the changes of the robot's internal systems. Therefore, when faults are occurring on the pitch sensory information, the AHN1 remains capable of influencing the robot wheel speed based on the terrain roughness by using the frontal area distance data instead.

It is important to note that although the implementation of the AHN1 might be considered rather similar to dual-channel fault-tolerance systems in traditional safety critical systems [106, 107, 108], the key purposes of both systems are fundamentally different. In the case of dual-channel fault-tolerance systems, its main purpose is specifically to cope with faults (one way is by providing redundancy in the form of dedicated additional sensing channels). However, for the AHN1, its main focus is not on fixing specific faults but rather on maintaining homeostasis of a system when encountering with internal and external environmental changes using hormone dynamics. It is only because some cases of internal environmental changes can be induced by component's faults (as considered in this research). In addition, as explained previously, rather than requiring a dedicated spare sensor, inspired by biological processes, the AHN1 acquires and responds to environmental cues from another available sensor already equipped on the robot, in order to help the robot to adapt and deal with both internal and external environmental changes.

Figure 5.1 also displays a distinguish feature of AHNs comparing to other previous artificial hormone systems, especially the Artificial Endocrine System (AES). This is the ability of AHNs which allows connections and interactions between several difference hormones by the construction of hormone networks. This feature helps AHNs to provide adaptability for autonomous robots in several different application scenarios, as will be shown further in this thesis.

The settings of inputs and mechanisms of HG1, HG2 and HG3 are shown in Figure 5.2 (a), (b) and (c) respectively. From Figure 5.2 (a) and (b), it can be noticed that both HG1 and HG2 is almost identical with the exception of the different signal inputs and the opposite control features set. Note that the Threshold values of 0.85 are empirically acquired from a preliminary experiment. The process of detecting conflicts of the pitch sensory information from the frontal area distance data utilized by HG3 is further

clarified below. In general, the conflicts are identified by the comparison between the estimated trends of the variations in the pitch sensory information and the variations in the frontal area distance data. The correlation of the sensory information is determined when both types of sensory information are following the same trends. From Figure 5.2 (c), HG3 processes the trends of sensory information in the Signal pre-processor. The variations of the sensory information are obtained by applying the SDs on the pitch sensory information and on the frontal area distance data in order to firstly acquire the changes of both types of information over a specified period of time. The slopes of both types of sensory information are then calculated over a specified period of time to obtain the estimated trends. Subsequently, the values of the trends are normalized to three cases (represented by three values). These are:

- (1): when the trends indicate positive slopes. This information implies that the roughness of terrain is likely to increase.
- (0): when the trends indicate zero slopes. This situation can either imply that the terrain is flat or the roughness of the terrain is constant.
- (-1): when the trends indicate negative slopes. This implies that the terrain roughness is likely to decrease.

The comparisons of the normalized trends (which identify the stimulation of the Pitch-Conflict hormone) are then performed in the Activation function of the HG3. A conflict is issued when the normalized trends at a specific time step of the sensory information from both sensors are not correlated. For example, when the normalized trend of frontal area distance data is (1) but the normalized trend of pitch sensory information is (-1). Note that the comparisons occur only when the normalized trend of frontal area distance data is not (0). The main reason is to prevent the HG3 from responding to the case of faults which might occur on the IR causing the sensor to report a constant value of zero. In addition, as explained previously, it can be noticed that HG3 only responds to conflicts of the pitch sensory information from the frontal area distance data. Although conflicts between the sensory information can happen because of either fault from the pitch or IR sensors, faults from IR are not considered by the HG3 because the robot mainly uses the sensory information from the pitch sensor to deal with rough terrain. However, this is by no means restrictive. With some modifications, faults on the frontal area distance data (or even on other sensory information) can be considered by the hormone networks. This issue will be discussed further in the generalization methods discussed in Chapter 7.

HG1		
<b>Signal inputs</b>	$SI_1$	Pitch angle of the robot (Pitch)
<b>Control inputs</b>	$CI_1$	Pitch Conflict hormone
<b>Signal pre-processor</b>	Standard deviation (SD)	$SI_{feature} = SD(SI_1)$
<b>Control features</b>	$CI_1$	Inhibitory control
<b>Threshold values</b>	$Th_1$	0.85
<b>Activation function</b>	Scaling linear function	$ActLevel = SI_{feature} / \maxLimitSDPitch$ <b>IF</b> $ActLevel > 1$ $ActLevel = 1$

(a)

HG2		
<b>Signal inputs</b>	$SI_1$	Frontal area distance data (IR)
<b>Control inputs</b>	$CI_1$	Pitch Conflict hormone
<b>Signal pre-processor</b>	Standard deviation (SD)	$SI_{feature} = SD(SI_1)$
<b>Control features</b>	$CI_1$	Stimulatory control
<b>Threshold values</b>	$Th_1$	0.85
<b>Activation function</b>	Scaling linear function	$ActLevel = SI_{feature} / \maxLimitSDIR$ <b>IF</b> $ActLevel > 1$ $ActLevel = 1$

(b)

HG3		
<b>Signal inputs</b>	$SI_1$	Frontal area distance data (IR)
	$SI_2$	Pitch angle of the robot (Pitch)
<b>Control inputs</b>	-	-
<b>Signal pre-processor</b>	Trend estimation	$SD1 = SD(SI_1)$ $SD2 = SD(SI_2)$ $Trend1 = Slope(SD1[x])$ $Trend2 = Slope(SD2[x])$ $SI_{feature}[Trend1, Trend2] = Normalize(Trend1, Trend2)$
<b>Control features</b>	-	-
<b>Activation function</b>	uncorresponding data detection	<b>IF</b> $SI_{feature}[Trend1] \neq 0$ <b>IF</b> $SI_{feature}[Trend1] \neq SI_{feature}[Trend2]$ $ActLevel = 1$ <b>THEN</b> $ActLevel = 0$ <b>ENDIF</b> <b>THEN</b> $ActLevel = 0$ <b>ENDIF</b>

(c)

Figure 5.2: The settings of (a) HG1 (b) HG2 (c) HG3 in the AHN1

Note also that each HG, in the AHN1, is set to have an implicit negative feedback control from its own hormone output. This feature is included in order to prevent the over saturation of hormone production on each gland as suggested in [85]. Therefore, the hormone release function of each HG which is used to define the hormone concentration at each time step is slightly modified from equation 4.1 (explained in section 4.1.1.1 and is redefined here in equation 5.1) to equation 5.2.

$$C_g(t) = ( \alpha_g \cdot ActLevel(t) ) + ( \beta_g \cdot C_g(t-1) ) \quad (5.1)$$

$$C_g(t) = ( \alpha_g \cdot \frac{ActLevel(t)}{(1 + C_g(t-1))} ) + ( \beta_g \cdot C_g(t-1) ) \quad (5.2)$$

As explained previously, the AHN1 enables the hormone system to change the sensory information used for the secretion of the Terrain Excitation hormone, however this is also not mandatory. Rather than switching from one type of sensory information to another, the AHN1 can also be used to only adjust the influential levels from several types of information. This is achievable with the inclusion of the Weight-Sum Hormone Receptor (HR\_WS). Illustrated in Figure 5.1, this hormone receptor is located at the conjunction between the Terrain Excitation hormone generated from the HG1 and from the HG2. Therefore, this HR can alter the weighting factors of the Terrain Excitation hormone generated from each gland. In principle, the influential level of the hormone generated from each gland can be changed to any values based on the concentration of the Pitch-Conflict hormone presented at the HR\_WS. This allows the Terrain Excitation hormone to be built up simultaneously from both types of information but with different confident levels.

However, for the experiment explained in the next section, only the case of entirely switching from one type of sensory information to another is investigated, thus the adjustments of the weight-sum based on the hormone concentration are not illustrated.

### 5.1.3 Experiment Setup

The test environment and robot used in this experiment is shown in Figure 5.3. There are two test scenarios in this experiment: when there is no fault induced on the pitch sensor and when a fault is introduced on the pitch sensory information. Note that the pitch fault implemented in this experiment is the case of stuck-at-zero. The pitch sensor always reports a constant value of zero. This situation causes the robot to be unaware of its actual pitch angle. Also note that the fault is injected immediately at the beginning of each run.

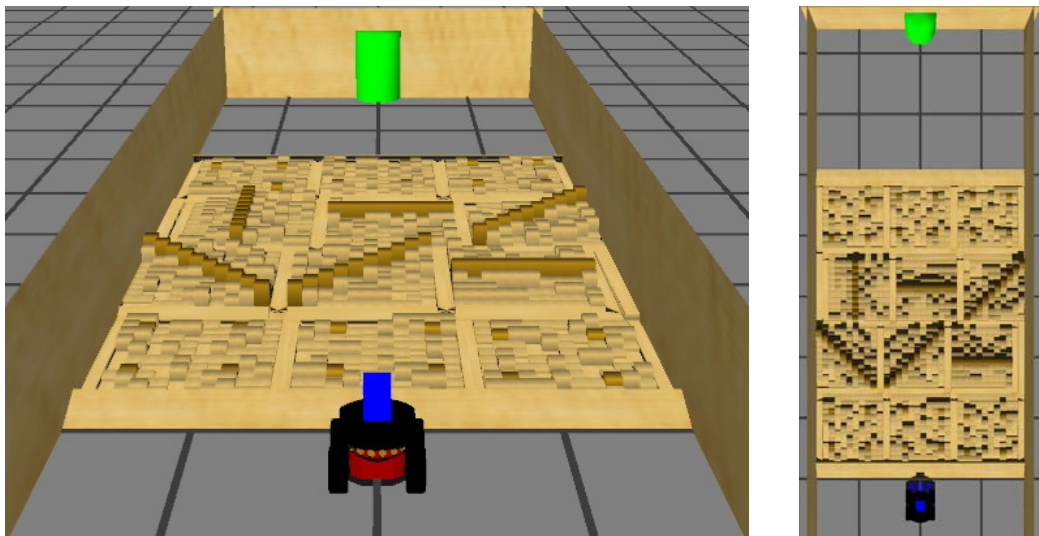


Figure 5.3: The robot and test arena used for the experiment of the AHN1

The  $\alpha_g$  and  $\beta_g$  values of each HG in the AHN1 are empirically acquired and set as shown in Table 5.1. This set of parameters is among the sets which provide best results in preliminary experiments. However, with an implementation of automatic methods for optimizing these parameters (e.g. evolutionary techniques), there may be some small improvements in the performance. However, this is considered a future work.

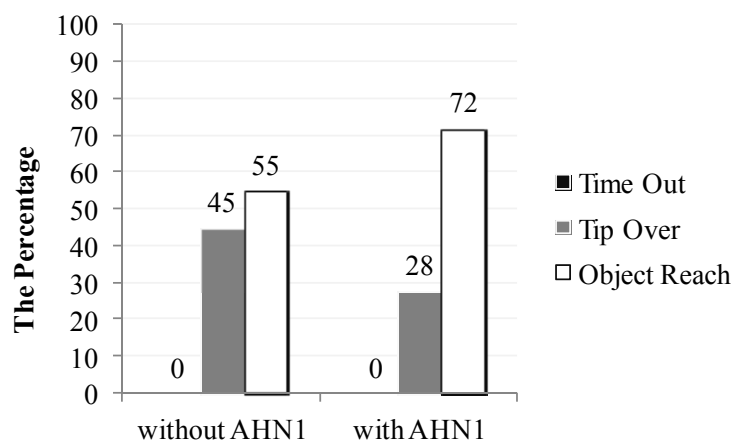
Table 5.1: The values of  $\alpha_g$  and  $\beta_g$  of each hormone gland in AHN1

	$\alpha_g$	$\beta_g$
<b>HG1</b>	0.3	0.5
<b>HG2</b>	1.0	0.9
<b>HG3</b>	0.2	0.8

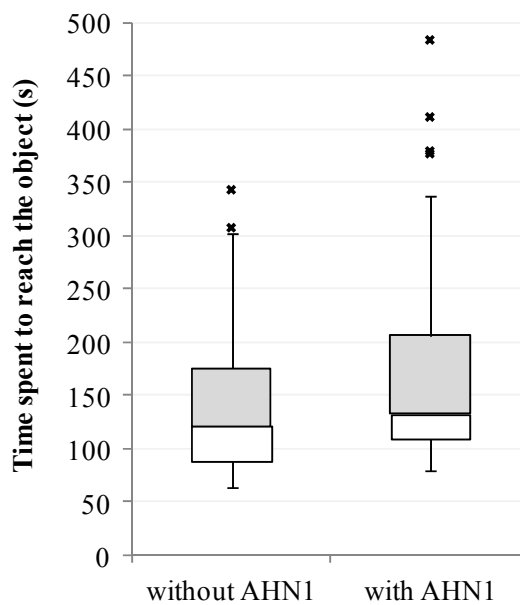
There are two test cases investigated in each test scenario. These are the cases when there is and there is no AHN1 implemented on the robot. Similar to the experiment in the previous chapter, each case is tested for 100 runs and the robot is allowed to perform its task for 15 minutes. The robot performance in achieving both test scenarios is presented in the next sub-section.

### 5.1.4 Results

Figure 5.4 and Figure 5.5 present the robot performance in the cases when there is no pitch fault implemented and when the pitch fault is injected to the robot respectively.



(a)



(b)

Figure 5.4: The robot performance in the fault free scenario (a) reporting in Time out, Tip Over and Object Reach metrics (b) displaying in box plots of time spent the robot uses to reach the target object

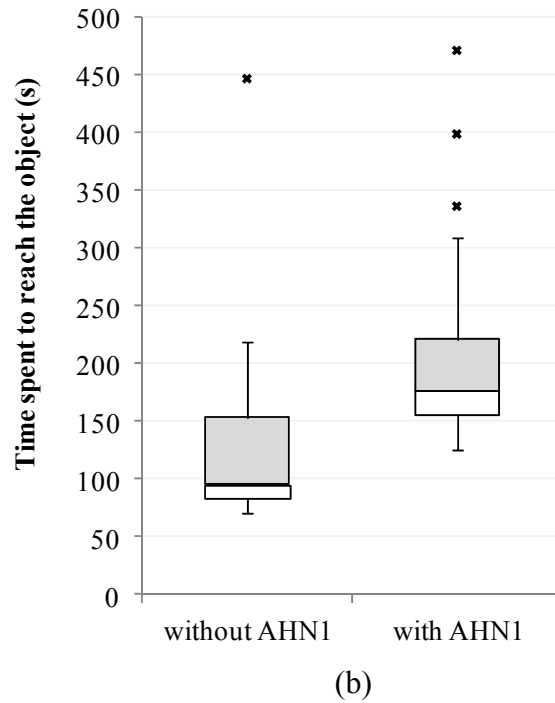
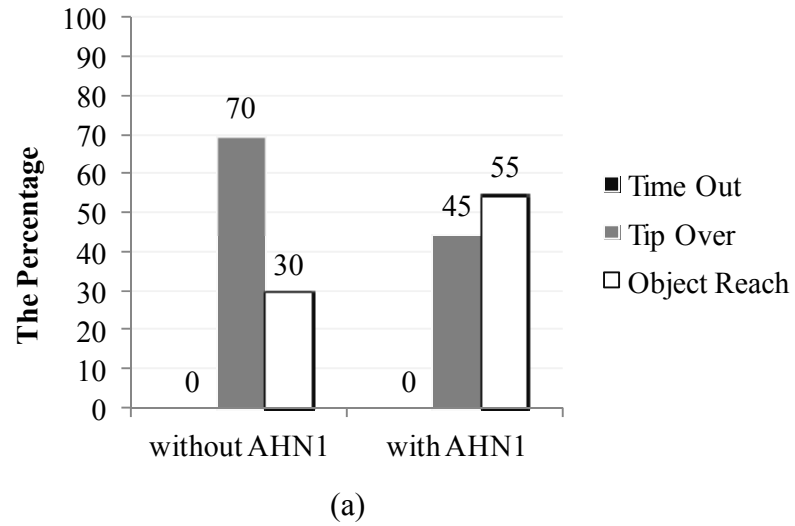


Figure 5.5: The robot performance in the pitch fault scenario (a) reporting in Time out, Tip Over and Object Reach metrics (b) displaying in box plots of time spent the robot uses to reach the target object

From the results of the robot performance in the fault free scenario (Figure 5.4 (a)), with the implementation of AHN1 on the robot, the robot performance is improved by 17% (to reach 72%) comparing to the case when there is no AHN1 implemented on the robot. Without the AHN1, however, the robot is still able to reach the target object at 55%.

Comparing the results on both scenarios, it can be observed that the pitch fault can severely affect the robot's performance. Without the AHN1, the number of times the object is reached is reduced by 25% (to 30). With the AHN1, the robot performance is also decreased by 17% (to 55) comparing to when there is no pitch fault. However, when the pitch fault occurs, with the AHN1, the robot performance remains better than when there is no AHN1 implemented. Actually, the robot is still able to keep its performance similar to when there is no pitch fault and the AHN1 is not implemented on the robot (55%).

From Figure 5.4 (b) and Figure 5.5 (b), the results also show that with the implementation of the AHN1, the robot requires longer time to reach the target object. This is a direct consequence of the speed adjustment effects from the hormone network. Further analysis and discussion on how the AHN1 can remain helpful for the robot even with the presence of the pitch fault is presented in the next sub-section.

### **5.1.5 Discussion and Analysis**

It has to be noted that when the pitch fault is injected to the robot systems, this can affect not only the main robot controller (unable to activate the Retreat behaviour when the robot pitch angle is critical) but also the artificial hormone system (no stimulation on the Terrain Excitation hormone from changes of the pitch sensory information). As a consequence, the robot performance is decreased when the pitch fault occurs. However, with the implementation of the AHN1, even when the pitch fault occurs, the AHN1 remains capable of secreting the Terrain Excitation hormone by using the sensory information from the frontal area distance infrared sensor instead, which results in the better robot performance reported. The ability of the robot to adapt to the internal environmental change is the direct consequences from the dynamic interplay between hormones in the AHN1. These interactions of the hormones are illustrated in the next sub-section.

#### **5.1.5.1 The Hormone Interactions**

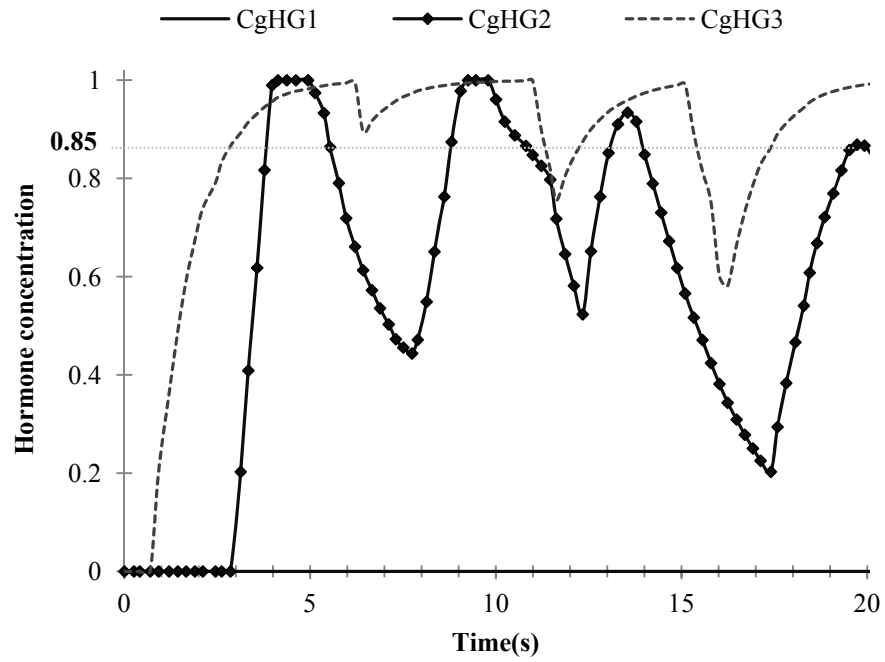
In order to illustrate the interplays between hormones in AHN1, Figure 5.6 (a), Figure 5.7 (a) and Figure 5.8 (a) show examples of the hormone interactions when the pitch fault is injected in the robot at different times; these are at 0, 9 and 15 seconds,

respectively. Note that the threshold values of the Pitch-Conflict hormone concentration ( $C_gHG3$  – the dotted line) which are set to activate or deactivate the stimulation of the Terrain Excitation hormone from the HG1 and HG2 are 0.85.

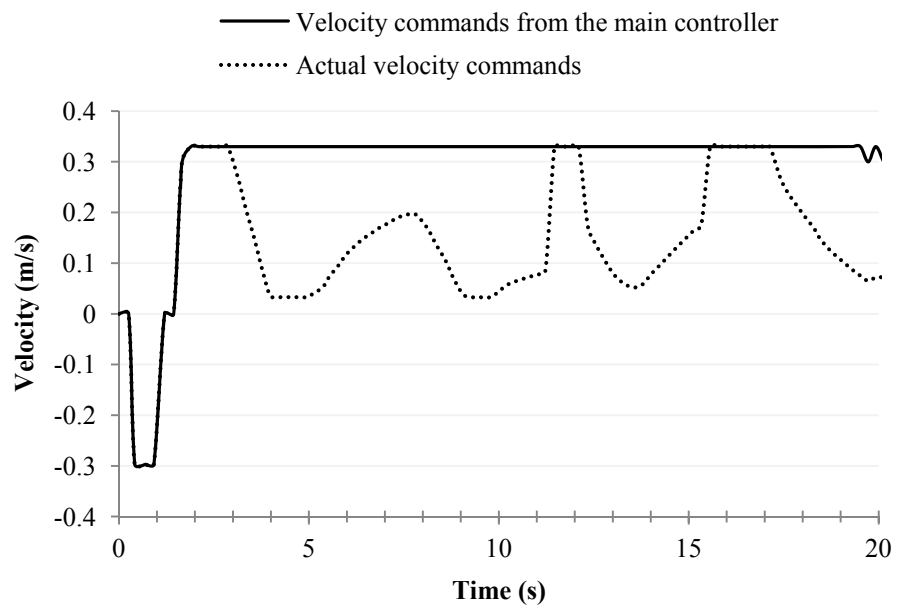
In Figure 5.6 (a) when the pitch fault is injected from the start of the run, it can be noticed that the Pitch-Conflict hormone ( $C_gHG3$  – the dotted line) begins to build up almost immediately from the start. In addition, since the pitch fault is injected from the beginning, the HG1 hormone is never built up as the pitch sensor always report the constant value of zero. Considering the robot velocity shown in Figure 5.6 (b), it can be seen that the robot remains able to reduce its speed even in the presence of the pitch fault by responding to the  $C_gHG2$  (the dotted full black line) instead.

In Figure 5.7 (a) when the pitch fault is injected after 9 seconds, at the beginning, the concentration of the Pitch-Conflict hormone is lower than the threshold value because there are no significant or frequent conflicts between the sensory information. In this time period, the secretion of the Terrain Excitation hormone is responsive to the changes of the robot pitch angle ( $C_gHG1$  – the solid line), while HG2 remains inactive. However, after 9 seconds, the Pitch-Conflict hormone concentration begins to build up from the accumulation of sensory conflicts occurring. Until at around 12 seconds, when the hormone concentration of HG3 exceeds the threshold value, HG2 then starts to secrete its hormone and the secretion of the Terrain Excitation hormone is then taken over by HG2. Figure 5.7 (b) illustrates that there is no difference between the velocity commands from the main controller and the actual velocity commands in the first 5 seconds. In the period between 5 to 10 seconds, the robot velocity is reduced based on the changes of HG1 hormone. However, after 12 seconds, even though there is no presence of the HG1 hormone, the robot velocity can also be decreased but now corresponding to the concentration of HG2 hormone instead.

Rather Similar to Figure 5.7, in Figure 5.8 when the pitch fault is injected after 15 seconds, it can be noticed that the HG2 hormone is kept inactive almost of the time from the beginning and the robot velocity responses directly to the HG1 hormone. Until at 19 seconds when  $C_gHG3$  exceeds the threshold, the  $C_gHG2$  then starts to build up and the robot velocity begins to respond to the HG2 hormone.

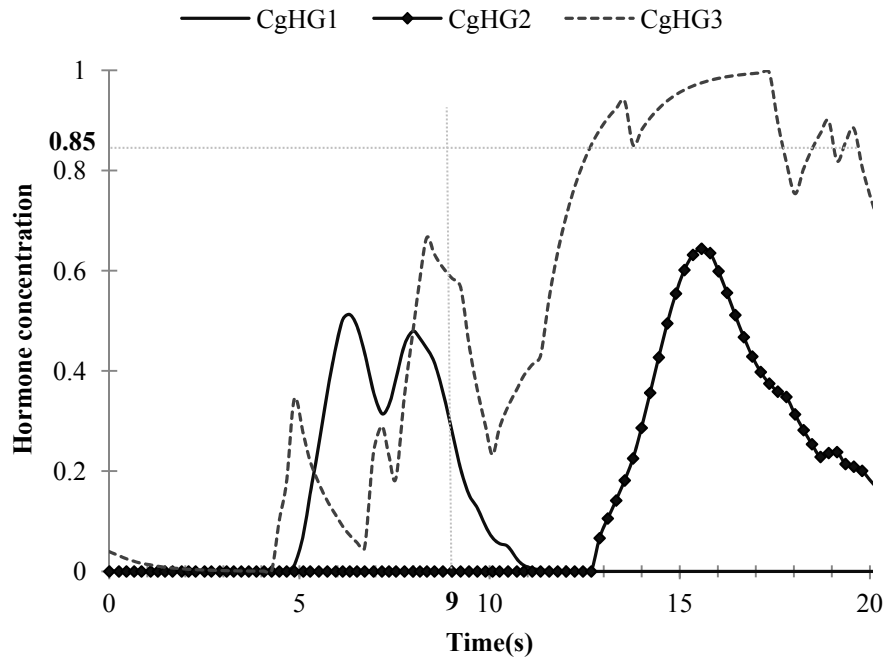


(a)

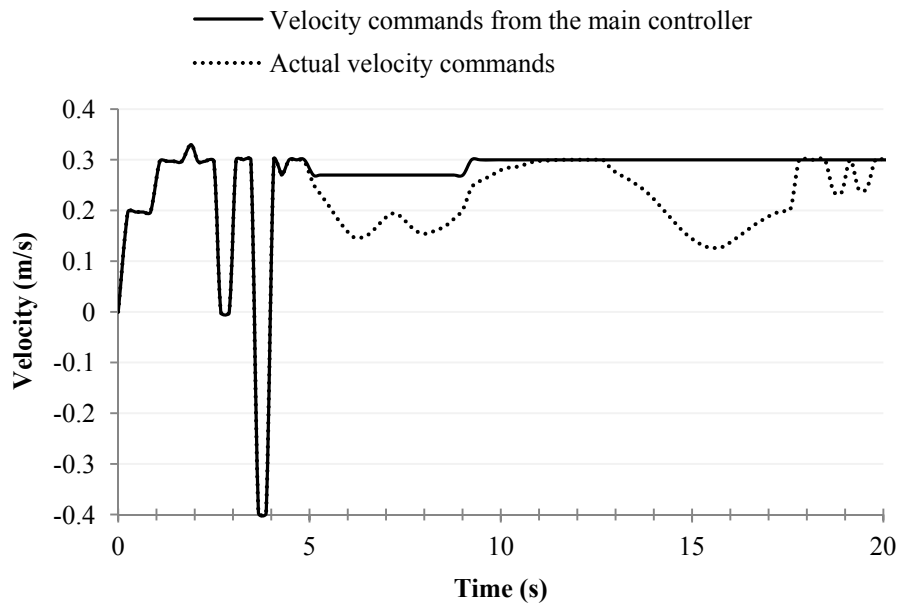


(b)

Figure 5.6: (a) An example of the hormone interactions in AHN1 from a single robot run when the pitch fault is injected from the beginning of the run (b) The robot wheel velocity corresponding to the hormones shown in (a)



(a)



(b)

Figure 5.7: (a) An example of the hormone interactions in AHN1 from a single robot run when the pitch fault is injected after 9 seconds (b) The robot wheel velocity corresponding to the hormones shown in (a)

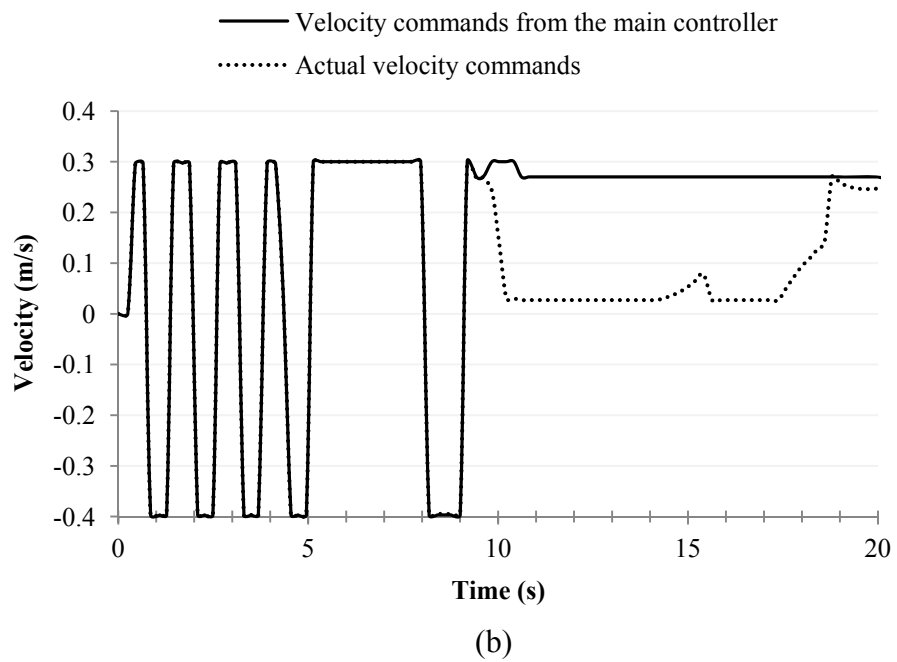
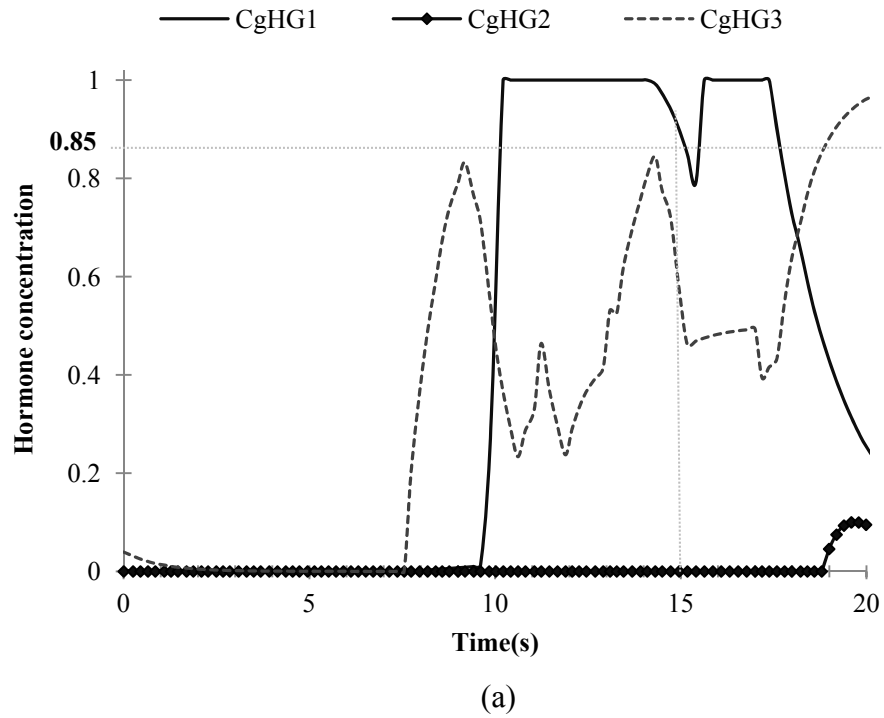


Figure 5.8: (a) An example of the hormone interactions in AHN1 from a single robot run when the pitch fault is injected after 15 seconds (b) The robot wheel velocity corresponding to the hormones shown in (a)

### 5.1.5.2 Tip Over Positions

The influence of the AHN1 in helping the robot deal with both the internal and the external environmental changes can also be observed from the tip over positions of the robot. Figure 5.9 and Figure 5.10 illustrate the tip over positions of the robot in the fault free and pitch fault scenarios respectively.

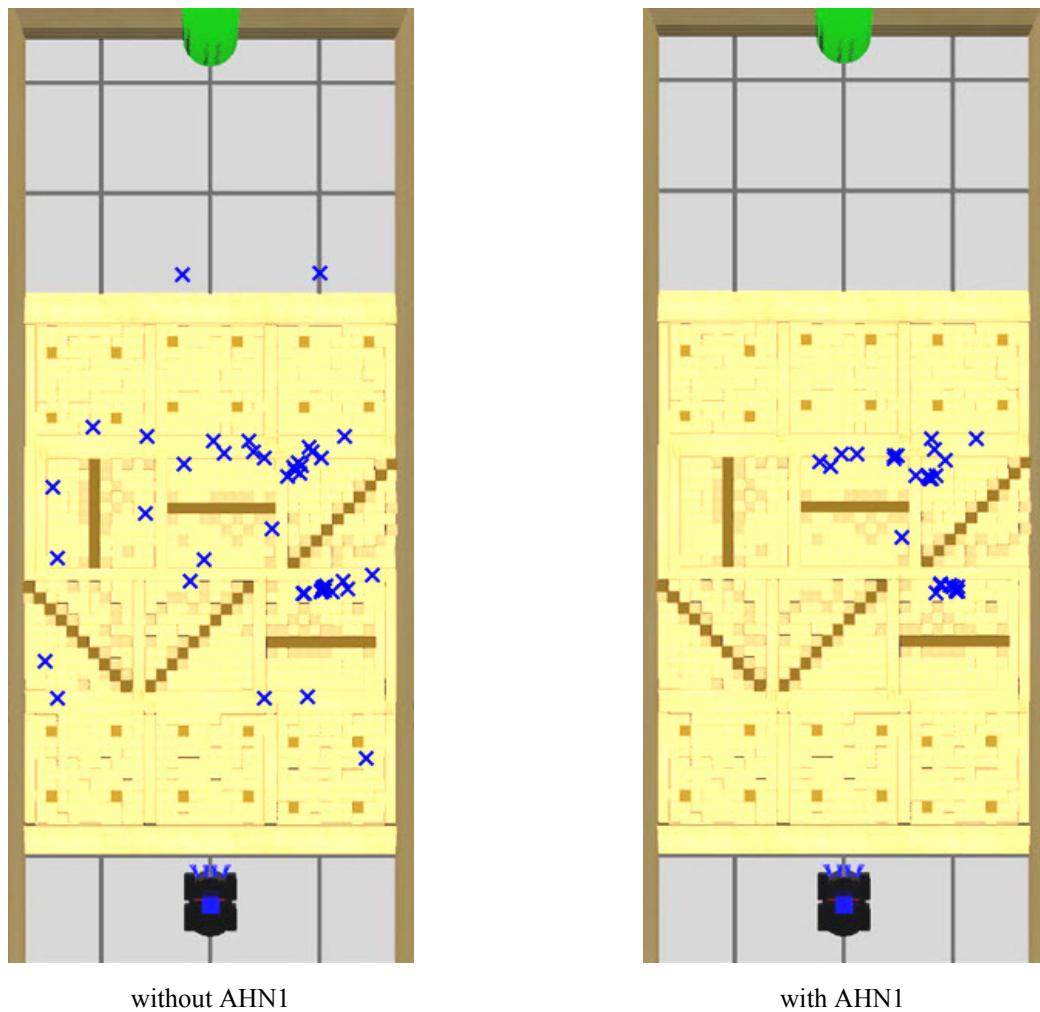


Figure 5.9: The tip over positions of the robot in the fault free scenario

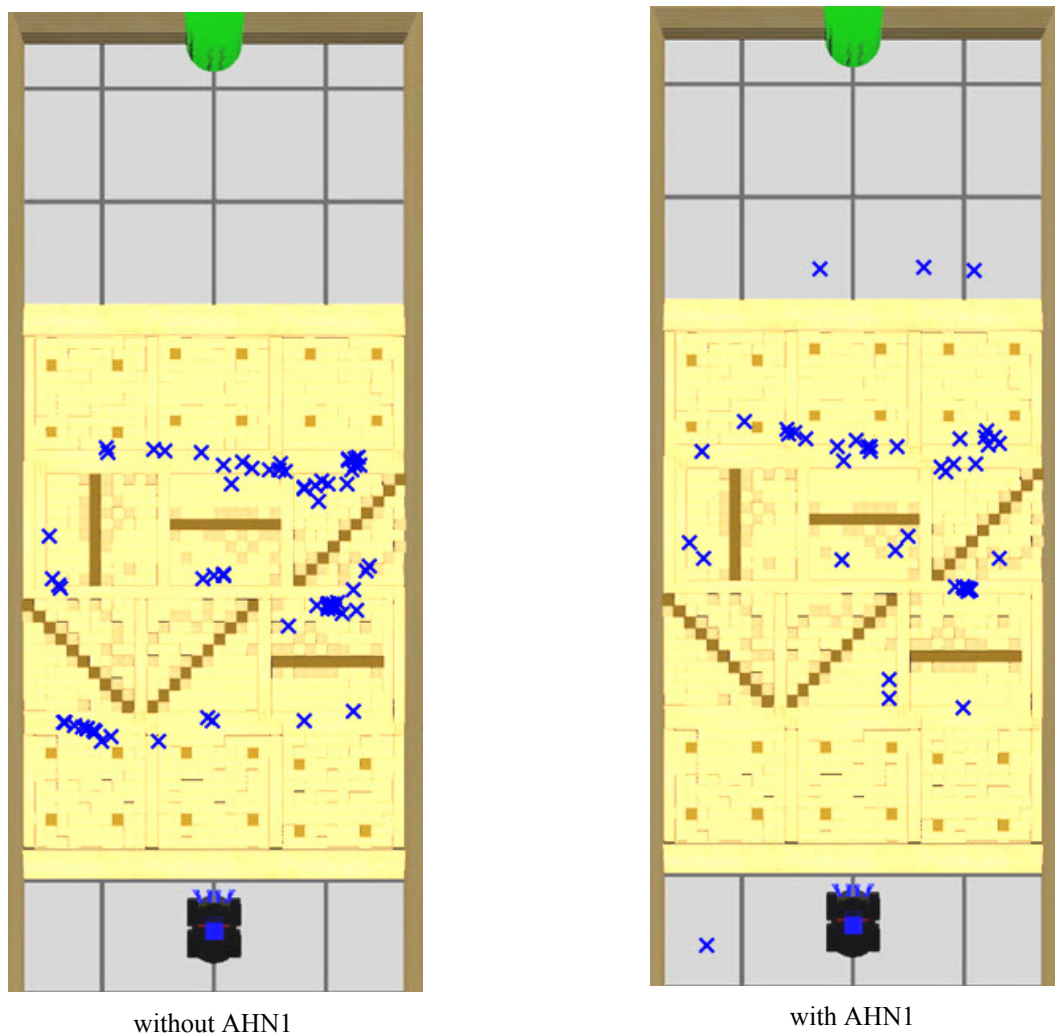


Figure 5.10: The tip over positions of the robot in the pitch fault scenario

It is shown in Figure 5.9 that, without the AHN1, the robot's tip over positions are spread widely over the rough areas of step-fields 2x and 3x. However, with the addition of the AHN1, the areas in which the robot tips over are reduced to be mainly on the upper parts of the step-fields 23 and 33. Comparing to the case when the pitch fault occurs (Figure 5.10), it can be observed that losing the ability to sense the pitch angle significantly increases the robot's chances of tipping over and widens the areas in which the robot tips over. Nevertheless, with the inclusion of the AHN1, the robot can increase its chances of survival comparing to when the pitch fault occurs but no AHN1 is implemented on the robot. The tip over positions show that the AHN1 helps reduce the number of tips over on some difficult areas such as the step-field 23 and 33 (less dense marks) and entirely prevent the tips over when the robot negotiates the diagonal hills around the step-filed 21 and 22.

The ability of the AHN1 in helping the autonomous robot cope with the case when an internal environmental change occurs on the robot sensor is shown in this section. There is also another crucial case of internal environmental changes on the robot considered in this research. The situation is further described and investigated in the next section.

## **5.2 Artificial Hormone Network 2 (AHN2)**

In the previous section, the AHN1 is assisting an autonomous robot to deal with a case of internal environmental changes induced by a fault in a sensory unit of the robot. This section explores the Artificial Hormone Network 2 (AHN2), a hormone network designed to cope with a second case of internal environmental changes considered in this research. This internal environmental change is the case when a fault occurs in the main locomotion systems, one of the robot's wheels. For a wheeled robot, faults occurring on the robot's wheels could severely affect the robot and could entirely ruin robot missions. The wheel fault considered in this research is the case when a robot wheel stops responding to any commands from the robot's controller. However, the wheel rotor is not locked, thus the wheel remains able to be turned freely by external forces applied to the wheel. The implementation of this type of faults can affect the robot movement and decrease the possibility of the robot accomplishing its tasks when the robot is operating in both flat and rough terrain environments. Therefore, the investigations of this type of internal environmental variations will be evaluated in both environments.

### **5.2.1 Background**

The locomotion system of the Pioneer-2 AT robot employed in this research (in simulation) is a 4-wheeled skid-steering drive mechanism. For this type of locomotion systems, the robot movements are normally controlled by the relative velocities of the left and the right side wheels of the robot. This is rather similar to the movement control exhibited in the differential-drive mechanism, except that the skid-steering drive mechanism also requires the presence of wheel slippage when making a turn because all wheels are aligned longitudinal [109, 110]. Because of the relations with the ground-wheel interactions and the skidding effects applied on the robot's movements, acquiring the kinematic model of such system is usually very complex as shown in work

presented in [109, 111]. An alternative way is to employ a simpler kinematic model based on the differential-drive mechanism (i.e. assuming non-slip and pure-rolling conditions [112]). For this mechanism the robot will move in a straight line (without rotation) when the velocities of the left and the right side wheels are equal. While the same speed on the left and the right side wheels of the robot, but in the opposite directions, normally causes the robot to rotate (without the transition). Other different wheel velocities will result in the combination of both transition and rotation of the robot corresponding to the velocity on either side [113]. Therefore, these types of the locomotion systems (skid-steering and differential drive mechanisms) are normally very sensitive to disturbance because only slight changes in the velocity of each wheel or in the ground-wheels reaction forces can easily change the robot course. This is one of the main reasons for the changes in orientations when the robot is moving on rough terrain, mentioned in section 4.2.1. Furthermore, it is not only the effects from external environments which can change the robot's movements but also the effects from internal environments, such as the existence of faults on the robot's wheels, also play a big part in affecting the movements of the robot.

When the changes of the robot movements occur, however, one key source of information which could imply the errors of the robot's movements is the conflicts between the robot's target turn velocity (commanded from the robot controller) and the robot's actual turn velocity. Note that, normally, the actual turn velocity of a robot can be obtained approximately using gyroscopes or IMUs [114, 115]. Therefore, when a difference between the robot's actual turn velocity and the robot's target turn velocity is detected, this environmental cue could imply that there might be an effect from either internal or external environmental changes on the robot. A possible effective way for the robot to response to these changes is by making velocity compensations on its wheels. Responding to the environmental cue in this way is expected to help retain the moving directions and maintain the travelling routes of the robot.

The implementation of the AHN2 is proposed based on the concepts explained. There are two levels of velocity compensations which can be induced by the AHN2.

- 1) When the conflicts between the target turn and the actual turn of the robot are not permanent or frequent (these may be evoked by temporarily wheel slippage, non-permanent external forces or transient faults), the AHN2 will encourage the robot to make a transient velocity compensation corresponding to the cues.

- 2) When the differences are detected permanently or frequently (these may be happened because of regular external forces or permanent robot faults), this situation will induce the robot to adjust its kinematic model with an aim to update the model as close to the current robot's conditions as possible.

### **5.2.2 Implementation of AHN2**

Overall, there are three main groups of Hormone Glands, which are HG4x, HG5x and HG6x, in the proposed AHN2 as shown in Figure 5.11. The HG4x (contains HG41 and HG42) is the fundamental group of HGs in the AHN2 which respond to the environmental cue of the conflicts between the target and actual turn velocity of the robot. This hormone group is considered the key driver of the whole hormone network in the AHN2. As shown in the figure, the hormones generated from HG41 and HG42 are connected to the Control Inputs of the remaining HG in the network via the stimulatory control feature. This simply means that without the HG41 and HG42 hormones, the remaining HGs would not be activated. The main reason is because the differences between the target and actual turn velocity of the robot are the key environmental cues which urge the robot to respond to effects from environmental changes. Without the indications of the robot's turn velocity errors, there is no need for the robot to make the velocity compensations. In general, HG41 and HG42 are considered to have the same functionality. Both glands take the same inputs but respond to opposite cues. HG41 hormone is stimulated by a situation when environmental cues imply that the robot is turning more to the right than desired. On the other hand, HG42 responds to the environmental cues which imply that the robot is turning more to the left. Therefore, when the hormone concentration of HG41 hormone is built up, it can be implied that the robot is turning more to the right. In contrast, the build up of HG42 hormone concentration implies that the robot is turning more to the left. Note that for the robot systems used in the research, when the robot is turning right (clockwise), the turn velocity is measured in negative values. When the robot is turning left (counter-clockwise), the turn velocity is measured in positive values.

HG5x (contains HG51, HG52, HG53 and HG54) is responsible for the changes of the robot kinematic model. The HGs in this group respond to the conflicts between the target forward velocity and the actual forward velocity on either side of the robot. As shown in Figure 5.11, HG51 and HG52 handle the conflicts on the right side of the

robot, while HG53 and HG54 handle the conflicts on the left side of the robot. Note that the velocity on either side of the robot is measured as the average between the velocity of the front and the rear wheel on each side. HG51 secretes its hormone when the actual right side forward velocity is faster than expected, whereas HG52 secretes its hormone when the actual right side forward velocity is slower than expected. HG53 and HG54 operate in a similar way to HG51 and HG52 but are responsible for the left side of the robot.

HG6x (contains HG61 and HG62) directly responds to the HG4x hormones. When the hormone concentrations of HG41 and HG42 are more than the thresholds set on HG61 and HG62 respectively, the hormone concentrations of HG41 and HG42 can directly stimulate the production of hormones HG61 and HG62. Therefore, the secretion of the HG61 hormone can imply that the robot is turning more to the right than expected, while the secretion of the HG62 hormone can imply that the robot is turning more to the left.

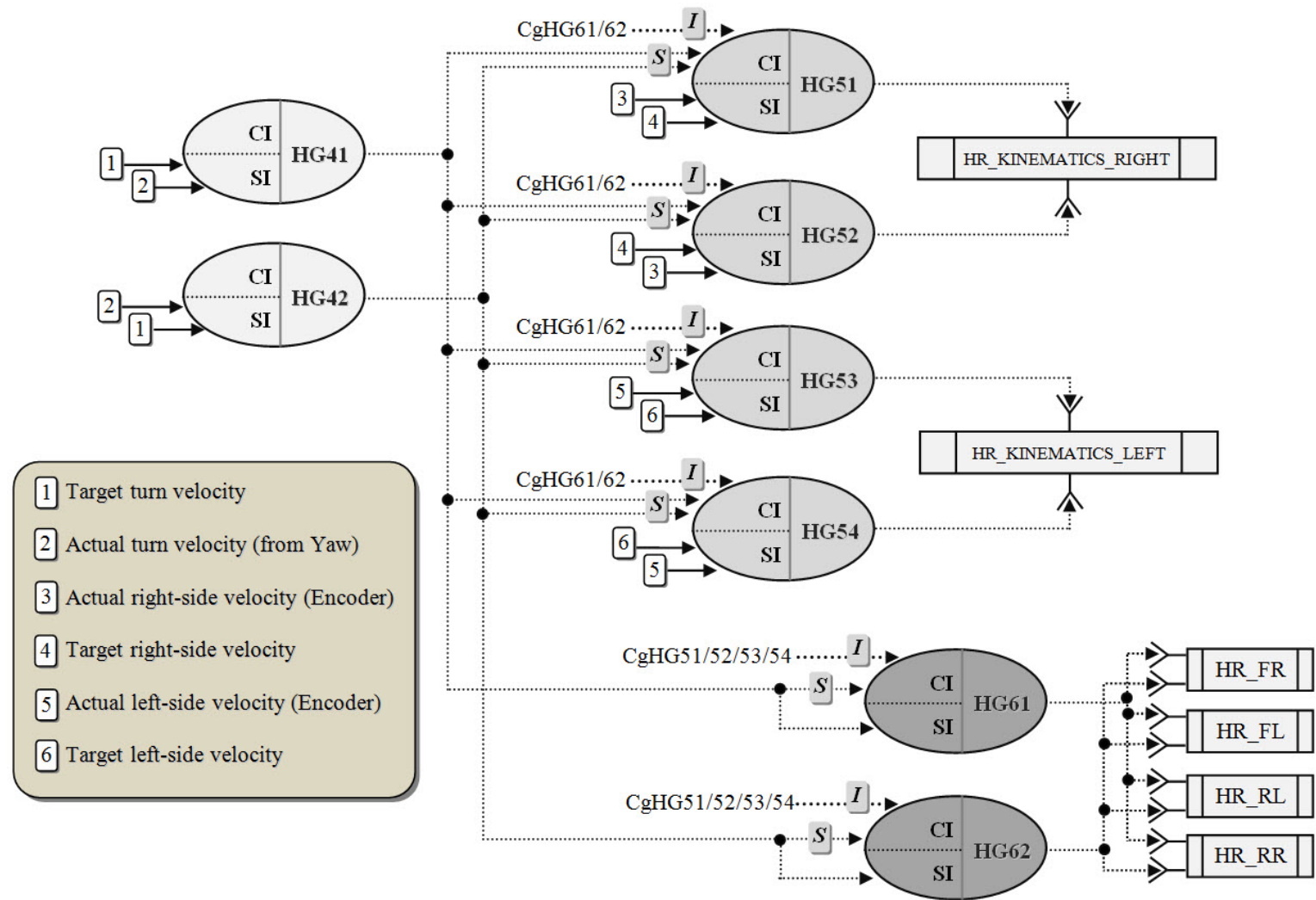


Figure 5.11: The Artificial Hormone Network 2 (AHN2)

### 5.2.2.1 Hormone Glands in the AHN2

Figure 5.12 illustrates the settings of HG41 and HG42. It is shown that the conflicts between the target and actual turn velocity of the robot are detected by the differentiation function in the Signal pre-processor of both glands. The opposite environmental cues which stimulate either gland are shown by the contrary Signal pre-processor functions presented. The Activation functions of both glands use the sigmoid function. This means that slight differences between the target and actual turn velocity (which are common for the robot) are generally considered not significant. Only large conflicts between the target and actual turn velocity of the robot can stimulate the production of both hormones.

HG41 / HG42		
<b>Signal inputs</b>	$SI_1$	Target turn velocity
	$SI_2$	Actual turn velocity
<b>Control inputs</b>	-	-
<b>Signal pre-processor</b>	Differentiation function	$SI_{feature} = (SI_1 - SI_2) / SI_1$ (for HG41)
		$SI_{feature} = (SI_2 - SI_1) / SI_1$ (for HG42)
<b>Control features</b>	-	-
<b>Activation function</b>	Sigmoid function	$t = SI_{feature} - 6$
		$ActLevel = (1 / (1 + \exp(-t)))$

Figure 5.12: The settings of HG41 and HG42

The settings of HG51 & HG52 and HG53 & HG54 are shown in Figure 5.13 and Figure 5.14 respectively. As mentioned earlier, all the HGs in HG5x respond to the conflicts between the target and actual velocity on either side of the robot. The conflicts are detected in the Signal pre-processor in each gland in the similar way to the ones explained for HG41 and HG42. However, as can be observed, all four glands in the HG5x consider different signal information to the HG4x. The HG51 and HG52 take the actual and target right side velocities, while the HG53 and HG54 take the actual and target left side velocities. A linear function is used in the Activation function of every gland in the HG5x. Therefore, the environmental cues from the related conflicts on each gland can linearly stimulate the production of the hormone on its gland. Regarding the inputs which can control the production of each hormone in the HG5x (CI), all four HGs in the HG5x have the HG41 and HG42 hormones connected to their Control Inputs via the stimulatory control (at  $CI_3, CI_4$ ). This enables the HG5x to produce its hormones only when the conflicts between the actual and target turn velocity of the robot are detected. However, apart from the HG41 and HG42 hormones, the glands in HG5x also

have the HG61 and HG62 hormones connected to their Control Inputs via the Inhibitory control feature (at  $CI_1, CI_2$ ). The main reason for the inclusion of these two control inputs is to prevent an unstable behaviour emerging on the robot. It was observed in early experiments that the robot repeatedly adjusted the velocity on the left and the right sides and moved uncontrollably. It was subsequently found that the undesirable behaviour was caused by the cyclic effects between the velocity compensations of HG5x and HG6x. Generally, when the transient velocity compensations were stimulated by the HG6x hormones, this could introduce the conflicts considered by the HG5x (the differences between the target and actual forward velocity on either side of the robot). This condition, then, stimulated the production of the HG5x hormones which resulted in the adjustment of the robot's kinematic factor. This kinematic adjustment then caused the differences between the target and the actual turn velocities of the robot, so the HG6x hormones were re-stimulated again and so on. Cyclic velocity compensations then caused the robot to move uncontrollably. Therefore, in order to impede this unwanted behaviour, the HG5x and HG6x glands are set to produce their hormones only when the hormone concentrations from another group are lower than the set threshold.

HG51 / HG52		
<b>Signal inputs</b>	$SI_1$	Actual right-side velocity
	$SI_2$	Target right-side velocity
<b>Control inputs</b>	$CI_1$	$C_gHG61$
	$CI_2$	$C_gHG62$
	$CI_3$	$C_gHG41$
	$CI_4$	$C_gHG42$
<b>Signal pre-processor</b>	Differentiation function	$SI_{feature} = (SI_1 - SI_2) / SI_2$ (for HG51)
		$SI_{feature} = (SI_2 - SI_1) / SI_2$ (for HG52)
<b>Control features</b>	$CI_1$	Inhibitory control
	$CI_2$	Inhibitory control
	$CI_3$	Stimulatory control
	$CI_4$	Stimulatory control
<b>Threshold values</b>	$Th_1$	0.1
	$Th_2$	0.1
	$Th_3$	0.1
	$Th_4$	0.1
<b>Activation function</b>	Linear function	$ActLevel = SI_{feature}$ <b>IF</b> $ActLevel > 1$ $ActLevel = 1$ <b>IF</b> $ActLevel < 0$ $ActLevel = 0$

Figure 5.13: The settings of HG51 and HG52

HG53 / HG54		
<b>Signal inputs</b>	$SI_1$	Actual left-side velocity
	$SI_2$	Target left-side velocity
<b>Control inputs</b>	$CI_1$	$C_gHG61$
	$CI_2$	$C_gHG62$
	$CI_3$	$C_gHG41$
	$CI_4$	$C_gHG42$
<b>Signal pre-processor</b>	Differentiation function	$SI_{feature} = (SI_1 - SI_2) / SI_2$ (for HG53)
		$SI_{feature} = (SI_2 - SI_1) / SI_2$ (for HG54)
<b>Control features</b>	$CI_1$	Inhibitory control
	$CI_2$	Inhibitory control
	$CI_3$	Stimulatory control
	$CI_4$	Stimulatory control
<b>Threshold values</b>	$Th_1$	0.1
	$Th_2$	0.1
	$Th_3$	0.1
	$Th_4$	0.1
<b>Activation function</b>	Linear function	$ActLevel = SI_{feature}$ <b>IF</b> $ActLevel > 1$ $ActLevel = 1$ <b>IF</b> $ActLevel < 0$ $ActLevel = 0$

Figure 5.14: The settings of HG53 and HG54

Figure 5.15 shows the settings of HG61 and HG62. These two glands directly respond to the HG41 and HG42 hormone concentrations. However, the HG41 and HG42 hormones are connected to both the Signal Input ( $SI_1$ ) and Control Input ( $CI_3$ ) of HG61 and HG62 respectively. Therefore, the HG61 and HG62 hormones can only be stimulated by the HG41 and HG42 hormones when the hormone concentrations of HG41 and HG42 are higher than the thresholds. In addition, for similar reasons to prevent the cyclic velocity compensation effects explained previously, the HG5x hormones are also connected to the Control Inputs of HG61 and HG62 via the Inhibitory control feature (at  $CI_1$ ,  $CI_2$ ,  $CI_3$ , and  $CI_4$ ).

Note that, similar to the AHN1, every HG (in the AHN2 explained) is also set to have an implicit negative feedback control from its own hormone output.

HG61 / HG62		
<b>Signal inputs</b>	$SI_1$	$C_gHG41$ (for HG61)
		$C_gHG42$ (for HG62)
<b>Control inputs</b>	$CI_1$	$C_gHG51$
	$CI_2$	$C_gHG52$
	$CI_3$	$C_gHG53$
	$CI_4$	$C_gHG54$
	$CI_5$	$C_gHG41$ (for HG61) $C_gHG42$ (for HG62)
<b>Signal pre-processor</b>	Linear function	$SI_{feature} = SI_1$
<b>Control features</b>	$CI_1$	Inhibitory control
	$CI_2$	Inhibitory control
	$CI_3$	Inhibitory control
	$CI_4$	Inhibitory control
	$CI_5$	Stimulatory control
<b>Threshold values</b>	$Th_1$	0.2
	$Th_2$	0.2
	$Th_3$	0.2
	$Th_4$	0.2
	$Th_5$	0.2
<b>Activation function</b>	Linear function	$ActLevel = SI_{feature}$ <b>IF</b> $ActLevel > 1$ $ActLevel = 1$ <b>IF</b> $ActLevel < 0$ $ActLevel = 0$

Figure 5.15: The settings of HG61 and HG62

### 5.2.2.2 Hormone Receptors in the AHN2

As shown in Figure 5.11, the HG61 and HG62 hormones are connected to front-left, front-right, rear-left and rear-right Hormone Receptors (HR\_FL, HR\_FR, HR\_RL and HR\_RR). These HRs, as shown in Figure 5.16, are connected to the velocity command of each robot wheel. The transient velocity compensations are set to occur at these positions. When there is an implication from the environmental cues that the robot is turning more to the right side than expected, AHN2 will encourage the robot to temporarily increase the velocity on the right side and decrease the velocity on the left side of the robot and via versa. These are achieved by the settings of these HRs as shown in Figure 5.17. The four HRs take the similar inputs but utilize them contrarily as shown in the Receptor functions (Figure 5.17). This basically enables the differences between HG61 and HG62 to have the opposite effects on the left and the right side of

the robot (increase one and decrease another). Each HR can then induce the velocity compensation on its dedicated wheel according to the values of each hormone receptor ( $HRLevel$ ) as shown in the Target action.

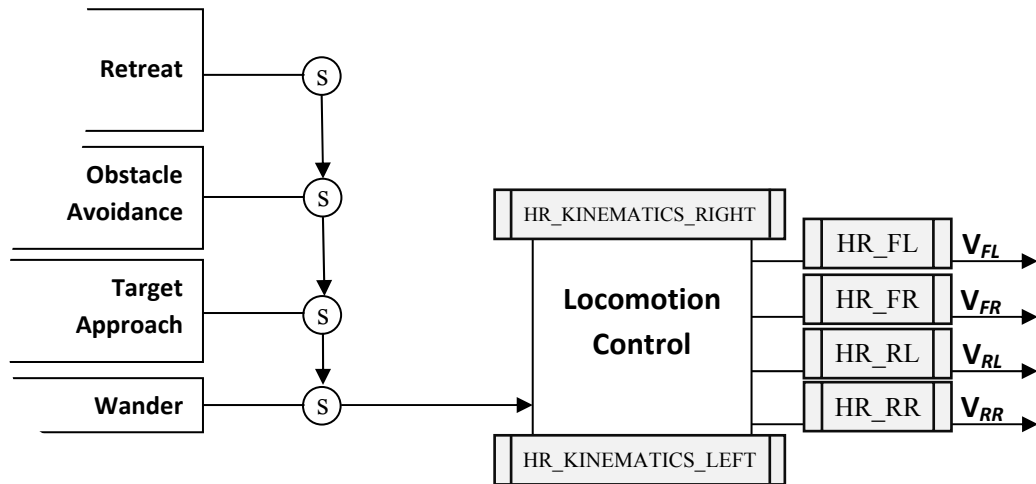


Figure 5.16: The AHN2 hormone receptors located on the main robot controller

HR_FL / HR_RL / HR_FR / HR_RR		
<b>Hormone inputs</b>	$HI_1$	$C_g HG61$
	$HI_2$	$C_g HG62$
<b>Receptor function</b>	Differentiation function	$RepLevel(t) = HI_2 - HI_1$ (for HR_FL & HR_RL)
		$RepLevel(t) = HI_1 - HI_2$ (for HR_FR & HR_RR)
<b>Receptor feature</b>	Direct effect	$HRLevel(t) = RepLevel(t)$
<b>Target action</b>	Front-left-wheel speed	$V_{FL}(t) \cdot (1 + HRLevel(t))$
	Rear-left-wheel speed	$V_{RL}(t) \cdot (1 + HRLevel(t))$
	Front-right-wheel speed	$V_{FR}(t) \cdot (1 + HRLevel(t))$
	Rear-right-wheel speed	$V_{RR}(t) \cdot (1 + HRLevel(t))$

Figure 5.17: The settings of HR\_FL, HR\_FR, HR\_RL and HR\_RR

Two other Hormone Receptors in the AHN2 are the Left Kinematics Hormone Receptor and the Right Kinematics Hormone Receptor (HR\_KINEMATICS\_LEFT and HR\_KINEMATICS\_RIGHT). These two HRs are responsible for the adjustment of the robot kinematic model. Therefore, they are located at the Locomotion Control unit on the main robot controller as shown in Figure 5.16. The kinematic adjustment is based on the concentrations of HG5x hormones. The key concept of the kinematic adjustment is

when there is the indication of the conflicts between the target and actual velocity on either side of the robot, the AHN2 will induce the kinematic adjustment on the related kinematics factors correspondingly so as further velocity commands from the Locomotion control unit is more likely to generate less conflicts in the velocity. For example, if there is an indication that the actual right side velocity is permanently or frequently slower than the target right side velocity (which might occur because of a right side wheel fault), the AHN2 will increase the front-right and rear-right wheel kinematic factors. Thus, further velocity commands on the right wheels can be increased and the actual turn velocity of the robot may be closer to the target turn velocity. The settings of the Right Kinematics and Left Kinematics Hormone Receptors are shown in Figure 5.18 (a) and (b). HR\_KINEMATICS\_RIGHT takes the HG51 and HG52 hormones (responsible to the right side conflicts) as their inputs, while HR\_KINEMATICS\_LEFT takes the HG53 and HG54 hormones (responsible to the left side conflicts) as their inputs. The Receptor functions of both HRs use a scaling differentiation function to determine the values of *RepLevel*. However, the Receptor features of both HRs are set to the Accumulative effect. This feature not only allows the kinematic factors to be collectively increased or decreased, but also helps restraint the kinematic factors after the new adjusted kinematics have been accomplished and the conflicts as well as HG5x hormones have ceased. Each kinematic factor is then adjusted proportionally based on the values of *HRLevel* as shown in the Target action. Note that the values of *HRLevel* in Figure 5.18 are restricted to 2, since this value is enough to make each robot wheel speed to reach the speed limit (0.7 m/s).

HR_KINEMATICS_RIGHT		
<b>Hormone inputs</b>	$HI_1$	$C_{gHG51}$
	$HI_2$	$C_{gHG52}$
<b>Receptor function</b>	Scaling differentiation function	$RepLevel(t) = (HI_2 - HI_1) / 2$
<b>Receptor feature</b>	Accumulative effect	$HRLevel(t) = RepLevel(t) + HRLevel(t-1)$
<b>Target action</b>	Front-right-wheel kinematic factor	$FR\_kinematic\_factor(t) \cdot (1 + HRLevel(t))$
	Rear-right-wheel kinematic factor	$RR\_kinematic\_factor(t) \cdot (1 + HRLevel(t))$

(a)

HR_KINEMATICS_LEFT		
<b>Hormone inputs</b>	$HI_1$	$C_{gHG53}$
	$HI_2$	$C_{gHG54}$
<b>Receptor function</b>	Scaling differentiation function	$RepLevel(t) = (HI_2 - HI_1) / 2$
<b>Receptor feature</b>	Accumulative effect	$HRLevel(t) = RepLevel(t) + HRLevel(t-1)$
<b>Target action</b>	Front-left-wheel kinematic factor	$FL\_kinematic\_factor(t) \cdot (1 + HRLevel(t))$
	Rear-left-wheel kinematic factor	$RL\_kinematic\_factor(t) \cdot (1 + HRLevel(t))$

(b)

Figure 5.18: The settings up of (a) HR\_KINEMATICS\_RIGHT  
(b) HR\_KINEMATICS\_LEFT

In summary, the AHN2 is activated when the conflicts between the target turn velocity and the actual turn velocity of the robot are developed. The persistence of these environmental cues first stimulates the productions of the HG41 and HG42 hormones, which, in turn, activate the HGs in HG5x and HG6x. In general, if the conflicts are evoked from temporarily or insignificant environmental effects (such as transient wheel slippages), the HG61 and HG62 are likely to secrete their hormones and cause the robot to make the transient velocity compensations accordingly. However, if there are any permanent faults occurring on either side of the robot wheels (which cause the conflicts between the target and actual forward velocity on either side of the robot), the corresponding hormones from HG5x will be produced and secreted. This condition will then influence the robot to update its kinematic model to reflect the current situations.

Because of the quite complex interactions between several related hormones in the AHN2, it may be difficult to perceive the full functions of the hormone network, without perceiving the actual interplay between the hormones. Therefore, the demonstrations of these hormone interactions will be illustrated in the discussion and analysis section after the experiment results have been shown in the next section.

As mentioned earlier in this section, when a fault occurs on a robot wheel, this can affect the robot operating in both flat and rough terrain. Therefore, the AHN2 will be evaluated on an autonomous robot operating on both flat and rough terrain environments. The flat terrain will be considered in Experiment I, Experiment II considers the rough terrain environment.

### **5.2.3 Experiment I: Flat Terrain Environment**

In this experiment, the AHN2 is investigated in helping an autonomous robot deal with the case of robot's actuator faults induced by an unresponsive wheel. The robot is set to operate in a flat terrain environment in this experiment.

#### **5.2.3.1 Experiment Setup**

The robot and test arena employed in this experiment are shown in Figure 5.19. The test arena is measured 340 cm by 1200 cm and is enclosed by walls. The terrain in this arena is all level. The task of the robot is to approach the green cylinder object located at the opposite end of the arena. There are 10 test cases evaluated in this experiment. They are established from the cases when the AHN is and is not implemented on the robot over five different robot's wheel fault cases (2 x 5). The five cases of the robot's wheel fault are as follow:

- 1) When there is no wheel fault injected on the robot (No fault)
- 2) When the wheel fault is injected to the robot's rear-right wheel (RR fault)
- 3) When the wheel fault is injected to the robot's rear-left wheel (RL fault)
- 4) When the wheel fault is injected to the robot's front-right wheel (FR fault)
- 5) When the wheel fault is injected to the robot's front-left wheel (FL fault)

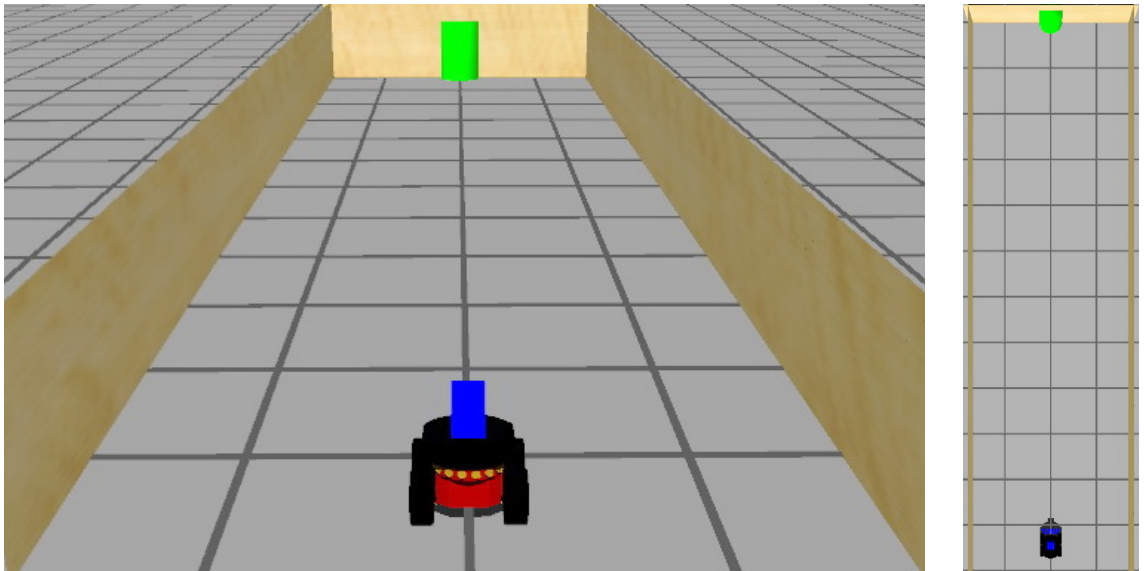


Figure 5.19: The robot and the test arena employed in Experiment I

Note that in the cases of no AHN, the robot accomplishes its task using only the behaviour-based robot controller. In the cases when the AHN is implemented on the robot, apart from the behaviour-based robot controller, the robot is also equipped with both the AHN1 and the AHN2 (presented in Figure 5.1 and Figure 5.11 respectively). The values of  $\alpha_g$  and  $\beta_g$  of the AHN1 are similar to the ones shown in Table 5.1, while the values of  $\alpha_g$  and  $\beta_g$  of the AHN2 are illustrated in Table 5.2.

Table 5.2: The values of  $\alpha_g$  and  $\beta_g$  of each hormone gland in the AHN2

	$\alpha_g$	$\beta_g$
<b>HG41 / HG42</b>	0.5	0.8
<b>HG51 / HG52 / HG53 / HG54</b>	0.5	0.8
<b>HG61 / HG62</b>	0.2	0.4

Similar to the previous experiments, the robot is tested for 100 runs in each case and at the beginning of each run the robot is randomly located on its starting position area. Note that in this experiment the robot is allowed to operate for only 5 minutes in each run because, without the rough terrain in the test arena, the time required for the robot to reach the target object is significantly decreased.

### 5.2.3.2 Results

Figure 5.20 shows the robot performance based on the performance metrics

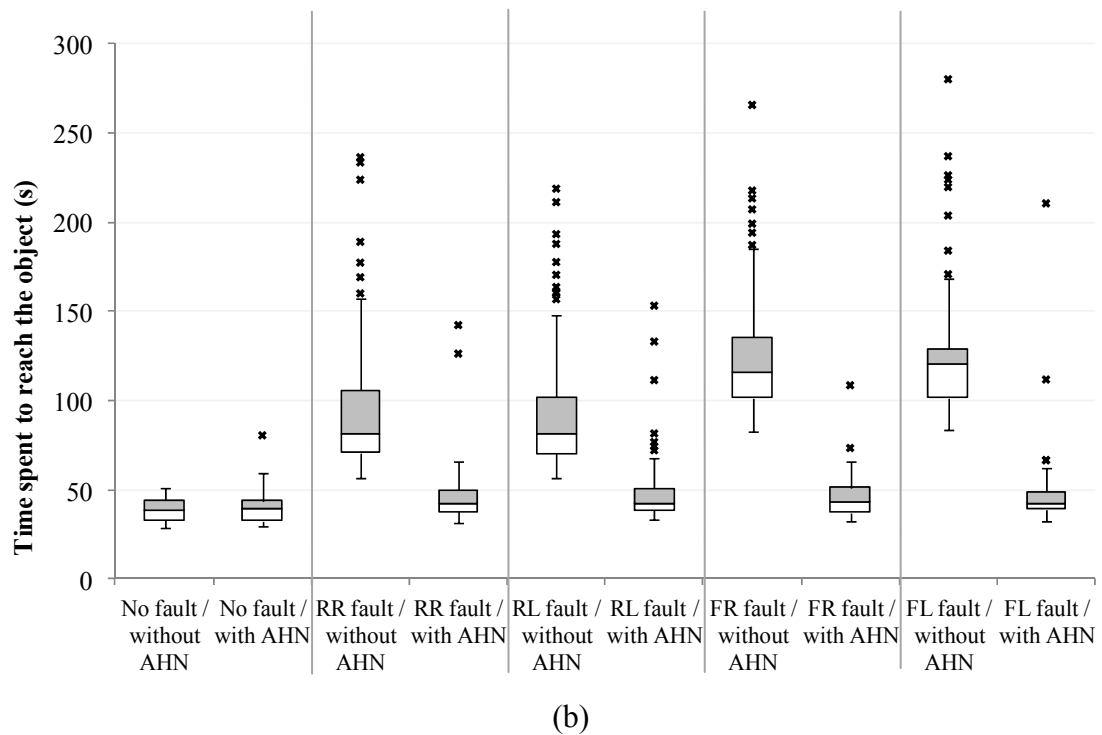
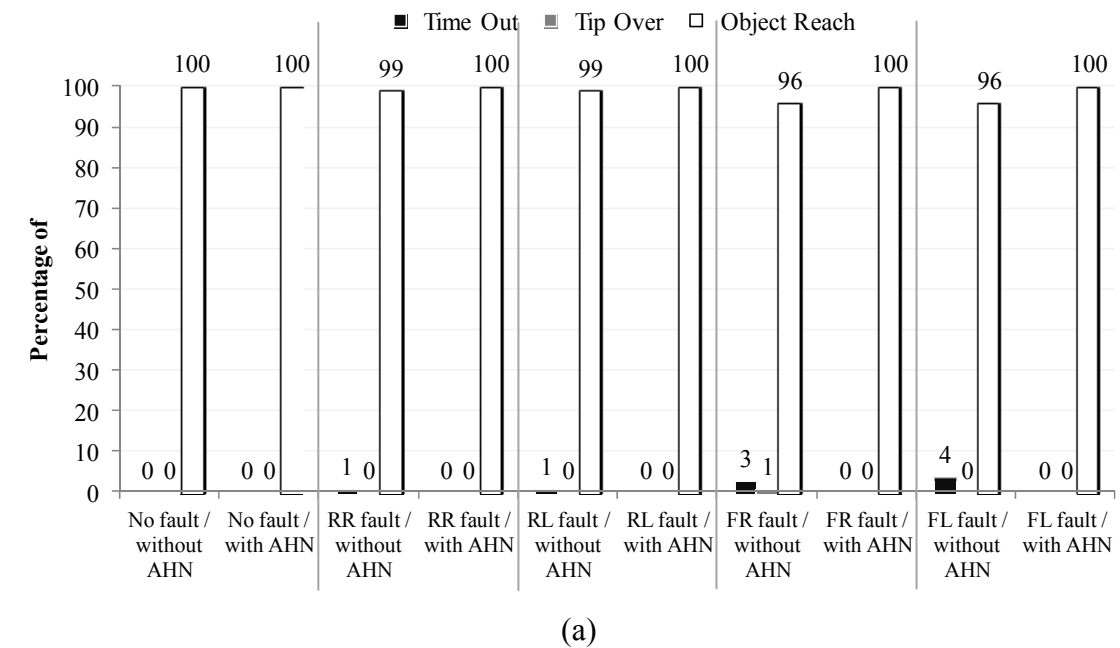


Figure 5.20: The experiment results of the robot operating in the flat terrain environment (a) reporting the robot performance in Time Out, Tip Over and Object Reach metrics (b) showing Time Spent the robot used to reach the target object

The results clearly show that there is little difference in term of the number of times the robot can reach the target object. With the AHN, the robot does reach the target 100% in every test case. Without the AHN, the robot produces just the small number of Time Out in each test case when the wheel fault occurs. Note that the unlikely event of the Tip Over shown in the case when the fault is injected to the front-right wheel and there is no AHN implemented on the robot is caused by the unusual situation when the robot struggles in a corner and climbs on a wall (because of unexpected movements induced by the wheel fault), and then tips over.

Nevertheless, when considering the time spent by the robot to reach the target object, it is shown that when the wheel fault happens, the robot with the AHN requires statistically less time to reach the target object. It can be observed that the time spent on each case is just slightly longer than when there is no wheel fault injected in the robot.

### **5.2.3.3 Discussion and Analysis**

Considering the actual robot movement, generally without the AHN, when the fault occurs on either side of the robot, the robot is likely to turn more to that side. For example, when the fault is injected to a right side wheel, the robot is likely to turn more to right because of the unbalanced velocities on the left and the right side wheels of the robot. It can be expected that this situation should directly affect the robot movements and significantly decrease the robot performance. However, as shown in the results, when there is the wheel fault injected in the robot (without the AHN), the robot remains able to reach the target object in almost every run. This is due to the fact that the test arena is enclosed by walls and the robot can manage to utilize this condition by slowly tracking along the walls in order to reach the target object even when a wheel fault occurs on the robot.

Figure 5.21 illustrates some examples of the routes taken by the robot. As can be noticed in Figure 5.21 (b) and (c), when the wheel fault occurs on the right side and on the left side of the robot, it keeps moving to the right and to the left respectively (the green dotted lines). However, in most situations when the robot is moving close to a wall, the robot can manage to track along the wall and finally reach the target object. The wall tracking behaviour emerges from switching between the Target Approach and the Obstacle Avoidance behaviours. In general, when the robot is close to a wall (on the side that the wheel fault occurs) and is commanded to move forward in order to

approach the target object, the wheel fault then causes the robot to turn slightly to the wall rather than go straight forward. This condition then activates the Obstacle Avoidance behaviour which forces the robot to turn away from the wall. Subsequently, the robot is trying to move forward again in order to approach the target but the robot is still forced by the wheel fault to move slightly back to the wall again and so on. This situation is also the main reason for the longer time required for the robot to reach the target when there is no AHN implemented. Because the no-AHN robot can reach the target only by tracking along the walls, the need to switch between the behaviours causes the robot to move slower on average and hence the longer time spent reaching the target.

As shown in the results, however, the no-AHN robot obtains the Time out in only a few runs. Generally, this happens in the situations when the robot cannot track along the walls as in the example shown in Figure 5.21 (d). It can be observed that when the robot cannot keep track with the walls, it keeps moving in a circle as shown by the forward spiral route. This is the result from the moving commands from the Target Approach and Wander behaviours combining with the effects from the front-right wheel fault.

Comparing to the case of the AHN robot, the robot traces (the blue solid lines) show that when the wheel fault is injected in the robot, the robot can keep moving quite similarly to the case when there is no wheel fault injected in the robot. This shows that the velocity compensation effects evoked by the AHN can better balance the velocity of either side wheels and can diminish the effects from the wheel fault.

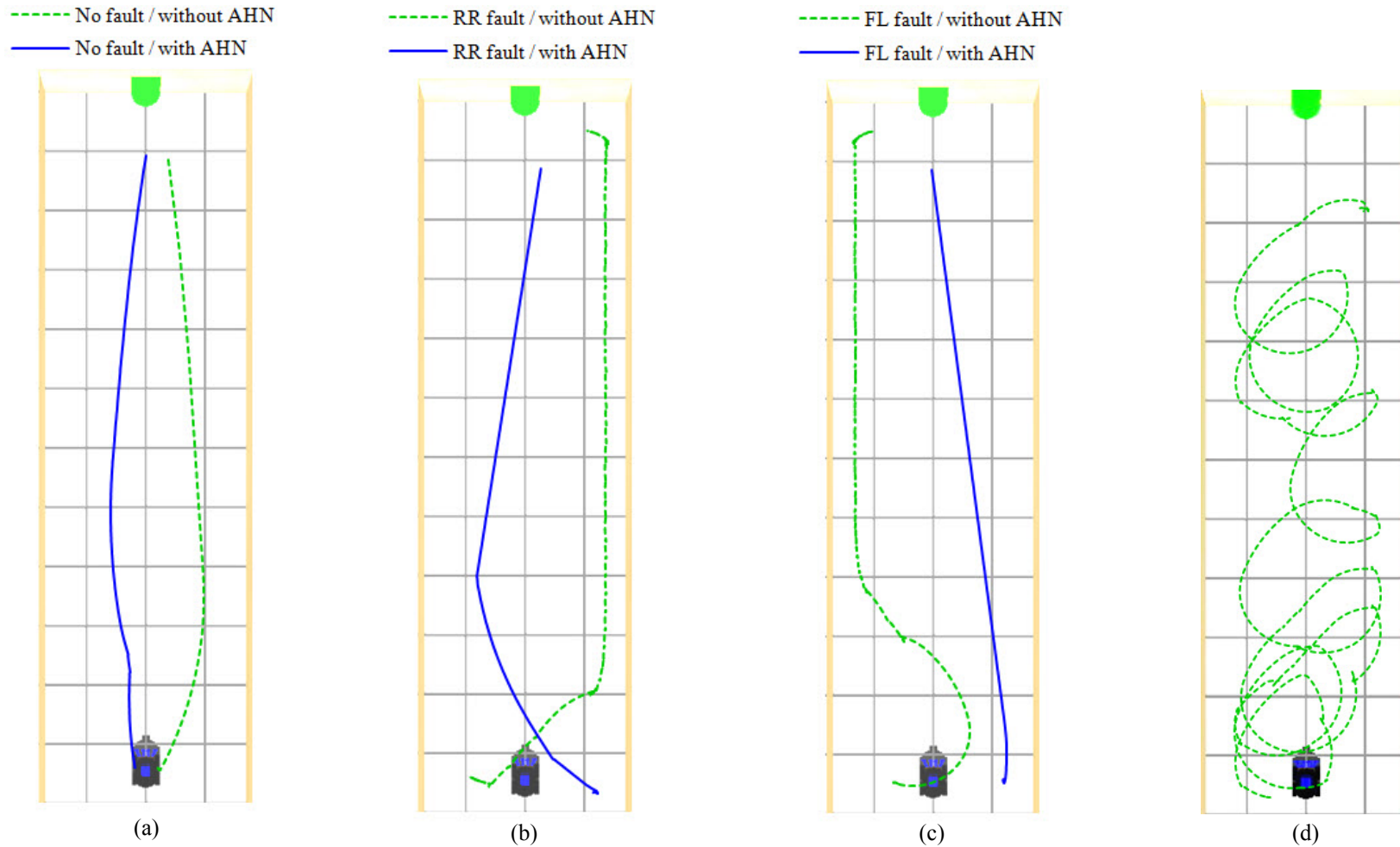


Figure 5.21: The robot traces when the AHN is and is not implemented on the robot in the cases of (a) no wheel fault (b) rear-right wheel fault (c) front-left wheel fault. (d) An example of robot trace in the case of Time Out

In order to illustrate the interplay between the hormones in the AHN2 and show how the velocity compensations induced by AHN2 can influence the robot when the wheel fault is injected in the robot, Figure 5.22 shows an example of the interactions among the hormones and how the robot's kinematic factor is changed by AHN2. Note that the example is derived from the case when there is a rear-right wheel fault. As explained previously, it is the conflicts between the target turn velocity and the actual turn velocity of the robot which is the key factor activating AHN2. As shown in Figure 5.22 (a), the differences between the target turn velocity (the solid line) and the actual turn velocity (the dotted line) stimulate the production of HG41 and HG42 hormones. The secretions of the HG41 and HG42 hormones then activate the HG5x glands which respond to the conflicts between the velocities on either side of the robot. Figure 5.22 (b) illustrates the variations of the HG51 and HG52 hormone concentrations in response to the conflicts between the actual and the target right side velocities. Because, in this case, the fault is injected to the rear-right wheel, it can be seen that there are significant differences between the actual and the target right side velocities in the first 4 seconds. This condition starts to stimulate the production of HG52 hormone at around 1 second. The changes of HG52 concentration directly affect the front-right and rear-right kinematic factors, hence the increasing of the Right Side Kinematic Factors (the dotted full black line in Figure 5.22 (b)). However, the HG52 hormone is immediately decreased even though the conflicts are still presented. This is because there are no significant conflicts on the target and actual turn velocities of the robot in that period (as shown in Figure 5.22 (a)) which results in the decreasing of hormones HG41 and HG42. This, in turn, deactivates the HG5x glands. Nevertheless, after 5 seconds, the HG5x glands are re-activated again and the differences between the actual and the target right side velocities then re-stimulate the HG52 hormone which results in the further increments of the Right Side Kinematic Factors. It can be noticed in Figure 5.22 (b) that the conflicts between the actual and the target right side velocities keep decreasing. One of the main reasons is because of the increasing value of the Right Side Kinematic Factors. As shown in Figure 5.22 (c), the increasing values of the Right Side Kinematic Factors influence the robot to increase the velocity commands on the right side. The affect from the velocity compensations can be noticed in the increase of the Hormone-modified velocity commands shown in Figure 5.22 (c). From the figure, it can be observed that, at the beginning, the Original Velocity Command, the Hormone-Modified Velocity Command and the actual front-right velocity are all equal. Note that the actual rear-right velocity is at zero because the rear-right wheel is the fault-injected wheel. However, the increasing

values of the Right Side Kinematic Factors subsequently influence the robot to increase the velocity commands on the right side, which in turn increases the velocity of the front right wheel and reduces the conflicts between the actual and the target right side velocities. Note that the changes of rear-right wheel velocity (even when the fault is injected on the wheel) are induced by the forces from the three-remaining working wheels which drive the robot and also cause the rear-right wheel to turn. As mentioned, the faulty wheel is only unresponsive to the velocity commands but remains able to be turned freely by external forces.

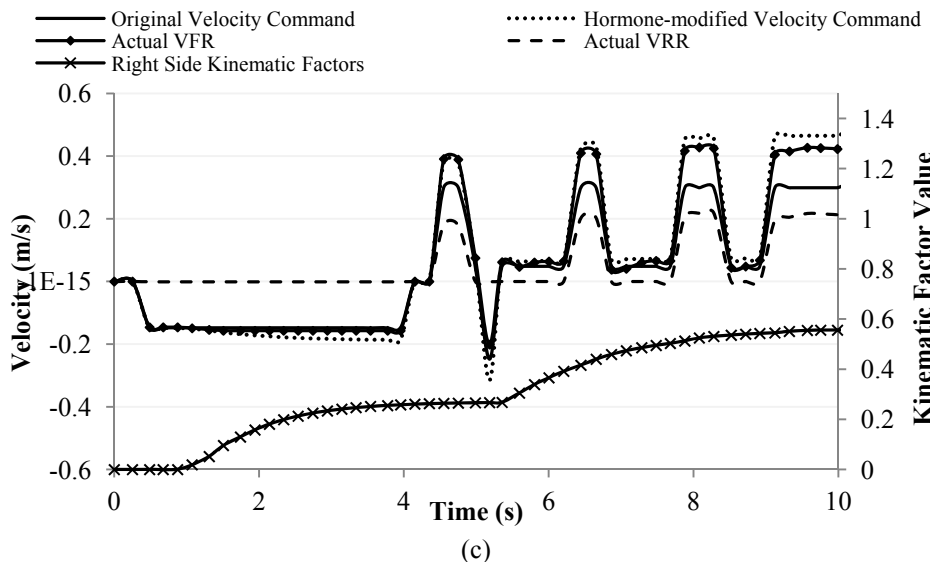
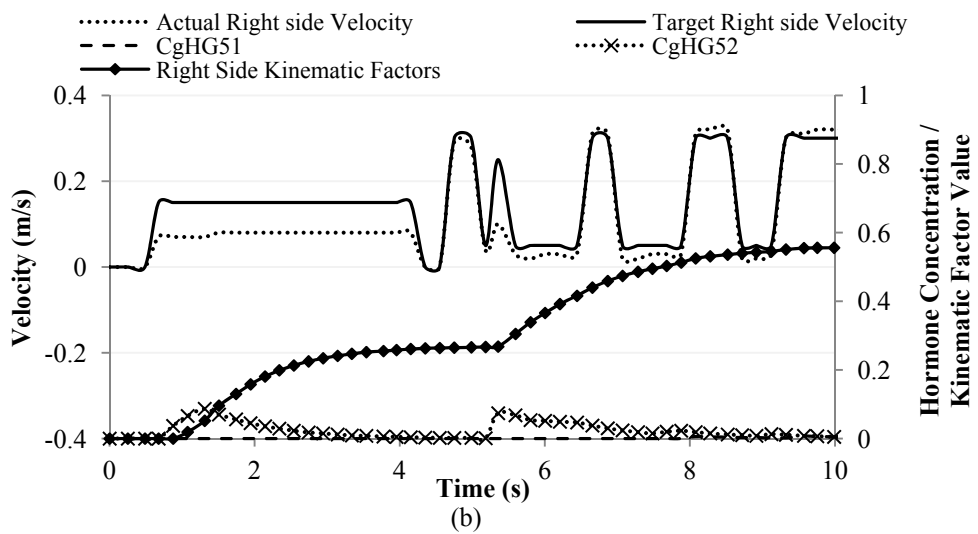
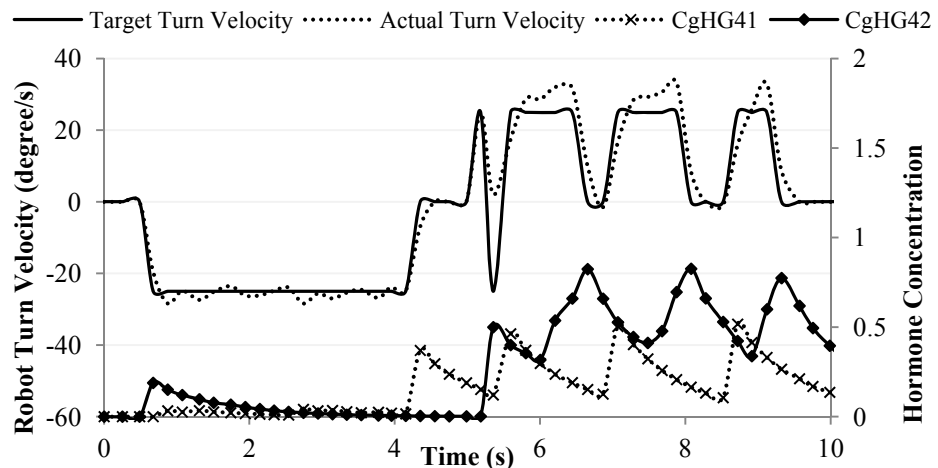


Figure 5.22: (a) the changes of HG41 and HG42 hormone concentrations based on the conflicts between the robot's target and the robot's actual turn velocity (b) the changes of the right side kinematic factor influenced by HG51 and HG52 hormones (c) the variation of the robot's actual right wheel velocities induced by the AHN2 hormones. Note that data in each figure is obtained from a single robot run.

Apart from adjusting the robot's kinematic factors in order to evoke the velocity compensation, AHN2 also influences the robot's movements by inducing the transient velocity compensation. An example of the hormone interactions in AHN2 which influences this velocity compensation technique is shown in Figure 5.23. This example is derived from the case when there is no wheel fault injected in the robot and it is moving over a rough terrain. As shown in Figure 5.11, HG61 responds to the HG41 hormone, while HG62 responds to the HG42 hormone. In Figure 5.23 (a) and (b), the rough terrain causes the conflicts between the target turn velocity and the actual turn velocity of the robot which in turn influence the secretions of HG61 and HG62 hormones. Figure 5.23 (c) and (d) illustrate how the front-left and front-right wheel velocities are influenced by the concentrations of HG61 and HG62 hormones. The transient velocity compensation is induced by the differences between the HG61 and HG62 hormone concentrations (as shown in Figure 5.17). As explained the transient velocity compensation influences the robot to increase the velocity on one side and decrease the velocity on the other side, this can be noticed from the opposite compensations between the front-left and front-right velocity shown in Figure 5.23 (c) and (d).

In this section, the investigation of the AHN in helping an autonomous robot operating in a flat terrain environment has been reported. The next section will be the case of the robot operating in a rough terrain environment.

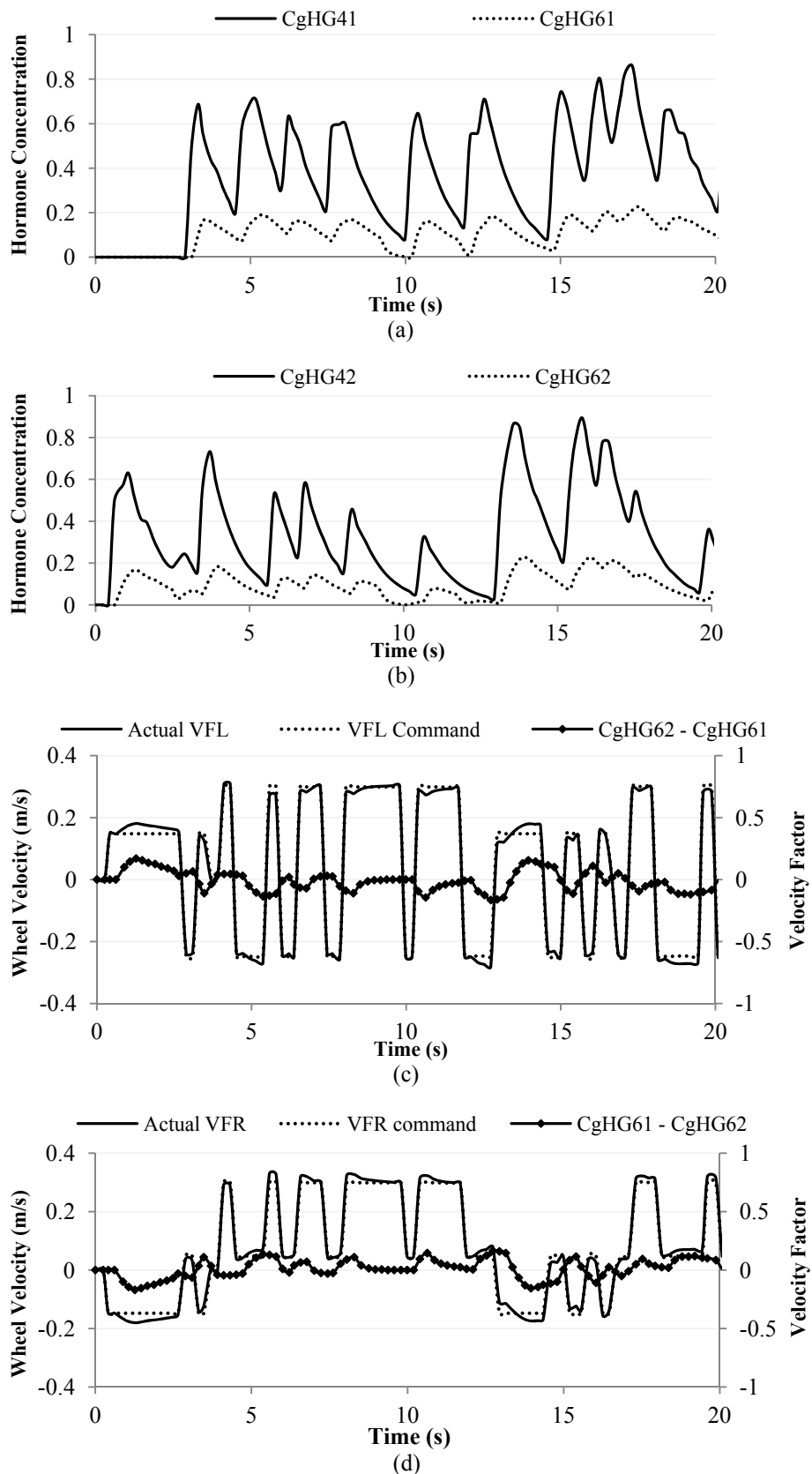


Figure 5.23: (a) the variations of the HG61 hormone based on hormone concentrations of the HG41 hormone (b) the variations of the HG62 hormone based on hormone concentrations of the HG42 hormone (c) The effects of HG61 and HG62 hormone concentrations on the front-left wheel velocity (d) The effects of HG61 and HG62 hormone concentrations on the front-right wheel velocity. Note that data in each figure is obtained from a single robot run.

## 5.2.4 Experiment II: Rough Terrain Environment

This experiment investigates the robot performance in the cases of the wheel fault when the robot operates in a rough terrain environment.

### 5.2.4.1 Experiment Setup

The robot and the test arena used in this experiment are shown in Figure 5.24. The test arena is almost identical to the test arena used in Experiment I, except the inclusion of the rough terrain located between the target object and the robot's starting position area. Other setups in this experiment are also the same as Experiment I with the only exception being the time allowed for the robot to perform the task. In this experiment the time limit is set to 45 minutes in each run. The increase of this time limit is necessary because of the addition of the rough terrain. The increasing time limit was derived from a preliminary experiment which found that in 90% of the runs, the robot either reaches the object or tips over within 45 minutes.

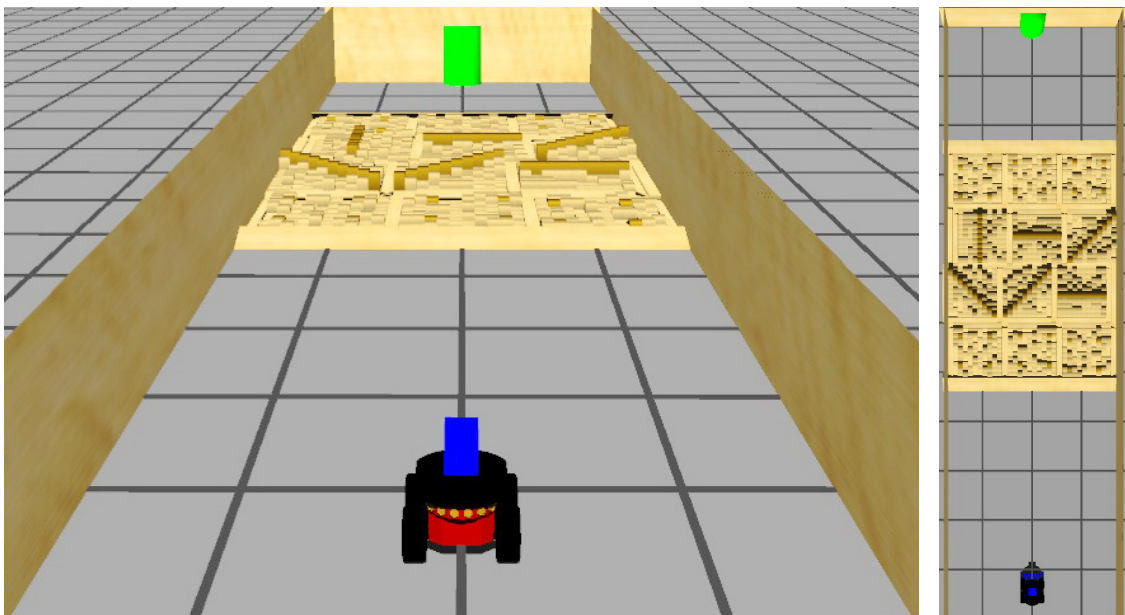
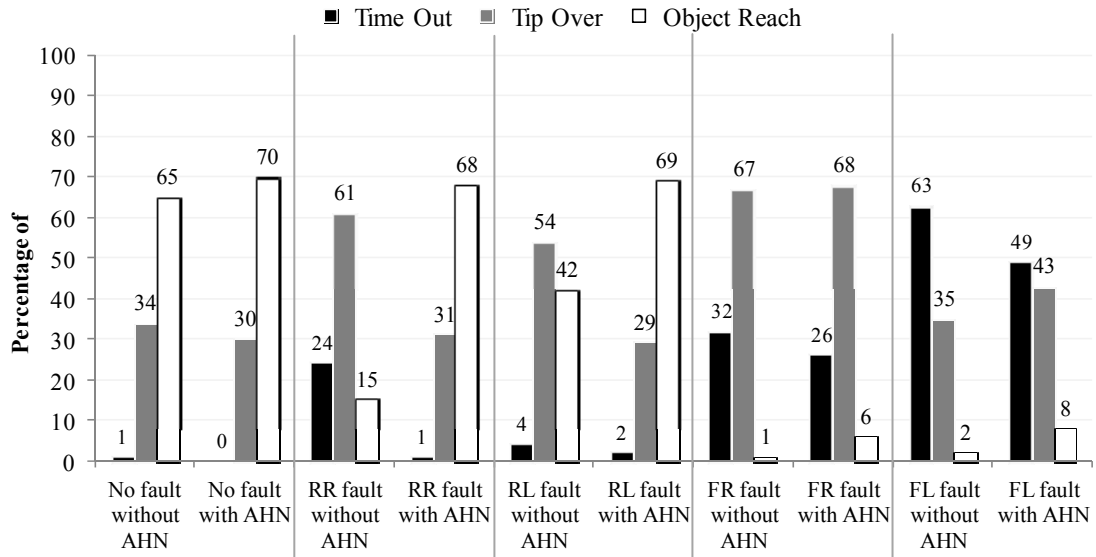


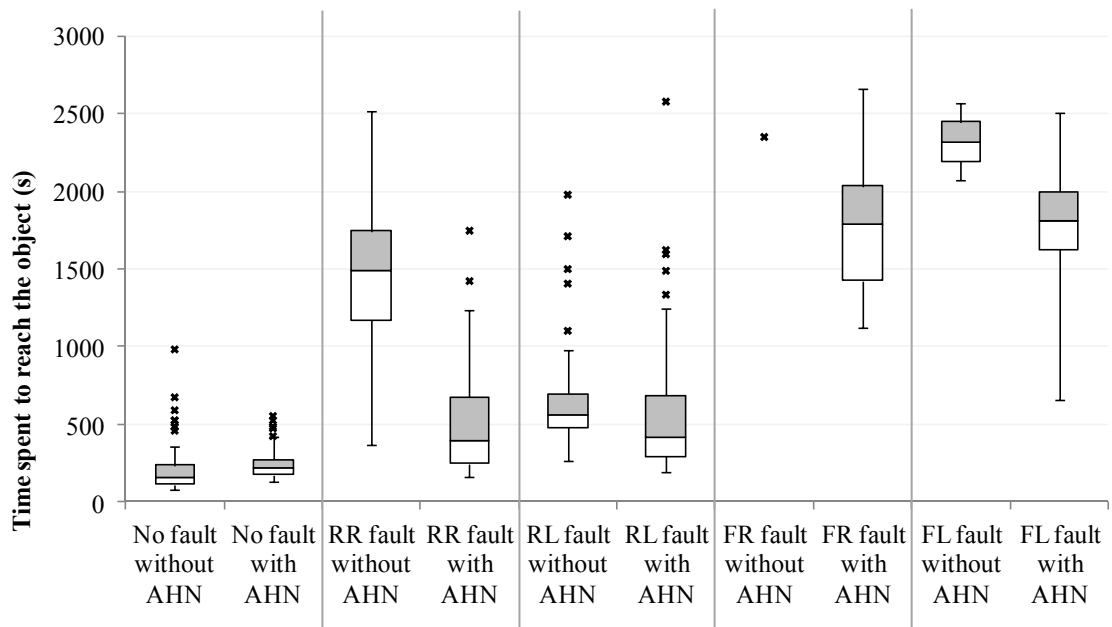
Figure 5.24: The robot and test arena employed in Experiment II

### 5.2.4.2 Results

Figure 5.25 shows the results of the robot based on the performance metrics.



(a)



(b)

Figure 5.25: The results of the robot performance in Experiment II (a) reporting in Time Out, Tip Over and Object Reach metrics (b) showing Time Spent the robot used to reach the target object

Considering the cases when the wheel fault is injected to the rear wheels (RL and RR), the results show that the no-AHN robot is significantly affected by the fault. The Tip Over rates are increased by over 20% (to 61 and 54) and the Object Reach rates are decreased by over 23% (to 15 and 42). The Time Out rates are also increased to 24 and 4. However, with the AHN, the robot is hardly affected by the wheel fault on the rear wheels. The Object Reach rates are reduced by just 2% and 1% (to 68 and 69). The Tip Over rates are almost identical to the case when there is no wheel fault (31 and 29 comparing to 30) and only just 1% and 2% increase shown in the Time Out.

Nevertheless, in the cases when the fault occurs on the front wheels (either left or right), the robot performance is severely decreased on both the no-AHN and the AHN robots. In the cases of the front-right wheel fault, The Tip Over rates of the no-AHN and the AHN robots are increased to 67 and 68 respectively. The robot can only manage to reach the target object 1% of the time (without the AHN) and 6% of the time (with the AHN). In the case when the fault is injected on the front-left wheel, the no-AHN and the AHN robots can reach the object only 2% and 8% of the time respectively and the Time Out rates are significantly increased to 63% and 49%. It can be noticed that in these cases the performance of AHN robot is better than no-AHN robot by less than 10%. However, in these very difficult situations, the AHN robot is still able to perform better by 5% and 6%. Investigating the actual robot movements, it can be observed that one of the key reasons for these more severe effects when the fault is injected to the front wheels (compared to the rear wheels) is the loss of the uplifting force from the broken wheels. Generally, when the robot first negotiates rough terrain, it is the two front wheels which begin to negotiate the terrain. However, with only one wheel driving in the front, the robot is regularly forced to turn to the side of a fault wheel because of both the high friction and missing uplift forces on the broken wheels to move the robot over irregular terrain. This condition constantly changes the robot's direction and makes it almost impossible for the robot to keep moving in the desired direction.

#### **5.2.4.3 Discussion and Analysis**

In order to illustrate the effects of the wheel fault on the robot, Figure 5.26 to Figure 5.30 show the positions where the robot obtains the maximum displacement and the positions where the robot tips over in each run. The green circles represent the maximum displacement positions, while the blue crosses represent the tip over

positions. Figure 5.26 to Figure 5.30 show the cases when there is no wheel fault, when the fault is injected to the rear-right wheel, when the fault is injected to the rear-left wheel, when the fault is injected to the front-right wheel and when the fault is injected to the front left wheel respectively.

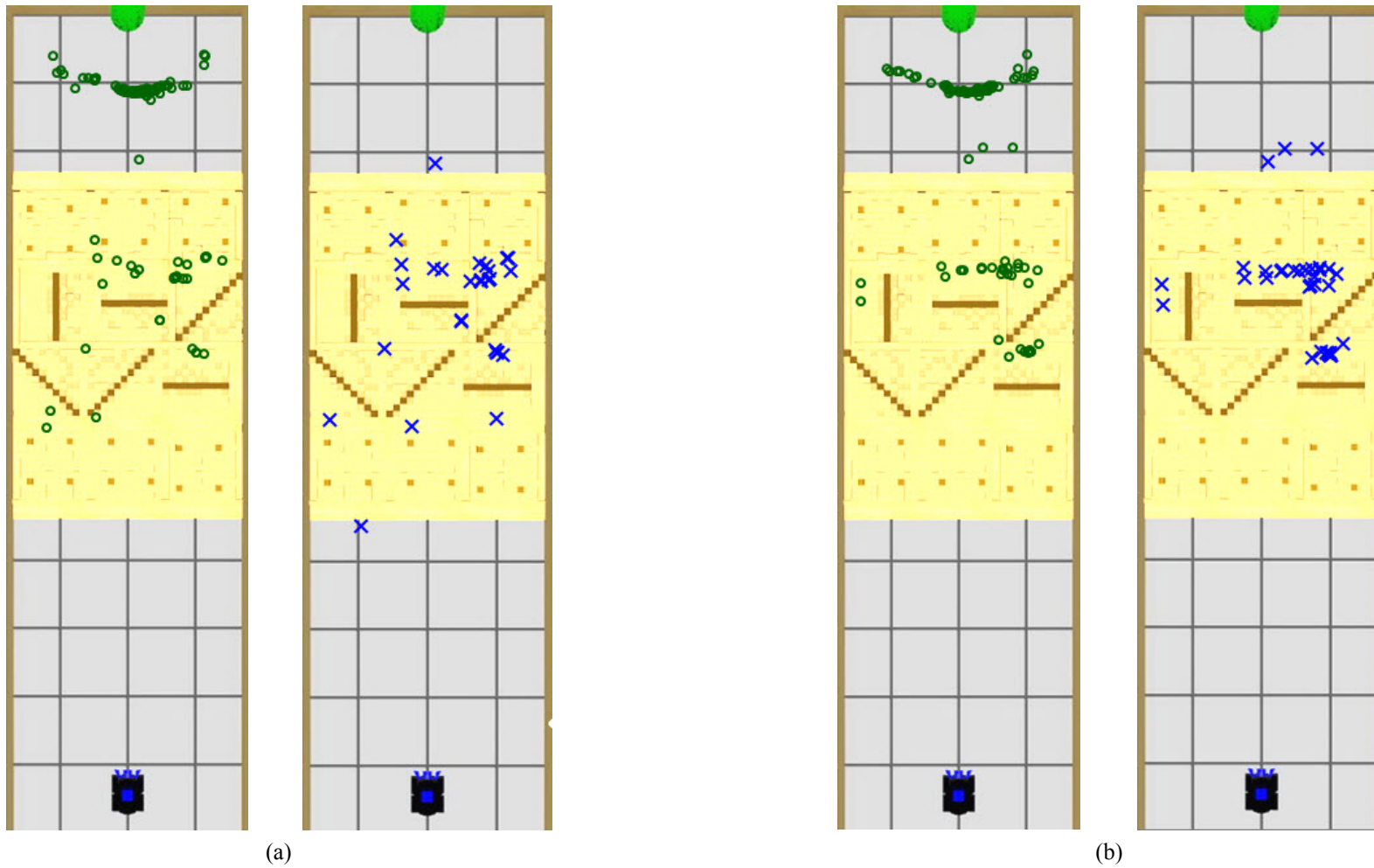


Figure 5.26: The maximum displacement (the green circles) and tip over (the blue crosses) positions in the case of no wheel fault  
 (a) with no AHN (b) with the AHN implemented on the robot

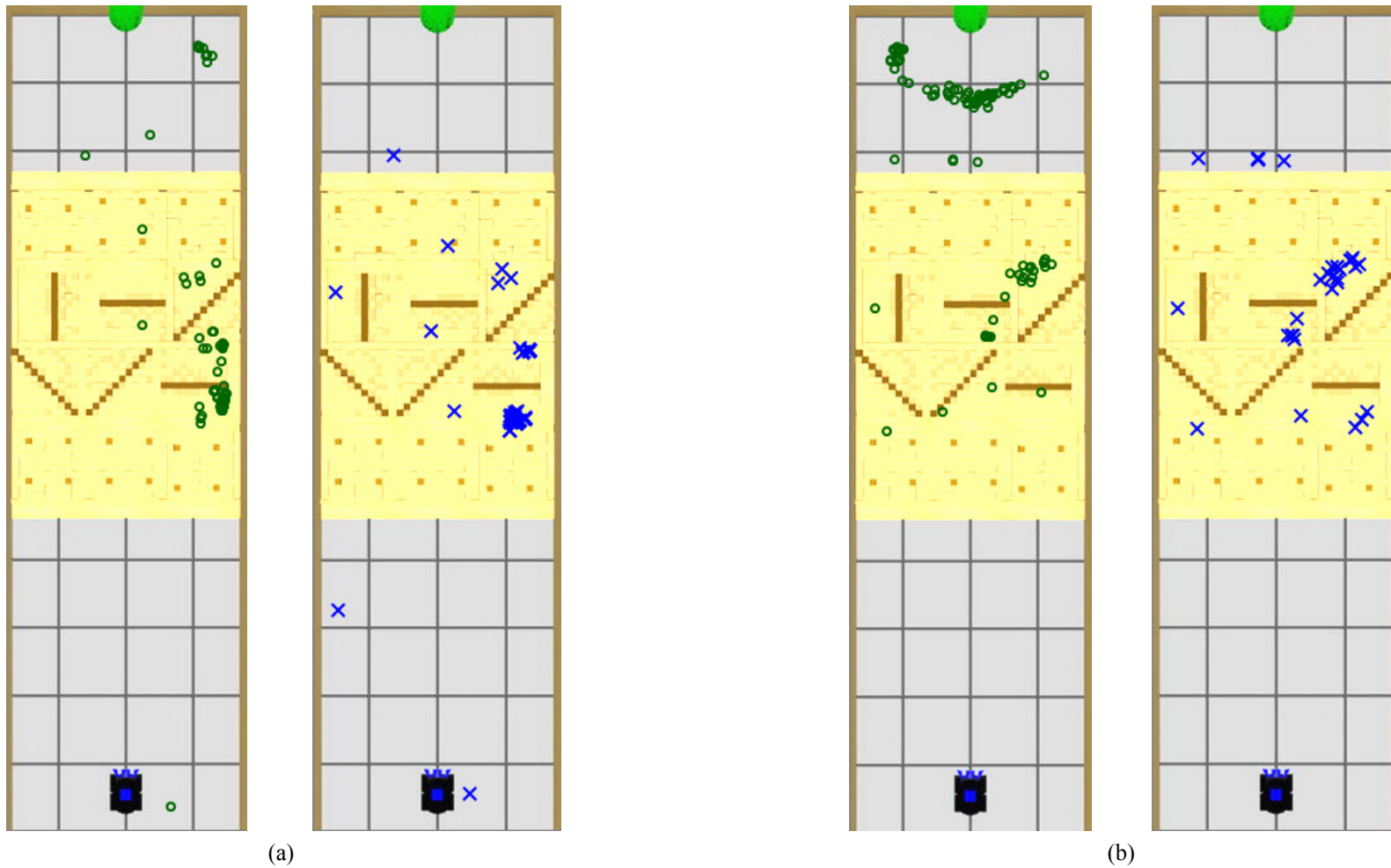


Figure 5.27: The maximum displacement (the green circles) and tip over (the blue crosses) positions in the case of rear-right wheel fault (a) with no AHN (b) with the AHN implemented on the robot

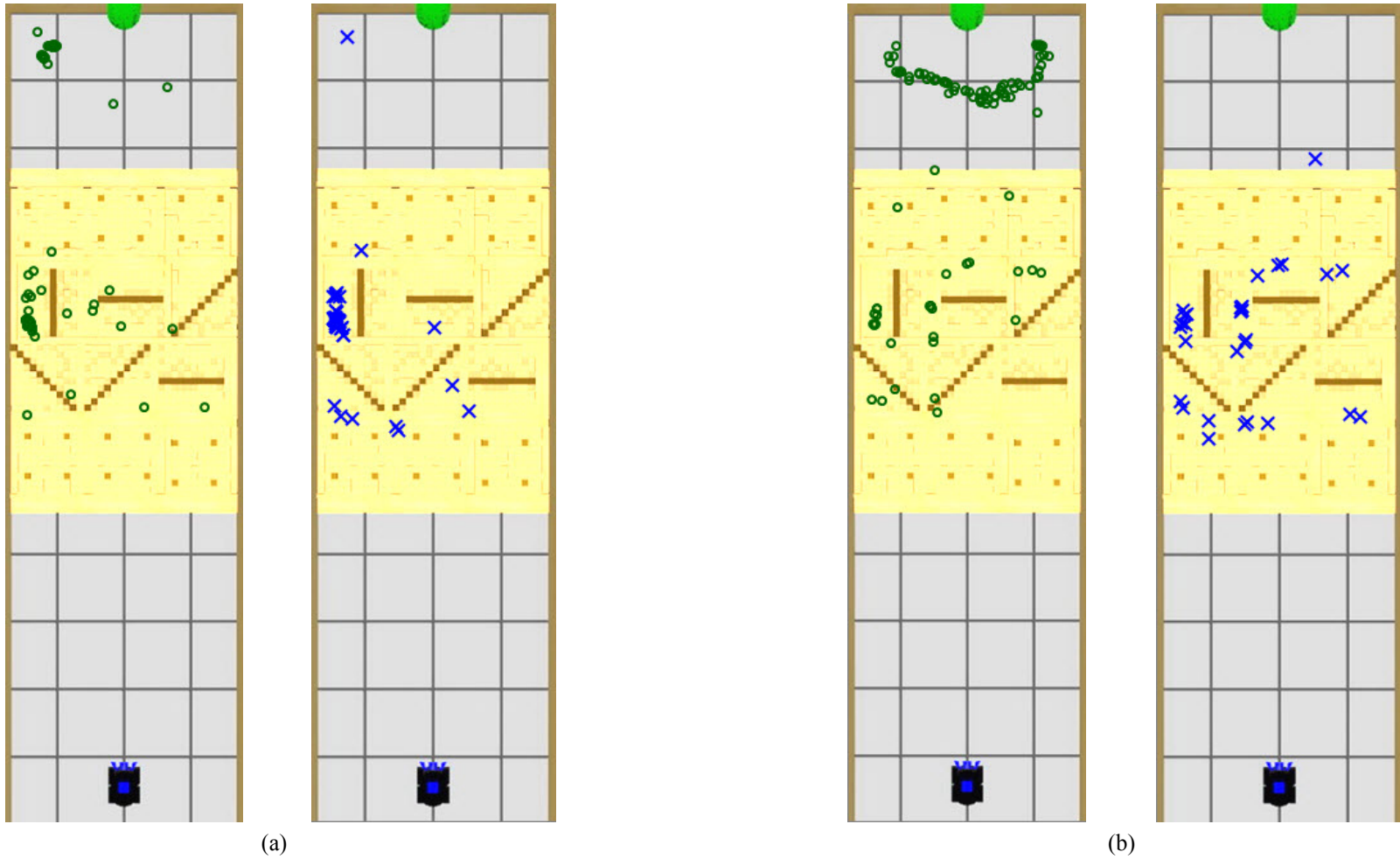


Figure 5.28: The maximum displacement (the green circles) and tip over (the blue crosses) positions in the case of rear-left wheel fault  
 (a) with no AHN (b) with the AHN implemented on the robot

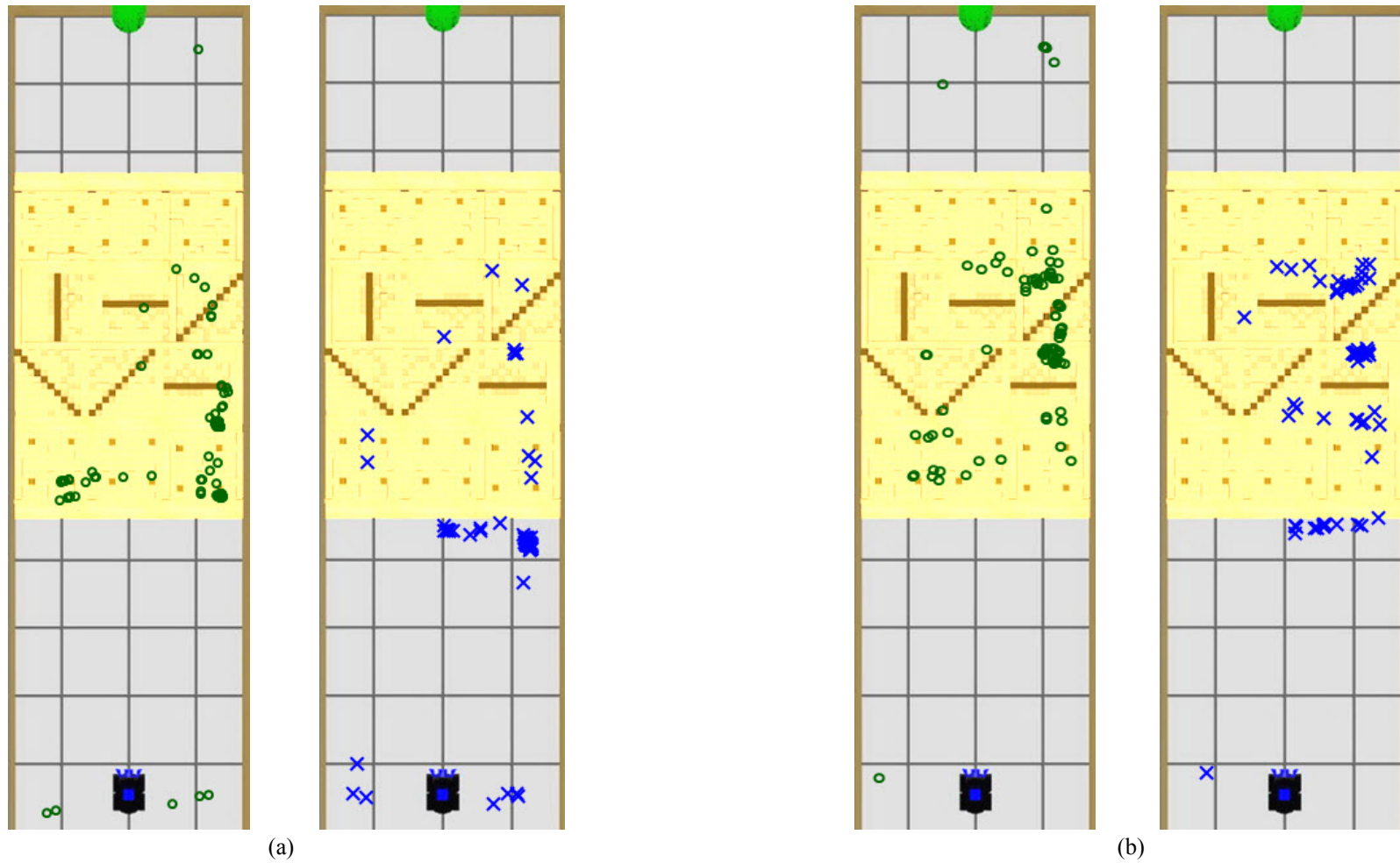


Figure 5.29: The maximum displacement (the green circles) and tip over (the blue crosses) positions in the case of front-right wheel fault (a) with no AHN (b) with the AHN implemented on the robot

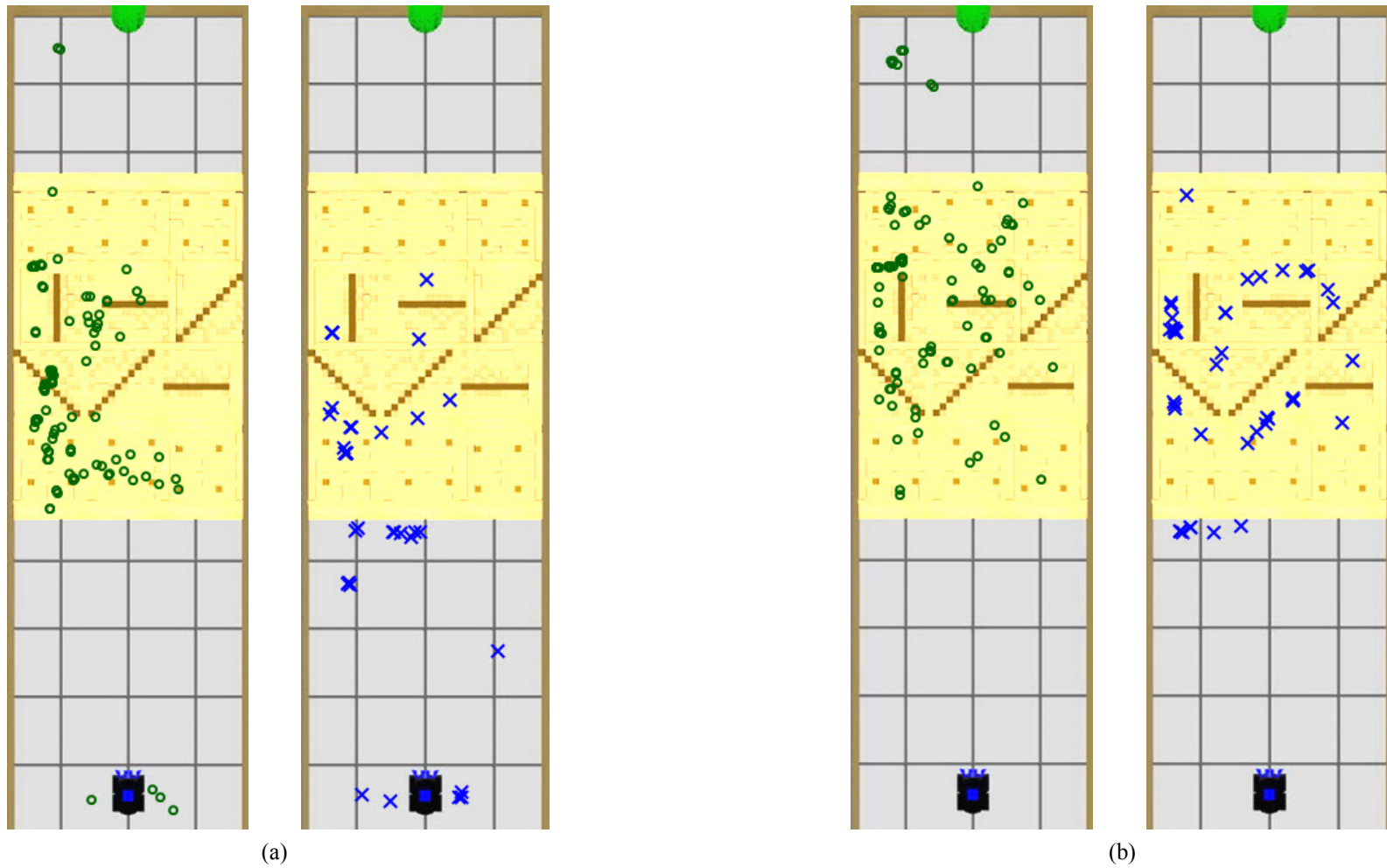


Figure 5.30: The maximum displacement (the green circles) and tip over (the blue crosses) positions in the case of front-left wheel fault  
 (a) with no AHN (b) with the AHN implemented on the robot

- **Rear-right wheel fault** (Figure 5.27)

In this case when there is no AHN implemented on the robot, the robot is likely to move to the right. This causes the robot to travel mostly along the right part of the arena which can be noticed from the maximum displacement and tip over positions which are located mostly on the right side of the test arena. As mentioned previously, the step-field 23 and 33 are considered the most difficult areas for the robot. The rear-right wheel fault significantly affects the robot's performance partly because the fault forces the robot to move mostly to the right side of the arena, thus the robot inevitably has to negotiate the step-field 23 and 33 regularly. This situation frequently causes the robot to tip over around the areas as shown by the maximum displacement and tip over positions in Figure 5.27 (a). However, when the AHN is implemented on the robot, the velocity compensations help adjust the velocity of the robot wheels. Consequently, the robot is able to move more freely to either side of the test arena (not restricted to only the right side). From the maximum displacement positions, it can be noticed that the robot can reach the target object from either side but less frequent from the right side. The main reason is because, even though the AHN can help compensating the wheel velocity, the rough terrain at the step-field 33 remains rather difficult to deal with. Therefore, when the robot traverses through this area, there remains a high possibility that the robot will tip over as can be noticed from the tip over positions which are located mostly on the upper part of the step-field 33.

- **Rear-left wheel fault** (Figure 5.28)

With the similar effects from the rear-right wheel fault, without the AHN, the robot is likely to move to the left side of the test arena and tip over mostly on the left side of the step-field 31. With the AHN, however, the robot can move better throughout either side of the arena which helps increase the robot performance in reaching the target object. However, because of the effects from the wheel fault, the tip over positions are widen to other parts of the rough areas (not only the step-field 33) as shown by the tip over positions in Figure 5.28 (b).

- **Front-right wheel fault** (Figure 5.29)

As shown in the figure, the robot performance in this case is severely decreased. Without the AHN, the maximum displacement positions show that the robot can

barely move beyond the step-field 2x and mostly tips over at the beginning of the rough terrain on the right side of the test arena. With the AHN, although the robot reaches the target object on only a few occasions, the robot can occasionally move further up the field beyond the step-field 2x. However, the robot still tips over frequently at the step-field 23 and 33.

- **Front-left wheel fault (Figure 5.30)**

Rather similar effects to the case of front-right wheel fault, without the AHN, the robot is likely to move to the left and struggles to travel beyond the step-field 3x. With the AHN, however, the robot shows good potential to reach the target object (if more time was allowed). As shown by the maximum displacement positions in Figure 5.30 (b), the robot is able to reach the step-field 4x several times without tipping over. Therefore, it is potentially possible that the robot might be able to reach the target object if the time limit is increased.

## 5.3 Summary

The main objective of this chapter is to investigate the two suggested AHNs in helping an autonomous robot deal with the internal environmental changes considered in this research. These are the changes in the robot systems induced by the cases of a sensor fault and an actuator fault.

The AHN1 is the hormone network designed principally to assist an autonomous robot to cope with the case of internal environmental changes induced by a sensor fault. The robot's pitch sensor is selected for the implementation of the sensor fault primarily because the pitch sensory information is one of the most essential pieces of information required by the robot to traverse on rough terrain. Faults on the pitch sensory information not only affect the robot's behaviour generated by the main controller but also the secretions of the hormones in the artificial hormone system, as both systems use the pitch information as one of their inputs. The performance of the robot presented in Figure 5.26 and Figure 5.27 show that the AHN1 can help the robot to reach the target object more often and tip over less often, comparing to when there is no AHN implemented on the robot (both on the cases when the pitch fault is injected and is not injected in the robot). This indicates that the AHN1 can provide the robot with the ability to adapt to the internal environmental variation evoked by the pitch fault. With

the AHN1, the robot remains capable of adjusting its wheel speed when moving on rough terrain by relying on an alternative cue provided from another sensor (frontal area distance IR), instead of responding to fault information from a broken sensor (pitch sensor). The results imply that the AHNs can be utilized to help increase the robot's chance of survival and to strengthen the possibility of the robot to achieve its tasks in unstructured environments.

For the case of internal environmental variations induced by a wheel fault, the case of an unresponsive wheel is considered. This condition effects the robot's movements and reduces the robot performance to accomplish its tasks. The results reported in Figure 5.20 and Figure 5.25 show that with the implementations of the AHN2 on the robot, it is able to perform better (higher Object Reach rate and lower Tip Over rate) on both flat and rough terrain environments. Generally, the interactions among the hormones, which are secreted in response to the environmental cues from the robot's movement conflicts, are the key in helping the robot to adapt to the internal variations induced by the wheel fault. The hormones urge the robot to make the velocity compensations corresponding to the implications notified by environmental information. However, the cases of the robot's front wheel fault remain a big challenge for the AHN2 as the results show that the robot is hardly able to reach the target object in these cases. Despite this issue, Figure 5.29 and Figure 5.30 give a promising indication that the robot can perform better when the AHN2 is implemented on the robot. The results show that the robot can traverse closer to the target object compared to when there is no AHN implemented on the robot. More importantly, it can be observed that the robot is more likely to acquire a higher Object Reach rate, if a longer operation time is allowed.

Note that in this research the AHNs are not used directly as a fault detection system but more as a self-monitoring system responding to environmental cues. The key utilization of the AHNs is to help maintain the healthy robot states when autonomous robots encounter the effects of both internal and external environmental changes. This feature consequently provides adaptability for autonomous robots to work in unstructured environments. With the purposes of the hormone gland mechanisms which allow other hormones or signal from other sources to influence the productions of hormones on any glands, it is clearly possible to apply the AHNs with any other systems. For example, one might design an AHN responding to fault detection signals provided by other dedicated fault detection systems. These signals can easily be applied to the AHN by connecting them to the inputs of any related hormone glands in order for the gland to

secrete its hormone correspondingly. On the other hand, one might also expect hormones from an AHN to be capable of influencing other systems. This can also be easily applied by locating hormone receptor(s) on those particular systems and constructing the hormone receptor(s) to respond accordingly. These attributes will be further elucidated in Chapter 7.

In this chapter, two AHNs designed specifically for helping an autonomous robot deal with internal environmental changes were presented. Nevertheless, it is obvious that AHNs can be constructed in many other different ways in order to provide other adaptation of behaviours for autonomous robots. Additionally, the parameters and mechanisms inside each hormone gland can also be altered in order to modify the production and the secretion behaviours of each hormone. The ability to be constructed using automatic design methods is also the key insight of the proposed AHN architecture. Therefore, in the next chapter, the use of an off-the-shelf automatic design method to create the AHNs will be explored.

## Chapter 6

# Cartesian Genetic Programming Artificial Hormone Network

In the previous chapter, two examples of artificial hormone networks, the AHN1 and AHN2, which are designed to assist an autonomous robot to deal with the cases of both internal and external environmental changes, were elucidated. It can be observed that two hormone networks which provide different adaptability can be constructed from the same fundamental mechanisms of an AHN, the Hormone Gland and the Hormone Receptor. The ability of an AHN, which allows the interplay between several hormones and enables the production and secretion of hormones based on different aspects of environmental cues as illustrated in Chapters 4 and 5, is the key feature in allowing an AHN to provide several adaptation mechanisms for autonomous robots.

Even though it has been shown that an AHN can be designed by the user, some desired adaptability may require much more complex hormone networks, which potentially demands huge effort to be designed properly by the user. It has also been shown that the variations in values of related parameters in the same hormone systems can change the production of hormones, which in turn alters the robot's performance. In addition, if such ideas are to be generalised to operate in many environments on various robots, this type of hand-design is not appropriate. Optimizing the values of every parameter may require very deep understanding of the problems or a huge amount of time to fine-tune the parameters. Therefore, applying intelligent design methods, in order to allow AHN to be constructed automatically to provide desired adaptability for autonomous robots, is considered important.

In this Chapter, evolutionary computing methods are considered as a way to “design” the AHN and as an initial step towards making such systems more generic for the future. Undoubtedly, there are various forms of evolutionary computation which can potentially be used to design the AHN, for example Genetic Algorithm (GA) [116], Genetic Programming (GP) [117], Cartesian Genetic Programming (CGP) [118] or Implicit Context Representation Cartesian Genetic Programming (IRCGP) [119].

However, the standard CGP is selected, in this research as an intelligent design method to explore the ability of AHN to be designed automatically for specific adaptive tasks, mainly because the corresponding representation of CGP is considered appropriate to the basic requirements of the AHN design. As shown in the previous chapters when, designing an AHN, one needs to consider both the connections between hormone glands and the production and secretion of a hormone on each gland. These requirements can be achieved suitably using CGP, as will be shown in this chapter. Moreover, there have also been some examples that report good results of using CGP to represent architectures with similar requirements (e.g. [120, 121]). In section 6.1, a brief introduction to CGP is given, while the representation of an AHN in CGP, proposed in this research, is elucidated in section 6.2. A set of experiments conducted to investigate the performance of Cartesian Genetic Programming Artificial Hormone Network is illustrated in section 6.3, and the summary of this chapter is given in section 6.4.

## **6.1 A Brief Introduction to Cartesian Genetic Programming**

CGP is a variant of GP. Simply put, the major difference is that conventional GP is represented by trees whilst CGP is represented by directed graphs. Originally, CGP was proposed as a directed acyclic two-dimensional array of computational nodes [122]. Although there is no fundamental restriction on applying CGP using a cyclic array, there have been only a few implementations of this concept (e.g. [123, 124]).

Figure 6.1 illustrates the general form of CGP. There are three main types of components in CGP. These are program inputs, program outputs and computational nodes. In general, program inputs are where signal data is connected to a CGP array, while program outputs are where the data processed by the CGP array are provided. Each computational node defines operations of the CGP array.

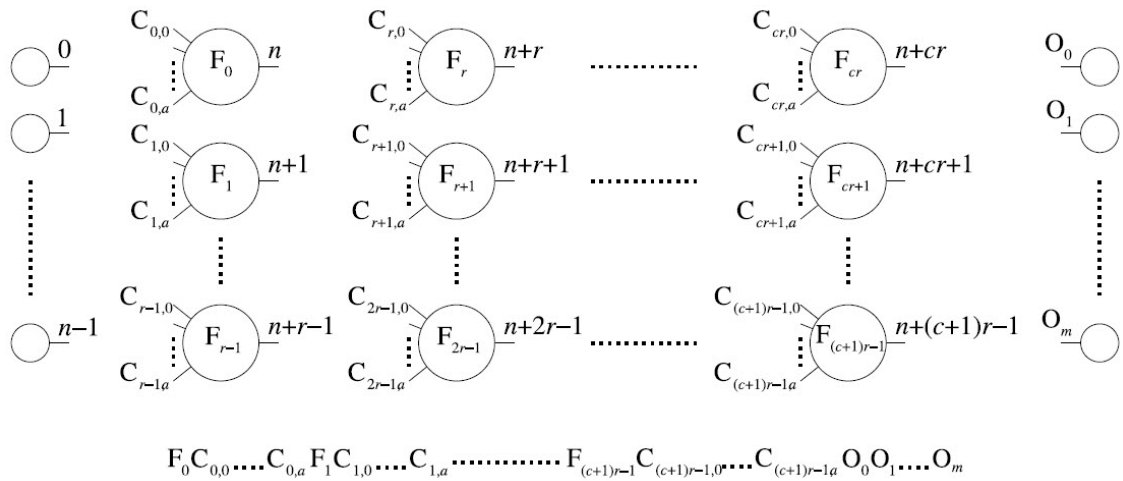


Figure 6.1: General form of CGP [122]

Usually, a computational node in CGP is defined by a function gene and a number of connection genes. The function gene ( $F_i$ ) is used to determine what operations are set to perform in a node. These operations are defined as functions in a lookup table. Thus, the primitive functions of computational nodes in CGP can be designed by the user and stored in the function lookup table. The connection genes ( $C_{i,j}$ ) define where the node gets its data from. One connection gene is used to define one data input of the node. Therefore, if for example a node has 10 inputs, 10 connection genes are required to define a node.

The total number of computational nodes in CGP is determined by the product of *the number of columns* and *the number of rows*. Both parameters can be set freely to any positive integer values by user. However, it has to be noted that computational nodes in CGP take their inputs in the direct and feed-forward manners. This means that any nodes can only take its inputs from the outputs of the nodes in the previous columns or from the program inputs. There is also another parameter called *levels-back* which determines how many previous columns that the computational nodes can take their inputs from. For example, if levels-back is set to be one, the computational nodes can only takes their inputs from the outputs of the nodes in the previous column or the program inputs. On the other hand, if levels-back is set to be 10, the nodes are able to take their inputs from the outputs of any nodes in the previous 10 columns or the program inputs. There is a special case of CGP which is used in a number of CGP implementations. This is the case when the number of row is set to be one [122, 125]. In this case, the maximum number of computational nodes allowed is determined by the

number of columns. The number of previous nodes that the input data can be received from is directly determined by the levels-back value.

The genotype representation of CGP is shown at the bottom in Figure 6.1. Note that the genes in CGP genotypes are represented by integers. As can be noticed, the CGP genotype is defined in the form of the aggregation of the gene representations from the first computational node to the last computational node followed by the program outputs. The function gene ( $F_i$ ) defines the operations of the computational node  $i$ . The integer value set on  $F_i$  represents the address of the function lookup table, which in turn determines the data operations of the node. Connection gene ( $C_{i,j}$ ) determines where input  $j$  of node  $i$  gets its data from. The possible integer values set on  $C_{i,j}$  need to comply with the restrictions explained (the number of columns which a node can get its data from which are determined by the levels-back value). For the program outputs ( $O_m$ ), only one integer value is used to define each program output. This value determines where the output gets its data from.

An example of CGP genotypes and its representation as a digital combinational circuit is shown in Figure 6.2 (a) and (b). There are four inputs, four outputs and 10 logic gates in the circuit. These are represented by four program inputs, four program outputs and 10 computational nodes respectively. As shown in Figure 6.2 (b), the inputs and the outputs of each logic gate are labelled numerically from 0 to 13. The CGP representation shown in Figure 6.2 (a) is the aggregation of the genes which represents the digital circuit from the first logic gate (number 4) to the last logic gate (number 13) followed by the four outputs. Each set of genes (the numbers in the round rectangular) shown in Figure 6.2 (a) represents a component in Figure 6.2 (b) labelled correspondingly. For example, the set of three numbers in the first round rectangular (labelled 4) in Figure 6.2 (a) represents the upper left-most logic gate (also labelled 4) in Figure 6.2 (b). The underlined number in each set represents the function of the computation node (which is the type of logic gates defined in the function lookup table) and the remaining two numbers in the set represent the connection genes. In this example, there are four primitive functions in the function lookup table. These are [0] AND, [1] AND with one input inverted, [2] XOR and [3] OR. Note that the numbers in the brackets are the function addresses. For example, the first set of genes in Figure 6.2 (a) contains values 0 0 2. This set determines the upper left-most logic gate in Figure 6.2 (b). Therefore, this logic gate is AND (defined by 0), which gets its two inputs from Input A and Input C (defined by 0 2). It can be observed that the last four set of genes in

Figure 6.2 (a) (which represent the four outputs) contain only one value in each set. As explained, the value is used to determine where the output gets its data from. For instance, the Output D has the gene value set to 13. This determines that this Output gets its data from the output of the computational node (logic gate) labelled 13. However, in this example, the outputs from nodes six and ten are not used in the circuit. The sets of genes, which belong to the nodes whose output is not used, are called inactive genes. As can be noticed, this type of gene is encoded in CGP genotypes but is not expressed in the phenotypes. The ability to carry inactive genes shown in CGP is considered one of the most important features of CGP, as investigated in [118, 125, 126]. The studies show that this feature can provide a neutral effect which is the key in helping CGP to achieve high fitness.

The mutation operator and 1 + 4 evolutionary strategy are normally used in the variation and selection processes of CGP. Also, in the case when an offspring genotype has the same fitness score with the parent and there are no other offspring genotypes having better fitness scores, the offspring genotype will be promoted as the new parent. The key reason is to make use of the neutral drift provided by inactive genes

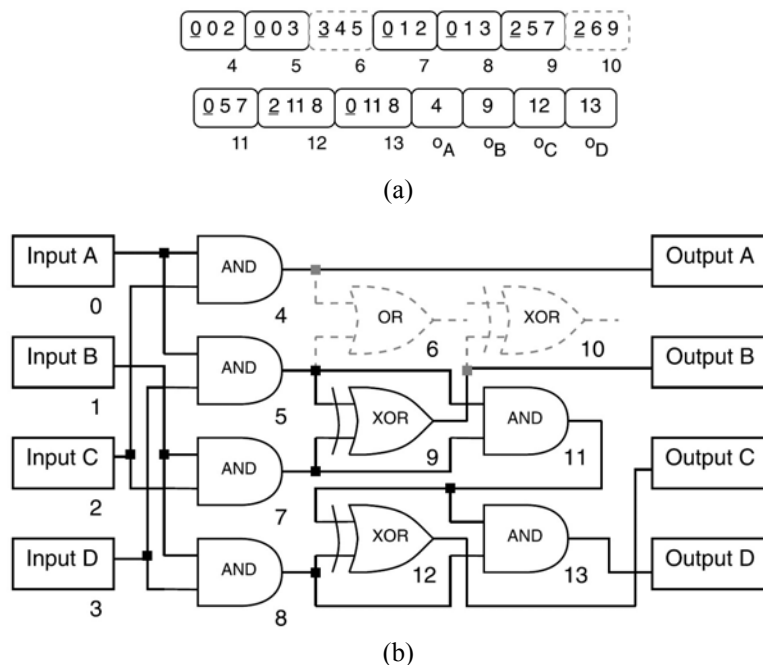


Figure 6.2: An example of CGP genotypes (a) and its representation as a digital combinational circuit (b) [122]

## 6.2 Implementation of Cartesian Genetic Programming Artificial Hormone Network (CGP-AHN)

To implement Cartesian Genetic Programming Artificial Hormone Network (CGP-AHN), some modifications on the CGP genotype representation are needed in order to enable an AHN to be encoded by CGP and to allow CGP to construct an AHN which is able to provide desired adaptability for autonomous robots. The case of internal environmental changes induced by a robot wheel fault (presented in section 5.2) is considered to explore the implementation of a CGP-AHN reported in this chapter. Figure 6.3 illustrates the CGP representation of the AHN for helping autonomous robots deal with the case. As can be observed in the figure, the program inputs represent the inputs of the AHN. Each computational node is used to represent a Hormone Gland (HG), and the program outputs are defined as Hormone Receptors (HRs).

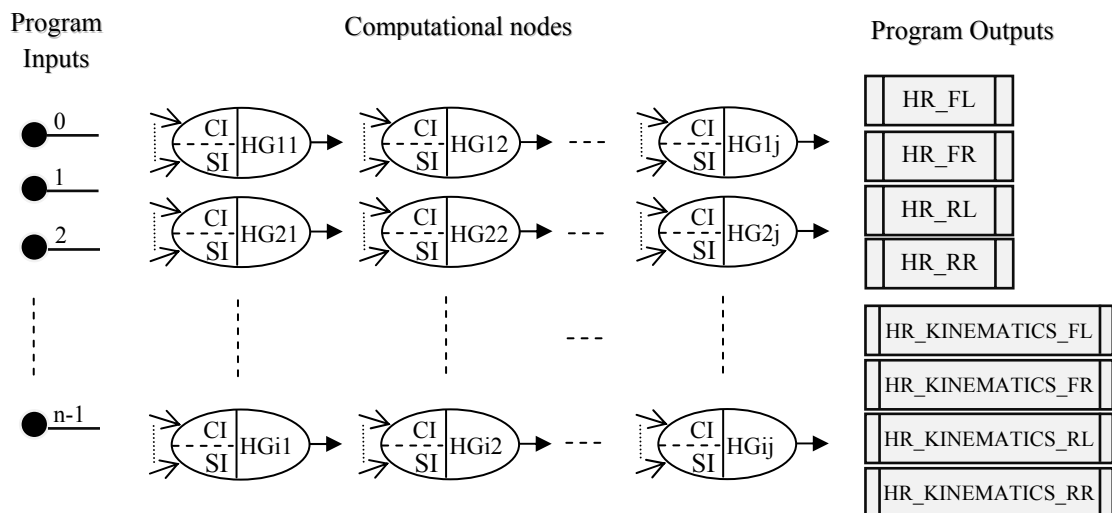


Figure 6.3: The representation of CGP-AHN

## **6.2.1 CGP-AHN Representation**

The representations of the three main types of CGP-AHN components are further elucidated in the following three sub-sections.

### **6.2.1.1 Program Inputs (AHN Inputs)**

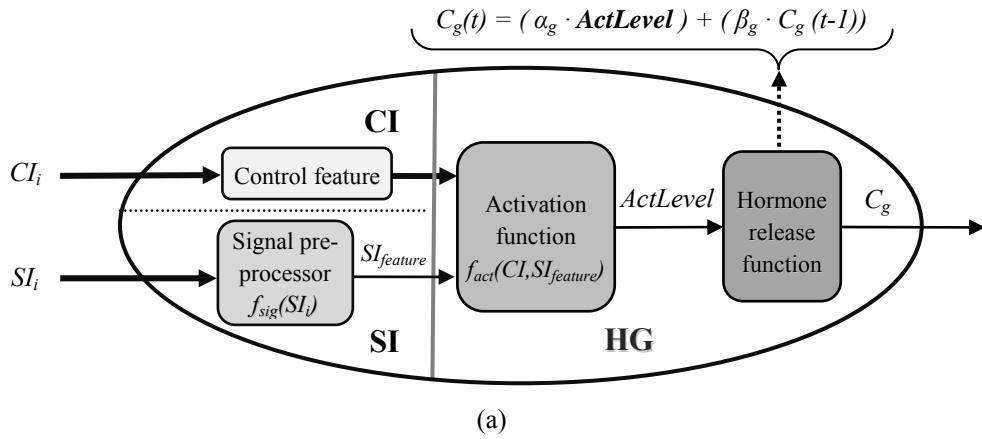
In this implementation, there are 24 input signals provided at the program inputs. They are labelled numerically as shown in Table 6.1. Almost all of the signal inputs are information related to the locomotion of the robot. Note that the signal information used by the AHN2 (explained in section 5.2.2), which is designed to cope with the same case of internal environmental changes evaluated in this implementation, is also included in among the 24 signal inputs.

Table 6.1: The 24 data inputs provided at the program inputs of the CGP-AHN

<b>Input Number</b>	<b>Input Data</b>	<b>Input Descriptions</b>
0	0	The constant vaule of zero
1	1	The constant vaule of one
2	Target Turn Velocity	Robot's turn velocity as commanded by the main robot controller
3	Target Left-side Velocity	Forward velocity on the left side of the robot as commanded by the main robot controller
4	Target Right-side Velocity	Forward velocity on the right side of the robot as commanded by the main robot controller
5	Target FL Velocity	Front-left-wheel velocity as commanded by the main robot controller
6	Target FR Velocity	Front-right-wheel velocity as commanded by the main robot controller
7	Target RL Velocity	Rear-left-wheel velocity as commanded by the main robot controller
8	Target RR Velocity	Rear-right-wheel velocity as commanded by the main robot controller
9	Actual Turn Velocity	Robot's actual turn velocity obtained from the robot's sensors
10	Actual Left-side Velocity	Forward velocity on the left side of the robot obtained from the wheel encoders
11	Actual Right-side Velocity	Forward velocity on the right side of the robot obtained from the wheel encoders
12	Actual FL Velocity	Front-left-wheel velocity acquired from the front-left-wheel encoder
13	Actual FR Velocity	Front-right-wheel velocity acquired from the front-right-wheel encoder
14	Actual RL Velocity	Rear-left-wheel velocity acquired from the rear-left-wheel encoder
15	Actual RR Velocity	Rear-right-wheel velocity acquired from the rear-right-wheel encoder
16	FL Speed Factor	Front-left-wheel speed factor parameter
17	FR Speed Factor	Front-right-wheel speed factor parameter
18	RL Speed Factor	Rear-left-wheel speed factor parameter
19	RR Speed Factor	Rear-right-wheel speed factor parameter
20	FL Kinematic Factor	Front-left-wheel kinematic factor parameter
21	FR Kinematic Factor	Front-right-wheel kinematic factor parameter
22	RL Kinematic Factor	Rear-left-wheel kinematic factor parameter
23	RR Kinematic Factor	Rear-right-wheel kinematic factor parameter

### **6.2.1.2 Computational nodes (Hormone Glands)**

Computational nodes are used to represent Hormone Glands in the AHN. As explained in section 4.1.1, there are a number of mechanisms defined in a HG. In general, altering the functions of each mechanism and changing how HGs are connected together can modify the operations of an AHN. Therefore, in order to allow the CGP-AHN to utilize these properties, the genotype of a computational node is designed to have 32 genes. Figure 6.4 (a) illustrates the mechanisms of HG and Figure 6.4 (b) displays how each mechanism of HG is encoded in the genotype.



Gene Locus		Gene Definition	
Connection Genes	1	C <sub>0</sub>	Cl <sub>0</sub> control input
	2	C <sub>1</sub>	Cl <sub>1</sub> control input
	3	C <sub>2</sub>	Cl <sub>2</sub> control input
	4	C <sub>3</sub>	Cl <sub>3</sub> control input
	5	C <sub>4</sub>	Cl <sub>4</sub> control input
	6	C <sub>5</sub>	Cl <sub>5</sub> control input
	7	C <sub>6</sub>	Cl <sub>6</sub> control input
	8	C <sub>7</sub>	Cl <sub>7</sub> control input
	9	C <sub>8</sub>	SI <sub>0</sub> signal input
	10	C <sub>9</sub>	SI <sub>1</sub> signal input
Function Genes	11	F <sub>0</sub>	Signal pre-processor
	12	F <sub>1</sub>	Signal parameter
	13	F <sub>2</sub>	Cl <sub>0</sub> control feature
	14	F <sub>3</sub>	Cl <sub>1</sub> control feature
	15	F <sub>4</sub>	Cl <sub>2</sub> control feature
	16	F <sub>5</sub>	Cl <sub>3</sub> control feature
	17	F <sub>6</sub>	Cl <sub>4</sub> control feature
	18	F <sub>7</sub>	Cl <sub>5</sub> control feature
	19	F <sub>8</sub>	Cl <sub>6</sub> control feature
	20	F <sub>9</sub>	Cl <sub>7</sub> control feature
	21	F <sub>10</sub>	Cl <sub>0</sub> threshold vaule
	22	F <sub>11</sub>	Cl <sub>1</sub> threshold vaule
	23	F <sub>12</sub>	Cl <sub>2</sub> threshold vaule
	24	F <sub>13</sub>	Cl <sub>3</sub> threshold vaule
	25	F <sub>14</sub>	Cl <sub>4</sub> threshold vaule
	26	F <sub>15</sub>	Cl <sub>5</sub> threshold vaule
	27	F <sub>16</sub>	Cl <sub>6</sub> threshold vaule
	28	F <sub>17</sub>	Cl <sub>7</sub> threshold vaule
29	F <sub>18</sub>	Activation function	
30	F <sub>19</sub>	Activation parameter	
31	F <sub>20</sub>	$\alpha_g$	
32	F <sub>21</sub>	$\beta_g$	

(b)

Figure 6.4: (a) The mechanisms of Hormone Gland (b) The definition of each gene locus in the genotype of computational node

There are two types of genes in the genotype of each computational node as shown in Figure 6.4 (b). These are:

### 1) Connection genes

Among the 32 genes used to define a computational node, 10 genes are dedicated as connection genes. These genes define where the node gets its signal information from. However, because there are two types of inputs for a HG, which are Control Input (*CI*) and Signal Input (*SI*), the connection genes are also separated into both types of inputs. As shown in Figure 6.4 (b), the first eight genes (gene loci 1 to 8) are set as *CI*s and the remaining two genes (gene loci 9 to 10) are defined as *SI*s. In principal, the total number of connection genes and the number of genes divided for *CI* and *SI* can be defined freely by the user. In this implementation, however, they are defined as explained because it was shown that only a maximum of six inputs are used by the HGs of the AHN2 illustrated in the previous chapter thus, in order to provide room for evolution, 10 inputs (8 *CI* + 2 *SI*) are set for the HGs in CGP-AHN.

### 2) Function genes

The remaining 22 genes in the genotype of each computational node are defined as the function genes. These genes are used to determine the functions and parameters of the HG mechanisms as follow:

- **Signal pre-processor and Signal parameter**

These two parameters are located at gene loci 11 and 12 respectively. Changing these two parameters generally alters the aspects of environmental information (environmental cues) which are responded to by a HG. Table 6.2 shows the 16 primitive functions defined for the *Signal pre-processor* and how the *Signal parameter* is used in each function. Other functions can also be defined in the *Signal pre-processor* but in this implementation it is expected that these functions should be able to help extract useful information from the inputs provided. It can also be noticed that all the functions used in the AHN2 are also included in the table. Note that the *Signal parameter* value is allowed to change from 0 to 20, and every divider operation in the function is protected. If the value of denominator is zero the output is set to be zero.

Table 6.2: The 16 primitive functions defined for the Signal Pre-processor and how the Signal parameter is used in each function

Function Address	Function	Function Description
0	$SI_0 / \text{Signal parameter}$	$SI_0$ which is scaled by signal parameter value
1	$SI_1 / \text{Signal parameter}$	$SI_1$ which is scaled by signal parameter value
2	$(-SI_0) / \text{Signal parameter}$	Negative value of $SI_0$ which is scaled by signal parameter value
3	$(-SI_1) / \text{Signal parameter}$	Negative value of $SI_1$ which is scaled by signal parameter value
4	$\text{Abs}(SI_0) / \text{Signal parameter}$	Absolute value of $SI_0$ which is scaled by signal parameter value
5	$\text{Abs}(SI_1) / \text{Signal parameter}$	Absolute value of $SI_1$ which is scaled by signal parameter value
6	$(SI_0 - SI_1) / \text{Signal parameter}$	The difference of $SI_0$ from $SI_1$ which is scaled by signal parameter value
7	$(SI_1 - SI_0) / \text{Signal parameter}$	The difference of $SI_1$ from $SI_0$ which is scaled by signal parameter value
8	$\text{Abs}(SI_0 - SI_1) / \text{Signal parameter}$	Absolute value of the difference between $SI_0$ and $SI_1$ which is scaled by signal parameter value
9	$(SI_0 + SI_1) / \text{Signal parameter}$	Summation between $SI_0$ and $SI_1$ which is scaled by signal parameter
10	$\text{SD}(SI_0, \text{Signal parameter})$	Standard deviation of $SI_0$ over a sampling period specified by signal parameter value
11	$\text{SD}(SI_1, \text{Signal parameter})$	Standard deviation of $SI_1$ over a sampling period specified by signal parameter value
12	$\text{Average}(SI_0, \text{Signal parameter})$	Average value of $SI_0$ over a sampling period specified by signal parameter value
13	$\text{Average}(SI_1, \text{Signal parameter})$	Average value of $SI_1$ over a sampling period specified by signal parameter value
14	0; when $\text{Abs}(SI_0 - SI_1) \leq \text{Signal parameter}$ 1; when $\text{Abs}(SI_0 - SI_1) > \text{Signal parameter}$	Check difference (whether $SI_0$ and $SI_1$ differ more than a value specified by signal parameter value)
15	0; when $\text{Abs}(SI_0 - SI_1) > \text{Signal parameter}$ 1; when $\text{Abs}(SI_0 - SI_1) \leq \text{Signal parameter}$	Check not difference (whether $SI_0$ and $SI_1$ differ less than a value specified by signal parameter value)

- **Control feature**

As explained in Chapter four, any inputs connected to a HG via *CI* are subjected to one of the control features. Table 6.3 lists all the possible control features and their addresses in the lookup table. Each of the possible eight *CI* can set its control feature separately from gene locus 13 to gene locus 20 as shown in Figure 6.4 (b).

Table 6.3: The control features and their addresses

Control feature address	Feature
0	No control feature
1	Inhibitory control
2	Stimulatory control
3	Positive feedback
4	Negative feedback

- **Threshold value**

The threshold value is available on any *CI*s which have the control feature set to Inhibitory control or Stimulatory control. This value is used to determine when the value of the *CI* can activate or deactivate the production of hormone in a HG. Similar to the control feature genes, there is a threshold value gene dedicated for each *CI*, thus the threshold value of each *CI* can be set separately (from gene locus 21 to gene locus 28). Note that the values of these genes can be set between 0 and 100 which represent the threshold values between 0.00 and 1.00.

- **Activation function and Activation parameter**

These two parameters (located at gene loci 29 and 30) determine the production of hormone in a HG based on its input signals as explained in section 4.1.1.2. Table 6.4 shows the three primitive functions defined in this implementation and how an Activation parameter is used in each function.

Table 6.4: The three primitive functions of the Activation function and how the Activation parameter is used in each function

Activation function address	Activation function	Function descriptions
0	$SI_{feature} / \text{Activation parameter}$	Linear function of the Signal Pre-processor output which is scaled by activation parameter value
1	$(1 / (1 + \exp(-t)))$ when $t = (SI_{feature} - \text{Activation parameter})$	Sigmoid function of the Signal Pre-processor output which is subjected to a decrement by activation parameter value
2	0; when $SI_{feature} \leq \text{Activation parameter}$ 1; when $SI_{feature} > \text{Activation parameter}$	Threshold function of the Signal Pre-processor output

- $\alpha_g$  and  $\beta_g$

The stimulation and decay rates of a HG can be determined at gene locus 31 and gene locus 32 respectively. The valid values of both genes are between 0 and 100 which represent the values between 0.00 and 1.00.

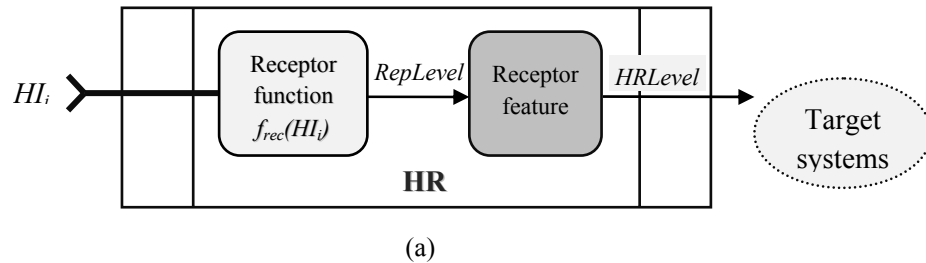
### 6.2.1.3 Program Outputs (Hormone Receptors)

As shown in Figure 6.3, the implementation of CGP-AHN contains eight program outputs which represent eight HRs as listed in Figure 6.5.

Program output	Hormone receptor
0	FL Speed Factor Hormone Receptor
1	FR Speed Factor Hormone Receptor
2	RL Speed Factor Hormone Receptor
3	RR Speed Factor Hormone Receptor
4	FL kinematic Factor Hormone Receptor
5	FR kinematic Factor Hormone Receptor
6	RL kinematic Factor Hormone Receptor
7	RR kinematic Factor Hormone Receptor

Figure 6.5: The eight Hormone Receptors represented by the program outputs

In contrast to the genotype of program outputs in CGP which contains only one gene, the program output genotype of CGP-AHN is set to include five genes in order to represent the mechanisms of HR. Figure 6.6 illustrates the definition of each gene locus and the fundamental mechanisms of HR.



	Gene Locus		Gene Definition
Connection Genes	1	C <sub>0</sub>	HI <sub>0</sub>
	2	C <sub>1</sub>	HI <sub>1</sub>
Function Genes	3	F <sub>0</sub>	Receptor feature
	4	F <sub>1</sub>	Receptor function
	5	F <sub>2</sub>	Receptor parameter

(b)

Figure 6.6: (a) The fundamental mechanisms of Hormone Receptor (b) The definition of each gene locus in the program output genotype

Similar to the genotype of computational nodes, there are also two types of genes in the program output genotype. These are:

### 1) Connection genes

Two genes are dedicated as the connection genes in the program output genotype of CGP-AHN as shown in Figure 6.6 (b). These genes (gene loci 1 and 2) are used to define where the hormone receptor gets its data from.

### 2) Function genes

Three genes are assigned to determine the mechanisms of HR as follow:

- **Receptor feature**

As explained in section 4.1.2.2, the Receptor feature of each HR can be set as the *Direct effect* or the *Accumulative effect*. These two features are defined in the lookup table shown in Table 6.5.

Table 6.5: The two receptor features

<b>Receptor feature address</b>	<b>Feature</b>
0	Direct effect
1	Accumulative effect

- **Receptor function and Receptor parameter**

These two genes are used to determine how the data of receptor inputs can determine the hormone receptor value. Table 6.6 illustrates the 16 primitive functions of the Receptor function and how the Receptor parameter is used in each function. Similar to the functions of Signal pre-processor, the primitive functions of the Receptor function can be defined freely by the user. The value of Receptor parameter is defined as being between 0 and 20 and every divider operation in the functions is protected.

Table 6.6: The 16 primitive functions of the Receptor function and how the Receptor parameter is used in each function

Function Address	Function	Function Description
0	$HI_0 / \text{Receptor parameter}$	$HI_0$ which is scaled by receptor parameter value
1	$HI_1 / \text{Receptor parameter}$	$HI_1$ which is scaled by receptor parameter value
2	$(-HI_0) / \text{Receptor parameter}$	Negative value of $HI_0$ which is scaled by receptor parameter value
3	$(-HI_1) / \text{Receptor parameter}$	Negative value of $HI_1$ which is scaled by receptor parameter value
4	$\text{Abs}(HI_0) / \text{Receptor parameter}$	Absolute value of $HI_0$ which is scaled by receptor parameter value
5	$\text{Abs}(HI_1) / \text{Receptor parameter}$	Absolute value of $HI_1$ which is scaled by receptor parameter value
6	$(HI_0 - HI_1) / \text{Receptor parameter}$	The difference of $HI_0$ from $HI_1$ which is scaled by receptor parameter value
7	$(HI_1 - HI_0) / \text{Receptor parameter}$	The difference of $HI_1$ from $HI_0$ which is scaled by receptor parameter value
8	$\text{Abs}(HI_0 - HI_1) / \text{Receptor parameter}$	Absolute value of the difference between $HI_0$ and $HI_1$ which is scaled by receptor parameter value
9	$(HI_0 + HI_1) / \text{Receptor parameter}$	Summation between $HI_0$ and $HI_1$ which is scaled by receptor parameter
10	$\text{SD}(HI_0, \text{Receptor parameter})$	Standard deviation of $HI_0$ over a sampling period specified by receptor parameter value
11	$\text{SD}(HI_1, \text{Receptor parameter})$	Standard deviation of $HI_1$ over a sampling period specified by receptor parameter value
12	$\text{Average}(HI_0, \text{Receptor parameter})$	Average value of $HI_0$ over a sampling period specified by receptor parameter value
13	$\text{Average}(HI_1, \text{Receptor parameter})$	Average value of $HI_1$ over a sampling period specified by receptor parameter value
14	0; when $\text{Abs}(HI_0 - HI_1) \leq \text{Receptor parameter}$ 1; when $\text{Abs}(HI_0 - HI_1) > \text{Receptor parameter}$	Check difference (whether $HI_0$ and $HI_1$ differ more than a value specified by receptor parameter value)
15	0; when $\text{Abs}(HI_0 - HI_1) > \text{Receptor parameter}$ 1; when $\text{Abs}(HI_0 - HI_1) \leq \text{Receptor parameter}$	Check not difference (whether $HI_0$ and $HI_1$ differ less than a value specified by receptor parameter value)

### 6.2.2 Example of CGP-AHN Encoding

In this section, an example of AHN represented by CGP is illustrated in order to help clarify the implementation of CGP-AHN. The genotype of the CGP-AHN is shown in Figure 6.7 (a), while the representation of the genotype as an AHN is shown in Figure 6.7 (b).

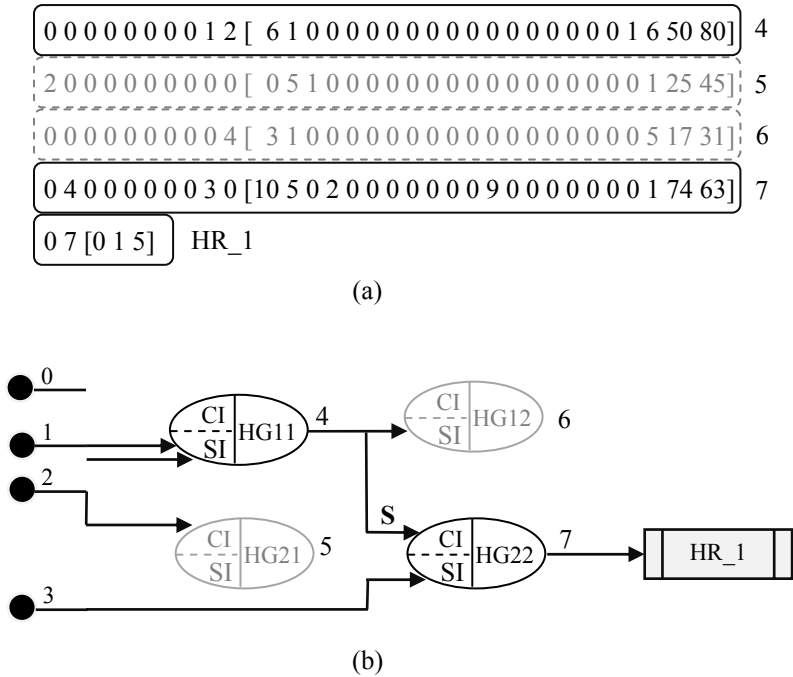


Figure 6.7: (a) An example of CGP-AHN genotype (b) The AHN decoded from the genotype shown in (a)

From the figure, it can be observed that there are four program inputs, four computational nodes and one program output in this CGP-AHN representation. The program inputs and the outputs of computational nodes are labelled numerically from 0 to 7 as shown in the figure. In Figure 6.7 (a) the genes located before the brackets represent the connection genes, while the genes shown in the brackets are the function genes.

For Node 4 (HG11), it can be observed in Figure 6.7 (a) that its gene locus 9 and gene locus 10 have the values of 1 and 2. This means that Node 4 takes its inputs from Input 1 and Input 2 at  $SI_0$  and  $SI_1$  respectively (refer to Figure 6.4). The values of Signal pre-processor and the Signal parameter genes (at gene loci 11 and 12) are set as 6 and 1 respectively. Referring to Table 6.2, this means that Node 4 takes the difference of Input 1 from Input 2 (function 6) with the scaling value of one (Signal parameter equals to

one). The Activation function and Activation parameter (at gene loci 29 and 30) are set to 1 and 6 respectively. This means that the activation function of Node 4 is set to be the sigmoid function with the output value of Signal pre-processor to be decreased by 6 (referred to Table 6.4). The gene locus 31 and gene locus 32 which determine the stimulation and decay rates of HG11 are set to 50 and 80 respectively. This determines the values of  $\alpha_g$  and  $\beta_g$  which are set to 0.5 and 0.8 respectively. Note that Input 0 of CGP-AHN is always set to be the constant value of zero, therefore any connection genes which are set to be '0' indicates that there is no signal connected to that input, as an example shown in the first eight connection genes of Node 4.

For Node 5 and Node 6, since the outputs of HG21 and HG12 are not used, these two nodes are inactive (coloured in grey).

For Node 7, there are two inputs connected to the node. The output from Node 4 is set as a control input at  $CI_l$  (defined by gene locus 2), while Input 3 is set as a Signal input at  $SI_l$  (defined by gene locus 9). The control feature of  $CI_l$  (the output from Node 4) is set to the Stimulatory control because gene locus 14 is set to 2 (refer to Table 6.3) and the Threshold value of  $CI_l$  is set to 0.09 because gene locus 22 is set to 9 (refer to Figure 6.4). The standard deviation of the signal data from the Input 3 over five sampling time steps are regarded as the environmental cue for activating the hormone production of Node 7 because gene loci 11 and 12 are set to 10 and 5 respectively (refer to Table 6.2). The linear function is used in the Activation function as defined by gene loci 29 and 30, while the values of  $\alpha_g$  and  $\beta_g$  are set to 0.74 and 0.63 respectively (as defined by gene loci 31 and 32).

For the program output (HR\_1 hormone receptor), the output from Node 7 is set as the input of the HR as defined by gene locus 2 (refer to Figure 6.6). The receptor feature is set to be the Direct effect as defined by gene locus 3 (refer to Table 6.5). The value of  $HRLevel$  which effects the target system of this HR is influenced by the value of the output from Node 7 which is scaled by 5 because gene loci 4 and 5 are set to 1 and 5 respectively (refer to Table 6.6).

This section illustrates an example of how a genotype of CGP-AHN can be used to represent an AHN and also how an AHN can be encoded in a CGP-AHN representation. In the next section, experiments on CGP-AHN for helping an autonomous robot deal with a case of internal environmental changes induced by a wheel fault are evaluated.

## 6.3 Experiments

Three experiments are conducted in this section in order to explore the ability of an AHN to be “designed” by CGP and to investigate the performance of an autonomous robot implemented with an AHN evolved by CGP-AHN compared to the robot implemented without AHN and with the AHN2 illustrated in the previous chapter. Experiment I focuses on investigating the AHNs evolved by CGP. Experiment II compares the robot performance when the robot is implemented with no AHN, with AHN2 and with CGP-AHN. Experiment III investigates the performance of AHNs in helping the robot operate in a different (one in which the CGP was not evolved in) environment.

The amount of time required in running CGP-AHN, especially in the evaluation process, plays a significant role in establishing the test scenario employed in these experiments. Even though, the robot and environments implemented in this research are simulated, the initial setup of the whole test systems used in this research makes it impossible to speed up the simulation process. Therefore, the simulation needs to be run in real-time. For this reason, careful considerations have to be made in designing the experiments in order to ensure that the expected number of experiments can be accomplished in a viable time.

As shown in the flat terrain environment experiment reported in section 5.2.3, without rough terrain in the test environment, the average time required for the robot to reach the target object is significantly decreased over that with rough terrain. Consequently, flat terrain experiment is considered in the experiments in this section. The case of internal environmental changes induced by a robot’s wheel fault when the robot is operating in a flat terrain environment is used to investigate the performance of CGP-AHN.

### 6.3.1 Experiment I: Initial test on CGP-AHN

The main objective of this experiment is to investigate the ability of CGP-AHN to evolve AHNs which can help an autonomous robot deal with the case of robot’s wheel faults. The test scenario in this experiment mimics the flat terrain environment experiment reported in section 5.2.3 with some modification. The robot and test arena

employed in this experiment is shown in Figure 6.8. The size of the test arena is decreased to 340cm x 400cm.

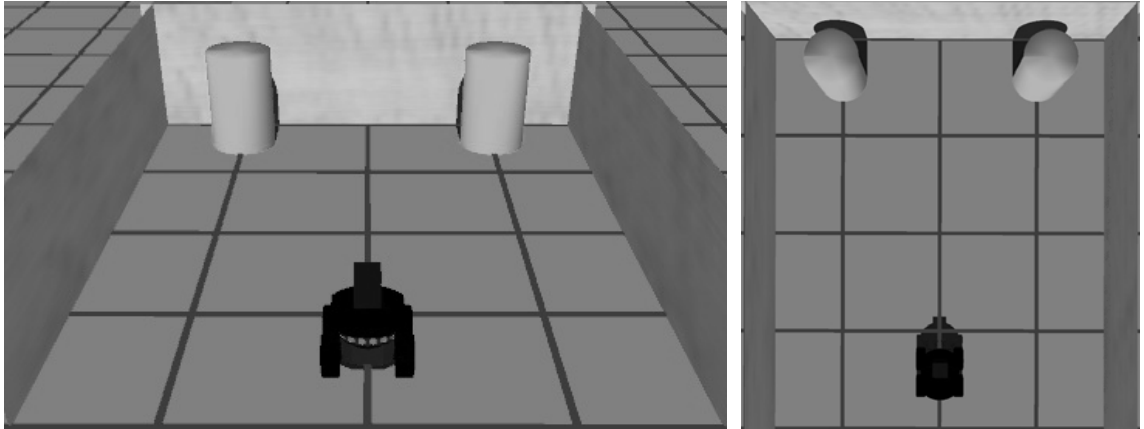


Figure 6.8: The robot and test arena employed in Experiment I (note that only one target object is presented at a time in the experiment)

### 6.3.1.1 Experiment Setup

- **Test Procedures**

As shown in the experiment in section 5.2.3, there are five fault test cases performed on the robot. These include when there is no wheel fault, when the fault occurs on front-left wheel, when the fault occurs on front-right wheel, when the fault occurs on rear-left wheel and when the fault occurs on rear-right wheel. However, in order to reduce the time required to evaluate each CGP-AHN individual, only three fault test cases are performed in this experiment. Each CGP-AHN individual is evaluated based on its performance in helping the robot operate in the three test cases which are defined as follow:

- 1) **Rear-right wheel fault**

In this case, the fault is injected to the rear-right wheel. As shown in Figure 6.9, in this case the target object is located on the left side of the arena. The main reason is because when the fault occurs on the right side of the robot, the robot is likely to move to the right. Locating the target object on the left is to evaluate whether a CGP-AHN individual can help adjust the robot's locomotion so as the

robot can reach the target object which is located at the opposite side of the wheel fault.

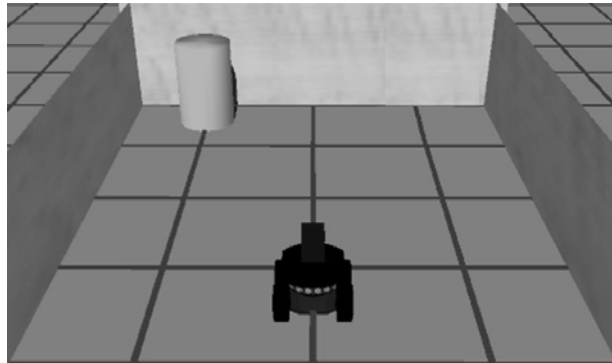


Figure 6.9: The target object position in the rear-right wheel fault test case

### 2) Rear-left wheel fault

In contrast to the previous test case, in this case, the fault is injected to the rear-left wheel and the target object is located on the right side of the test arena as shown in Figure 6.10.

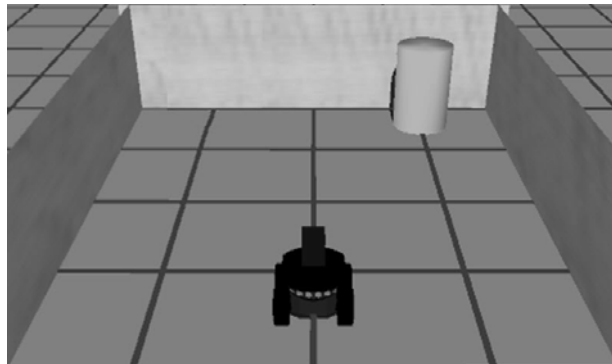


Figure 6.10: The target object position in the rear-left wheel fault test case

### 3) No wheel fault

The final test case is when there is no fault injected on the robot wheels. In this case, the target object is randomly located either on the left or on the right as shown in Figure 6.9 and Figure 6.10. In this case, without the wheel fault, an AHN should not negatively affect

the robot by preventing it to reach the target object located on either side.

Note that the starting position of the robot is fixed at the same position in every test case as shown in both Figure 6.9 and Figure 6.10. Each CGP-AHN individual is tested once on each test case.

Therefore, the performance of each CGP-AHN individual is evaluated based on the robot performance after the robot has been tested three times, once on each test case.

- **Fitness Function**

Fitness functions play a crucial role in evolutionary computing [127]. There are various techniques for helping accelerate the convergence of solutions, especially in problems where every run is expensive. In general, these approaches allow the fitness functions to change over time with the main aim to reduce the number of generations required to obtain an acceptable solution [128]. However, as the complexity of the test scenario employed in this experiment has already been reduced (as explained previously) thus only a static fitness function is investigated in this research. Other different fitness functions are considered beyond the scope of this research. The fitness function which is used to evaluate the performance of each CGP-AHN individual in this experiment is described further below.

Each CGP-AHN individual is evaluated based on the number of times that the robot can reach the target object, the average time spent to reach the target object and the average displacement between the robot and the target object. The fitness function used to assign the fitness score for each CGP-AHN individual is shown in Figure 6.11. This fitness function is designed based on the insights that:

- 1) The key performance is measured on the ability to help the robot reach the target object either when there is, or there is not, a wheel fault injected on the robot. Therefore, the better CGP-AHN

individual is the one which can help the robot reach the target object more often.

- 2) In the case when CGP-AHN individuals can help the robot to reach the target object in all three test cases, the better individual is the one which can help the robot reach the target object faster on average.
- 3) In the cases when the robot is unable to reach the target object in all three test cases, the better individual is the one which can bring the robot closer to the target object on average.

```

IF the_number_of_object_reach < 3
    IF average_displacement < 0.2
    THEN average_displacement = 0.2
    IF average_displacement > 2.236
    THEN average_displacement = 2.236
    fitness2 = (1.098231827 - (0.491159136 x average_displacement)) x 100
ELSE
    fitness2 = (1 - (average_time_to_reach / maximum_time_allowed)) x 100
ENDIF

fitness1 = the_number_of_object_reach x 100
fitness_score = fitness1 + fitness2

```

Figure 6.11: The fitness function for evaluating CGP-AHN individuals

As can be noticed in Figure 6.11, the fitness score is calculated from the values of two fitness terms which are *fitness1* and *fitness2*. The value of *fitness1* is obtained from the number of times the robot can reach the target object (*the\_number\_of\_object\_reach*) which is subjected to the weighting factor of 100. As explained in the previous sub-section, each CGP-AHN individual is tested three times, one on each test case. Therefore, each CGP-AHN individual can obtain the base score (*fitness1*) of 0, 100, 200 or 300 depending on the number of test cases which the robot can reach the target object.

In the case of *fitness2*, the value of this term is obtained based on whether the robot can reach the target object in all three test cases (as shown in Figure 6.11). In general, when the robot is able to reach the target object in all three test cases, *fitness2* is calculated based on the average time spent to reach the target object. On the other hand, if the robot is unable to reach the target object in all three test cases, *fitness2* is calculated from the average displacement between the robot and the target object.

There are two parameters related to the calculation of *fitness2* when the robot is able to reach the target object in all three test cases. These are *average\_time\_to\_reach* and *maximum\_time\_allowed*.

The *maximum\_time\_allowed* is defined by the maximum time limit the robot is allowed to operate in each test case. This time limit is set to 10 seconds. This means that in each test case the robot is allowed to operate for 10 seconds. From a preliminary experiment, it is found that the robot without the injection of the wheel fault is able to reach the target object in the test arena within less than 10 seconds but when the wheel fault is injected on a robot wheel, the robot requires more than 10 seconds to reach the target object. Therefore, it is expected that the CGP-AHN individual which can improve the robot's locomotion when the wheel fault occurs is the individual which can help the robot reach the target object within 10 seconds even when the fault is injected on a robot wheel.

The *average\_time\_to\_reach* is the average time the robot used to reach the target object in all three test cases. Put simply, it is the summation of the time spent to reach the target object in the test cases of rear-right wheel fault, rear-left wheel fault and no wheel fault divided by three.

Another parameter used for the calculation of *fitness2* when the robot cannot reach the target object in all three test cases is the *average\_displacement*. This value is obtained from the average displacement between the robot and the target object on all three test

cases. However, it should be noted that the displacement is measured from the centre position of the target object to the robot heading test vector as shown in Figure 6.12. The robot heading test vector is a vector pointing from the centre of the robot along the robot heading direction. The test vector is used instead of the robot centre position mainly because the robot heading direction is also needed to effectively define the displacement. Using the robot centre position, it is impossible to know which direction the robot is heading in. When the robot is at its starting position, the displacement between the target object and the robot heading test vector is measured 2.236 m, while when the robot reaches the target object the displacement is measured approximately 0.2 m. Therefore, the *fitness2* value, in the cases when the robot is unable to reach the target object in all three test cases, is defined as shown in Figure 6.11 in order to give the score of zero when *average\_displacement* is more than or equal to 2.236 m (the robot is at its starting position or further away) and the score of 100 when *average\_displacement* is less than or equal to 0.2 m.

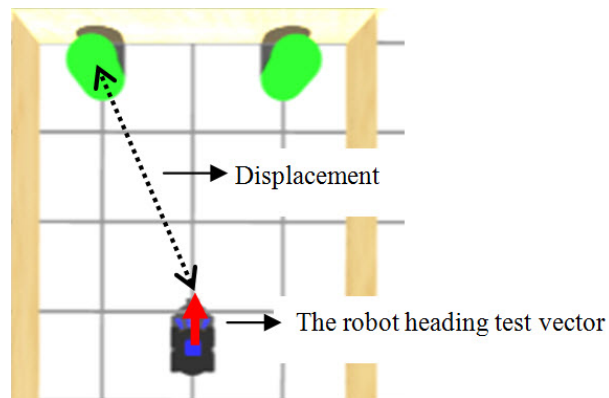


Figure 6.12: The measuring of displacement between the centre of the target object and the robot heading test vector

In summary, with this fitness function, when the robot is unable to reach the target object in all three test cases, a CGP-AHN individual can gain the fitness score between 0 to less than 300 depending on the average displacement between the target object and the robot heading test vector, as well as the number of times the robot can reach the target object. On the other hand, when the robot is able to reach the target object in all

three test cases, a CGP-AHN individual can obtain the fitness score from more than 300 to approximately 370 depending on how long it takes for the robot to reach the target object. The highest possible fitness score is approximately 370 (not 400) mainly because the maximum translation speed of the simulated Pioneer2-AT robot used in this research is 70 cm/s. The ‘travel displacement’ the robot has to cover in order to reach the target object is approximately 2.1 m. Therefore, if the robot constantly moves at its maximum speed, the robot would need approximately 3 seconds to reach the target object. This situation gives the fitness score of approximately 370. Note that although the displacement between the centre of the target object to the robot heading test vector is measured 2.236 m when the robot is at its starting position, the ‘travel displacement’ is measured only 2.1 m because the displacement is measured to the centre of the target object. However, the robot does not need to travel to the centre of the target object to be classified as ‘reaching the target object’. The robot only has to move close to the target object at a certain distance in order to reach the target object and the ‘travel displacement’ between the position where the robot is classified as ‘reaching the target object’ and the starting position of the robot is measured approximately 2.1 m.

- **CGP Parameter Settings**

The parameters of CGP used in this experiment are set as follow:

- 1) The number of columns : 80
- 2) The number of rows : 1
- 3) Levels-back : 80
- 4) Evolutionary Strategy : 1 + 4
- 5) Mutation rate : 1%
- 6) The number of generations : 500

Similar to most CGP implementations, the CGP-AHN in this experiment has the number of rows equals to one and the levels-back equals to the number of columns [122, 125]. The maximum number of computational node is 80 and every computational node can take its inputs from any

previous nodes on the left. Because each computational node contains 32 genes and each program output has 5 genes, this means that a genotype contains 2,600 genes  $((32 \times 80) + (5 \times 8))$ . Thus, with the mutation rate of 1%, normally up to 26 genes would be mutated from a parent to create an offspring.

The parameter settings shown is based on the work reported in [125]. The study found that the computational effort required to find a successful solution in an evolutionary run of CGP is low when the genotype size is large and the mutation rate is low. The implementation of CGP-AHN in this chapter follows this finding and attempts to use the parameter settings which are more likely to achieve fast evolution. Therefore, the mutation rate in this experiment is set to 1%. The maximum number of computational nodes is set to 80 because it is shown in the AHN2 (in the previous chapter) that eight HGs are enough to help the robot deal with the case of internal changes considered in this experiment, thus 80 nodes are expected to be large enough.

It is clear that there are other CGP-AHN parameter settings which are also worth investigating in order to evaluate the performance of the system. However, because of the time constraints, this issue is left for future work.

With the experiment setups explained in this section, the maximum time required to evaluate a CGP-AHN individual is 30 seconds as the maximum time allowed in each test case is 10 seconds and each individual is tested on three test cases. There are five individuals evaluated in each generation (1 + 4 evolutionary strategy). Thus, each generation requires the maximum of 150 seconds  $(30 \times 5)$ . The number of generations set for each evolutionary run is 500 and the experiment is set to operate for 40 evolutionary runs. Therefore, the maximum time required to run this experiment is 3,000,000 seconds  $(150 \times 500 \times 40)$  or approximately 833 hours.

### 6.3.1.2 Results

The results of 40 CGP-AHN evolutionary runs are shown in Figure 6.13. The fitness scores shown in the box plot are acquired from the fitness score after 500 generations of each evolutionary run. It can be observed from the plot that the successful configurations of AHN (the one that gains the fitness score more than 300) can be found in almost every evolutionary run. The highest fitness score obtained is 359.33 and the lowest fitness score is 281.76.

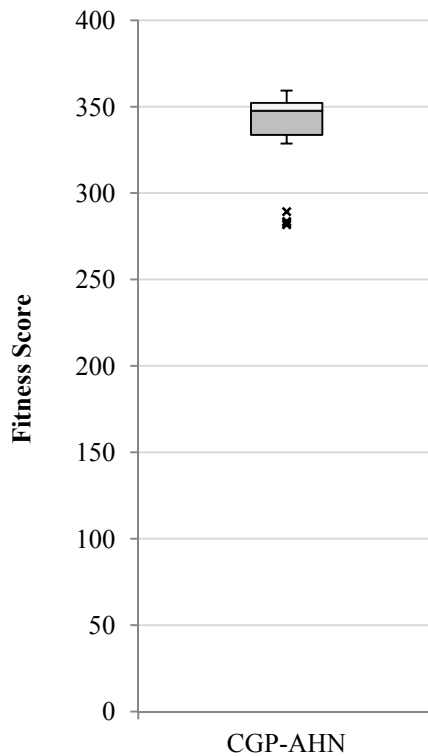


Figure 6.13: The fitness scores of 40 evolutionary runs in Experiment I

### 6.3.1.3 Analyse and discussion

For further investigation, the best and average fitness scores obtained on each generation of AHNs, which obtain the minimum (excluding the outliers), the median and the maximum fitness scores (as shown in Figure 6.13), are illustrated in Figure 6.14 (a), (b) and (c) respectively. These three AHN configurations are referred further in this chapter as the Min, the Med and the Max AHNs, respectively.

As shown in Figure 6.14, the best fitness scores obtained in the first generations from the Min, the Med and the Max AHNs are 177.03, 178.04 and 278.96 respectively. These mean that the best AHN configurations at the first generations of the Min and the Med AHNs can help the robot to reach the target object in only one out three test cases and the average displacement between the target object and the robot is approximately 0.81 m (refer to the fitness function described). On the other hand, the best AHN configurations at the first generations of the Max AHN can help the robot reach the target object in two out three test cases and the average displacement between the target object and the robot is approximately 0.63 m. Subsequently, the fitness scores of each AHN configuration are developed gradually as shown in Figure 6.14. Finally, the best AHN configurations at the 500<sup>th</sup> generations of the Min, the Med and the Max AHNs obtain the fitness scores of 328.67, 347.33 and 359.33 respectively. These mean that at the 500<sup>th</sup> generation, all three AHNs can help the robot reach the target object in all three test cases and the robot spends 7.133, 5.267 and 4.067 seconds on average to reach the target object, respectively.

As can be noticed in Figure 6.14, the leaps in the values of fitness scores between 100 & 200, 200 & 300 and 300 & 400 indicate the situations when the number of times the robot reaches the target object are changed because these situations can change the fitness scores as high as a factor of 100, as explained previously in the fitness function section.

From Figure 6.14, it may also suggest that the acceptable solutions might not be difficult to acquire. One of the main reasons is because of the reduction in complexity of the test scenarios, as explained previously. However, in more complex scenarios (e.g. the ones investigated in chapters 4 and 5), this might not be the case.

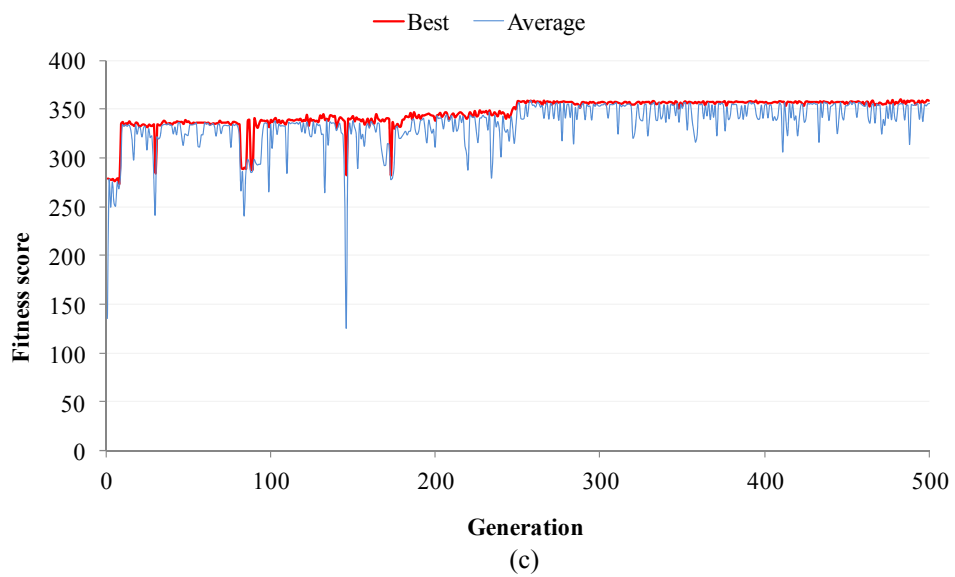
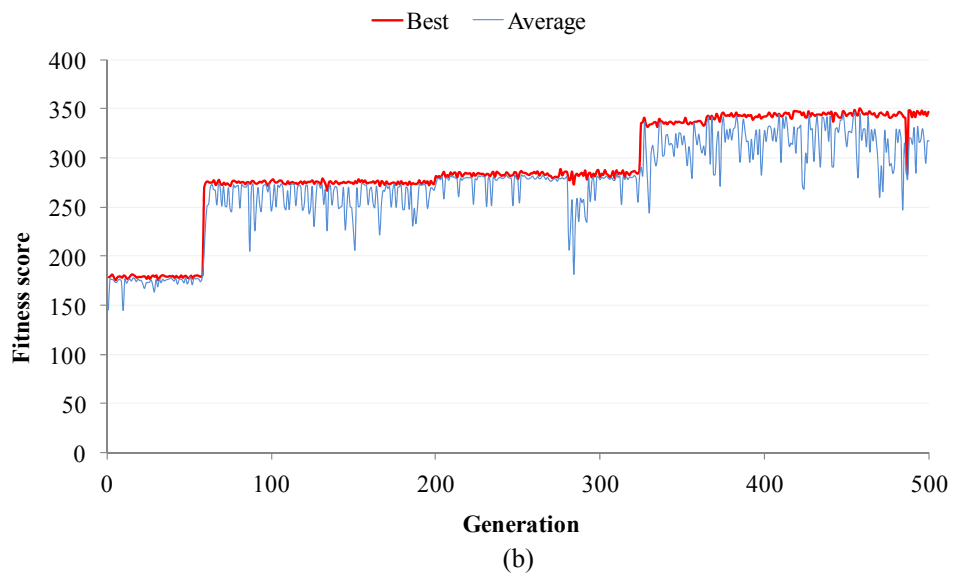
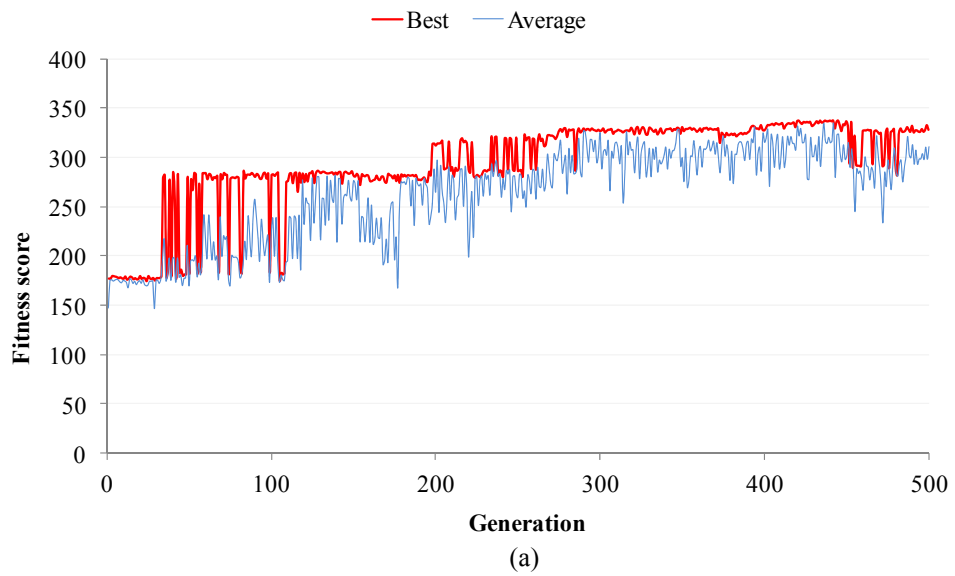


Figure 6.14: The best and average fitness scores over 500 generations from a single evolutionary run of (a) the Min AHN, (b) the Med AHN and (c) the Max AHN.

It can be observed that the best fitness scores do not keep increasing even though elitism is implemented. Three main reasons behind this issue are as follow:

**1) The uncertainty in Gazebo simulation**

Generally, for the robot simulated in Gazebo, although the robot and the target object are positioned exactly at the same places in two different runs, the routes taken by the robot in both runs are not always exactly the same; the route can be slightly different. Because of this, the fitness score in each run can be slightly different even through the robot is implemented with the same CGP-AHN individual.

**2) The possibility of the sudden change in the fitness scores**

With the fitness function explained, it can be observed that the fitness score can be changed rather significantly depending on whether the robot can or cannot reach the target object in each test case. Because of the tight time limit (10 seconds) allowed in each test case, the results show that in the cases when a CGP-AHN individual which is able to help the robot reach the target object at very close to the time limit is selected to be the new parent. There is a high possibility that when this individual is re-tested again in the next generation, the slightly different routes taken causes the robot to miss the target object, which in turn decreases the fitness score.

**3) The non-deterministic nature of the test scenario**

As explained in the Test Procedures sub-section, in the no wheel fault test case, the target object is randomly located either on the left side or on the right side of the test arena. This causes the changes in the fitness score because there is a possibility that the chosen parent is an individual which is only able to help the robot reach the target object located on a particular side of the test arena. When the individual is re-tested in the next generation and the target object is randomly located on another side, the robot might not be able to reach the target object in time.

Considering the number of active nodes, the best AHN configuration has 65 active nodes. However, for the CGP-AHN representation used in this work, it is possible that even if the output of a node is connected to another node, the node of that output may not be classified as active because it may not actually be used. For example, if the output of Node1 is connected to a Control Input of Node2 but the control feature of that input is set to “no control feature”. In this case, the output of Node1 is not actually being used, thus the Node1 is not classified as active. Therefore, if considering only the actual active nodes, the best AHN configuration has only 51 active nodes.

### **6.3.2 Experiment II: Comparing the performance of no AHN, AHN2 and the best CGP-AHN**

In order to further investigate the performance of CGP-AHN in helping the robot deal with the case of internal environmental changes induced by the wheel fault, this experiment focuses on the comparisons of the robot performance between the robots implemented with no AHN, with AHN2 and with CGP-AHN.

It is obvious that from the 40 evolutionary runs in Experiment I, several different good configurations of AHN are obtained. However, only the best AHN configuration from an evolutionary run which gains the highest fitness score (the Max AHN) is selected for further investigation in this experiment. Therefore, there are three systems investigated in this experiment. These are:

- 1) The robot implemented without any AHNs (No AHN)
- 2) The robot implemented with the AHN2 illustrated in Chapter 5 (AHN2)
- 3) The robot implemented with the best CGP-AHN obtained in the previous experiment (CGP-AHN)

#### **6.3.2.1 Experiment Setup**

The robot and the test arena employed in this experiment are similar to the ones used in the previous experiment as shown in Figure 6.8. Moreover, the three systems are also set to be investigated on the same test procedures described in section 6.3.1.1. The performance of each system is evaluated using the fitness function explained in the previous experiment. However, there is no evolution running in this experiment. The main objective of this experiment is to compare the performance of the three systems in

performing the test scenario used in the previous experiment. Nevertheless, because of the stochastic nature of the test scenario explained in the previous section, in this experiment, each system is tested for 40 runs.

### 6.3.2.2 Results

Figure 6.15 shows the performance of the three systems. The box plots present the system performance based on the fitness score obtained from 40 runs on each system. Note that applying Mann-Whitney U test between the results of the three systems, the significance test shows that the results of the three systems are significantly different ( $p$ -value  $< 0.05$ ).

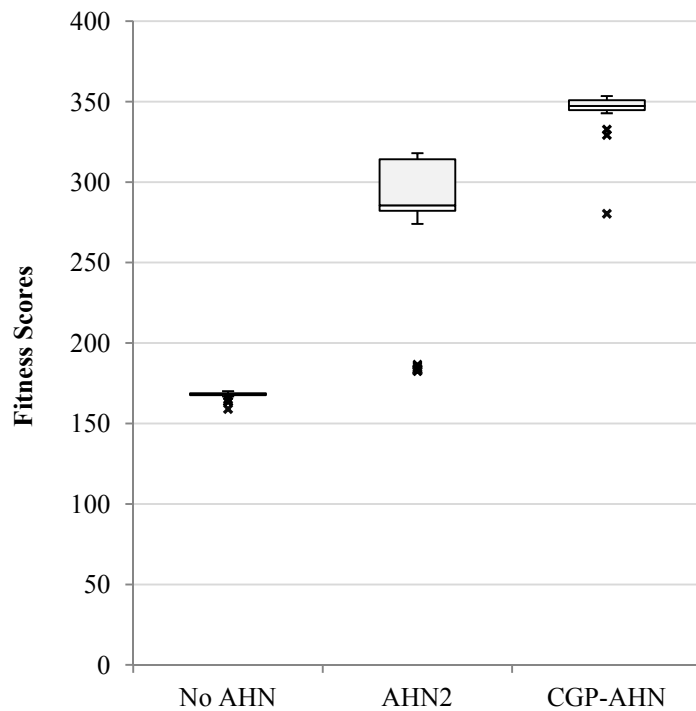


Figure 6.15: The performance of the three systems in term of the fitness score obtained from 40 runs on each system

### **6.3.2.3 Discussion**

In Figure 6.15, it can be observed that the CGP-AHN performs the best. The robot can reach the target object in all three test cases (the fitness score more than 300) in almost all of the runs. In the case of the AHN2, although the robot is unable to reach the target object in all three test cases in every run, most of the times the robot is able to reach the target object in at least two out of three test cases. However, when there is no AHN implemented on the robot, it can be observed that the robot can reach the target object only in one test case (the fitness score more than 100 but less than 200) and this is the case when there is no wheel fault.

The results from both Experiment I and Experiment II indicate that AHN configurations, constructed by CGP, can help the robot deal with the case of internal environmental changes induced by the wheel fault when the robot operates in the flat terrain arena. However, it is interesting to investigate further whether the best CGP-AHN is capable of assisting the robot operate in different test arenas on the same case of internal environmental changes. This issue is the main attention of the next experiment.

### **6.3.3 Experiment III: Generalization Test**

The main objective of this experiment is to investigate whether the best CGP-AHN can assist the robot to reach the target object located at other positions which are different from the target object's positions in the environment in which the best CGP-AHN were evolved. The main reason is to evaluate whether the better performance of the best CGP-AHN shown in the previous experiment was obtained because the best CGP-AHN was evolved in that particular environment.

#### **6.3.3.1 Experiment Setup**

The robot and test arena employed in this experiment are shown in Figure 6.16. The size of the arena is measured 540cm x 700cm. It can be observed that in this experiment the target object is located at five positions which are different from the positions used in both Experiment I and Experiment II. It is worth mentioning that, even though there are five target objects shown in Figure 6.16, this is just for the illustration purposes. In the experiment, only one of these target objects is presented at one of the locations at a time.

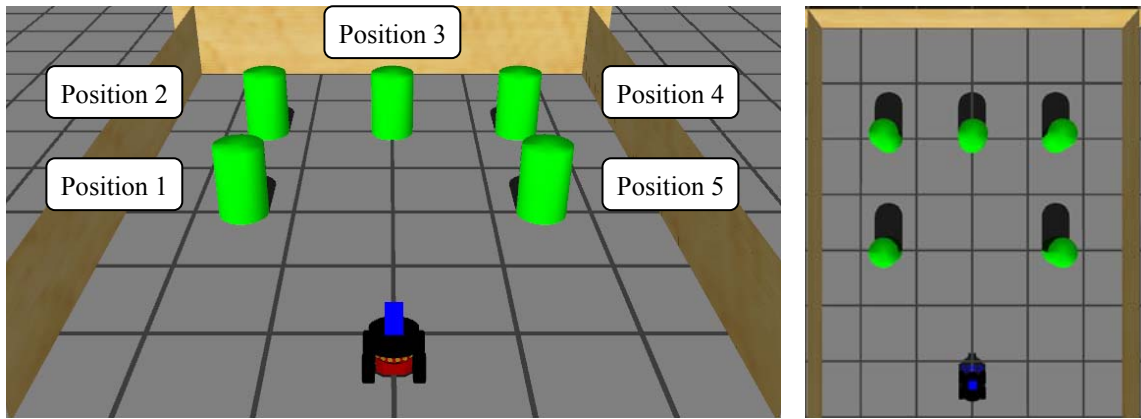


Figure 6.16: The robot and the test arena employed in Experiment III

The test procedures in this experiment are based on the three test cases used in Experiment I and Experiment II (rear-right wheel fault, rear-left wheel fault and no wheel fault test cases). However, instead of operating once in each test case, in this experiment, the robot must be operated for five times in each test case. Moreover, in these five runs, the position of the target object is changed to cover all five locations shown in Figure 6.16. Therefore, there is the total number of 15 test cases to be evaluated on each system as follow:

- 1) Rear-right wheel fault / target object at Position 1
- 2) Rear-right wheel fault / target object at Position 2
- 3) Rear-right wheel fault / target object at Position 3
- 4) Rear-right wheel fault / target object at Position 4
- 5) Rear-right wheel fault / target object at Position 5
- 6) Rear-left wheel fault / target object at Position 1
- 7) Rear-left wheel fault / target object at Position 2
- 8) Rear-left wheel fault / target object at Position 3
- 9) Rear-left wheel fault / target object at Position 4
- 10) Rear-left wheel fault / target object at Position 5
- 11) No wheel fault / target object at Position 1
- 12) No wheel fault / target object at Position 2
- 13) No wheel fault / target object at Position 3
- 14) No wheel fault / target object at Position 4
- 15) No wheel fault / target object at Position 5

Similar to the previous experiment, no evolution is operated. The three systems (No AHN, AHN2 and CGP-AHN) are investigated in this experiment. Each system is tested for 40 times. The performance of each system is evaluated by the same fitness function used in the previous two experiments. However, because of the variations in the test arena and the number of test cases, there are some changes on the fitness function parameters.

The *maximum\_time\_allowed* is increased to 30 seconds. This means that the robot is allowed to operate at the maximum of 30 seconds in each test case. In addition, because of the increasing number of test cases, the value of *the\_number\_of\_object\_reach* can be changed from 0 to 15 depending on the number of test cases when the robot reaches the target object. Therefore, the performance of the systems in term of the fitness score in this experiment can have values from 0 to less than 1600.

### **6.3.3.2 Results**

The performance of the three systems is shown in Figure 6.17. The box plots present the performance of each system in term of the fitness scores obtained from 40 runs on each system. The highest fitness scores obtained by the No AHN, AHN2 and CGP-AHN are 1,552, 1,567.47 and 1,580.44 respectively. Note that the Mann-Whitney U test results indicate that the results of the three systems are significantly difference ( $p$ -value < 0.05).

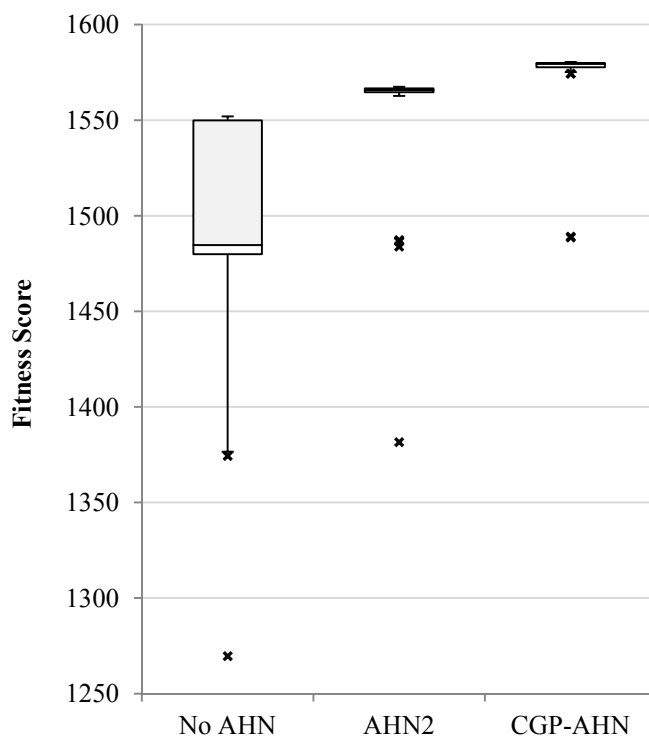


Figure 6.17: The box plots present the fitness scores obtained from 40 runs on each system

### 6.3.3.3 Analysis and discussion

From Figure 6.17, it can be observed that, in the majority of the runs, both AHN2 and CGP-AHN can consistently help the robot reach the target in all 15 test cases, comparing to the case of No AHN where the system performance is more inconsistent. The results indicate that the best CGP-AHN is not only specialized for the environment in which the AHN was initially evolved but is also able to help the robot operate in the new environment, where the target object is located at different locations. Further analysis on how the best CGP-AHN helps the robot cope with the case of internal environmental changes induced by the wheel fault is further discussed on the issue of time spent and the robot traces. Note that the analysis is based on the best runs of each system shown in Figure 6.17.

- **Time Spent**

Table 6.7 shows the time spent by the robot on each system in order to reach the target object in each test case. Similar to the results shown in the flat terrain environment experiment reported in section 5.2.3, the presence of the wheel fault generally causes the robot to spend a longer time reaching the target object

because the internal change induced by the wheel fault affects the locomotion system of the robot.

With the implementations of the AHNs (either the AHN2 or the best CGP-AHN), the robot is able to adjust its locomotion system and is better adapted to the changes as shown by the shorter time spent on average to reach the target object. It can be observed that the better performance of the CGP-AHN shown in Figure 6.17 comes from the fact that the CGP-AHN not only helps the robot to reach the target object but also allows the robot to move faster. As can be noticed from Table 6.7, the robot never spends longer than 10 seconds to reach the target object when the wheel fault occurs in the case of the CGP-AHN. In contrast, without the best CGP-AHN, the robot spends more than 10 seconds on average when the wheel fault is injected

Table 6.7: The time spent to reach the target object on each test case. Each average time spent is calculated from the same fault case over five positions of the target object

Test case	Target object position	Time spent (s)			Average time spent (s)		
		No AHN	AHN2	CGP-AHN	No AHN	AHN2	CGP-AHN
1	Position 1	12.4	8.4	4.2	17.6	10.5	5.4
2	Position 2	23.0	14.6	7.2			
3	Position 3	19.6	13.8	6.6			
4	Position 4	22.0	10.4	6.2			
5	Position 5	10.8	5.4	3.0			
6	Position 1	8.8	5.2	4.6	17.7	10.6	7.0
7	Position 2	20.6	10.4	8.2			
8	Position 3	23.2	12.4	6.8			
9	Position 4	22.8	16.2	9.4			
10	Position 5	13.0	9.0	6.0			
11	Position 1	6.2	6.2	3.8	8.0	8.1	5.2
12	Position 2	9.2	9.4	7.2			
13	Position 3	8.8	8.8	5.8			
14	Position 4	9.4	9.6	6.2			
15	Position 5	6.2	6.6	2.8			

- **Robot Traces**

Figure 6.18 illustrates the robot routes taken by the three systems on each test case. Considering the No AHN system, it can be observed that the wheel fault causes the robot to move slightly to the side that the fault is injected and the robot needs to keep doing regular turns in order to reach the target object (this can be observed from the routes which are rather coarse). With the AHN2, the velocity compensations help adjust the robot movement, and the robot can stay better on track as can be observed from the routes.

However, in the case of the CGP-AHN, when the fault is injected to the rear-right wheel, it can be observed that the best CGP-AHN influences the robot to move in right-curve routes but is able to make huge left turns when needed in order to reach the target object, as shown in Figure 6.18 (a). It is interesting that the robot approaches the target object in the case when there is no wheel fault (Figure 6.18 (c)) in quite similar ways to the case when the fault is injected to the rear-right wheel. This indicates that the best CGP-AHN influences the robot to move in a way that there is very little differences in the routes taken whether there is no wheel fault or there is the rear-right wheel fault occurring. Furthermore, considering on the case of rear-left wheel fault Figure 6.18 (b), the best CGP-AHN is able to influences the robot to take the straight routes and make either left or right turns in order to reach the target object.

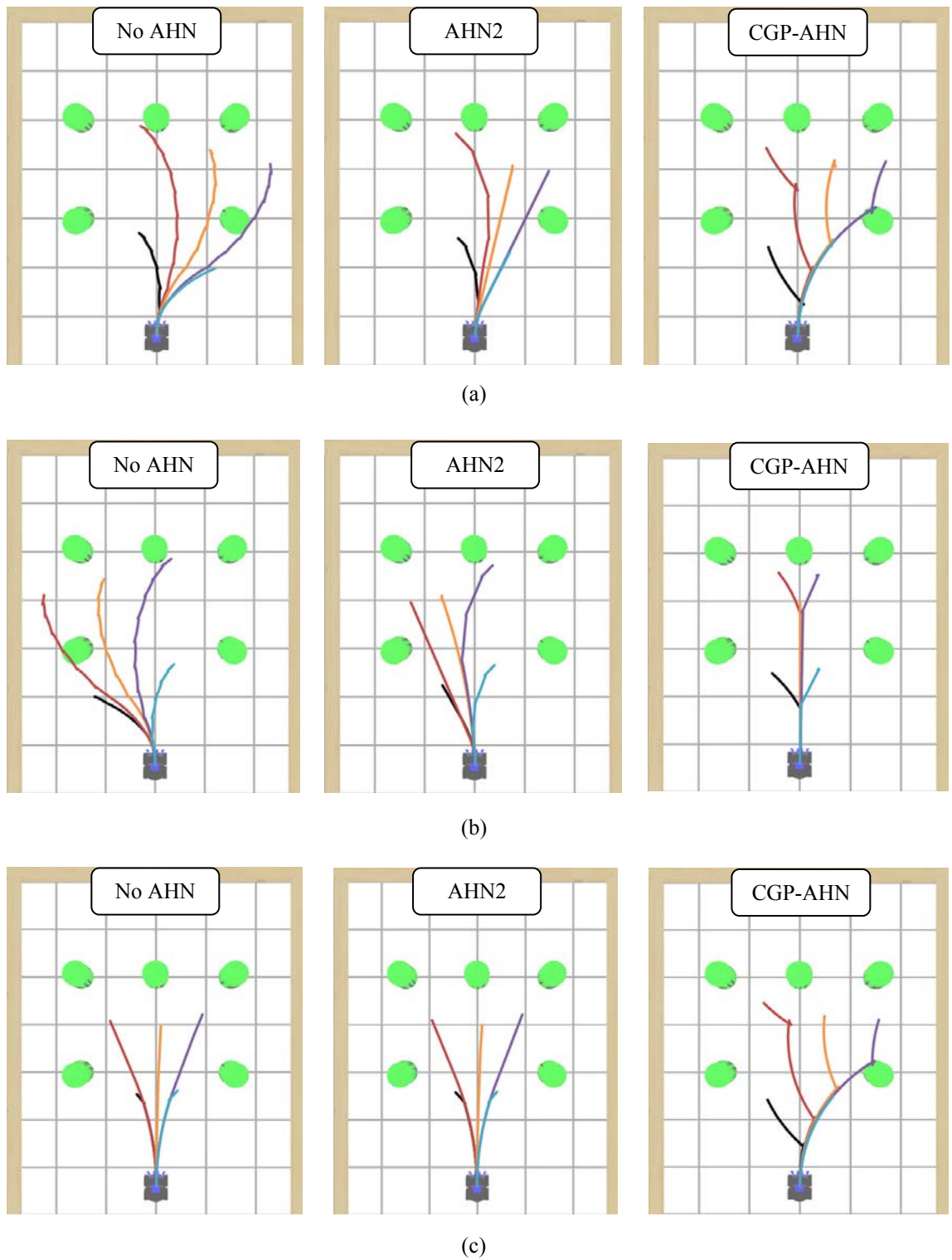


Figure 6.18: The robot routes taken by each system in the case of (a) rear-right wheel fault (b) rear-left wheel fault (c) no wheel fault. Note that each trace colour represents routes taken to reach the target object at each particular position as follow: Black (Position1), Red (Position2), Orange (Position3), Purple (Position4) and Blue (Position5)

Further investigation into the configuration of the best CGP-AHN is clearly needed in order to understand how the best CGP-AHN operates and helps the robot cope with the change. However, it is hardly possible to deduce meaningful information by drawing the hormone networks because they are constructed from more than 50 computational nodes with a huge number of connections between the nodes. Nevertheless, one possible way to perceive the effects of the best CGP-AHN is to investigate the changes of values at its program outputs (hormone receptors). As introduced in section 6.2.1.3, there are eight program outputs representing eight hormone receptors in this CGP-AHN representation. Observing the changes of the values of all program outputs, it is found that there are only three program outputs whose values are changed when the robot is in operation. These are the program outputs 4, 5 and 6 which correspond to the FL kinematic factor, FR kinematic factor and RL kinematic factor respectively. These three parameters are changed in a way that their values keep increasing to a certain value when the robot is operating. The outcome of this behaviour is to increase the velocity of front-left, front-right and rear-left wheels. It can be perceived that this situation correlates to the robot movements shown in Figure 6.18. Because the best CGP-AHN influences the velocity increment on both left wheels but only on one right wheel (front-right), this condition causes the robot to be more likely to move to the right. This is the reason for the right-curve routes shown by the robot. In the case when the fault occurs on the rear-right wheel, the velocity increment on the rear-right wheel is cancelled out because of the fault. In this case, the best CGP-AHN is only able to increase the velocity on one wheel of both sides (which are front-right and front-left), thus the velocity on both sides are much more balanced. This is the reason for the straight routes shown in Figure 6.18 (b).

The main objective of this chapter is to explore the ability of AHN to be constructed by an automatic design method. The results from all three experiments correspondingly indicate that the AHNs, which are able to help an autonomous robot cope with the case of internal environmental changes induced by the wheel fault, can be constructed automatically using CGP.

## 6.4 Summary

In this chapter, one of the key aspects of an Artificial Hormone Network, the ability to be designed automatically to provide adaptability for autonomous robots, is investigated. As shown in the previous two chapters, generally AHNs can be designed by the user to help autonomous robots deal with different environmental changes. However, it can also be observed that not only can the hormone networks be constructed in a number of ways but the mechanisms and parameters of Hormone Glands in the networks can also be established differently. Therefore, the ability of AHN to be constructed automatically using an off-the-shelf intelligent design method is considered useful. CGP is utilized to investigate this ability because of its representation as a two-dimensional grid of computational nodes which is deemed appropriate to represent an AHN.

Three experiments were conducted in this chapter with the main purpose to investigate the performance of AHN configurations evolved by CGP. The case of internal environmental change induced by the wheel fault when an autonomous robot operates in flat terrain environment is employed as the test scenario. Results show that the best CGP-AHN individual obtained is not only able to help the robot deal with the case of internal environmental changes in the test environment where the individual was evolved but can also help the robot operate in a different test environment.

In this chapter, the performance of CGP-AHN was investigated in only one test scenario. Not only a number of test scenarios but also a number of CGP parameter settings might also be investigated in order to further evaluate the performance of CGP-AHN. However, the significant time required to evaluate each CGP-AHN individual on the test environments used in this research plays a very significant role in obstructing these investigations.

Investigating CGP-AHN in providing adaptability for an autonomous robot operating in rough terrain environments is certainly one of the most interesting test scenarios. For example, in the case of internal environmental changes induced by the sensor fault investigated in section 5.1 or the case of internal environmental changes induced by the wheel fault when the robot operates in the rough terrain environment investigated in section 5.2.4.

Although, identifying the exact time required to investigate CGP-AHN on these test scenarios is difficult without first running some preliminary experiments, the estimated time might be acquired. Considering just one evolutionary run of 500 generations with 1+4 evolutionary strategy, there are 2,500 individuals need to be evaluated (if only the offspring genotypes are evaluated, the number can be decreased to 2,000 individuals). In the case of the sensor fault investigated in section 5.1, assumed that each individual is tested for only 50 runs (instead of 100 in the original experiment) and the maximum time allowed is reduced to just 5 minutes (instead of 15 minutes), the maximum time required to evaluate one individual is 250 minutes. If 2,500 individuals are needed (as explained above), one evolutionary run would require the maximum of 625,000 minutes which is approximately 434 days.

It can be noticed that the time required to evaluate each individual plays the vital role in the time to investigate the CGP-AHN. Therefore, decreasing the time required in the evaluation process is considered the most important issue. One possible solution is to reduce the size of the test arena and the complexity of the test terrain, thus the robot can perform the assigned task faster and the time allowed to operate can be reduced. This is the solution used for the test scenario investigated in this chapter. Another solution is to implement the test environments using other robot simulators which are capable of physics simulations but also allow the speed up of simulations.

In the next chapter, methodologies for extending the AHN architecture for other robotic application scenarios will be discussed.

## **Chapter 7**

### **Generalisation Methodology**

The AHN is proposed in this research as a mechanism which assists autonomous robots to deal with both internal and external environmental changes. The key driver of the system is the cues from environments which influence the production and secretion of hormones. The dynamic interactions between hormones, in turn, adjust the robot's systems and provide adaptability for autonomous robots to deal with environmental changes and to operate in dynamic environments.

The two fundamental mechanisms of the AHN, the Hormone Gland (HG) and the Hormone Receptor (HR), were illustrated in Chapter 4. Subsequently, it has been shown in Chapter 5 that the two mechanisms can be constructed in a different manner in order to create hormone networks which can provide different adaptability for various autonomous robot situations. For instance, the AHN1 is designed to help autonomous robots deal with different terrain roughness and the case of internal environmental changes induced by sensor faults. In contrast, the AHN2 is constructed to assist autonomous robots to cope with the effects from both terrain roughness and actuator faults. It is shown that different hormone networks can be achieved by the alteration of the functions and parameters of HGs and HRs, as well as the changing of the connections and interactions between them.

This chapter concentrates on providing methodologies on how the proposed AHN1 and AHN2 can be generalised in order to cope with other application scenarios and how to extend the AHN for other robotic application scenarios. Section 7.1 focuses on the methodologies for extending the proposed AHN1 and AHN2 for other types of robots and applications, while section 7.2 discusses the methods for constructing the AHN for other application scenarios. Section 7.3 gives the summary of this chapter.

## **7.1 Methodology for Extending the AHN1 and AHN2**

This section provides guidelines on how to apply the AHN1 and the AHN2 for other types of robots and other application scenarios different from the ones elucidated in Chapter 4 and Chapter 5.

### **7.1.1 Extending the AHN1 for Other Types of Robots**

The proposed AHN1 elucidated in Chapter 5 is designed mainly to help autonomous robots deal with the affects of external environmental changes caused by rough terrain and the internal environmental changes induced by sensor faults. One of the key features which gives the AHN1 the capability of being implemented on different types of robots is that the production of hormones in the AHN1 are driven by the environmental cues which are perceived directly through the robots' sensors and are obtained from the interactions of the robots with the environments where the robots operate. Therefore, when the AHN1 is implemented on different robots, the production of hormones in the AHN1 are driven differently, and appropriately, corresponding to the environmental cues perceived by the sensors on each particular robot and the interactions of each robot with the environments in which it operates.

There are some general requirements of the systems which are expected to be implemented directly with the proposed AHN1. Because the proposed AHN1 responds to two main environmental cues, which are the robot's stability and the conflicts between two corresponding sensory inputs which imply the robot's stability, the target robots must have sensing systems which are able to provide similar kinds of sensory information. For example, the target robots may have two sensory channels which can provide information about the stability of the robot but are at different levels of confidence (such as the pitch and the frontal area distance sensory information explained in Chapter 5).

For the methods to implement the AHN1, generally, the main sensory data expected to provide information about the robot's stability must be connected to the HG1, while the less confident sensory information must be connected to the HG2. In addition, both sensory channels must be connected to HG3 where the *Signal pre-processor* is set to detect the conflicts that imply negative changes in the main sensory information. Regarding the HR\_MC, this hormone receptor should be located with the velocity

commands of the target robots so that the hormones can influence the speed of the robot.

### 7.1.2 Extending the AHN1 for Other Robotic Applications

Apart from extending the AHN1 for different types of robots, with slight modification, the hormone network can also be extended for other application scenarios as well. One of the main features of the AHN1 is the ability to switch or adjust the confidence levels of the information utilized to accomplish assigned tasks when the indication of sensor malfunctioning is detected. Chapter 5 illustrated an example of the AHN1 helping an autonomous robot deal with rough terrain. The proposed AHN1 was able to switch to use the information from the frontal area distance sensor to help the robot cope with terrain roughness when there is an indication that the pitch sensory information is unreliable. However, the AHN1 can also be extended to other tasks by switching or adjusting the confident levels of other sensory information or even increasing the number of sensory inputs, for example see Figure 7.1.

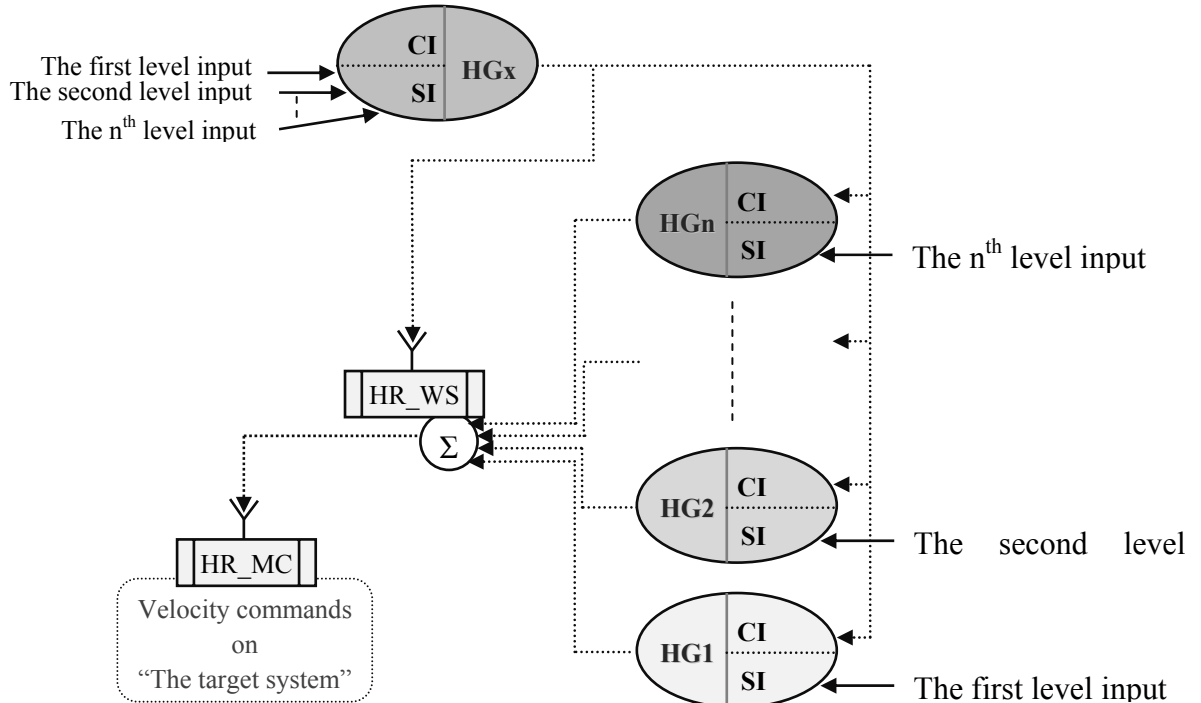


Figure 7.1: The generalisation of AHN1 for other applications

As mentioned in the previous sub-section, the main requirement of the target robot is that it must have sensory systems which are capable of providing the same information but can be at different levels of confidence. For example, in the situation when the AHN1 is expected to help an autonomous robot adjust its speed based on the dynamics of surrounding environments. The robot may be expected to decrease its speed when its surrounding objects are moving rapidly and to increase its speed back to a normal level when its surrounding objects are rather more static. In this case, the robot may be equipped with laser range sensors and ultrasonic sensors which are used mainly for close-range and long-range obstacle avoidance or motion planning, respectively. However, the information from these two types of sensors can also provide an indication about the dynamics of surrounding objects. The sensory information from the laser range sensors (which is likely to provide the more reliable indicator) can be connected to the HG1. The sensory information from the ultrasonic sensors (which is likely to provide the less reliable indicator) can be connected to the HG2. The sensory information from both types of sensors is connected to the HG3 which assesses the conflicts of information indicating faults in the laser range sensors as the environmental cue. In this situation, the AHN1 can continue to assist the robot by adjusting its speed based on the dynamics of surrounding environments even when faults occur on the laser range sensors by switching to use the sensory information from the ultrasonic sensors instead.

Some modifications can also be made in order to optimize the hormone network for different applications. For instance, the rates at which each hormone is produced and secreted can be altered by changing  $\alpha_g$  and  $\beta_g$ . Moreover, rather than switching entirely from one source of sensory information to the others (as shown in Chapter 5), there may be a case in which the robot is expected to only adjust the confidence levels of information from each source. This can be implemented on the HR\_WS introduced in section 5.1.2. The hormone concentration of the hormone connected to HR\_MC can be defined as the combination between the weight-sum of several hormone concentrations, instead of the hormone concentration from just one hormone.

### **7.1.3 Extending the AHN2 for Other Type of Robots**

As explained in section 5.2, the AHN2 is proposed mainly to help maintain the locomotion of skid-steering robots in the presence of both external environmental

changes induced by terrain conditions and internal environmental changes evoked by wheel faults, by influencing the velocity compensations corresponding to these changes. However, generally the AHN2 can also be extended to provide the adaptability for other types of robots. Some general requirements for designers of the robots which might be implementing the AHN2 are as follow:

- 1) The movements of the target robots must be the results of relative velocities from either side of the robots. For example, six or eight-wheel skid-steering robots which have their wheels aligned in the similar way to the Pioneer2- AT robot.
- 2) Depending on the type of wheel fault, generally, in order for AHN2 to reach full potential, the velocity on either side of the target robot should be the results of more than one actuator. With just one actuator on either side (for example in the case of 2-wheel differential drive robot), only transient velocity compensation can be induced by the AHN2. The kinematic adjustments may not be as effective because there are no additional actuators to induce the velocity compensation.
- 3) Since one of the velocity compensation effects influenced by the AHN2 is the kinematic adjustments, the target robot must have its locomotion control based on kinematics so that the velocity compensation can take affects.

In order to implement the AHN2 on a target robot (refer to Figure 7.2), the actual and the target turn velocity of the robot must be connected to the HG4x, while the target and actual forward velocity from either side of the robot must be connected to the HG5x. Regarding the hormone receptors in the AHN2, the HR\_KINEMATICS\_LEFT and HR\_KINEMATICS\_RIGHT must be connected to the kinematic locomotion control of the target robot so that the hormones can influence the locomotion control systems and adjust the robot's movement accordingly. However, the HR\_FL, HR\_FR, HR\_RL and HR\_RR can be extended to cover the number of corresponding wheels occupied on the target robot.

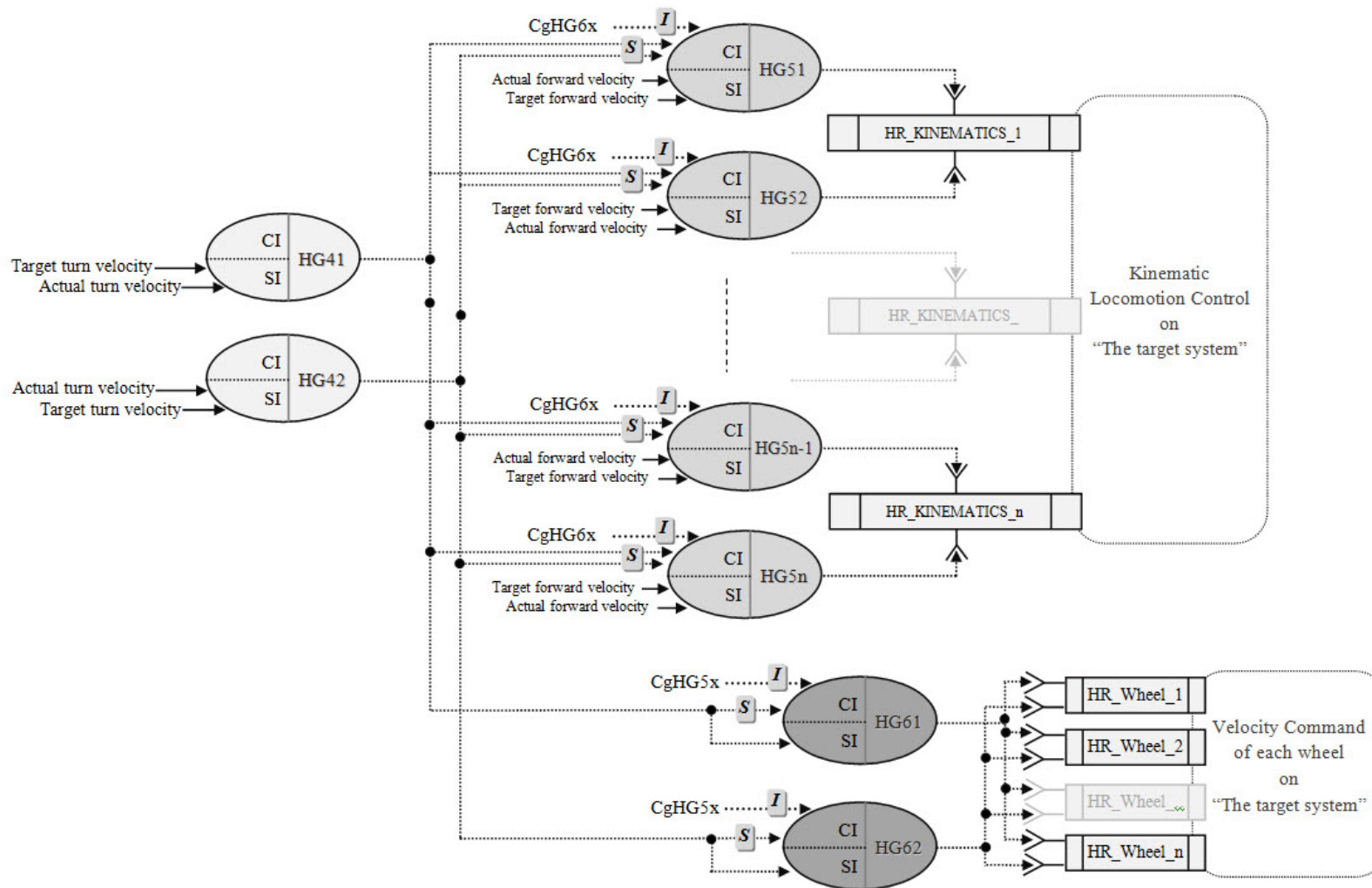


Figure 7.2: The generalisation of AHN2 for other robots

## 7.2 Methodology for Extending the AHN Architecture for Other Application Scenarios

The previous section concentrates on the methodologies for extending the proposed AHN1 and AHN2 illustrated in Chapter 5 to other robotic applications and other types of robots. However, for the AHN architecture, other different constructions of hormone networks, any other input signals or other different effects on target systems, can also be established to provide different adaptability for other robotic application scenarios. Therefore, this section provides a discussion for the general methods for extending the AHN architecture to provide other desired adaptabilities and to help autonomous robots operate in other application scenarios.

Generally, in order to implement the AHN on other robotic systems, there are two fundamental requirements needed to be met by the target robots:

- 1) The target robots must be able to sense the environmental information. Put simply, they must have sensors or sensory units which are able to provide environmental information for the robots.
- 2) The behaviours of the target robots must be able to be changed by the modifications of parameters in the control units of the robots. Therefore, hormones from the AHN can induce adaptation in the robots.

The two main types of mechanisms in the AHN are Hormone Glands and Hormone Receptors. Generally, any parameters on the control units of the target robots which are expected to be altered by hormones must have HR(s) attached, thus hormones can influence the robots. In addition, any sensory information which is expected to be used to provide environmental cues must be connected to the Signal Inputs of HG(s). The general guidelines for the designing of the AHN are given as follows:

### Regarding the HGs (refer to Figure 7.3)

- 1) The sensory information which is expected to be used directly to provide environmental cues and stimulate the productions of hormones should be connected to HGs through the *Signal Inputs*.
- 2) The aspects of environmental information or the environmental cues can be derived from any Signal Input of a HG by functions assigned in the *Signal pre-processor* of a HG (refer to section 4.1.1.3).

- 3) The signal information which is expected to control the hormone production of a HG should be connected to the HG via the *Control Inputs*.
- 4) The desired control affects of the signal information connected to a HG via the *Control Inputs* can be assigned at the *Control feature* (refer to section 4.1.1.4).
- 5) The mapping between the production of hormone and the aspects of environmental information, or put simply how the hormone level is produced based on the values derived from the environmental cues, can be set in the *Activation function* (refer to section 4.1.1.2).
- 6) The rates, at which the hormone is expected to be secreted and the time interval in which the hormone is expected to be presented in the system when there are no more hormone stimulations, can be set at the *stimulation rate* ( $\alpha_g$ ) and the *decay rate* ( $\beta_g$ ) respectively. In general, the higher value should be set on the stimulation rate when the hormone is expected to be more sensitive to the environmental cues and the lower value should be set on the decay rate if the hormone is expected to decrease quicker when there is no hormone stimulation (refer to section 4.1.1.1)

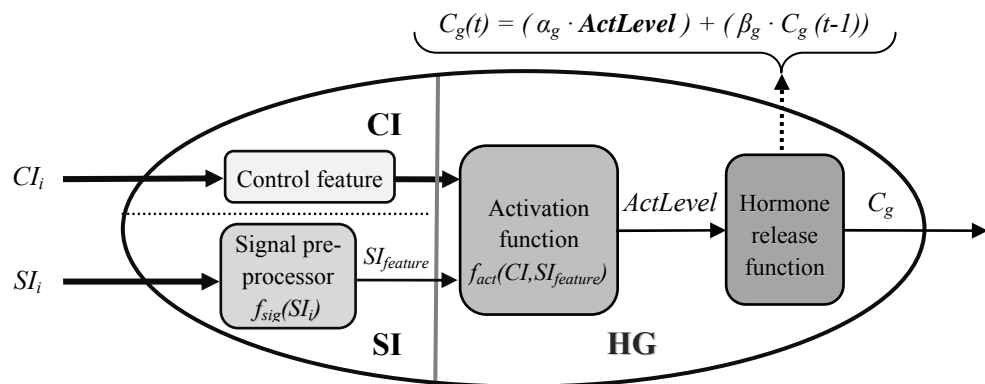


Figure 7.3: The fundamental mechanisms of Hormone Gland

#### Regarding the HRs (refer to Figure 7.4)

- 1) The hormone(s) which is expected to influence target systems (induce the adaptability) should be connected to the inputs of the hormone receptor located at the corresponding locations.
- 2) The changes in the values of hormone receptor (which is used to influence the changes of the target systems) based on the associated hormone receptor inputs

can be determined by the functions assigned in the *Receptor function* (refer to section 4.1.2.1).

- 3) The effect of the hormone receptor value over the target systems can be set to be the *Direct effect* or the *Accumulative effect* at the *Receptor feature* (refer to section 4.1.2.2)

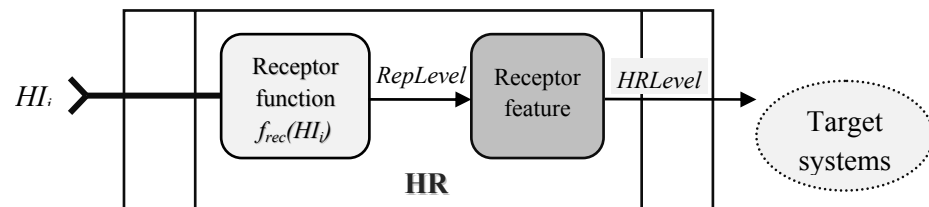


Figure 7.4: The fundamental mechanisms of Hormone Receptor

### Regarding the settings of hormone networks

In general, the adaptability provided by the AHN can emerge depending on the connections and interactions between HGs, HRs and target systems, as well as, the settings of each component in the AHN. Therefore, an understanding of the desired adaptability is required in order to assign the functions and parameters in each component and to define the connections between components in the AHN. However, these can also be achieved in a generic way by using intelligent design methods such as evolutionary or learning techniques. Details depend somewhat on the technique used, but generally the design methods must be implemented in the way which enables them to alter the settings of each component and the interactions between each component in order to allow various constructions of the AHN to provide the desired adaptability. Chapter 6 illustrated, with a simple example, that using an evolutionary method, in this case CGP-AHN, the construction of the AHN could be evolved and that this evolved system not only performed to a level of adaptability that was acceptable but actually performed better than the “hand-coded” system.

## 7.3 Summary

One of the key propositions of the AHN proposed in this research is the ability to use its fundamental mechanisms to design hormone networks which can provide different adaptability control for autonomous robots. It has been shown in this thesis that different hormone networks can be constructed to provide different adaptability mechanisms depending on environmental signals and internal faults. These hormone networks can induce behaviour alterations on autonomous robots in order to help the robots deal with different environmental changes. Examples are the AHN1, which is designed to help autonomous robots cope with rough terrain and the internal environmental change induced by the sensor fault, and the AHN2 which is constructed to help autonomous robots deal with the case of external environmental changes induced by terrain and internal environmental changes evoked by the wheel faults. All the hormone networks illustrated are constructed from the same fundamental mechanisms which are the Hormone Gland and the Hormone Receptor. However, by changing the settings of each component as well as the connections and interplay between the components, the hormone networks which provide different adaptation for autonomous robots can be constructed.

This chapter further describes the methodologies for extending the AHN to provide adaptability on different robotic applications and different types of robots. The general guidelines on how to extend the proposed AHNs on other types of robots and on other robotic applications are exemplified in this chapter. In addition, the general requirements of the target systems expected to be implemented with the AHN are also provided.

The next chapter will give the conclusions of the research reported in this thesis and will provide ideas for possible future work.

# Chapter 8

## Conclusions and Future Work

This chapter will give an overall summary on the research reported in thesis. Section 8.1 provides the conclusions on the key contents of each chapter including a discussion related to the hypothesis stated in Chapter 1. Section 8.2 describes the key contributions of this research, while section 8.3 elucidates the future work.

### 8.1 Thesis Summary

Autonomous robots capable of operating in unstructured real-world environments can be considered in a number of useful applications in human-hazardous environments such as search and rescue in collapsed buildings or reconnaissance in disaster scenarios. However, there remain a number of issues which need further development in order to accomplish autonomous robots having such abilities. One of the fundamental issues imposed on such robots is the ability to deal with the dynamics and unpredictability of these unstructured real-world environments. Autonomous robots operating in such environments require the ability to deal with changes which are very common in such environments. Generally, both internal and external environmental changes can occur and affect the robot performance. For this reason, adaptability is considered one of the most crucial features in such robot systems. Turning attentions towards nature, it can be observed quite clearly that biological organisms can cope very well with environmental variations. It has been noted that one of the key features which help biological organisms deal with the dynamics of the real-world is the ability to adapt using environmental cues. Chapter 1 discussed these issues and provided some examples of the utilization of environmental cues in order to increase the chances of survival and to help cope with environmental variations shown in biological organisms.

The introduction to the test environments employed throughout this research was the main focus of Chapter 2. It began by giving the general overview of the Robocup Rescue Robot competition and explaining the reference test environments which were

used as the representative environments employed in this research. Subsequently, the 3D robot simulator, called Gazebo, which was used as the simulation tool for the robots and environments employed in this research was introduced. Moreover, this chapter also explained in some detail the simulated Pioneer2-AT robot, its controller and its main tasks as well as the simulated environments referenced from the test arenas of the Robocup Rescue Robot competition. Finally, the performance metrics assigned to investigate the robot performance and the introduction to the environmental changes considered in this research were also described in this chapter.

Using the hormone system as the mechanism in response to environmental cues and in providing adaptability is one of the key inspirations of this research. Chapter 3 started by giving some examples of the hormone utilizations in response to environmental cues shown in biological organisms. Then, two systems closely related to the hormone system, the endocrine and the homeostasis systems, were also introduced. This chapter reviewed the two mainstream architectures, the Neuro-Endocrine System and the Artificial Homeostasis Hormone System, which use artificial hormones to regulate internal states and adjust system dynamics of artificial systems. The chapter ended with descriptions of the key approaches of this research which can be summarized as follows:

- To create a hormone-inspired mechanism which is able to provide adaptability for autonomous robots in order to deal with both internal and external environmental changes
- To propose a generic hormone network architecture, which is capable of being manually or automatically designed, to provide adaptability for different robotic applications and to be applied on various robotic systems

Chapter 4 first gave an introduction to the fundamental mechanisms of the novel Artificial Hormone Network (AHN) proposed in this research. These were the Hormone Gland (HG) and the Hormone Receptor (HR). The HG was proposed as the mechanism responsible for the production and secretion of hormones based on the aspects of environmental information, while the HR was suggested as the channel for hormones to affect the target systems. The fundamental structures and components of both mechanisms were also elucidated in the chapter. The description in this chapter illustrated the properties of each component and hinted at how hormone networks can be constructed from the two fundamental mechanisms. Subsequently, an example was

introduced for the hormone system constructed in order to help autonomous robots deal with the case of external environmental changes induced by rough terrain. The experiment conducted in this chapter demonstrated that the hormone system could help the robot better deal with rough terrain and better accomplish the assigned task. The results showed that the hormone system can help the robot reduce the occurrence of tips over and increase the number of times the target object was reached, compared to the robot operating without the hormone system. Furthermore, this chapter also illustrated the dynamics of hormones in helping the robot adjust its internal system based on the variation of external environments and showed how the hormone system can be used to provide adaptability for autonomous robots.

Chapter 5 presented the implementations and experiments of two AHNs, AHN1 and AHN2, which were designed principally for helping autonomous robots cope with the case of internal environmental changes induced by sensor faults and the case of internal environmental changes evoked by wheel faults, respectively. The AHN1 was further developed from the hormone system described in Chapter 4. This hormone network illustrated how a network of hormones can be constructed to help autonomous robots deal with both the case of external environmental changes caused by terrain roughness and the case of internal environmental changes induced by faults in the sensory system of the robot. The fault implemented was injected to the pitch sensory information of the robot. This condition generally caused the robot to become unaware of its pitch orientation and meant the hormone system was unable to secrete the hormone based on the variations of the robot's pitch orientation. The results obtained from the experiment in section 5.1.3 showed that this situation affected the robot's performance significantly as the robot's tip over rate was increased when the fault occurs. However, the results also showed that with the implementation of the AHN1 on the robot, it remained able to keep its performance similar to when there was no pitch fault and the AHN1 was not implemented on the robot (normal operation).

The AHN2 was designed to assist autonomous robots adapt their locomotion control depending on both the case of external environmental changes induced by rough terrain and the case of internal environmental changes evoked by faults on the robot's wheels. The AHN2 was evaluated on both the cases when the robot operated in a flat terrain environment and in a rough terrain environment. The results obtained in section 5.2.3 showed that, in the flat terrain test environment when the wheel faults occurred, the AHN2 could assist the robot in reaching the target object faster, on average, compared

to the case when there was no AHN2 implemented on the robot. For the case of the rough terrain environment investigated in section 5.2.4, the results also showed that the AHN2 could help increase the robot's performance when the fault occurred on the robot's wheels. Finally, Chapter 5 also illustrated the generic nature of the AHN as it was shown that two different hormone networks, AHN1 and AHN2, which provide different adaptability for autonomous robots can be constructed from the fundamental mechanisms of the AHN (i.e. HGs and HRs).

Chapter 6 investigated an initial step towards making the AHN more generic by evaluating the ability of the architecture to be constructed automatically to provide desired adaptability for autonomous robots using Cartesian Genetic Programming (CGP). The chapter started with a brief introduction to the CGP. Then, the implementation of CGP on the AHN, called CGP-AHN, as well as an example of CGP-AHN encoding, were described. The implementation investigated in this chapter focused on evolving hormone networks which were able to help autonomous robots cope with the case of internal environmental changes induced by wheel faults on the robot operated in a flat terrain environment. The representation of CGP on the AHN, including how CGP could alter the functions and parameters of each mechanism in the AHN, was illustrated. The results obtained from a series of experiments showed that the robot implemented with the AHN configuration acquired from the CGP-AHN not only performed to an acceptable level in the test scenarios but also performed better than the robot implemented with the AHN2 (investigated in Chapter 5) and the robot implemented without any AHNs. As a significant amount of time was required to evaluate CGP-AHN individuals within the test environments employed, the experiments conducted in this chapter were restricted only to the case of internal environmental changes induced by the robot's wheel faults on the robots operating in the flat terrain environment. Experiments of CGP-AHN on other scenarios such as rough terrain were considered beyond the scope of this thesis.

It was shown throughout the thesis that the AHN architecture can be constructed to provide different adaptability for different robotic applications, Chapter 7 further discussed the methodologies for extending AHN1 and AHN2 as well as the AHN architecture in general for other robots and other robotics applications, in order to provide insights into how to apply the AHN architecture in other robotic application scenarios.

### 8.1.1 Testing the Hypothesis

The hypothesis of this research was presented in section 1.4 and was stated as follow:

*“A flexible hormone-inspired architecture is able to exploit environmental cues in order to provide adaptability for autonomous robots to deal with variation effects of both internal and external environmental changes in simulations of unstructured real-world environments”*

Chapter 2 elucidated every aspects of the test environments employed in this research. As explained, even though a robot simulator was used throughout this research, every experiment was conducted in a physically-realistic robot simulator which is not only able to simulate 3D objects but is also able to simulate the dynamic interactions between objects and environments. Furthermore, the simulated test scenarios used in this research were inspired from the Robocup Rescue robot competition. As described in section 2.1, the test arenas used in this robot competition were developed from many stages of real-world collapsed building by the National Institute of Standards and Technology (NIST). Therefore, the test environments employed in this research are considered to be a realistic reflection of unstructured real-world environments. Regarding the environmental variations considered in this research, as introduced in section 2.6 and presented in the experiments throughout Chapters 4, 5 and 6, both internal and external environmental changes were investigated in this research. These were the cases of external environmental changes induced by rough terrain and the cases of internal environmental changes caused by faults in the autonomous robot’s sensory and actuator units.

The capability of the hormone-inspired architecture, the *Artificial Hormone Network (AHN)*, to provide adaptation for autonomous robot was evaluated in the experiments reported in Chapters 4 and 5. The results from every experiment correspondingly showed that the AHNs can help adjust the robot’s behaviours and the control systems depending on the environmental variations. The robot implemented with the AHNs acquired the higher number of Object Reach than the robot implemented without the AHNs in every test case. Regarding the environmental cues exploited in the AHN, section 5.1 showed that the AHN1 can utilize the variations and conflicts between the pitch and frontal area distance sensory information of the robot as the environmental cue to provide adaptability. Section 5.2 illustrated that the conflicts between target and

actual velocity of the robot can be utilized by the AHN as environmental cues to adjust the locomotion control of the robot in the presence of both the internal environmental change induced by wheel faults and the external environmental change caused by rough terrain.

The ability to be designed to provide adaptability for different robotic application scenarios was clearly shown by the AHN1 and the AHN2 in Chapter 5. Both hormone networks were constructed from the same fundamental mechanisms of the AHN architecture: the Hormone Gland (HG) and the Hormone Receptor (HR). However, with different settings on each component and different interactions between the mechanisms, various hormone networks, which can provide different adaptability in order to cope with different environmental changes, can emerge. Furthermore, the general guidelines for applying the AHN architecture on different robotic applications were also discussed in Chapter 7.

Regarding the ability to be constructed automatically using an off-the-shelf intelligent design method, Chapter 6 presented the implementation of CGP on the AHN (CGP-AHN). CGP was selected as the technique for “designing” the AHN in this chapter because the CGP representation was considered suitable for the requirements to design the AHN architecture. The results from the experiments conducted in this chapter also illustrated that CGP can be used to “design” AHNs which can provide adaptability in a specific robotic application scenario. It was shown that AHNs evolved by CGP can help an autonomous robot cope with the case of internal environmental changes induced by the wheel faults.

From this discussion, the experiments conducted and results obtained in this thesis, it is concluded that the hypothesis stated in Chapter 1 has been shown to be upheld.

## 8.2 Contributions

The key contributions of the research reported in this thesis can be described as follow:

- **An implementation of a hormone-inspired architecture for providing adaptability to autonomous robots that operate in unstructured simulated real-world environments**

One of the main interests in this research is to provide a system which is able to help create adaptable robots capable of operating in unstructured real-world environments. This is one of the most important issues in robotics since the ability of autonomous robots in dealing with dynamic unpredictability of unstructured real-world environments remains a vital issue. However, almost all of the related work (as introduced in section 3.3) only investigates the utilizations of hormone-inspired architectures on autonomous robots that operate in structured environments. On the other hand, this research considers an application in autonomous robot search and rescue scenarios, which is considered one of the most active real-world robotic applications in unstructured environments. Although, as explained in chapter 2, the robot and test environments employed in this research were simulated, careful considerations were taken in order to investigate the proposed system on test environments and scenarios which reflect unstructured real-world robotic applications as closely as possible.

- **A hormone-inspired architecture which can assist autonomous robots deal with both internal and external environmental changes**

In other previous hormone-inspired architectures which are proposed for helping maintain homeostasis of robots in the face of environmental variations, only cases of external environmental changes are considered. However, in real-world robot application scenarios, both internal and external environmental changes can have significant effects on the operations of autonomous robots. The AHN architecture is the first hormone-inspired system which displays the ability to provide adaptability for autonomous robots in dealing with both internal and external environmental changes. As illustrated in chapter 5, the AHNs not only can help autonomous robots cope with the external environmental changes in the case of different terrain roughness, but can also help autonomous robot deal with the cases of internal environmental changes induced by faults occur in sensor

and actuator units. However, it has to be noted that the AHN architecture is not proposed as a fault detection system but as a system to maintain homeostasis and to provide adaptation from the affects of environmental changes.

- **A hormone-inspired architecture which enables the creation of hormone networks**

As described in chapter 3, the hormone mechanisms used in the AHN architecture is extended from the Artificial Endocrine System (AES) proposed in the neuro-endocrine system [70]. However, the key additional feature proposed in the AHN is the novel ability to create hormone networks, by allowing the different connections and interactions between several hormones. This is one of the key aspects of the AHN architecture which provides adaptability for autonomous robots in several different applications.

- **The first implementation of CGP for evolving a hormone-inspired architecture**

Exploiting automatic design methods in order to create hormone-inspired architectures for different robotic application scenarios is important. Previous work (e.g. [96]) has examined the use of Evolutionary Algorithm to evolve Artificial Homeostatic Hormone System for robots to perform specific tasks. This research, however, investigates the first implementation of CGP to represent the AHN architecture and to construct AHNs which are able to provide desired adaptability for autonomous robots (Chapter 6). CGP is able to create different hormone networks by altering the functions and parameters of each HG and HR as well as changing connections and interactions between each mechanism.

## 8.3 Future Work

- **Investigations of the AHN on other robotic applications and implementations on real robots**

The main test scenario investigated in this research is the case of a wheel-robot exploring test arenas while encountering environmental changes induced by rough terrain as well as sensor and wheel faults. Undoubtedly, there are a number of other unstructured real-world robotic application scenarios which could be investigated, for example, the cases of autonomous flying or submarine robots performing reconnaissance in outdoor environments. In these scenarios, the robots may encounter different environmental conditions. The changes of air or water currents may affect the robot movements, the variations of lighting condition or temperatures could cause incorrect perceptions in the sensory systems, or even faults occurring on the robot's components may decrease the robot's performance to accomplish assigned tasks. The implementations of AHNs designed to help the robots cope with these application scenarios should be very useful in further developments of the AHN for assisting autonomous robots operating in unstructured real-world environments.

Moreover, even though the robot simulator employed in this research is a physically-realistic simulator, reality gaps remain unavoidable. Therefore, further investigations of the AHN architecture on real physical robots and environments are considered another step forward. However, because of reality gaps, evaluating the proposed architecture on real physical robots may require some tweaks. As illustrated throughout this thesis, hormones in AHNs respond directly to environmental information imposed on implemented robots and interactions of the robots with environments in which the robots are situated. Therefore, one of the key important issues, which need to be aware of, is these perceptions and interactions may be different in actual real-world environments. Noises in actual real-world sensors are generally inevitable. In addition, physical real-world robots are vastly imposed with more complex physical effects from environments. Different types of terrains, such as sand, soil or grass, can have different effects on robots. Various other changes in components of robots can also occur. Thus, fine-tuning of the architecture is certainly important to adjust hormone dynamics in different physical real-world robots and scenarios, for

example, modifications in the stimulation and decay rates ( $\alpha_g$  and  $\beta_g$ ) in order to appropriately adjust the production of hormone for particular robots and environments.

- **Further investigations on CGP-AHN**

As explained in Chapter 6, due to time and resource consideration, only one CGP parameter setting and one test scenario were investigated on CGP-AHN. In order to further evaluate the performance of CGP-AHN, there is no doubt that testing CGP-AHN on different CGP parameter setting (e.g. different maximum number of nodes or mutation rates) and on different robotic application scenarios (e.g. rough terrain environments) are important. Another interesting investigation is to enable the cyclic array representation of CGP on the AHN in order to allow the creation of more complex hormone networks. Moreover, investigating the use of different fitness functions which can speed up the convergence of solutions (e.g. dynamic selectivity scaling function [129] or Gaussian process fitness function models [128]) is also worth considering.

As also mentioned in Chapter 6, the time-consuming experiments on the CGP-AHN are partly due to the issues on the robot simulator which is unable to speed up the simulation. Further investigations of CGP-AHN would be recommended to be evaluated on a test environment which is able to reduce the significant amount of time required in the evaluation process of CGP-AHN individuals.

- **Further developments of the AHN architecture**

In biological organisms, the time intervals in which each particular hormone can exist in an organism are different. Some hormones may take effect and decay in minutes but some may take longer to decay, even hours or days [69, 70]. However, with the *hormone release function* used in the AHN architecture (section 4.1.1.1), it is very difficult, if not impossible, to specifically define the time interval in which hormones are expected to be presented on target systems, only by setting the values of  $\alpha_g$  and  $\beta_g$ . As such, alternative functionality of the hormone release function is considered useful; the functionality which allows

the user to identify the specified time period in which hormones can take effect on target systems by settings of related parameters.

In this research, the AHN is used directly to induce specific changes on autonomous robots. However, in nature, it has been suggested that hormones can also have indirect effects on the developments of organisms in subsequent stages or even subsequent generations [57]. This phenomenon sheds some light on the utilizations of AHNs on the artificial developmental system [130, 131]. A possible application may be the use of AHNs to help set developmental stages of artificial systems based on the environmental information in order to develop artificial systems which are suitable for different environmental contexts.

Chapter 6 has investigated the use of evolutionary systems on the AHN architecture. However, another interesting implementation is the use of online learning techniques to create adaptive AHN, as first introduced in [87]. As illustrated throughout the thesis, the characteristics of each hormone network can be changed depending on the alterations of each mechanism and the interactions between components in each hormone network. Therefore, applying online learning methods to change characteristics of hormone networks should definitely be useful for autonomous robots working in long-term scenarios. The online learning techniques may be applied to associate useful environmental inputs to hormone networks or associate the secretion of hormones in response to different environmental cues in order to create adaptive hormone networks which are also capable of online adaptation.

# Bibliography

- [1] *Unimate*, <http://en.wikipedia.org/wiki/Unimate>, (Access on: 2012, October )
- [2] *1961: Installation of the First Industrial Robot*, <http://world-information.org/wio/infostructure/100437611663/100438659325>, (Access on: October, 2012)
- [3] *1961: A peep into the automated future*, <http://www.capitalcentury.com/1961.html>, (Access on: 2012, October)
- [4] "World Robotics - Industrial Robots 2012", IFR Statistical Department, 2012.
- [5] "A Roadmap for US Robotics: From Internet to Robotics", the Computing Community Consortium (CCC), 2009.
- [6] *The Start of a Revolution*, <http://www.prsrobots.com/1961.html>, (Access on: 2012, October)
- [7] *Unimate Series Information*, <http://www.prsrobots.com/uninfo.html>, (Access on: 2012, October)
- [8] "World Robotics - Service Robots 2012", IFR Statistical Department, 2012.
- [9] D. J. Spero, "A Review of Outdoor Robotics Research", Department of Electrical and Computer Systems Engineering, Monash University, Melbourne, Australia, 2004.
- [10] *iRobot Roomba*, <http://www.irobot.com>, (Access on: 2012, October)
- [11] *Robomow*, [www.robomow.com](http://www.robomow.com), (Access on: 2012, October)
- [12] *The da Vinci® Surgical System*, <http://www.davincisurgery.com/davinci-surgery/davinci-surgical-system/>, (Access on: 2012, October)
- [13] *Paro Therapeutic Robot*, <http://www.parorobots.com/>, (Access on: 2012, October)
- [14] *iRobot Packbot* [www.irobot.com](http://www.irobot.com), (Access on: 2012, October)
- [15] *Robonaut* <http://robonaut.jsc.nasa.gov/default.asp>, (Access on: 2012, October)
- [16] "Global Trends 2025: A Transformed World", the National Intelligence Council (NIC), 2008.
- [17] Ulrich Nehmzow and Carl Owen, "Robot navigation in the real world: Experiments with Manchester's FortyTwo in unmodified, large environments", *Robotics and Autonomous Systems*, vol. 33, pp. 223-242, December 2000.
- [18] Tony Prescott, Martin Pearson, Ben Mitchinson, J. Charles Sullivan, and Anthony Pipe. (2009) Whisking with robots: From rat vibrissae to biomimetic technology for active touch. *IEEE Robotics and Automation Magazine*. 42-50.

- [19] Tony Prescott, Martin Pearson, Charles Fox, Mat Evans, Ben Mitchinson, Sean Anderson, and Tony Pipe, "Towards biomimetic vibrissal tactile sensing for robot exploration, navigation, and object recognition in hazardous environments", in *Proceedings of 4th IARP workshop: Robots for risky Interventions and Environmental Surveillance- maintenance (RISE)*, Sheffield, 2010.
- [20] G. C. Nandi and Debjani Mitra, "Development of a Sensor Fusion Strategy for Robotic Application Based on Geometric Optimization", *Journal of Intelligent and Robotic Systems*, vol. 35, pp. 171-191, 2002.
- [21] Rolf Pfeifer, Max Lungarella, and Fumiya Iida. (2007) Self-organization, embodiment, and biologically inspired robotics. *Science*. 1088-1093.
- [22] Fumitoshi Matsuno and Satoshi Tadokoro, "Rescue Robots and Systems in Japan", presented at the IEEE International Conference on Robotics and Biomimetics, 2004.
- [23] Angela Davids, "Urban search and rescue robots: from tragedy to technology", *IEEE Intelligent Systems*, vol. 17, pp. 81-83.
- [24] Jacob Adelman *Japan Taps U.S. Robots For Nuclear Reactor Cleanup Help*, [http://www.huffingtonpost.com/2011/04/18/japan-reactor-cleanup-us-robots\\_n\\_850344.html](http://www.huffingtonpost.com/2011/04/18/japan-reactor-cleanup-us-robots_n_850344.html), (Access on: 2012, October)
- [25] Robert Charette *The Rise of Robot Warriors*, <http://spectrum.ieee.org/robotics/military-robots/the-rise-of-robot-warriors>, (Access on: 2012, October)
- [26] Marc Raibert, Kevin Blankespoor, Gabriel Nelson, Rob Playter, and a. t. B. Team, "BigDog, the Rough-Terrain Quadruped Robot", in *In Proceedings of the 17th IFAC World Congress*, 2008.
- [27] Serge Kernbach, Eugen Meister, Florian Schlachter, Kristof Jebens, Marc Szymanski, Jens Liedke, Davide Laneri, Lutz Winkler, Thomas Schmickl, Ronald Thenius, Paolo Corradi, and Leonardo Ricotti, "Symbiotic Robot Organisms: REPLICATOR and SYMBRION Projects", in *Proceeding of Performance Metrics for Intelligent Systems Workshop*, Gaithersburg, MD, USA, 2008, pp. 62-69.
- [28] Francesco Mondada, Giovanni C. Pettinaro, Andre Guignard, Ivo W. Kwee, Dario Floreano, Jean-Louis Deneubourg, Stefano Nolfi, Luca Maria Gambardella, and Marco Dorigo, "Swarm-Bot: a New Distributed Robotic Concept", *Autonomous Robots*, vol. 17, pp. 193-221, 2004.
- [29] Manuele Brambilla, Eliseo Ferrante, Mauro Birattari, and Marco Dorigo, "Swarm robotics: A review from the swarm engineering perspective", Université Libre de Bruxelles, Brussels, Belgium, 2012.
- [30] *Someone please call a tow truck*, <http://www.areavoices.com/astrobob/index.cfm?blog=63955>, (Access on: 2012, October)
- [31] Sasha R.X. Dall, Luc-Alain Giraldeau, Ola Olsson, John M. McNamara, and David W. Stephens, "Information and its use by animals in evolutionary ecology", *Trends in Ecology & Evolution*, vol. 20, pp. 187-193, April 2005.

- [32] Katherine Herborn, "Variation in response to environmental cues when foraging", PhD thesis, Faculty of Biomedical and Life Sciences, University of Glasgow, Glasgow, May 2012.
- [33] Ned H. Kalin and Steven E. Shelton, "Defensive Behaviors in Infant Rhesus Monkeys: Environmental Cues and Neurochemical Regulation", *Science*, vol. 243, pp. 1718-1721, March 1989.
- [34] Kenneth J. Lohmann, Catherine M. F. Lohmann, Llewellyn M. Ehrhart, Dean A. Bagley, and Timothy Swing, "Geomagnetic map used in sea-turtle navigation", *Nature*, vol. 428, pp. 909-910, 2004.
- [35] D. F. H. Grocott, "Maps in Mind – How Animals Get Home? ", *The Journal of Navigation*, vol. 56, pp. 1-14, 2003.
- [36] Massimo Pigliucci, *Phenotypic Plasticity: Beyond Nature and Nurture*. The Johns Hopkins University Press, 2001.
- [37] Anurag A. Agrawal, "Phenotypic Plasticity in the Interactions and Evolution of Species", *Science*, vol. 294, pp. 321 – 326, October 2001.
- [38] Stephen C. Stearns, "The evolutionary significance of phenotypic plasticity: phenotypic sources of variation among organisms can be described by developmental switches and reaction norms", *BioScience*, vol. 39 pp. 436-445, 1989.
- [39] *Prey Learn The Future*, <http://z-letter.com/2009/11/01/prey-learn-the-future/>, (Access on: 2012, October)
- [40] *Great Hanshin earthquake*, [http://en.wikipedia.org/wiki/Kobe\\_earthquake](http://en.wikipedia.org/wiki/Kobe_earthquake), (Access on: 2012, October)
- [41] Hiroaki Kitano and Satoshi Tadokoro. (2001) RoboCup Rescue A Grand Challenge for Multiagent and Intelligent Systems. *AI Magazine*.
- [42] *Rescue Robot League*, [http://en.wikipedia.org/wiki/Rescue\\_Robot\\_League](http://en.wikipedia.org/wiki/Rescue_Robot_League), (Access on: 2012, October)
- [43] *Urban Search and Rescue Robot Competitions: Arenas*, <http://www.isd.mel.nist.gov/projects/USAR/arenas.htm>, (Access on: 2012, October)
- [44] *Performance Metrics and Test Arenas for Autonomous Mobile Robots*, <http://www.nist.gov/el/isd/testarenas.cfm>, (Access on: 2012, October)
- [45] *Urban Search and Rescue Robot Competitions*, <http://robotarenas.nist.gov/competitions.htm>, (Access on: 2012, October)
- [46] "Robocup Rescue Robot League Arenas: Major Component Descriptions", 2008.
- [47] *Gazebo* <http://playerstage.sourceforge.net/index.php?src=gazebo>, (Access on: 2012, October)
- [48] Nathan Koenig and Andrew Howard, "Design and Use Paradigms for Gazebo, An Open-Source Multi-Robot Simulator", presented at the In Proceedings of 2004 IEEE/RSJ International Conference on Intelligent Robots and Systems, Sendai, Japan, 2004.

- [49] *The Player Project* <http://playerstage.sourceforge.net/index.php?src=index>, (Access on: 2012, October)
- [50] Brian Gerkey, Richard T. Vaughan, and A. Howard, "The Player/Stage Project: Tools for Multi-Robot and Distributed Sensor Systems", in *In Proceedings of the 11th International Conference on Advanced Robotics (ICAR 2003)*, Coimbra, Portugal, June 2003, pp. 317-323.
- [51] *OGRE – Open Source 3D Graphics Engine*, [www.ogre3d.org](http://www.ogre3d.org), (Access on: 2012, October)
- [52] *Open Dynamics Engine* <http://www.ode.org/>, (Access on: 2012, October)
- [53] *Pioneer 3-AT*, <http://www.mobilerobots.com/ResearchRobots/P3AT.aspx>, (Access on: 2012, October)
- [54] Ronald C. Arkin, *Behavior-Based Robotics*. Cambridge, MA: MIT Press, 1998.
- [55] Rolf Pfeifer and Josh Bongard, *How the body shapes the way we think: a new view of intelligence*. The MIT Press, 2006.
- [56] John C. Wingfield and Alexander S. Kitaysky, "Endocrine Responses to Unpredictable Environmental Events: Stress or Anti-Stress Hormones?", *Integrative and Comparative Biology*, vol. 42, pp. 600-609, 2002.
- [57] Alfred M. Dufty Jr, Jean Clobert, and Anders P. Møller, "Hormones, developmental plasticity and adaptation", *Trends in Ecology & Evolution*, vol. 17, pp. 190-196, 2002.
- [58] Knut Schmidt-Nielsen, *Animal Physiology: Adaptation and Environment*, 5 ed.: Cambridge University Press 1997.
- [59] Clifford Ladd Prosser, *Adaptational Biology: Molecules to Organisms* 99 ed.: Wiley-Interscience, 1986.
- [60] Jerry D. Jacobs and John C. Wingfield, "Endocrine control of life-cycle stages: a constraint on response to the environment?", *Condor*, pp. 35-51, 2000.
- [61] Ellen D. Ketterson, Jonathan W. Atwell, and Joel W. McGlothlin, "Phenotypic integration and independence: Hormones, performance, and response to environmental change", *Integrative and Comparative Biology*, vol. 49, pp. 365-379, 2009.
- [62] Hanno Wolters and Gerd Jürgens, "Survival of the flexible: hormonal growth control and adaptation in plant development", *Nature Reviews Genetics* pp. 305-317, 2009.
- [63] George B. Johnson and Peter H. Raven, "How Plants Grow in Response to the Environment", in *Biology*, 6 ed: McGraw-Hill Higher Education, 2002.
- [64] U. Bernabucci, N. Lacetera, L. H. Baumgard, R. P. Rhoads, B. Ronchi, and A. Nardone, "Metabolic and hormonal acclimation to heat stress in domesticated ruminants", *Animal*, vol. 4, pp. 1167-1183, 2010.
- [65] Michal Horowitz, "Heat acclimation: phenotypic plasticity and cues to the underlying molecular mechanisms", *Journal of Thermal Biology*, vol. 26, pp. 357-363, 2001.

- [66] Robert J. Denver, "Environmental Stress as a Developmental Cue: Corticotropin-Releasing Hormone Is a Proximate Mediator of Adaptive Phenotypic Plasticity in Amphibian Metamorphosis", *Hormones and Behavior*, vol. 31, pp. 169-179, 1997.
- [67] Robert J. Denver, Nooshan Mirhadi, and M. Phillips, "Adaptive plasticity in amphibian metamorphosis: response of *Scaphiopus hammondi* tadpoles to habitat desiccation", *Ecology*, vol. 79, pp. 1856-1872, 1998.
- [68] Robert J. Denver, "Evolution of the Corticotropin-releasing Hormone Signaling System and Its Role in Stress-induced Phenotypic Plasticity", *Annals of the New York Academy of Sciences*, vol. 897, pp. 46-53, 1999.
- [69] Charles G.D. Brook and Nicholas J. Marshall, *Endocrinology* 4ed.: Blackwell Science, 2001.
- [70] Mark Neal and Jon Timmis, "Timidity: A useful mechanism for robot control?", *Informatica*, vol. 27, pp. 197-204, 2003.
- [71] Ellen D. Ketterson and Val Nolan Jr., "Adaptation, Exaptation, and Constraint\_A Hormonal Perspective", *The American Naturalist*, vol. 154, pp. 4-25, 1999.
- [72] Mark Neal and Jon Timmis, "Once More Unto the Breach: Towards Artificial Homeostasis?", in *Recent Developments in Biologically Inspired Computing*, 2005, pp. 340-365.
- [73] Ezequiel A. Di Paolo, "Organismically-inspired robotics: homeostatic adaptation and teleology beyond the closed sensorimotor loop", in *Dynamical systems approaches to embodiment and sociality*, K. Murase and Asakura, Eds., ed Adelaide: Advanced Knowledge International, 2003, pp. 19-42.
- [74] Patrícia Vargas, Renan Moioli, Leandro N. de Castro, Jon Timmis, Mark Neal, and Fernando J. Von Zuben, "Artificial Homeostatic System: A Novel Approach", in *Advances in Artificial Life*. vol. 3630, ed: Springer 2005, pp. 754-764.
- [75] Wei-Min Shen, Behnam Salemi, and Peter Will, "Hormone-inspired adaptive communication and distributed control for CONRO self-reconfigurable robots", *IEEE Transactions on Robotics and Automation*, vol. 18, pp. 700-712, 2002.
- [76] Wei-Min Shen, Peter Will, Aram Galstyan, and Cheng-Ming Chuong, "Hormone-Inspired Self-Organization and Distributed Control of Robotic Swarms", *Autonomous Robots*, vol. 17, pp. 93-105, 2004.
- [77] Andrew J. Greensted and Andy M. Tyrrell, "Fault Tolerance via Endocrinologic Based Communication for Multiprocessor Systems", in *Evolvable Systems: From Biology to Hardware*. vol. 2606, ed, 2003, pp. 24-34.
- [78] Andrew J. Greensted and Andy M. Tyrrell, "An endocrinologic-inspired hardware implementation of a multicellular system", in *NASA/DoD Conference on Evolvable Hardware* 2004, pp. 245-252.
- [79] Andrew J. Greensted and A. M. Tyrrell, "Implementation results for a fault-tolerant multicellular architecture inspired by endocrine communication", presented at the NASA/DoD Conference on Evolvable Hardware 2005.

- [80] Joanne Walker and Myra Wilson, "Hormone-inspired control for group Task-Distribution", in *Proc. Towards Autonomous Robotic Systems*, 2007, pp. 1-8.
- [81] Joanne Walker and Myra Wilson, "A performance sensitive hormone-inspired system for task distribution amongst evolving robots", in *IEEE/RSJ International Conference on Intelligent Robots and Systems*, Nice, France, 2008, pp. 1293-1298.
- [82] Dario Floreano and Claudio Mattiussi, "Neural Systems", in *Bio-Inspired Artificial Intelligence: theories, methods, and technologies*, ed: MIT Press, 2008, pp. 163-267.
- [83] Julian J. Henley and David P. Barnes, "An Artificial Neuro-Endocrine Kinematics Model for Legged Robot Obstacle Negotiation", in *Proceedings of the 8th ESA Workshop on Advanced Space Technologies for Robotics and Automation*, ESTEC, Noordwijk, The Netherlands, 2004.
- [84] Colin Sauze and Mark Neal, "A Biologically Inspired Approach to Long Term Autonomy and Survival in Sailing Robots", in *Proceedings of the International Robotic Sailing Conference*, Breitenbrunn, Austria, 2008, pp. 6-11.
- [85] Jon Timmis, Lachlan Murray, and Mark Neal, "A Neural-Endocrine Architecture for Foraging in Swarm Robotic Systems", in *Nature Inspired Cooperative Strategies for Optimization (NICSO 2010)*, ed: Springer, 2010, pp. 319-330.
- [86] Orlando Avila-García and Lola Cañamero, "Hormonal modulation of perception in motivation-based action selection architectures", in *Proceedings of the Symposium on Agents that Want and Like: Motivational and Emotional Roots of Cognition and Action, AISB 05: Social Intelligence and Interaction in Animals, Robots and Agents*, 2005, pp. 9-16.
- [87] Jon Timmis, Mark Neal, and James Thorniley, "An adaptive neuro-endocrine system for robotic systems", in *IEEE Workshop on Robotic Intelligence in Informationally Structured Space (RIISS '09)*, 2009, pp. 129-136.
- [88] Renan C. Moioli, Patricia A. Vargas, Fernando J. Von Zuben, and Phil Husbands, "Towards the Evolution of an Artificial Homeostatic System", in *IEEE Congress on Evolutionary Computation (CEC 2008)*, 2008, pp. 4023-4030.
- [89] Renan C. Moioli, Patricia A. Vargas, and Phil Husbands, "A Multiple Hormone Approach to the Homeostatic Control of Conflicting Behaviours in an Autonomous Mobile Robot", in *IEEE Congress on Evolutionary Computation (CEC '09)*, 2009, pp. 47-54.
- [90] Patricia A. Vargas, Renan C. Moioli, Fernando J. Von Zuben, and Phil Husbands, "Homeostasis and evolution together dealing with novelties and managing disruptions ", *International Journal of Intelligent Computing and Cybernetics*, vol. 2, pp. 435-454, 2009.
- [91] Patricia A. Vargas, Ezequiel A. Di Paolo, and Phil Husbands, "Preliminary investigations on the evolvability of a non-spatial gasnet model", in *Proceedings of the 9th European Conference on Artificial life (ECAL 2007)*, 2007.

- [92] Phil Husbands, Tom Smith, Nick Jakobi, and Michael O'Shea, "Better living through chemistry: Evolving gasnets for robot control", *Connection Science*, vol. 10, pp. 185-210, 1998.
- [93] Thomas Schmickl and Karl Crailsheim, "Modelling a hormone-based robot controller", in *In Proc. of the 6th Vienna International Conference on Mathematical Modelling (MATHMOD-09)*, Vienna, Austria, 2009.
- [94] *SYMBRION Project website*, [www.symbion.eu](http://www.symbion.eu), (Access on: 2012, October)
- [95] Jurgen Stradner, Heiko Hamann, Thomas Schmickl, and Karl Crailsheim, "Analysis and implementation of an artificial homeostatic hormone system: A first case study in robotic hardware", presented at the The 2009 IEEE/RSJ International Conference on Intelligent Robots and Systems (IROS'09), 2009.
- [96] Jurgen Stradner, Heiko Hamann, Thomas Schmickl, Ronald Thenius, and Karl Crailsheim, "Evolving a novel bio-inspired controller in reconfigurable robots", in *Advances in Artificial Life. Darwin Meets von Neumann*. vol. 5777, ed: Springer-Verlag, 2009, pp. 132-139.
- [97] Heiko Hamann, Jurgen Stradner, Thomas Schmickl, and Karl Crailsheim, "A hormone-based controller for evolutionary multi-modular robotics: From single modules to gait learning", in *Proceedings of the IEEE Congress on Evolutionary Computation (CEC'10)*, 2010, pp. 244-251.
- [98] Heiko Hamann, Jurgen Stradner, Thomas Schmickl, and Karl Crailsheim, "Artificial hormone reaction networks: Towards higher evolvability in evolutionary multimodular robotics", in *Proc. of the ALife XII Conference*, 2010, pp. 773-780.
- [99] J. Andrew Bagnell, David Bradley, David Silver, Boris Sofman, and Anthony Stentz. (June 2010) Learning for Autonomous Navigation: Advances in Machine Learning for Rough Terrain Mobility. *IEEE Robotics & Automation*. 74-84.
- [100] Jean-Francois Lalonde, Nicolas Vandapel, Daniel Huber, and Martial Hebert, "Natural terrain classification using three-dimensional lidar data for ground robot mobility", *Journal of Field Robotics*, vol. 23, pp. 839-861, November 2006 2006.
- [101] Cang Ye and Johann Borenstein, "A Method for Mobile Robot Navigation on Rough Terrain", presented at the International Conference on Robotics and Automation, New Orleans, LA, 2004.
- [102] Alan J. Benson, "Motion Sickness", in *Medical Aspects of Harsh Environments*, ed Washington, DC: Government Printing Office, 2002.
- [103] *Motion sickness* <http://www.nhs.uk/conditions/Motion-sickness/Pages/Introduction.aspx>, (Access on: 2012, November)
- [104] *Motion sickness: Wikipedia*, [http://en.wikipedia.org/wiki/Motion\\_sickness](http://en.wikipedia.org/wiki/Motion_sickness), (Access on: 2012, November)
- [105] *Motion Sickness*, <http://www.brooksidepress.org/Products/OperationalMedicine/DATA/operationalmed/Manuals/GMOManual/clinical/Motion%20sickness.html>, (Access on: 2012, November)

- [106] John C. Knight, "Safety Critical Systems: Challenges and Directions", in *Proceedings of the 24rd International Conference on Software Engineering*, 2002, pp. 547 - 550.
- [107] Bev Littlewood and John Rushby, "Reasoning about the Reliability of Diverse Two-Channel Systems in which One Channel is "Possibly Perfect"", *IEEE Transactions on Software Engineering*, 2011.
- [108] Ricky W. Butler, "A Primer on Architectural Level Fault Tolerance ", 2008.
- [109] Anthony Mandow, Jorge L. Martinez, Jesus Morales, Jose L. Blanco, Alfonso Garcia-Cerezo, and Javier Gonzalez, "Experimental kinematics for wheeled skid-steer mobile robots", presented at the International Conference on Intelligent Robots and Systems, 2007.
- [110] Dariusz Pazderski and Krzysztof Kozłowski, "Trajectory Tracking of Underactuated Skid-Steering Robot", presented at the American Control Conference, 2008.
- [111] J.C. Alexander and J.H. Maddocks, "On the Kinematics of Wheeled Mobile Robots", *The International Journal of Robotics Research*, vol. 8, pp. 15-27, 1989.
- [112] Guy Campion, Georges Bastin, and Brigitte D'Andrea-Novet, "Structural Properties and Classification of Kinematic and Dynamic Models of Wheeled Mobile Robots", *IEEE Transactions on Robotics and Automation*, vol. 12, pp. 47-62, 1996.
- [113] Krzysztof Kozłowski and Dariusz Pazderski, "Modeling and control of a 4-wheel skid-steering mobile robot", *International Journal of Applied Mathematics and Computer Science*, vol. 14, pp. 477-496, 2004.
- [114] Hakyong Chung, Lauro Ojeda, and Johann Borenstein, "Accurate mobile robot deadreckoning with a precision-calibrated fiber-optic gyroscope", *IEEE Transactions on Robotics and Automation*, vol. 17, pp. 329-336, 2001.
- [115] Georgia Anousaki and Kostas J. Kyriakopoulos, "A dead-reckoning scheme for skid steered vehicles in outdoor environments", in *Proceeding of IEEE International Conference on Robotics and Automation*, New Orleans, LA, 2004., pp. 580–585.
- [116] David E. Goldberg, *Genetic Algorithms in Search, Optimization, and Machine Learning*, 1989.
- [117] John Koza, *Genetic Programming: On the programming of computers by means of natural selection*: MIT Press, 1992.
- [118] Julian F. Miller and Peter Thomson, "Cartesian Genetic Programming", in *Genetic Programming*, ed: Springer Berlin Heidelberg, 2000, pp. 121-132.
- [119] Stephen L. Smith and Michael A. Lones, "Implicit Context Representation Cartesian Genetic Programming for the Assessment of Visuo-Spatial Ability," in *Proceeding of IEEE Congress on Evolutionary Computation (CEC) 2009*, ed. Trondheim, 2009.

- [120] Paul Bremner, Mohammad Samie, Gabriel Dragffy, Anthony. G. Pipe, and Yang Liu, "Evolving Cell Array Configurations Using CGP", in *Proceedings of the 14th European conference on Genetic programming*, 2011, pp. 73-84.
- [121] Maryam Mahsal Khan, Gul Muhammad Khan, and Julian F. Miller, "Evolution of Neural Networks using Cartesian Genetic Programming", presented at the IEEE Congress on Evolutionary Computation (CEC), 2010.
- [122] Julian F. Miller, "Cartesian Genetic Programming", in *Cartesian Genetic Programming*, Julian F. Miller, Ed., ed: Springer-Verlag, 2011, pp. 17-34.
- [123] Yang Liu, Gianluca Tempesti, James A. Walker, Jon Timmis, Andrew M. Tyrrell, and Paul Bremner, "A Self-scaling Instruction Generator Using Cartesian Genetic Programming", in *Genetic Programming*. vol. 6621, Sara Silva, *et al.*, Eds., ed: Springer Berlin Heidelberg, 2011, pp. 298-309.
- [124] James Alfred Walker, Yang Liu, Gianluca Tempesti, and Andy M. Tyrrell, "Automatic Code Generation on a MOVE Processor Using Cartesian Genetic Programming", in *Evolvable Systems: From Biology to Hardware*. vol. 6274, ed: Springer Berlin Heidelberg, 2010, pp. 238-249.
- [125] Julian F. Miller and Stephen L. Smith, "Redundancy and Computational Efficiency in Cartesian Genetic Programming", *IEEE TRANSACTIONS ON EVOLUTIONARY COMPUTATION*, vol. 10, pp. 167-174, April 2006 2006.
- [126] Tina Yu and Julian Miller, "Neutrality and the Evolvability of Boolean Function Landscape ", in *Proceedings of European Conference on Genetic Programming*, 2001, pp. 204-217.
- [127] Andrew L. Nelson, Gregory J. Barlow, and Lefteris Doitsidis, "Fitness functions in evolutionary robotics: A survey and analysis", *Robotics and Autonomous Systems*, vol. 57, pp. 345-370, 2009.
- [128] Dirk Büche, Nicol N. Schraudolph, and Petros Koumoutsakos, "Accelerating Evolutionary Algorithms With Gaussian Process Fitness Function Models", *IEEE Transactions on Systems, Man and Cybernetics*, vol. 35, pp. 183-193, 2005.
- [129] Jose Allen Lima, Nuno Gracias, Henrique Pereira, and Agostinho Rosa, "Fitness Function Design for Genetic Algorithms in Cost Evaluation Based Problems", in *Proceedings of IEEE International Conference on Evolutionary Computation*, 1996, pp. 207-212.
- [130] Gunnar Tufte and Pauline C. Haddow, "Extending Artificial Development: Exploiting Environmental Information for the Achievement of Phenotypic Plasticity", *Lecture Notes in Computer Science, Evolvable Systems: From Biology to Hardware*, vol. 4684, pp. 297-308, 2007.
- [131] Gunnar Tufte, "Phenotypic, Developmental and Computational Resources: Scaling in Artificial Development", in *Proceeding of Genetic and Evolutionary Computation Conference 2008*.